sST2 as a candidate for dual biosensing with cTnI in presentations of myocardial infarction

A thesis submitted in partial fulfilment for the degree of Doctor of Philosophy

by

Olivia Jones

Lady Margaret Hall, University of Oxford

& Department of Physiology, Anatomy and Genetics

Trinity Term 2025

Word count: 33,803

Table of Contents

Abstract 1
List of Figures 1
List of tables 5
Acknowledgements 8
Declaration of contributions 13
Patent published 13
1. Introduction 15
1.1 Myocardial infarction (MI) and its impact worldwide 15
1.2 Troponin I 17
1.3 Diagnosis and treatment of MI 18
1.3.1 Diagnosis by electrocardiogram (STEMI vs NSTEMI) 18
1.3.2 Biomarkers for diagnosis 19
1.3.3 MI management 21
1.3.4 Risk stratification in MI patients 22
1.4 Suppression of tumorgenicity factor 2 (ST2) 25
1.5 Hypothesised contribution of sST2 to MI diagnosis and risk management and thesis rationale 29
1.6 Literature review of sST2 relation to MI 30
1.6.1 Search strategy 30
1.6.2 Evidence in literature to support thesis hypothesis 34
1.6.3 Evidence in the literature contradictive of the thesis hypothesis 37
1.6.4 Cell-based investigation of sST2 in MI-like injury 38
1.6.5 Existing immunoassays for sST2 39
1.7 Thesis hypotheses and aims 41
1.7.1 Hypotheses 41
1.7.2 Aims 41
2. The development of a human duplex assay for sST2 and cTnI 43
2.1 Introduction 43
2.1.1 Aim and hypothesis 43
2.1.2 Rationale 44
2.1.3 Enzyme linked immunosorbent assay (ELISA) 45
2.1.4 Analytical performance targets and justification 47
2.1.4.1 LoQ, LoB and LoD 48
2.2 Materials and methods 51
2.2.1 General assay materials 51

2.2.2 Fluorescence assay materials 52
2.2.3 Chemiluminescence assay materials 52
2.2.4 Antibody biotinylations 52
2.2.5 Single plex assay method 54
2.2.5.1 Antibody screening 54
2.2.5.2 Cardiac troponin I 55
2.2.5.3 sST2 56
2.2.6 Duplex assay method 56
2.3 Results 57
2.3.1 Selection of antibodies 57
2.3.2 Matrix effects assessment 58
2.4 Assay detection method 60
2.4.1 Optical density vs chemiluminescence 60
2.4.2 Biotin conjugation chemistries 63
2.5 Analyte commutability 66
2.6 Levers of sensitivity 69
2.6.1 Luminol formulation screen 69
2.6.2 Co-detection antibody screen 73
2.6.3 Assay diluent titrations 74
2.6.3.1 Calcium chloride 75
2.6.3.2 Magnesium chloride 76
2.6.3.3 Sodium chloride 77
2.6.3.4 Bovine serum albumin (BSA) 79
2.6.4 Final optimised single plex assay performance 80
2.7 Conversion of single plex to duplex assay 84
2.7.1 Interference studies 84
2.7.1.1 Analyte interference 84
2.7.1.2 Detection system interference 86
2.7.2 Quantum dot adoption for fluorescent signal distinction 88
2.7.3 Final duplex assay optimisations 91
2.7.5 Final assay validation 94
2.7.5.1 Linearity 94
2.7.5.2 LoD 95
2.5.7.3 Matrix equivalency 101
2.5.7.4 Precision 104
2.8 Pilot clinical study 104

2.9 Discussion 111
3. Mechanistic investigations of sST2 pathway activation and expression in *in vivo* and *in vitro* injury models 116
3.1 Introduction 116
3.1.1 Aim and hypothesis 116
3.1.2 Rationale 119
3.2 Methods 120
3.2.1 Mouse model study design 120
3.2.2 Surgical method 120
3.2.3 Assay development for mouse cTnI and sST2 targets 121
3.2.3 Cell culture and injury 122
3.2.4 rt-qPCR using SYBR green and TaqMan probes 123
3.3 Results 124
3.3.1 scRNA-seq for IL1rl1 in MI and uninjured mice 124
3.3.2 Murine characterisation of sST2 release profile 126
3.3.2.1 ELISA optimisation 126
cTnI 126
sST2 131
3.3.2.2 Assaying mouse serum post-LAD ligation for sST2 and cTnI 134
3.3.3 H9c2 injury modelling for MI and HF 138
3.3.3.1 Confirmation of sST2 expression pre and post differentiation 138
3.3.3.2 MI modelling with hypoxia 139
RT-qPCR 139
SDS-PAGE and Western blots 142
3.3.4 *IL1RL1* response in HF modelling with AngII 144
SDS-page and Western blots 146
3.3.5 sST2/IL-33 pathway comparison between models 148
3.4 Discussion 153
4. A clinical cohort evaluation of sST2 presence in myocardial infarction 160
4.1 Introduction 160
4.1.1 Aims and hypothesis 160
4.1.2 Rationale 161
4.2 Methods 161
4.2.1 Patient inclusion and exclusion criteria 161
4.2.2 Sample handling, preparation, transport and storage 165
4.2.3 96 well plate layout and study plan 165

4.2.4 Statistical analysis 167
4.3 Results 168
4.3.1 Control material 168
4.4 Comparison of duplex sST2 with commercial analysers 170
4.5 sST2 correlation with cTnI readings 173
4.6 sST2 response with diagnosis 177
4.7 sST2 reading broken down by time post MI symptom onset 181
4.8 MACE incidence (either HF or secondary MI) 184
4.8.1 Subsequent diagnosis of HF post-presentation to A&E 184
4.8.2 Second MI incidence and prediction 188
4.9 Discussion 190
5. Discussion 194
5.1 Contribution of this work to the field 194
5.2 Limitations 197
5.3 Future work 199
6. Conclusions and final remarks 202
7. Appendix 203
8. References 211

Abstract

sST2 is an emerging biomarker of interest for cardiovascular stress, where this thesis aims to isolate specific pathologies contributing to its serous release. On a molecular level, sST2 is a decoy receptor that intercepts IL-33 and sequesters its natural association with the transmembrane isoform of ST2: ST2L. This pathway, if not inhibited, signals to a cascade of transcription factors that upregulate cardioprotective chemokines and cytokines to reduce the severity of adverse remodelling processes such as hypertrophy post-injury. The work described in this thesis has a significant focus of developing an applicable solution of sST2 measurements in instances of MI. This was facilitated via a partnership with Osler Diagnostics, a point of care immunoassay development start-up (an Oxford University spinout), where a duplex assay for sST2 and cTnI was created, enabling a rapid solution for measuring both biomarkers simultaneously.

Chapter 2 describes the optimisation of this complex assay in 96-well plate ELISA format with novel techniques for improving sensitivity and specificity of biomarker detection, with the adoption of different detection methods for distinguishing each signal. The resulting assay achieved an LoD of 20ng/L for cTnI and 10.3ng/mL for sST2; this assay was then used to analyse biomarker levels in a clinical cohort of 215 MI patients, where sST2 levels were significantly ($P<0.0001$) higher in patients diagnosed with MI in comparison to a healthy "normals" cohort (n=37). In addition, sST2 had similar predictive ability for HF post-MI in comparison to NT-proBNP (AUC of 0.70 and 0.72, respectively). Chapter 3 involved investigative experiments pertaining to the molecular pathways involved in sST2 upregulation, and the effects of sST2 expression according to two injury models. Current literature disputes the attribution of MI and HF to upregulation of sST2, and so this chapter aimed to isolate the

contribution of both diseases to sST2 upregulation. These injury models utilised AngII to simulate HF, and H_2O_2 to induce ischemic injury, where sST2 on the transcript and protein level showed increased expression. Additionally, an *in vivo* model subject to coronary artery ligation characterised, for the first time, the release profile of sST2 post-MI in a controlled environment. This showed a 2.95-fold increase in sST2 released into sera within 24 hours of injury.

In conclusion, sST2 is a promising biomarker for MI and injury severity, providing additional information to what is already diagnostically available. More research should be conducted into sST2 and MI to continue building a dataset convincing enough to acquire commercial interest and funding to propel the addition of sST2 to MI investigative recommendations.

List of Figures

1. Introduction

Figure 1.1: Cardiac troponin comprises 3 subunits that mediate calcium ion-mediated contraction

Figure 1.2: MI is classified as STEMI or NSTEMI depending on ST wave behaviour.

Figure 1.3: IL-33 and ST2L interaction triggers downstream mediators of cytokinetic response to inflammation and injury.

Figure 1.4: Necrotic events in the myocardium (a.) result in upregulated hypertrophic signalling and thickening of the left ventricle wall (b.).

Figure 1.5: Scientific interest in sST2 as a biomarker for MI increased exponentially after the Critical Care Diagnostics patent in 2008.

Figure 1.6: A PubMed search for papers containing both phrases “soluble ST2” and “myocardial infarction produced 18 relevant results.

Figure 1.7: There is no trend between study sample size and support for sST2 as a use for MI diagnosis or prognosis.

2. The development of a human duplex assay for sST2 and cTnI

Figure 2.1.1: A diagrammatic visualisation of three different methods of ELISA.

Figure 2.1.2: A sandwich ELISA formation shown situated in a well of a 96 well plate.

Figure 2.1.3: A graphical demonstration, taken from the CLSI document EP17, of 3 important mathematical limits in assay development: LoB, LoD and LoQ.

Figure 2.1.4: An image taken from the Thermo Fisher NHS-SS biotinylation protocol showing the targeting of primary amines for biotin attachment via sulfo-NHS-SS-biotin.

Figure 2.1.5: The biotin reaction scheme taken from Thermo Fisher product 21911, showing the attachment of PEG-11 biotin to a protein with exposed sulfhydryl groups.

Figure 2.1.6: An example of 96 well plate layout for antibody screening exercises.

Figure 2.1.7: Tables to show, by colour conditional formatting, the size of signal to background ratios when antibodies are screened as both capture and detection antibodies.

Figure 2.1.8: Standard curves in PBS-T 0.1% or calf plasma as matrix to show sensitivity and linearity of the two best antibody pairs identified in Figure 2.1.7.

Figure 2.1.9: Matrix effects present in calf plasma prevents sensitivity and cTnI detection up to 1000ng/L.

Figure 2.2.1: 4PL plots to show sensitivity of the troponin assay in PBS-T and calf plasma in a chemiluminescent format (a and b) and optical absorbance (c and d).

Figure 2.2.2: The most optimal conditions for cTnI assay sensitivity was 40µg/ml capture antibody with 2µg/ml detection antibody and 2µg/ml polyHRP.

Figure 2.2.3: 4PL regressions shows no sensitivity in the initial pair, with improved sensitivity of the new pair for cTnI.

Figure 2.2.4: Biotin conjugation chemistry has a substantial impact on assay performance.

Figure 2.2.5: Mal-PEG11 linker achieved an increased slope of 4840 RLU/ng/ml compared to the NHS-SS linker at 10ng/ml sST2.

Figure 2.2.6: The recombinant (Hytest IC) cTnIC protein used for assay development does not corroborate the behaviour of clinical native cTnI.

Figure 2.2.7: RayBio recombinant cTnI resembles clinical troponin in assay response and therefore is a suitable calibrator.

Figure 2.2.8: Neogen K-blue luminol gives superior sensitivity to SuperSignal Pico and the old custom Neogen luminol formulation.

Figure 2.2.9: The introduction of a second detection antibody does not improve the ability of the assay to detect native troponin.

Figure 2.3.1: A titration of calcium chloride in the assay diluent shows an increase in signal to background ratio before plateauing and decreasing after 10mM.

Figure 2.3.2: The addition of 20mM magnesium chloride to assay diluent improved sensitivity (slope) to 8217RLU/ng/L.

Figure 2.3.3: Titrating sodium chloride into the assay diluent shows some, but minimal increase in sensitivity of the assay on top of the already added salts.

Figure 2.3.4: 0.3-1% BSA addition to assay diluent improves slope to 11994.7RLU/ng/L.

Figure 2.3.5: After optimisation, the cTnI single plex assay had an LoD of 29.28ng/L

Figure 2.3.6 – After optimisation, the sST2 duplex assay had an LoD of 6.07ng/ml.

Figure 2.3.7 – There is no cross-interference of analyte when a.) a high amount of sST2 is spiked into the troponin assay and b.) a high amount of troponin is spiked into the sST2 assay.

Figure 2.3.8 - Assay performance when a.) sST2 antibody at optimised concentration (1µg/ml) is spiked into the troponin detection solution, and b.) optimised concentration of troponin detection antibody (2µg/ml) is spiked into the sST2 assay.

Figure 2.3.9 – sST2 detection reagents do not interfere with the cTnI assay (a.). Vice versa, cTnI detection antibody do not interfere with sST2 fluorescent-based detection (b.).

Figure 2.4.1 - Standard curves with broad ranges of sST2 and cTnI concentration run on the duplex assay format show loss of linearity starting between 1000-2000ng/ml and 6250ng/L-12500ng/L, respectively.

Figure 2.4.2 – Duplex LoD for sST2 (a. and b.) using pooled plasma was at 24.8ng/ml, confounded by basal analyte. LoD for cTnI was at 11.3ng/L (c. and d.).

Figure 2.4.3 – A true "blank" human plasma pool sample is achievable via depletion of basal sST2 using antibody-conjugated magnetic particles.

Figure 2.4.4 - A revised experiment using pooled plasma depleted of basal sST2 analyte shows a more accurate LoD of 10.3ng/ml.

Figure 2.4.5 – Performance between EDTA and Lihep using the duplex assay is within error (error bars reflect SD), with the same equivalency observed between three different plasma donors.

Figure 2.4.6 –2-way ANOVA showed no significant difference between types of anticoagulated plasma and cTnI readings at lower (a.) and higher (b.) spikes, with sST2 showing the same effect (c. and d.)

Figure 2.4.7 - Correlation plots between sST2 and cTnI readings produced by the duplex assay in sequential resolution from a-c and d-f show.

Figure 2.4.8 – Duplex cTnI readings correlate strongly with the hospital cTnI measurements (Pearson r = 0.9311, 95% CI 0.8756 to 0.9623).

Figure 2.4.9 – The plasma sST2 levels of patients diagnosed with HF or MI (or both) are significantly higher than the average plasma level of sST2 in a cohort of normals (P<0.0001).

3. Mechanistic investigations of ST2L pathway activation and sST2 expression in vivo and in vitro injury models

Figure 3.1.1 – UMAP projections display the expression of various marker genes across different cell populations in the heart.

Figure 3.1.2 – Titrations of primary antibody with either 2µg/ml Ab (antibody) and polyHRP (a.) or 1µg/ml Ab and polyHRP (b.)

Figure 3.1.3 – 4PL regressions show sensitivity and linear range of one-step and two-step versions of the troponin assay, with increasing XY resolution from a-c.

Figure 3.1.4 – A demonstration of matrix effects in serum that are absent in assay diluent.

Figure 3.1.5 – The sST2 assay demonstrates similar sensitivity at both a 1 in 2 and a 1 in 4 sample dilution.

Figure 3.1.6 – When mice were subjected to LAD ligation, cTnI increased by 3000-fold within 24 hours, and then declines rapidly.

Figure 3.1.7 – sST2 is very responsive to LAD ligation in mice, with a 2.95-fold increase in the biomarker within 24 hours of infarction.

Figure 3.1.8 – Collectively, there is a negative correlation between signal obtained by the murine sST2 assay and day post-LAD ligation.

Figure 3.1.9 – ΔΔCT data (a.) shows a very minimal (~10%) decrease in expression of sST2 mRNA over a differentiation time course.

Figure 3.2.1 – Increased mRNA levels of *Il6*, *Tnf* and *Il1rl1* were observed after ischaemic injury with H2O2 at either 50µM or 100µM.

Figure 3.2.2 – Plots to show the relationship between mRNA levels of *Il1rl1* with other closely related interleukins.

Figure 3.2.3 – Longer periods of H_2O_2 incubation (plot a) show moderate increases of caspase-9, whilst most injury conditions mediated significant increases in α-smooth muscle actin (plot b).

Figure 3.2.4 - Relative expression of 100µM AngII for 24 hours shows increase of mmp9, pikc3b and IL-6 mRNA, however sST2 expression remains constant.

Figure 3.2.5 – Mean caspase-9 (plot a.) protein level increased with all concentrations of AngII (however only significantly so to 100µM for 24 hours, P=0.0005)), indicating increased apoptotic activity associated with hypertrophy and remodelling.

Figure 3.2.6 – AngII and H_2O_2 agonists have very different influences on the expression of the constituents of the IL-33/ST2L signalling pathway.

Figure 3.2.7 – sST2 protein expression increased in all injury conditions involving AngII and H_2O_2.

4. A clinical cohort observation of sST2 presence in MI

Figure 4.1.1 – sST2 readings collected for the assessment of MI-contributed plasma levels of the biomarker were screened and refined by the above criteria.

Figure 4.1.2 – A donut graph to show distribution of diagnoses among patients involved in the clinical cohort.

Figure 4.1.3 – Donut charts show the distribution of age and gender by all-cause with a total n=348.

Figure 4.1.4 - A 96 well plate design to show the layout of each clinical sample study plate, where this plate was repeated 17 times with different groups of 22 samples each run.

Figure 4.1.5 – A Levy-Jennings plot to show distribution of control sample (BioRad IntelliQ Cardiac Plus) on each plate for clinical sample measurement over time.

Figure 4.1.6 – A Levy-Jennings plot to show distribution of control sample (BioRad IntelliQ Cardiac Plus) on each plate for clinical sample measurement over time.

Figure 4.1.7 – Scatter plots to show agreement between cTnI measurement systems, where a) shows Siemens Centaur vs Abbott Architect, b) Duplex vs Abbott Architect and c) Duplex vs Siemens Centaur.

Figure 4.1.8 – sST2 does not correlates with cTnI in all-cause measurements of biomarker, however, correlates strongly in MI patients (P=<0.0001) when comparing duplex readings only.

Figure 4.1.9 – sST2 levels are significantly (P=<0.0001) higher in MI patients than a cohort of healthy individuals.

Figure 4.2.1 - sST2 is able to distinguish both (a.) NSTEMI (P=<0.0001) and (b.) STEMI (P=0.0381) from a healthy cohort. There is no difference in sST2 levels between STEMI and NSTEMI patients (plot c. P=0.3473).

Figure 4.2.2 – The median time between patient presentation to A&E and the sample which was donated to this study drawn was 2876 minutes (2 days).

Figure 4.2.3 – When patients were able to donate their plasma within 24 hours of MI, there was no correlation between time elapsed and sST2 concentration (plot a.) (P=0.9942). This was still true when normalising for size of infarct (cTnI) of the same sample (plot b.) (P=0.4602).

Figure 4.2.4 – Comparison of biomarker levels in entire patient cohort (all-cause) between HF (n=295) and non-HF (n=55) with corresponding ROC.

Figure 4.2.5 – Comparison of biomarker levels in MI subsection of clinical cohort (n=202: n=176 no HF and n=27 HF) with corresponding ROC.

Figure 4.2.6 - Comparison of biomarker levels in the MI cohort between second MI (n=113) and no second MI (n=92) with corresponding ROC.

7. Appendix

Figure 7.1.1 - The response when the sST2 assay is optimised for Osler Diagnostics proprietary development platform, showing feasibility for assay commercialisation.

Figure 7.1.2 - Analytes are unaffected by freeze-thaw cycles required for clinical study preparation.

List of tables

1. Introduction

Table 1.1 - Popular cardiovascular risk score systems are unique in their combination of considered variables

Table 1.2 – A summary of literature exploring the efficacy of existing ST2 assays

2. The development of a human duplex assay for sST2 and cTnI

Table 2.1 – A table to show comparison of epitope regions on capture and detection antibodies with the initial underperforming pair and the new, significantly more sensitive pair.

Table 2.2 - A table to list comparative signal to background ratios of various luminol formulations (left) with three different types of analyte.

Table 2.3 - Values representing signal obtained at low concentrations of troponin and their interpolated values from the standard curve run on that plate.

Table 2.4 - Values representing signal obtained at low concentrations of sST2 and their interpolated values from the standard curve run on that plate.

Table 2.5 - signal to background ratio using a checkerboard of different sST2 capture and detection antibody concentrations, whilst keeping quantum dot concentration equal to detection antibody.

Table 2.6 - A colour schematic to show various combinations of sST2 capture antibody coating with troponin antibody coating for best slope between 0-200ng/L for troponin and 0-300ng/ml for sST2.

Table 2.7 - The precision of the duplex assay at a wide concentration range of both cTnI and sST2, expressed as CV.

3. Mechanistic investigations of ST2L pathway activation and sST2 expression *in vivo* and *in vitro* injury models

Table 3.1 - Capture antibody (S215) is titrated in a checkerboard fashion with detection solution, which contains a fixed ratio (1:2) of secondary antibody (S103) with polyHRP.

Table 3.2 - After selection of 40µg/ml as capture antibody concentration, ratio and concentration of secondary antibody (S103) and polyHRP were titrated in a similar checkerboard fashion.

4. A clinical cohort observation of sST2 presence in MI

Table 4.1 – Normality and correlation significance data for cTnI measurements across all systems.

Table 4.2 – Statistical analysis shows significance in all cases for the correlation between cTnI and sST2 in MI patients.

7. Appendix

Table 7.1 – Primer sequences for RT-qPCR

Table 7.2 – Metadata from scRNA-seq analysis

Table 7.3 – A timetable for the execution of the clinical sample study, designed to ensure protection of analyte stability.

Table 7.4 – The results and comparison of a literature review on human clinical studies evaluating sST2 plasma levels in MI patients.

Table 7.5 – The results and comparison of a literature search where sST2 expression in cardiomyocytes (HL-1, AC16 or H9c2 cell line) has been explored.

Acknowledgements

This thesis and 4-year body of work is dedicated to my grandparents, Bob and Sheila Whitaker. Their encouragement and support has been extremely motivating in the most challenging portions of the work and I hope I can make them proud. Thank you also to my best friend, Lauren, who not only made me a godmother in 2023, but would sit on facetime with me for hours on end in silence whilst I wrote this thesis for moral support. Thank you also to my parents and my brother for their constant encouragement.

Thank you so much to my friends and colleagues at Osler Diagnostics who have been a tremendous support and a source of wisdom and guidance in what has been a new and daunting learning experience for me. Thank you specifically to Laura Baers, Barbara Simões, Aya Abdalla, Laure Carrique, Fatiha Taylor and Peter Reader. Your encouragement and mentorship made navigation of new topics much less intimidating and having their pastoral support in addition to the expertise was so appreciated. Additionally, a tremendous thank you to the financial contribution made by Osler Diagnostics and the executive team. Giving me the opportunity to read for a DPhil at Oxford alongside developing as a commercial scientist is a once in a million opportunity that I do not take for granted. I am immensely proud and grateful to be an employee of a company that values development so much so that they saw potential in an eager 22-year-old and have contributed so much to moulding me as a scientist.

Thank you to my college, Lady Margaret Hall for their award of my Alison Brading Memorial Scholarship by Prof. Margaret Matthews in 2023. The contribution fulfilled my ambition to expand my experiments and is greatly acknowledged.

Thank you to Tania Tenreiro, the lead of intellectual property at Osler Diagnostics. The IP surrounding this thesis has been tricky to navigate and took a lot of advisements from the

legal team in presenting a contract. Tania spent a lot of time handling this for me and also reading my thesis to give feedback. I have learned so much about commercial-academic collaborations through her expertise and greatly appreciate her technical support.

Thank you to Danielle Walker and Sheryl Bell-Rhone at NCARC for their assistance and correspondence in organising and delivering all of the information for the clinical cohort study. In addition, thank you to the patients at Salford Royal hospital for their generous donations to this research, alongside the healthy volunteers at Osler.

Finally, but no means least, thank you to my fantastic supervisors, Prof. Nicola Smart and Dr Konstantinos Psarros. Nicola has helped me navigate the unusual circumstance in which I proposed the concept of this work to her, and she has encouraged my concept from day 1 by taking me under her wing. Originally, this work started as a Master's degree and flourished into a much greater body of work and Nicola supported my transfer to DPhil without hesitation. I was equally supported by Costas, who has taught me so much about presenting and designing academic work and is the reason I have developed so much to this day. I could not have achieved my dream of getting a DPhil from the University of Oxford without my supervisors; words cannot convey how grateful I am.

List of abbreviations:

4PL – 4 parameter logistic

ACS – Acute coronary syndrome

AKI – Acute kidney injury

AngII – Angiotensin II

AP-1 – Activator protein 2

AUC – Area under curve

BP – Blood Pressure

BSA – Bovine serum albumin

C JUN – Cellular Jun

CI – confidence interval

cTnI – Cardiac troponin I

CLSI – Clinical and Laboratory Standards Institute

DMEM – Dulbecco's modified eagle medium

ECG - Electrocardiogram

EDTA – Ethylenediaminetetraacetic acid

GRACE – Global Registry of acute coronary events

HEART – History, ECG, Age, risk factors and troponin

HF – Heart Failure

HRP – Horse radish peroxidase

IL-33 – Interleukin-33

IL1RL1 – Interleukin 1 receptor-like 1

IRAK 1 – Interleukin-1 receptor-associated kinase 1

JNK – Jun N-terminal kinase

LAD – Left anterior descending

Lihep – Lithium Heparin

LoB – Limit of blank

LoD – Limit of detection

LoQ – Limit of quantification

MACE – Major adverse cardiac events

MAPK – Mitogen-activated protein kinase

MI – myocardial infarction

MiRNA – MicroRNA

MyD88 – Myeloid differentiation primary response 88

NF-κβ – Nuclear factor Kappa-light-chain-enhancer of activated B cells

NICE – National Institute of Health and Care Excellence

NSB – Non-specific binding

NSTEMI – non-ST elevated myocardial infarction

PBS-T – Phosphate buffered saline - tween

PCI – percutaneous coronary intervention

RLU – Relative light units

scRNA-seq – single cell RNA sequencing

SOX7 – SRY-box transcription factor 7

sST2 – Soluble suppression of tumorigenicity factor 2

STEMI – ST-elevated myocardial infarction

TIMI - Thrombolysis in myocardial infarction

TLR – Toll-like receptor

TMB - 3,3',5,5'-Tetramethylbenzidine

TTR – Time to result

UMAP – Uniform manifold approximation and projection

Declaration of contributions

I declare that the work described in this dissertation is completely my own. I produced my own DPhil topic initiative through reading and subsequent pitch to both Nicola Smart and a panel during interview. All experiments were completed solely by me, except for the following:

1. Surgery for MI simulation and extraction of serum (Chapter 3) performed by Dr Shih-Hsuan Mao at the Kennedy Institute of Rheumatology
2. scRNA-seq data produced from metadata (Chapter 3) by Jun Ying, a DPhil student in Mathilda Mommersteeg's group.

Patent published

"Diagnostic assay reagents comprising block co-polymers"

I was listed as an inventor in the International Patent Application No. PCT/EP2022/072601, which was published on 16 February 2023 as WO2023017132A1 (https://patents.google.com/patent/WO2023017132A1/en?oq=WO2023017132).

This application entered the national phase in Q1 2024 and the subsequent national phase applications are pending in the United States (US 18/682,753), Europe (EP22761002.9), China (CN2022800685092), Japan (JP2024508573) and Canada (CA3227288).

1. Introduction

1.1 Myocardial infarction (MI) and its impact worldwide

Colloquially referred to as a "heart attack", MI describes the death of cardiac tissue by oxygen starvation, usually due to an obstruction in the coronary arteries supplying the myocardium (Lu, Liu, Sun, Zheng, & Zhang, 2015). A recent meta-analysis involving over 5 million participants found that MI has a global incidence of 9.5% in those over 60 years old, and 3.8% in those under 60 years old (Salari, et al., 2023). This puts MI as the leading cause of death worldwide and subsequently an enormous strain on healthcare services (Moraes-Silva, Rodrigues, Coelho-Junior, Feriani, & Irigoyen, 2017). Not to mention, 1 in 5 of those who have an MI go on to have a second MI within 5 years, according to the American Heart Association (AHA). As a result, research into prevention and risk stratification of MI is in increasing demand in attempts to reduce event prevalence, particularly in this era of an aging population. Despite this, the proportion of MI events within the population continues to rise. In the UK, the British Heart Foundation (BHF) published new statistics in September 2024 revealing that someone in the UK is admitted to hospital due to MI every 6 minutes, which is around 220 people per day (BHF, 2024). Most detrimental about MI is the associated increased risk in mortality and life altering remodelling of the muscle based on time post symptom presentation, and the importance of addressing the infarct as quickly as possible. The relationship between time post presentation, treatment (usually Percutaneous Coronary Intervention, PCI) and mortality has been quantified multiple times and has repeatedly linked longer times between presentation to PCI with higher risk of adverse outcome such as death, subsequent MI or development of heart failure (HF) (Mills, et al., 2024).

In 2024, 1,822 patients diagnosed and treated for MI were assessed for the risk of combined adverse outcomes in 3 groups; those who were treated 60 mins, 90 mins, and 120

mins post-presentation (Mills, et al., 2024). It was discovered that even between 60 and 120 minutes, the risk of an adverse outcome within 1 year of infarction rises from 11.3% to 20.2%. That accounts for almost double the risk in just a 60-minute window of waiting to be treated (Mills, et al., 2024). A much earlier study conducted in 2010 similarly found that the difference between a 0–60-minute delay vs 61–120-minute delay caused an increase in mortality from 15.4% to 23.3% respectively (Terkelsen, et al., 2010). Even within the 14 years that have elapsed between these two studies, given the similar statistics, there is little suggestion of any significant improvement in MI survival with respect to time to treatment. However, a longitudinal study (1995-2015) assessing 6-month mortality shows an improvement in survival (regardless of time to treatment) over the 20-year period (Puymirat, et al., 2017). Data from FAST-MI (French Registry of Acute ST-Elevation or Non-ST-Elevation Myocardial Infarction) shows that in 14,423 patients (59% STEMI), mortality in STEMI patients decreased from 17.2%, to 6.9%, and 5.3% from 1995, 2010 and 2015 respectively. In NSTEMI patients, mortality decreased from 17.2%, to 6.9% and 6.3%, respectively, over the same time period (Puymirat, et al., 2017).

Although these data only account for 6-month mortality (when 30-day and post 1 year are of equal interest), the trends suggest an improvement in survival rates regardless of MI classification. Published data for mortality post MI within 30 days is currently at a rate of around 30%, with the five year mortality rates spread between 48.2-62.3%, which differs considerably to the findings of 6-month mortality previously outlined (Harrison, 2013) (Nadlacki, et al., 2021) (Taylor, et al., 2019). Notably in the FAST-MI study, median time from patient-reported onset of symptoms to hospital admission decreased from 240-168 minutes, and the use of reperfusion therapy also increased (from 49.5-82%) (Puymirat, et al., 2017). This is suggestive of multifactorial contribution to the decrease in mortality over the 20-year

period. With MI presenting such a sensitive relationship between time of onset and time of ischaemia alleviation, rapid identification and intervention could provide the key for better patient outcomes and reducing the loss of life.

In a post-COVID19 world, where scientists, government leaders and civilians are aware of now more than ever, the importance of rapid diagnostics, the efficacy of diagnostic solutions for all diseases are under a spotlight of scrutiny. In the context of MI, the prevention and risk assessment of patients has room for improvement given the propensity of this type of ischaemic injury to cause death.

1.2 Troponin I

Widely validated and practised is the reading of cardiac troponin I (cTnI) in the diagnosis of MI. cTnI contributes one of 3 subunits of cardiac troponin, pictured in Figure 1.1, that when bound by free calcium ions allows for the contraction of cardiac muscle via myofilament reorganisation (Bers, 2002). Naturally, in accordance with their interdependence for structure, troponin I and T demonstrate a 1:1 complex ratio in the myocardium. All subunits of troponin are known to be released upon cardiomyocyte necrosis in the event of acute coronary syndrome and ischaemia, either in complex or separately (Espinosa, et al., 2023). However, cTnI has demonstrated superior clinical utility over cTnT, due to its highly dynamic release profile, where a much larger concentration of cTnI (compared to cTnT) is detected in response to myocardial necrosis (Espinosa, et al., 2023) (Keller, et al., 2009). This is reflective of its sensitivity, and as a result provides enhanced ability to stratify risk early post-MI (Keller, et al., 2009). The nature of its release in serum, in that it comes directly from the breakdown of cardiac tissue rather than mRNA upregulation, makes troponin an extremely

specific and attractive biomarker for acute diagnosis. For the reasons explained, cTnI remains the gold standard diagnostic analyte for MI (Aydin, Ugur, Aydin, Sahin, & Yardim, 2019).

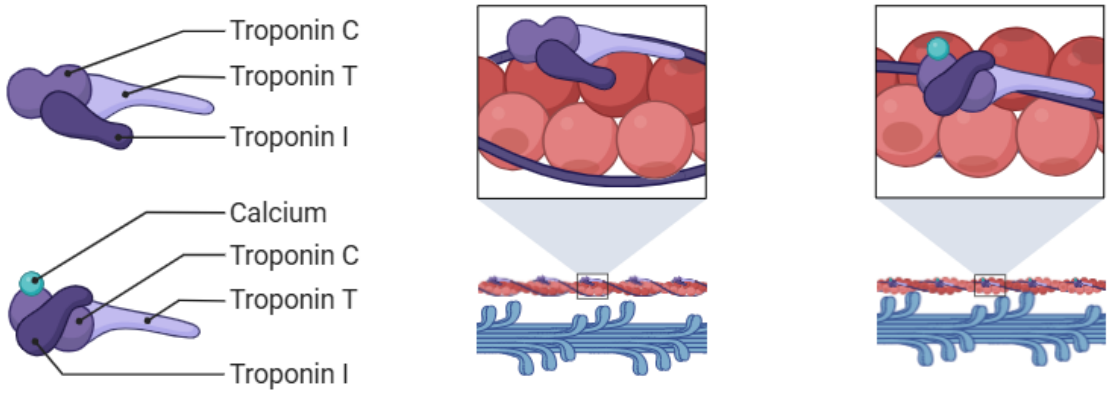

Figure 1.1 – Cardiac troponin comprises 3 subunits that undertake calcium ion-mediated contraction. *A schematic to demonstrate the contribution of troponin subunits to normal muscle function, including calcium ion mediation of contraction. Produced using BioRender.*

1.3 Diagnosis and treatment of MI

1.3.1 Diagnosis by electrocardiogram (STEMI vs NSTEMI)

An ECG is required and uniformly practised in the diagnosis of MI, for assessment of the severity of the occlusion and to categorise the pathology as STEMI (ST elevated myocardial infarction) or NSTEMI (non-ST elevated myocardial infarction). STEMI describes a total occlusion of a coronary artery for a prolonged period of time, characterised by an elevated ST wave on ECG assessment (Mitsis & Gragnano, 2021). On the other hand, NSTEMI involves only a partial occlusion of a coronary artery, considered the less severe form of MI (Martínez, et al., 2022). NSTEMI is the most commonly diagnosed phenotype at around 70%, with STEMI prevalence around 30% (Gandhi, et al., 2022). NSTEMI is characterised by ST depression on ECG but with the presence of high troponin serum concentrations. On the other hand, STEMI

is characterised by ST elevation in addition to high troponin serum concentrations. Figure 1.2 demonstrates the ECG traces of each aetiology.

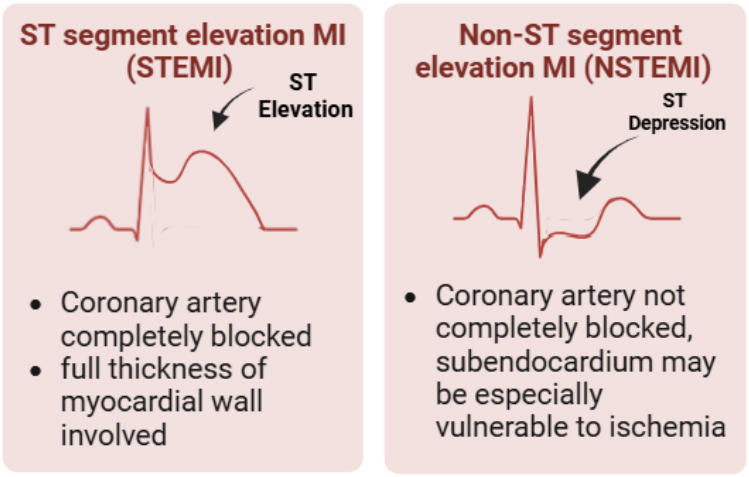

***Figure 1.2 – MI is classified as STEMI or NSTEMI depending on ST wave behaviour**. ECG behaviour of both STEMI and NSTEMI, where STEMI involves total occlusion and corresponding elevation of ST waves. Image produced using Biorender.*

Of course, ECG cannot be used as the sole method of diagnosis in MI, given that NTSEMI presentation on ECG can appear unremarkable despite the presence of ischaemia. ECG is also not specific for necrosis of the myocardium, unlike troponin. Therefore, the combination of ECG with biomarkers is standard practice as described in the following section.

1.3.2 Biomarkers for diagnosis

As mentioned, cardiac troponin (either I or T subunit) is the most important marker to assay in a suspected MI due to its high specificity. Troponin measurements are taken serially, as an observed increase in levels within a short period of time indicate a correlating degradation of myocardium integrity. Currently, the guidelines are for troponin to be measured as quickly as possible after the patient arrives at the hospital, and then 3 hours after

the initial blood draw. This allows clinicians to confirm a diagnosis alongside an ECG, but to also monitor the decrease in troponin after a hopefully successful intervention.

Another well-established biomarker in cardiovascular risk is NT-proBNP (N-terminal pro brain natriuretic peptide). NT-proBNP has been clearly defined in a cardiovascular physiological context after its debut in clinical practice in the mid-2000s. As a biomarker, it is exceptionally useful in measuring wall stress of the left ventricle, and correlates closely with left ventricular ejection fraction (LVEF) (Bay, et al., 2003). NT-proBNP release is mechanistically reliant on cardiomyocyte stretch in the left ventricle, initiating the transcription of its gene via activation of MAPK and calcineurin-NFAT signalling pathways (Cao, Jia, & Zhu, 2019). When stratifying risk of patients after MI, serial NT-proBNP measurements may be of use to understand strain of the left ventricle (i.e. by fluid overload, dilated or hypertrophic cardiomyopathy) their vulnerability to developing several unfavourable outcomes post-MI termed “MACE” (major adverse cardiovascular events). Patients that have experienced one or more MIs have a much higher risk of MACE compared to the healthy population, given the severe and irreversible nature of myocyte necrosis. Their susceptibility to MACE (including mortality) calls for constant improvement in the ability to predict and prevent such events occurring.

sST2 is the novel biomarker of interest in this thesis and is described in detail on a molecular level in the next section (1.4). Based on existing literature, it would appear that sST2 may aid in diagnosis and/or risk stratification during and after MI. According to these data collected on sST2 levels in MI patients, the biomarker appears to be raised above the clinical cutoff for a longer period of time in comparison to cTnI, the latter of which is known to have a short half-life of between 7-20 hours (Kristensen, et al., 2024). The half-life of sST2 is yet to

be defined. Given that troponin is released on necrosis, once the stimulator of the necrotic event is removed or alleviated, cTnI levels will decline. Conversely, due to the apparent multifaceted mechanism in which sST2 is released (necrosis, myocardial stretch, inflammation), sST2 could be measured routinely post admission after MI is confirmed to monitor the cardiac physiology of the patient.

1.3.3 MI management

Treatment for MI was not the primary focus of this work and is a significant area of ongoing improvement in cardiology. However, the quality of diagnosis and risk stratification of MI that is debated in this work does inform pathway of treatment and so it was relevant to harbour broad context in these pathways throughout this thesis to connect their implications on patient survival. In the UK, the National Institute for Health and Care Research (NICE) provide guidelines for treatment of all well-established health conditions, and these are followed by the NHS (National Health Service) uniformly. Management of MI differs depending on the extent of risk and perceived occlusion in the affected coronary artery (Meyers, et al., 2021). NICE recommends a 300mg dose of aspirin in all cases where MI is suspected as soon as the patient enters the hospital for both NSTEMI (NICE: NG185, 2020) and STEMI (NICE: NG185, 2020). Post ECG assessment where MI is classed as STEMI or NSTEMI, treatment starts to become branched based on severity.

Physiologically, STEMI presents a more urgent case than NSTEMI due to its completely occlusive nature, and so more aggressive intervention is recommended in this case, where a PCI (also known as coronary angioplasty) is performed, by placing a stent into the coronary artery to remove the occlusion and restore blood flow (NICE: NG185, 2020). The NICE guidelines recommend that PCI is offered to patients with STEMI (or high risk NSTEMI) if presenting within 12 hours, and if PCI can be performed within the following 2 hours. If PCI

cannot be performed within this time frame, fibrinolysis is conducted using drugs such as streptokinase and alteplase (NICE: NG185, 2020) (NICE: NG185, 2020). In severe NSTEMI presentations (e.g. with higher GRACE scoring and/or troponin), an immediate angiogram should be ordered with follow on PCI if required. If the PCI is not required, the architecture of the vasculature and predicted damage to the left ventricle should be considered in follow up therapy both from a pharmacological and rehabilitative perspective. In those with less severe NSTEMI, angiography is not currently recommended by NICE and instead, ticagrelor (anti-platelet medication) and aspirin should be offered (NICE: NG185, 2020). Interestingly, some research has found that despite differences in hypoxia and occlusion, mortality rates for those with STEMI and NSTEMI do not differ significantly (Takeji, et al., 2021) (Montalescot, et al., 2007). This has been attributed to more effective interventions being taken in STEMI compared to NSTEMI based on perceived risk, where one study found that patients with STEMI were more likely to undergo reperfusion therapy and receive more pharmacological intervention at discharge, although their quantitative risk factors (including but not limited to: BP, Killip class and diabetes diagnosis) did not differ between the groups (Montalescot, et al., 2007) (Brogan, et al., 2014). Clearly, judgement of risk is pivotal in selecting the most appropriate treatment after an infarction. The next section will discuss the current risk analysis conducted at point of MI diagnosis.

1.3.4 Risk stratification in MI patients

Clinicians utilise international scoring systems post or pre-MI to predict death or adverse outcome. Scoring systems demonstrate consideration of all factors contributing to cardiovascular health such as age, smoking status, Kilip class and HF status. The most common scoring systems are known as GRACE (Global Registry of Acute Coronary Events), TIMI

(Thrombolysis in Myocardial Infarction) and HEART (History, ECG, Age, Risk factors, Troponin). A depiction of the variables considered in each scoring algorithm is depicted in Table 1.1:

Variable		GRACE	HEART	TIMI
History	Age	X	X	X
	Doctors suspicion (opinion		X	
	Severe angina (≥2 events in the last 24hr)			X
	Aspirin use in last 7 days			X
	Kilip class	X		
Physical exam	Heart rate	X		
	Systolic BP	X		
ECG	ST deviation	X	X	X
	Repolarisation disorder, LBBB or pacemaker		X	
	Cardiac arrest at admission	X		
Biomarkers	Creatinine	X		
	Positive troponin or creatine kinase-MB	X	X	X
Risk factors	Atherosclerosis		X	
	CAD ≥50%			X
	Current smoker		X	X
	Diabetes mellitus		X	X
	Family history of CV disease		X	X
	Hypercholesterolemia		X	X
	Hypertension		X	X
	Obesity (BMI >30)		X	

***Table 1.1 – Popular cardiovascular risk score systems are unique in their combination of considered variables. Table** Adapted from Poldervaart et al. HEART and TIMI scoring has a bigger focus on risk factors in comparison to GRACE scoring.*

Clearly, there is diversity in the number of factors considered in scoring in addition to the factors themselves. In assessment of robustness and reliability, these scoring systems have been subject to review constantly since their publication and have demonstrated efficacy in

the prediction of risk to inform patient management. NICE guidelines published in NG185 and the ACFF/AHA guidelines for management of STEMI both suggest the use of a risk scoring algorithm during management decisions in STEMI/NSTEMI patients and specifically refer to GRACE scoring, inferring its popularity (ACCF/AHA Task Force on Practice Guidelines, 2017).

Recently, the use of GRACE scoring to predict specifically sudden cardiac arrest and sudden cardiac death longitudinally in 1,985 patients with MI, and found that just one SD increase in GRACE score was associated with 50% higher risk of sudden cardiac adverse events (Hautamäki, et al., 2024). However, there is disagreement in the comparative efficacy of all three risk scores. A research group based in University Medical Centre, Utrecht, has deemed GRACE scoring inferior to that of HEART and TIMI scoring, where AUC was calculated to be 0.73 (95% CI: 0.70-0.76%), 0.86 (95% CI: 0.84-0.88%) and 0.80 (95% CI: 0.78-0.83%) for GRACE, HEART and TIMI respectively (Poldervaart, et al., 2017) (Backus, et al., 2013).

In contrast, a far superior predictive value has been observed for GRACE scoring for 30-day mortality (AUC 0.87) in comparison to TIMI (AUC 0.60) in 1324 patients diagnosed with NSTE-ACS (non-ST elevation Acute Coronary Syndrome) (Schellings, et al., 2016). This was corroborated in a study that found GRACE scoring to be superior to TIMI in East Asian patients, which also introduces the question of whether these scoring systems are based on a wide variety of ethnic backgrounds (Yanqiao, Shen, Yutong, Linghong, & Ben, 2022). This topic has been investigated mainly with the GRACE system and has been found to have multiple cited incidences of ethnicity independence in risk stratification (Ogbu, Ayutyanont, Wilson, & Akhondi, 2023). However, there are also data in over 300,000 patients showing that GRACE overestimated risk in non-white ethnicities (Moledina, et al., 2022). Additionally, large cohorts

of Chinese, Malay, Indian and white patients having suffered MI found underestimation of risk in the Asian groups, which does not align with the findings of Yanqiao et al. (Chan, et al., 2011).

Risk stratification scoring for MACE is a routine practice in the UK but has never seen the addition of novel biomarkers to improve accuracy. Troponin alone cannot reflect the multiple pathologies that occur post MI including left ventricle strain, dilation or hypertrophy, but NT-proBNP as another popular cardiac biomarker is not released as a result of necrosis. Given that one of the scoring systems (HEART) even uses "doctor suspicion" as a factor in the algorithm shows propensity for flaw and bias, with room for expansion in the quantitative factors.

1.4 Suppression of tumorgenicity factor 2 (ST2)

Interleukin 1 receptor-like 1 (IL1RL1) is a 40kb gene, located on chromosome 2q21.1 in humans, that encodes the protein ST2 (Griesenauer & Paczesny, 2017). ST2 is part of the wider toll-like/interleukin-1 receptor-like (TL/IL-1) superfamily in which it shares 3 common leucine-rich immunoglobulin motifs with the IL-1 sub-group located on the extracellular domain of the protein (Kakkar & Lee, 2008). It exists in two predominant isoforms: as the transmembrane receptor (ST2L) and as a soluble, extracellular protein (sST2) (Ghali, et al., 2018) (Griesenauer & Paczesny, 2017). The ST2L isoform is cited to be fairly ubiquitous in humans, with expression identified in a variety of immune cells (macrophages, Th1 and Th2 lymphocytes, NK cells), as well as cardiomyocytes. The expression of sST2 is much more poorly defined. There is conflicting literature on the source of sST2 upregulation in the heart, with some citing that only endothelium and vascular cells provide combative expression of sST2 in response to myocardial stress (Brunetti, et al., 2023). Others suggest significant fibroblastic contribution to expression (Homsak & Gruson, 2020). This is juxtaposed with research

suggesting that highest cardiac source of sST2 mRNA expression was in cardiomyocytes and not at all in fibroblasts (Mildner, et al., 2010). It is entirely possible that injury mechanism dictates source of sST2 release, however this is understudied, and as a consequence, is one of the aims of this thesis to be later described in detail.

Between 1989 and 2005, ST2L was considered an orphan receptor until the discovery of its relationship with IL-33 initiated the next 20 years of research into sST2 in disease. It was subsequently elucidated through a variety of mechanistic investigations that the IL33-ST2L axis plays a vital role in the prevention of adverse remodelling of the heart (see Figure 1.3). This protective effect occurs upon the interaction of IL-33 (an alarmin) with ST2L, which is present in heterodimeric form with IL-1 Receptor Accessory Protein (IL-RAcP), to allow signalling via the adaptor protein MyD88 (Duchesne, Okoye, & Lacy, 2022). MyD88 acts to transduce signals from transmembrane proteins to the nucleus to promote transcription, and in the case of IL-33/ST2L, does so by further activating Interleukin-1 receptor-associated-kinase (IRAK4) and 9. After simultaneous IRAK 4 and 9 activation, TRAF6 is responsible for NF-κβ facilitation of inflammatory gene upregulation in the nucleus, mainly of chemokines and cytokines such as IL-5, IL-13 and MCP-1 (Duchesne, Okoye, & Lacy, 2022). Recuritment of macrophages and other immune cells, as a result of alarmin signalling, plays a role in preventing the progression of adverse tissue remodelling such as fibrosis and hypertrophy (Zhang & Dhalla, 2024). However, there is a biphasic contribution of many cytokines to cardiovascular health, where early release of immune modulating cytokines beneficially prevented pathogenesis, whereas in later phases, if continually released, they can have a negative effect. Cytokines can also be classed as pro-inflammatory, anti-inflammatory or both. For example, in the ST2L/IL-33 pathway, IL-13 is anti-inflammatory, and so there is a

disadvantage of IL-33-ST2L interception in instances of myocardial necrosis (Zhang & Dhalla, 2024).

This interceptive behaviour by decoying IL-33 is strongly associated with increased sST2 presence. By sequestering the ST2L binding site on IL-33 in the blood before interfacing the cell membrane, IL-33 is prevented from inducing the intracellular signalling detailed in the previous paragraph and thus, prevents the protection of the heart from irreversible damage (depicted in Figure 1.4).

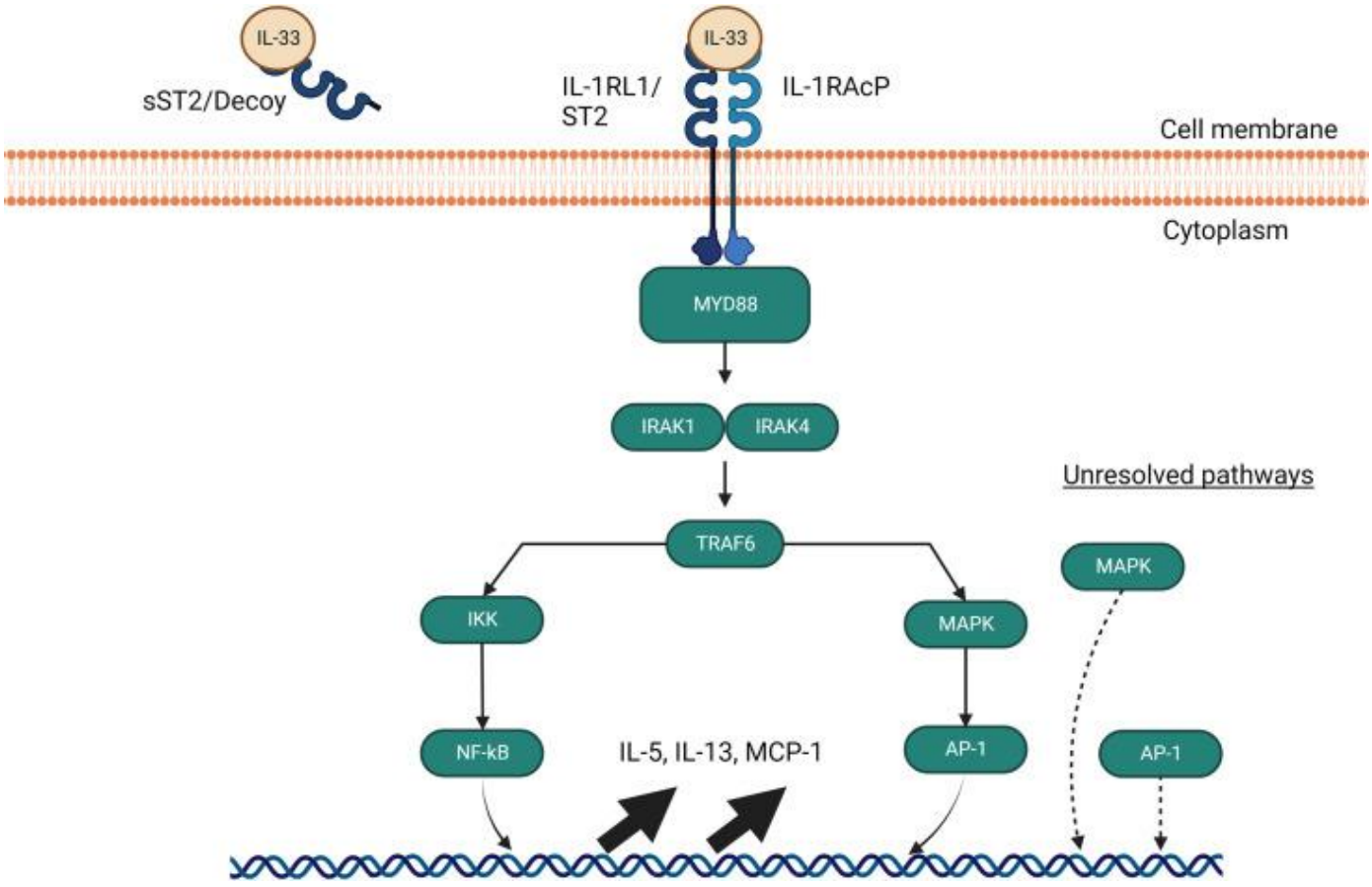

Figure 1.3 – IL-33 and ST2L interaction triggers downstream mediators of cytokinetic response to inflammation and injury. *When the decoy receptor, sST2 is serally present, IL-33 is sequestered from cell membrane interactions, rendering ST2L unable to participate in the upregulation of cardio-protective transcription factors. Figure produced by Duchesne et al., 2022.*

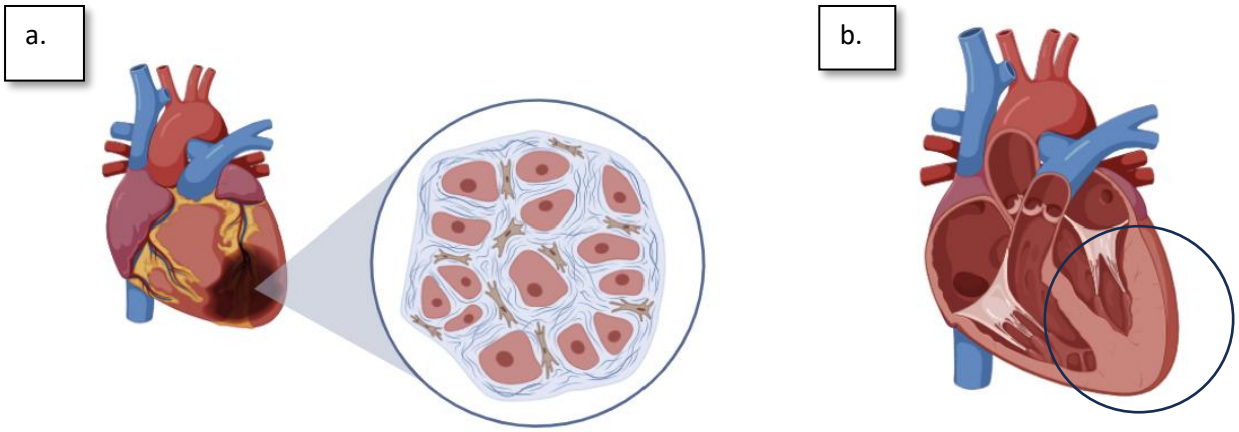

Figure 1.4 – Necrotic events in the myocardium (a) result in upregulated hypertrophic signalling and thickening of the left ventricle wall (b). *A visualisation of how ischaemia mediated necrosis initiates the formation of fibrotic tissue (a), as well as the remodelling of the left ventricle to become hypertrophic, where the hypertrophic wall is indicated with a circle (b). Figure produced using Biorender.*

Based on the type of injuries that observe hypertrophy such as ischaemia, myocardial stretch and chamber stress, it is plausible that sST2 release is multi-factoral, however its important to acknowledge that hypertrophy has multiple stimulators such as excessive Ca^{2+} signalling (Michael Attwaters, 2021). Overall, there is room for clarification of IL1RL1 expression drivers on the molecular and organ level, as well as isolating the source of circulating sST2. Despite unanswered questions, the serous presence of sST2 and the initial data available to demonstrate its physiological role makes for an attractive biomarker for heart disease in a clinical setting.

1.5 Hypothesised contribution of sST2 to MI diagnosis and risk management and thesis rationale

Given that heart disease is the number one cause of mortality worldwide, with MI being as prevalent as occurring in over 7 million people per year, there is an enormous drive to properly assess any novel contender for MI prevention, risk stratification and diagnosis (Piepoli, et al., 2016). Based on what is already known about sST2 and its molecular pathway leading to adverse remodelling, one could extrapolate its potential use in diagnostics/prognostics of heart disease. On a physiological level, if indeed sST2 is upregulated and serologically present in myocardial necrosis, measurements of the biomarker have the propensity to improve the personalisation of care of each MI patient, with the aim of preventing more deaths. If sST2 adds additional, physiologically unique information on top of currently quantified biomarkers, it could lead to personalised allocation of stronger interventions to those patients at greatest risk.

For example, if two patients diagnosed with NSTEMI had equal amounts of serous troponin, NT-proBNP, and a similar ECG profile, but one patient had higher sST2, clinicians may be inclined to implement stronger interventions/risk management to this patient, compared to a patient with lower sST2. This is highlighted in the previous section where current NICE guidelines do not recommend PCI or even angiography in the case of low risk NSTEMI (NICE: NG185, 2020). This contextualises the drawbacks of current risk scoring systems, that need to provide stronger predictive power. However, the question remains whether sST2 measurements could contribute to risk assessment for PCI and save lives as a result by preventing inappropriate under treatment of patients with ischaemia. This proposition of sST2 use is currently hypothetical, given the very small amount of data linking sST2 to MI thus far. Hence, this body of work is dedicated to elucidating a physiological link between the type of

injury observed with MI and circulating sST2 levels for its eventual application in modern medicine.

1.6 Literature review of sST2 relation to MI

1.6.1 Search strategy

To demonstrate the gap in the literature pertaining to this research, a literature review was conducted to quantify and evaluate clinical studies assessing measurement of sST2 in patients diagnosed with MI. The focus of this thesis is the application of sST2 measurements in humans with MI, and so the search was isolated in this way, however, for the purposes of exploring pathway and mechanism, papers exploring this in pre-clinical animal or cellular models will be described in section 1.5.4. Additionally, it was interesting to observe the trend in quantity of research undertaken to explore the link between ST2 and MI, and a simple search producing papers that included both of these terms up to the present day (19th February 2025) yielded an n of 929 results. The relationship between number of papers published and year is depicted in Figure 1.5:

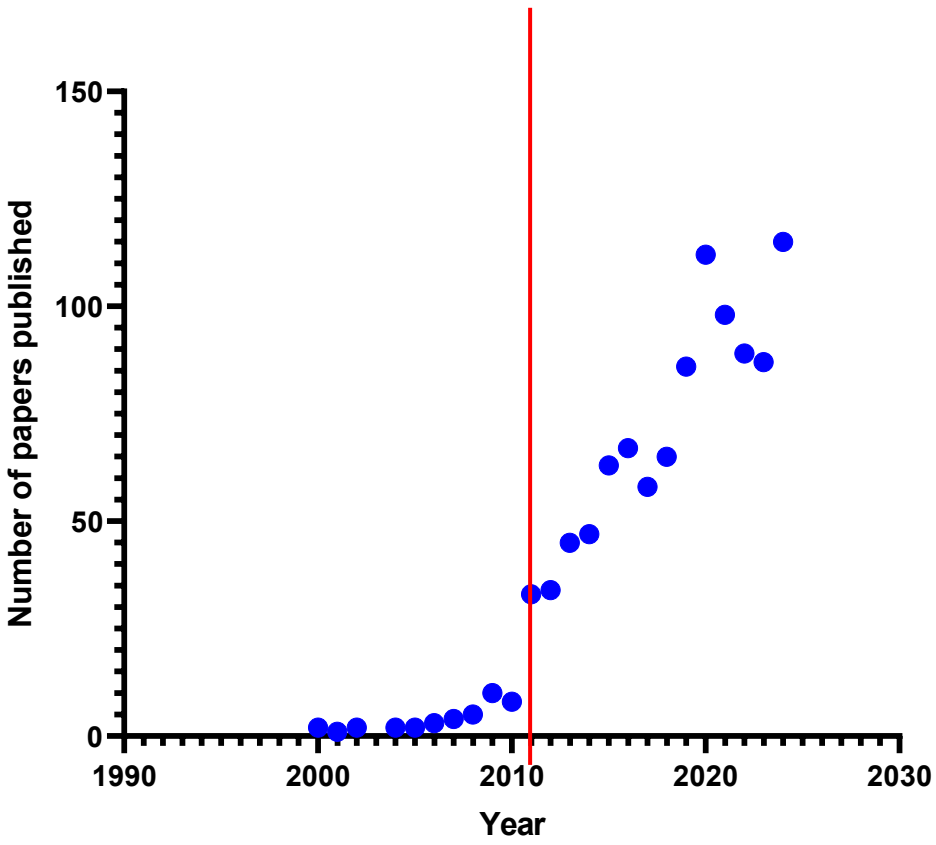

Figure 1.5 - Scientific interest in sST2 as a biomarker for MI increased exponentially after the Critical Care Diagnostics patent in 2008. *sST2 interest has steadily increased from 2000, with an exponential increase after discovery of its function as a decoy receptor in 2008. The red line demonstrates the time point in which the patent was filed for sST2 as a marker for cardiovascular disease, including but not exclusively MI.*

Clearly, there is an increasing interest in sST2 relation to MI injury since 2000 but this started to increase exponentially after further elucidation of its physiological function around 2008. Also relevant is the parallel commercial interest in sST2, which saw big investment upon the filing of a patent of sST2 as a biomarker in 2011 by Critical Care Diagnostics (International publication number WO 2011/127412 A2), marked by the red line in Figure 1.5. After the filing of this initial patent, more followed associating sST2 as a biomarker with outcome post-MI and as risk stratification for HF and other cardiovascular diseases.

The process of the literature review search terms and consolidation of papers is described in the flow chart (Figure 1.6) below:

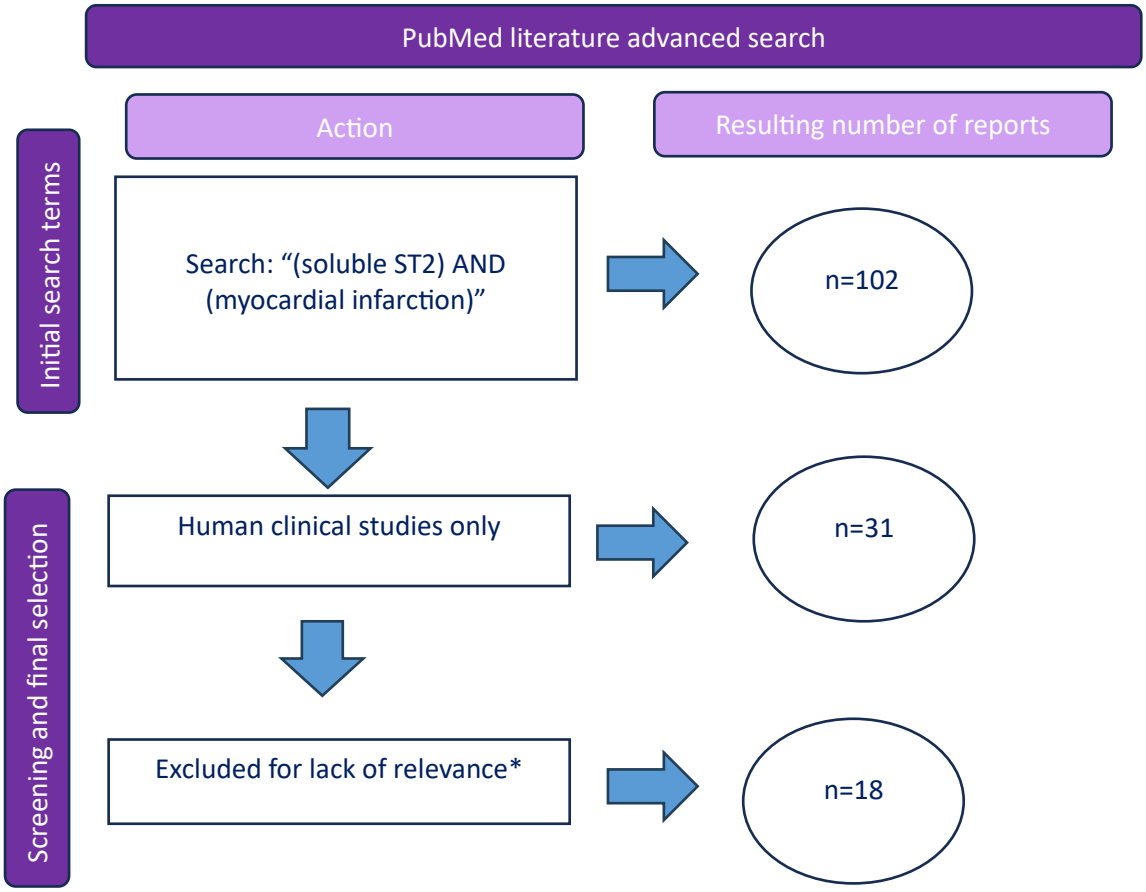

Figure 1.6 – A PubMed search for papers containing both phrases "soluble ST2" and "myocardial infarction produced 18 relevant results. *A third of papers identified in the initial search were of human clinical studies. *Reasons for exclusions" involved "ST2" being part of an ethics code, papers mentioning MI and sST2 in the introduction without being the focus of the paper, and sST2 being part of the title in references cited by the paper, without any mention of ST2 within the research.*

The literature review revealed several areas of interest for sST2 expression in humans with MI. Some papers investigated specific clinical outputs post MI such as left ventricular function recovery (Weir, et al., 2010) (Miñana, et al., 2018), whereas the vast majority characterised sST2 against MACE and cardiovascular death both within hospital and on discharge within various timepoints post MI. To systematically digest the literature review, studies can be separated into those that would support the hypothesis of this thesis (that sST2 is raised in MI in a severity dependent manner and is useful to measure alongside troponin)

and those that would alternatively support the null hypothesis (that sST2 is not raised in MI and therefore does not have use as a biomarker in this context).

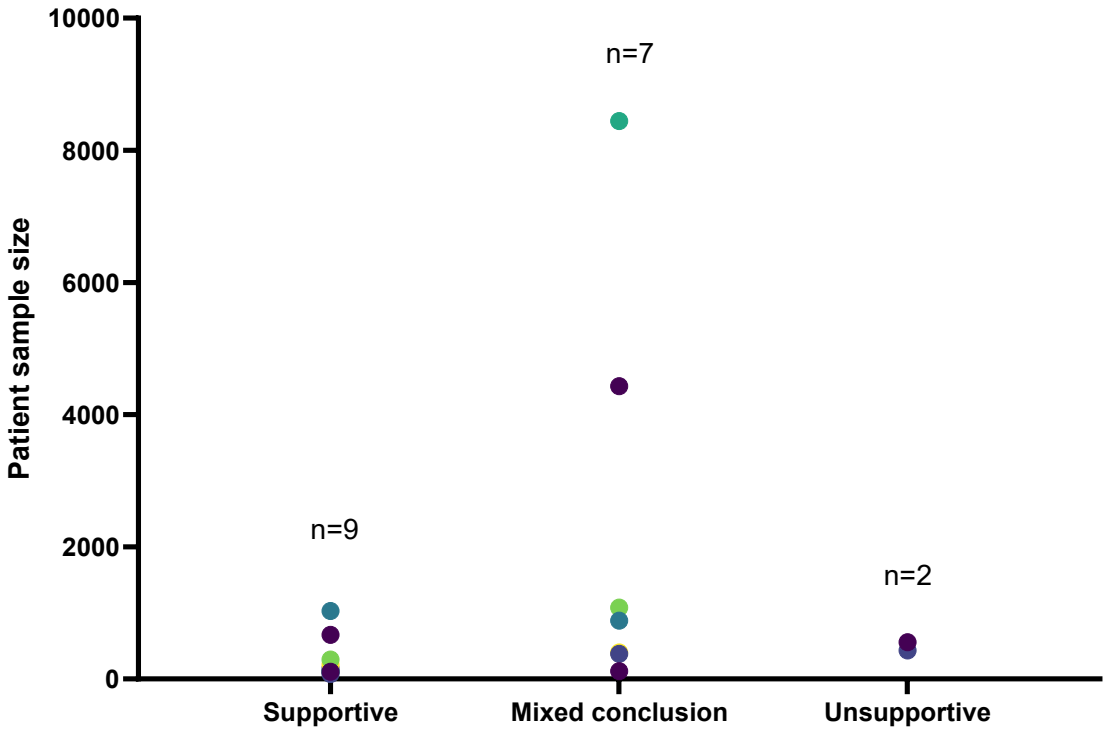

Figure 1.7 – There is no trend between study sample size and support for sST2 and its use for MI diagnosis or prognosis. *Small sample size could not be the reason for differing views on the efficacy of sST2 measurement in MI patients. Almost an equal number of papers supported or had mixed conclusions about sST2 in MI, reinforcing need for further elucidation in this area of cardiac physiology.*

Out of the 18 papers investigating the relation between sST2 and MI in humans, most papers were either supportive or mixed in regard to sST2 efficacy in a clinical setting. These papers were compared and tabulated in Appendix item F, Table 7.4, page 208-210. The above data were plotted for the observation of sample size in accordance with conclusion, and despite low n for the unsupportive group, it is clear that for mixed/ambiguous conclusions the average sample size was much higher, which may infer trustworthiness. Generally, studies with larger sample sizes are more likely to accurately represent the population and have tighter confidence intervals (Monti, Ambrogi, & Sardanelli, 2024). However, the paper with

the largest sample size (n=8444) in this analysis only observed sST2 ability to predict MI occurrence longitudinally in the general population, which is not the same disease cohort this thesis endeavours to evaluate. If this study was removed from Figure 1.7, the mean number of patients in studies are 307±325, 1216±1614 and 493±89 for supportive, mixed, and unsupportive groups, respectively. The second largest study sample size (n=4432) does find a benefit in sST2 predicting cardiovascular risk, however only investigated NSTE-ACS patients, which encompasses ECG negative ACS and MI patients and again, falls slightly outside the target cohort of exclusively MI (STEMI+NSTEMI) patients intended to be investigated in this work (O'Malley, et al., 2014). Of course, the literature review was not expected to yield studies with perfect alignment with the aims and methods of investigation intended for Chapter 4 of this thesis, however, points out that the existing studies with the largest sample sizes are some of the least relevant out of the 18-paper cohort. The lack of controlled studies with MI patients exclusive of unstable angina demonstrates an angle of pathophysiology yet to be properly investigated in the context of sST2.

1.6.2 Evidence in literature to support thesis hypothesis

Among the 18 papers resulting from a targeted PubMed literature search, 50% provide data that is wholly supportive of a use in measuring sST2 during acute MI diagnosis. In 2019, a study with 74 participants with MI saw that 78% of the cohort had sST2 levels raised above the clinical cutoff of 35ng/ml, with an additional observation that sST2 could independently predict MACE (Mzoughi, et al., 2019). Despite encouraging data, the sample size is a significant limitation in the confidence attributed to its conclusions. However, also in 2019, Liu et al. corroborated this finding in a larger sample size, where the highest quartile of sST2 readings in MI patients (total n=295, each quartile n=74) showed a significant (P=0.006) correlation

with MACE within one year of follow up. Having said that, another important contribution of this study is the observation that ROC analysis showed that despite sST2 correlating with MACE, it did not predict MACE more effectively than NT-proBNP or cTnI, even when in combination (Liu, et al., 2019). Other data describe relations between sST2 and anatomical maladaptations post-MI, which ultimately extrapolate to qualitative outcomes such as subsequent MI, HF or cardiac death. Miñana et al characterised several left ventricular remodelling manifestations using CMR where at even 1-week post-MI, sST2 was able to predict severity of LVEF. Again, sample size for this study was limited to 109 patients and when retrospectively calculated, did not have adequate power to associate sST2 with MI on a statistically significant level (Miñana, et al., 2018).

Aforementioned studies evaluating sST2 as a relative indicator of MI pathophysiology and its predictive power of outcome is essential in its advocation for measurement in suspected MI patients. However, equally critical is its separation from the effectiveness of current cardiac biomarkers (NT-proBNP, cTnI, cTnT) and the ability to demonstrate the additive power of sST2 measurement in a multi-marker approach. Despite being an older study, Dhillon et al. achieved a larger sample size (n=677) of patients with STEMI specifically, evaluating sST2 as a stand-alone biomarker but also in addition to NT-proBNP and GRACE scoring in its ability to predict re-infarction. It was observed that the combination of sST2 with GRACE scoring and NT-proBNP increased the c-statistic for 30-day mortality from 0.82 to 0.9, inferring a significant and distinct contribution of sST2 to current predictive power algorithms for MI patients (Dhillon, et al., 2013). This contradicts data from Liu et al., previously mentioned however Liu et al. reports on one year MACE in comparison to Dhillon et al.'s 30-day mortality. More recent research predicting mortality risk at 1 year after cardiogenic shock found that sST2 addition to GRACE scoring improved AUC from 0.75 to 0.84, however only 84% of the 219 patients had a

primary aetiology of MI (Hongisto, et al., 2021). In addition, cardiogenic shock is a secondary syndrome that has unknown implications for sST2 and involvement of inflammatory response.

Importantly, predicting adverse outcomes post-MI in the acute stages of disease presentation may lead to more rigorous interventions for those most at risk of MACE and prevent loss of life from a disease that continues to remain one of the top causes of death worldwide. Occurrences of MACE that result in both survival and death, as well as all-cause mortality require specific diagnosis distinction (i.e HF development, stroke, secondary MI) to appropriately attribute the source of any sST2 distribution, considering it's reported association with lung health in addition to the heart.

In the absence of a robust definition of sST2 half-life and release profile, it is of interest to observe sST2 changes over time in MI patients. In 2019, an observational study with 104 patients' biomarker data both 72 hours and 1 year post MI found that patients with significantly higher baseline levels of sST2 were more likely to develop HF after one year (Tymińska, et al., 2019). However, sST2 levels at one year did not correlate with outcome, suggesting that at this time point, the signalling pathway causing upregulation of sST2 is no longer activated by a disease process (Tymińska, et al., 2019). Despite their novel contribution to the field, this study lacks sample size, and an intermediate time point between immediately after MI and 1-year post-MI. One of the hypotheses of this thesis is that sST2 can be used in serial measurements to stratify risk and quantify damage, which is critical within the first month post-MI. This is not to suggest that sST2 cannot predict outcome when measured past this critical time frame, but with so much of its cellular origin unknown, one must first calculate precisely its window of utility.

An older study conducted in 2010 is the only clinical study (based on the literature search and extensive wider reading in the last 4 years) to have measured sST2 at multiple early time points post-ACS at 24, 48 and 72 hours (Eggers, et al., 2010). However, a significant limitation of this study which informs the intention of the work of this thesis is the lack of distinction between MI patients and those with unstable angina. Nevertheless, it was found that sST2 is increased in the serum of those with NSTE-ACS, however it could not independently predict outcomes when adjusted for the more well-established prognostic biomarker, NT-proBNP (Eggers, et al., 2010).

In summary, the initial experiments discovered in this literature review provide rationale for further investigation of sST2 in the context of MI, especially considering that there are currently very few clinical studies with statistically significant results in this area. If indeed sST2 is as useful for patient outcome as these data suggest, corroboration of this alongside the development of an applicable solution (experiments outlined in Chapter 2), could enable actionable improvements in this expansive area of cardiology.

1.6.3 Evidence in the literature contradictive of the thesis hypothesis

As is characteristic of novel experiments, the literature review also yielded studies that refute the use of sST2 measurements in MI. These are equally important to consider. Dhillon et al, a significant contributor of literature so far, published a separate paper on the efficacy of sST2 measurements in NSTEMI (as opposed to STEMI above) where they observed that in this aetiology, sST2 could not significantly contribute to NT-proBNP and GRACE scoring in the risk stratification of 30-day mortality (Dhillon, et al., 2011). Given that NSTEMI is less severe than STEMI, one could hypothesise that sST2 correlates with severity of vascular occlusion

and therefore MI, rendering sST2 useful but not raised in all MI patients. Subsequently, if this were true, it would be expected to observe a correlation between troponin and sST2, which is another relationship yet to be reliably established. Another interesting application of sST2 and predictive biomarkers in general, is the power of prediction of disease in healthy cohorts. One study with a large cohort (n=8444) of the healthy population of Finland is the only study to have extensively reviewed sST2 levels pre-cardiac event for the prediction of MACE. Here, the data showed an inability for sST2 to predict MACE (include MI), HF and death in those without CV disease, however, it was able to stratify risk of death in HF post diagnosis (Hughes, et al., 2014). This study does not support the use of sST2 as a routine CV risk screen in the healthy population, which is not necessarily completely unsupportive of the work of this thesis given that this work focuses on measurements post-MI. Despite that, the knowledge that sST2 is irrelevant for stratification of risk pre-MI provides context around its physiology and implies a stimulus-dependent nature to its release in serum.

Clearly, there is only a very small amount of research collecting sST2 levels from patients after MI, and some with very small sample sizes. sST2 as a cardiovascular biomarker is novel generally, but by comparison there are a total of 126 clinical studies associating sST2 with heart failure as opposed to the 18 for MI. The fact that multiple studies demonstrate unique contribution by sST2 to risk post-MI makes this an area that warrants further exploration.

1.6.4 Cell-based investigation of sST2 in MI-like injury

Investigative cell-based experiments are the foundation for data collection to allow the natural progression into human clinical studies. The most commonly used cardiomyocyte cell lines (H9c2, HL-1 and AC16) have only been utilised in studies investigating sST2 in 10 papers, 7 of which were published within the time frame of this research (2021-2025), showing the

subjects novelty. The information from these 10 papers in tabulated in Appendix item G, Table 7.5, page 211. Studies outside of cardiomyocyte expression of sST2 have been explored in 213 papers. This reveals a further gap in research exploring specifically cardiomyocyte expression of sST2 and the pathways activated in these cells pertaining to its release. In H9c2 cells, the relationship between the association of RND3 expression for sST2 signalling has been explored in the context of CM senescence, however not in an injury protocol (Wu, et al., 2024). There are two examples of the observation of sST2 expression as a result of hypoxic injury in H9c2 cells. One of these papers concluded a vital role of miR-128/SOX7 in the regulation of sST2 expression post-injury and the other promotes the use of Nicorandil™ in the alleviation of injury mediated by sST2 upregulation (Yang, et al., 2018) (Zheng, et al., 2022). A useful extrapolation of this work is the observed expression of sST2 in hypoxic injury to CMs, however the pathway leads to the alternative splicing of the soluble variant of ST2 remains unclear. Given the disagreement about which type of injury (HF or MI) promotes the greater upregulation of sST2 in humans, if at all, it would be useful to characterise the response of each injury and the relative activation of each component of the sST2 pathway.

1.6.5 Existing immunoassays for sST2

Adjacent to the main literature review, papers evaluating existing sST2 assays were also explored (see details in Table 1.2). There are other ELISA kits and lateral flow tests available that are not FDA approved and are designed for research purposes only, however, highlight the demand for well-performing assays in academia. Dieplinger and Mueller are the main contributing authors to the comparison of sST2 assays available on the market.

Author, Year published, PMID	Assay evaluated	Assay format	Number of samples tested	Main finding(s)
Dieplinger et al, 2009, 19699192	PRESAGE	ELISA	528	No significant difference in the performance of PRESAGE and MBL assays. However, did not test MI cohort, only HF and sepsis.
Mueller et al, 2012, 22743282	MBL	ELISA	45	When a sample was read with each assay, the resulting sST2 concentration reported was considerably different. Results should not be compared between assay methods, only within. Only used male participiants.
Dieplinger et al, 2015, 26483129	ASPECT-PLUS, MBL, PRESAGE	Lateral flow and ELISA	251	ASPECT-PLUS meets the analytical requirements for point of care testing and was comparable in performance to the FDA approved PRESAGE assay.
Hartopo, 2018, 30046467	ASPECT-PLUS	Lateral flow	95	In 95 patients with STEMI, sST2 predicted MACE (P=0.02)
Aurora et al, 2020, 32926842	Lab based (novel)	ELISA vs turbidimetric	721	Assays were equivalent in performance, however, only tested on patients with transient ischaemic attack, not MI.
Kim et al, 2023, 39076257	AFIAS, Ichroma, PRESAGE	Lateral flow and ELISA	420	The AFIAS and Ichroma point of care assays performed equivalent to the PRESAGE, without requiring a laboratory. Only tested HF patients.
Ye et al, 2023, 37649538	Pylon	Cyclic enhanced fluorescent immunoassay (automated)	240	This novel assay delivers a result in 10 mins with a repeatability CV of 6%, but does not state LoD/Loq.

Table 1.2 *– A summary of literature exploring the efficacy of existing sST2 assays*

1.7 Thesis hypotheses and aims

1.7.1 Hypotheses

Broadly speaking, the main hypothesis of this thesis was that sST2 is released in the bloodstream of patients suffering from MI, specifically because of molecular triggers involved in ischaemic pathology. Consequently, it was further hypothesised that sST2 can be used as a biomarker for MI, with potential for its use in risk stratification of MACE. However, as mentioned, elongating the time between patient presentation and MI diagnosis (and therefore, treatment) for the purpose of measuring biomarkers in addition to MI, defeats the purpose of preventing MACE. Therefore, it is also hypothesised that a cutting edge, duplex immunoassay that measures for cTnI and sST2 at the same time and within 30 minutes can be produced to overcome this practical obstacle.

1.7.2 Aims

To provide evidence to confirm or refute the above hypotheses, the work described in this thesis was designed to fulfil the following aims:

1. To produce the duplex assay for cTnI and sST2, meeting sensitivity and specificity requirements detailed in Chapter 2.
2. To characterise the release profile of sST2 *in vivo* post-MI.
3. To isolate the effect of ischaemic injury on sST2 expression on the cellular level (cardiomyocyte), and in turn, to consider both oxidative stress and HF-like injury on the IL-33/ST2L molecular pathway.
4. To evaluate levels of sST2 in a clinical cohort in relation to their matching cTnI levels.
5. To evaluate whether sST2 can predict reinfarction and HF.

2. The development of a human duplex assay for sST2 and cTnI

2.1 Introduction

2.1.1 Aim and hypothesis

The aim of this chapter was to evaluate the feasibility and attempt the development of an immunoassay that allows the simultaneous measurement of sST2 and cTnI (duplexed), using a single sample, with results that are validated and meet reasonable performance requirements. This assay would take form as an ELISA (enzyme linked immunosorbent assay) and should perform close or equal to industry standard by way of "time to result" (TTR), precision, Limit of detection (LoD) and linear range. These targets were quantitatively defined in section 2.1.4. The assay would require sufficient validation to build confidence in these limits and in the case of troponin, measurements were compared to a reference instrument: the Abbott Architect. The Abbott Architect is a commercial analyser that can perform immunoassays for many biomarkers, including cTnI. For the sST2 assay, there is no reference analyser available for measurement. Consideration of the assay performance in the desired matrix (plasma; EDTA or lithium heparin anticoagulants) must also be recognised and thoroughly assessed, alongside commercially available cardiac controls. The selection of matrix requirements is based on the current protocols for collecting blood from patients suspected of MI in Europe and the United States (in the UK, this recommendation is laid out in DG40, an NHS guideline published in August 2020). Adequate precision and reliability are also paramount assay performance parameters and will be realised using the aforementioned cardiac controls as well as sufficient repeats of clinical samples. This will particularly serve the second aim of this chapter, which is to produce an assay of high enough quality to utilise in a

clinical study for correlation analysis of MI diagnoses and MACE against sST2 levels. It is hypothesised that this is entirely possible, using novel assay development techniques and technology to differentiate markers. However, this chapter should be prefaced by stating that it would be overly optimistic to expect commercial grade performance with one scientist and 3 years of work. Instead, this chapter is an investigation into the feasibility of duplexing these biomarkers to a standard that can reliably differentiate and diagnose heart disease in a cohort of patients. However, the protocols developed should show commercial capability and promise given that additional finance and resource was provided for a continuation of the project. It is hypothesised that the assay resulting from this work could provide insight into MI risk stratification, with the additional measurement of sST2 to cTnI, beyond what is already ascertained in the biomarker workup in patients with acute heart disease.

2.1.2 Rationale

The only assay available for measurement of sST2 in humans is currently the Presage© assay supplied by Critical Care Diagnostics. This assay takes the form of a lab-based ELISA but has a TTR of 3 hours, which is an unacceptable length of time in acute situations of suspected MI. As explained, cardiac troponin is a firm member of the MI diagnostic criteria, so it is highly convenient to have any biomarkers of interest measured simultaneously, using the same sample, with results receival at the same time also. Contemporaneous measurements also control for any effects of age of sample on analyte integrity. This duplex solution for these biomarkers currently does not exist. If this thesis does reveal a clinical benefit in the measurement of sST2 alongside troponin, then this chapter will have already proven feasibility and protocol for hospitals to theoretically carry this out as soon as possible (given obvious caveats such as regulatory body approval). Multiplexed assays for biomarkers of acute disease have increased in popularity over the last decade of research in diagnostics, propelled further

by the outbreak of COVID-19. The pandemic shone the spotlight on the necessity for rapid diagnostics, and this chapter endeavours to address the need for innovation, specifically in heart disease.

2.1.3 Enzyme linked immunosorbent assay (ELISA)

This thesis relies on the concept of analyte detection by way of enzyme-mediated, light emitting or absorbing reactions proportional to analyte concentration. First discovered in the 1970's, several variations of ELISA exist today, including direct, sandwich and indirect ELISAs. Depictions of each assay type are made in Figure 2.1.1.

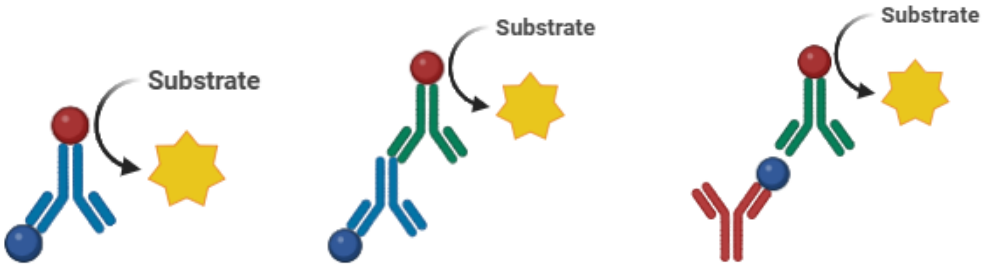

***Figure 2.1.1 - A diagrammatic visualisation of three different methods of ELISA**. Left to right: Direct, Indirect and Sandwich. The key is as follows: blue circle; analyte of interest, blue antibody; primary antibody, red circle: reporter, green antibody; secondary antibody, red antibody; coated capture. Image produced using BioRender.*

Each version of ELISA utilises an interaction between analyte, antibody, and a surface. Antigen may be coated to the surface of a well, for example in a 96 well plate, to be detected by labelled antibody incubated above it. In attempts to amplify signal, one may apply indirect ELISA protocol in which an anti-species labelled antibody is added after the incubation of the antibody specific to the analyte. Via identification of the Fc region of the IgG, the second anti-species antibody is able to associate a large amount of label required for substrate oxidation, removing the need for specificity in this step. Obviously, in cases where human or other animal

biological matrices are assayed for analyte, a direct or indirect ELISA approach is inappropriate, as it would be needlessly limiting to coat the entire protein content of that matrix into a well. Instead, a sandwich ELISA is commonly employed for the highly specific detection of analyte, using two or more specific antibodies with affinity for two or more non-competing epitopes. This type of assay is depicted in Figure 2.1.2 where the analyte is "sandwiched" between two specific antibodies targeting epitopes on opposite sides of the protein. Depending on protein folding and quaternary structure, antibody pairs for sandwich ELISAs will perform differently according to the amount of steric hinderance caused by targeting different epitopes on the target analyte.

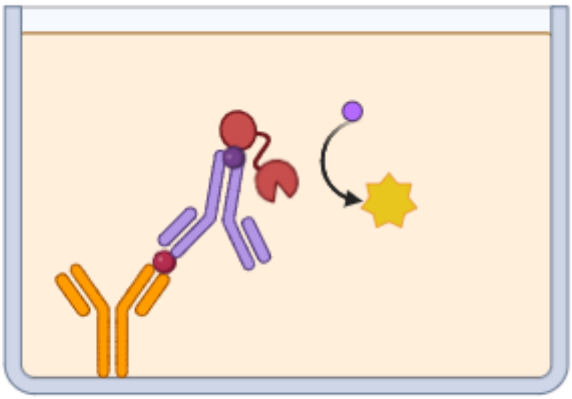

Figure 2.1.2 - A sandwich ELISA formation shown situated in a well of a 96 well plate. *Analyte (red circle) is captured by the primary antibody (orange), before being detected by a biotinylated secondary antibody (purple) and detected by a streptavidin conjugated reporter (two red circles) that enzymatically metabolises substrate to produce a light-related change. This can be light emitting (luminescence), a colour change for absorbance, or fluorescence. Image produced using BioRender.*

Another popular feature applied in ELISA, amongst other assays, is the significant inherent affinity of biotin to streptavidin, and the ability to conjugate both of these molecules to proteins and enzymes. Usually, biotin is conjugated to the detection antibody in sandwich

ELISA (referred to as biotinylation), whilst streptavidin is bound to a substrate activating enzyme, such as HRP. In diagnostics this is highly advantageous due to the fact that when detection antibody is exposed to the antibody-bound analyte, interactions occur extremely quickly (Bagai, et al., 2018).

2.1.4 Analytical performance targets and justification

In order to adequately fulfil the need for a rapid rule in/rule out MI screen, the duplex assay needs to be validated and rigorously tested against certain performance requirements. These parameters include LoQ, LoB, LoD, linearity, precision, TTR and sample volume requirement. The mathematical formula to determine these calculations is broken down in section 2.1.4.1. As for TTR, an appropriate comparator is the Abbott Architect assay, as mentioned in the introduction of this chapter. This analyser is a commonly chosen predicate device for FDA submission and validation due to its popularity across the US and Europe (Sherwood & Newby, 2014). The Abbott Architect assay currently has a run time of 16 minutes for high sensitivity troponin, with an additional minute required for NT-proBNP measurement. Therefore, to be remotely comparable to this analyser, TTR target is set at <30 mins. This would be a significant improvement compared to the current 3-hour ELISA kit produce by Critical Care Diagnostics for sST2. 250µL of plasma sample is sufficient for troponin measurement on the Abbot Architect with an additional 50µL required for an NT-proBNP measurement on top. For a 96 well plate ELISA, well capacity is capped at 300µL; less if the plate is shaking during incubations. For this reason, it is guaranteed that if development is successful, this assay will beat the Architect on sample volume and will only require a single volume for both cTnI and sST2 measurement.

The disclosed linearity limit of the Architect is set at 50,000ng/L, a target that this assay endeavours to achieve, however, realistically, the only clinically relevant cutoff for troponin is

set at the 99th percentile. This is the upper measurement of troponin detected in 99% of the healthy population, which is defined according to each diagnostic test. For example, one study defined 99th percentile as around 29.7ng/L for men, and 22.4ng/L for women (Mullins & Christenson, 2020). Another study found the Abbott Architect 99th percentile to be 15.6ng/L for women and 34.2ng/L for men, demonstrating some level of variability between populations and gender (Bagai, et al., 2018).

Considering that MI diagnosis is heavily dependent on the delta of troponin measurements after presentation to an emergency department, sensitivity around the 99th percentile is paramount. The important aspect to consider is at what point of troponin level would course of treatment differ. To contextualise, this, if the assay is not sensitive in lower ranges of troponin (e.g. 0-100ng/L), a delta of say, 30ng/L to 80ng/L, would not be realised, and so MI could be ruled out inappropriately. The introduction of high sensitivity troponin assays to diagnostics is an increasingly competitive field and one that this assay does not intend to match. The Abbott Architect LoQ is stated to be 3.5ng/L, with an LoD of 1.7ng/L. The purpose of this duplex development is not to replicate this level of sensitivity, but to assess troponin readings in those with MI, who, if suffer from this cardiac event, will have significantly higher troponin levels than the Architect LoD. Therefore, the target LoD target set for the duplex is 10ng/L. This is thought to be sufficient, accounting for reasonable error, to differentiate the 99th percentile of the population as assumed by previous studies quantifying the 99th percentile around 20ng/L (Bagai, et al., 2018) (Mullins & Christenson, 2020).

2.1.4.1 LoQ, LoB and LoD

The Clinical and Laboratory Standards Institute (CLSI), an FDA recommended organisation for the definition of verification standards, describes a methodology for the

determination of LoQ, LoB and LoD in their guideline titled EP17. A graph from this guideline is shown below in Figure 2.1.3 for the mathematical depiction of each of the three limits.

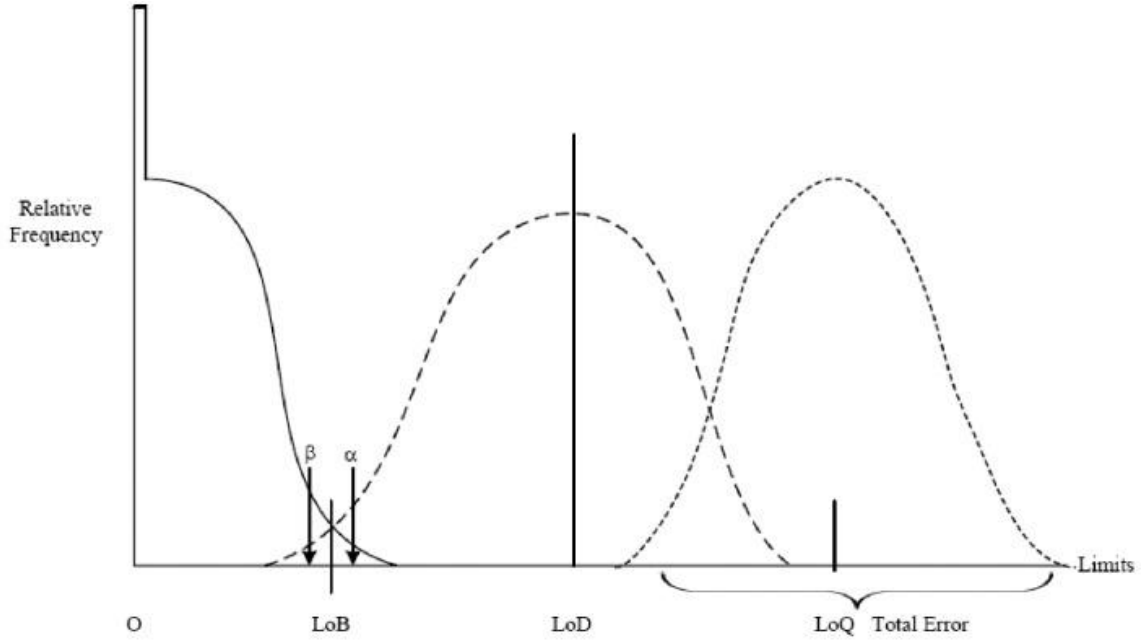

Figure 2.1.3 - A graphical demonstration, taken from the CLSI document EP17, of 3 important mathematical limits in assay development: LoB, LoD and LoQ. *Alpha and Beta type error are also highlighted around the LoB.*

LoD defines the lowest amount of analyte, within the capability of the assay, that can be robustly distinguished from the LoB. Alpha type I error describes the 5% of samples (1.645 SD) that will be incorrectly defined as containing analyte, when they are actually blanks, and a beta type II error denotes the opposite, whereby samples are assigned as blank when analyte is actually present. LoD calculations are further influenced by the number of replicates, gaussian distribution and CV (coefficient of variation). For example, a poor CV may cause the LoD to become worse (higher) due to uncertainty of the signal produced at the blank and the low concentration. The calculation for LoD is:

$$LoD = LoB + 1.645(SD\ of\ low\ concentration\ sample)$$

The LoB, defined by CLSI, is the highest apparent amount of analyte measured in a sample that is known to contain no analyte. This technically describes the degree of false positivity found in a validated blank calibrator matrix. It is paramount that the LoB (which is always more than 0) is lower than any clinically relevant cutoff value in a diagnostic immunoassay. The equation for LoB is as follows:

$$LoB = mean\ blank + 1.645(SD\ blank)$$

To enable LoD and LoB determination, raw assay signal is to be interpolated from a standard curve. Simply, this describes a range of analyte concentrations that are "spiked" at nominally assigned levels, usually in the form of recombinant protein, into a matrix that behaves equally to the target matrix. To be considered as "behaving equally", the standard curve matrix must exhibit the same degree of matrix effects (a term unpacked in section 2.3.2) as the target matrix. If a reproducible calibrator matrix cannot meet this requirement, standard curves can be run in the same matrix as the matrix of intended use (e.g. human plasma). In industry, it is required to formulate a matrix more reproducible than human plasma, but for the scope and purpose of this project, this is not required.

Most commonly in assays where analyte is measured, particularly in very small and very large amounts, a 4PL non-linear regression model is preferred due to the likely 'S' shape of the standard curve. This 'S' shape is exhibited at very low and very high concentrations, where measurements are outside of the linear range. Sometimes, in assay development experiments, a simple linear regression model is sufficient for fitting data points where there are fewer points in the standard curve and linearity is statistically confirmed. In cases where a decision must be made on the type of fit, or to evaluate the goodness of fit, a regression sum

of squares calculation can be made on the model. The equation below denotes the rearrangement of a 4PL regression to solve for χ (concentration), where A = theoretical response at zero concentration, B = slope factor, C = mid-range concentration (inflection point) and D = theoretical response at infinite concentration, as a demonstration of the interpolation method used throughout this thesis.

$$\chi = C\left(\frac{\mathrm{A} - D}{\gamma - D}\right) - 1^{\left(\frac{1}{\mathrm{B}}\right)}$$

Finally, the LoQ describes the ability of the assay in question to reliably measure, according to the restraints of predetermined limits of precision, the lowest possible amount of analyte. The LoQ can usually equal to the LoD, as long as the LoD meets these requirements.

2.2 Materials and methods

2.2.1 General assay materials

For optical density measurements, clear high binding MaxiSorp® 96 well plates (ThermoFisher – 442404) were purchased. For buffer preparations, the following components were purchased: PBS tablets (Merck - P4417), TBS concentrate (ThermoFisher - 28358), calcium chloride (Merck - 223506), magnesium chloride (Merck - M8266), Tween-20 (Fisher – BP337), Bovine serum albumin (Sigma – A3294). All (proprietary) troponin antibodies were supplied by Osler Diagnostics, as well as the polyHRP. sST2 antibodies were purchased from Hytest. For temperature-controlled incubation at 40 degrees, an orbital shaker and climate incubator was used for incubation steps. For antigen, three materials were trialled for cTnI detection including IC complex from Hytest (8ICR3), RayBiotech recombinant cTnI (227-

20168), and pooled plasma of donors with high native troponin measurements. For sST2, Hytest recombinant sST2 (8STR4) was used for calibration curves.

2.2.2 Fluorescence assay materials

Black high-adsorption 96 well plates (ThermoFisher – 437111) were used for fluorescent assays with streptavidin Q-dot800 for detection with anti-sST2 antibody. Fluorescent detection was only used for detection of sST2.

2.2.3 Chemiluminescence assay materials

The same black high-adsorption 96 well plates (ThermoFisher – 437111) were used for chemiluminescent measurements as for fluorescence (enabling simultaneous fluorescent and chemiluminescent measurements). Streptavidin PolyHRP supplied by Osler Diagnostics was used in detection solution containing biotinylated antibody for catalysis of luminol at the reading step. Luminol materials were trialled for sensitivity and consisted of the following products: 1) Custom luminol formulation – Neogen 2) SuperSignal Femto – ThermoFisher, 3) SuperSignal Atto - ThermoFisher, 4) SuperSignal Pico, 5) K-blue – Neogen.

2.2.4 Antibody biotinylations

To start, an NHS-SS (N-hydroxysulfosuccinimide disulfide) conjugation chemistry was used due to the availability of reagents and ease of protocol. This method of biotinylation utilises the lysine residues on the Fc region parallel to the disulfide bridge in the hinge region of the antibody. The biotin provided in the kit also provides a spacer arm to increase steric

favourability and access of the biotin to streptavidin-HRP, theoretically increasing sensitivity of the assay (see Figure 2.1.4).

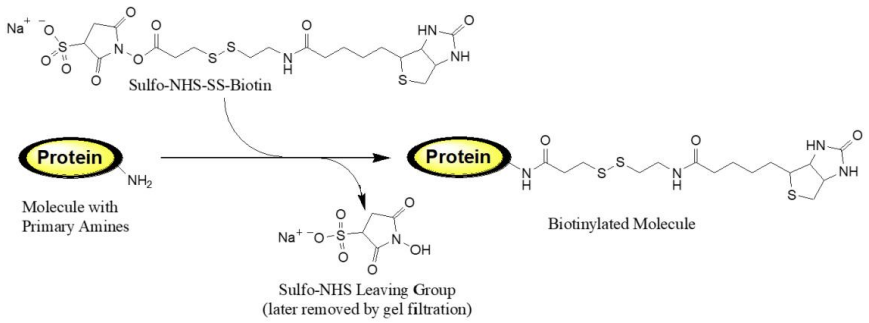

Figure 2.1.4 - An image taken from the Thermo Fisher NHS-SS biotinylation protocol showing the targeting of primary amines for biotin attachment via sulfo-NHS-SS-biotin.

Eventually, another biotinylation technique was applied that involves splitting the detection antibody in half down the disulfide bridge, then utilising the exposed thiol groups to attach biotin with a long linker arm (PEG-11). The reduction of the antibody to two halves further decreases the likelihood of reaction-limiting steric hindrance, allowing surface area and incubation kinetics to increase, giving superior sensitivity. A depiction of this conjugation chemistry is seen below in Figure 2.1.5 and was subsequently carried out for the final assay conditions for improved sensitivity.

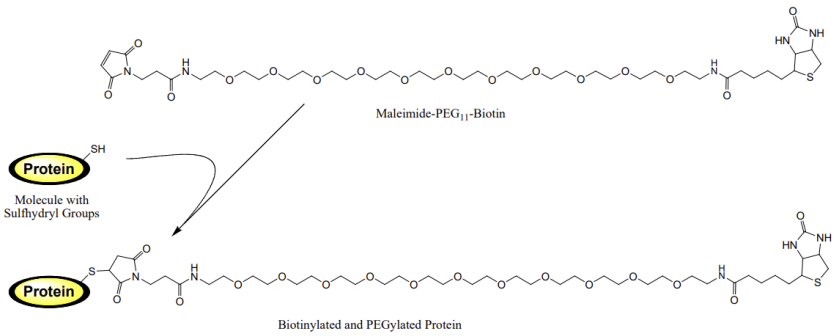

Figure 2.1.5 – The biotin reaction scheme taken from Thermo Fisher product 21911, showing the attachment of PEG-11 biotin to a protein with exposed sulfhydryl groups. *Exposure of sulfhydryl groups occurs as a result of antibody cleavage by 2-MEA.*

2.2.5 Single plex assay method

In the interest of clarity, the development of the duplex assay first involved the development of optimal assays in single plex format, until duplexing was later attempted, as described in the latter parts of this chapter. Conditions for running all variants of the assays attributed to producing data are captured in this section (2.2.5) and section 2.2.6.

2.2.5.1 Antibody screening

Anti-sST2 and anti-troponin I antibodies were obtained from Osler Diagnostics through Hytest for screening. The screening exercise in 96 well plate format resembled a checkerboard, whereby every antibody was trialled as a capture (coated to the surface of the well), and also conjugated with biotin to use as a detection antibody with streptavidin-polyHRP. All antibodies were coated in either PBS or bicarbonate buffer to determine whether coating performance was dependent on pH. Concentration of antibody coated ranged from 80µg/ml down to 5µg/ml. A positive sample containing a large amount of analyte (500ng/L for troponin and 300ng/ml for sST2) and a negative (blank) sample was used to determine signal to background ratio. Detection antibody concentration was also titrated in a 90 degrees direction to capture antibody. A depiction of one of these 96 well plates is detailed below in figure 2.1.6:

			Capture antibody concentration / ug/ml											
			80	40	20	10	5	0	80	40	20	10	5	0
Detection antibody and HRP concentration / ug/ml			1	2	3	4	5	6	7	8	9	10	11	12
2	Positive sample	A	PBS coat						Bicarb coat					
1		B												
0.5		C												
0		D												
2	Negative sample	E												
1		F												
0.5		G												
0		H												

Figure 2.1.6 – An example of 96 well plate layout for antibody screening exercises. *All antibodies are trialled as capture and detection. Capture antibody was titrated in a horizontal fashion, repeating twice for each half of the plate. Detection antibody was titrated vertically, again repeating for each half of the plate to allow for two different samples (one positive for analyte, one negative) to be measured.*

An incubation time of 20 minutes was selected initially for screening, and the sample matrix and detection diluent consisted of PBS-T 0.1% with 5% BSA. 50µL of sample was added to the well immediately before 50µL of detection solution, commencing the 20-minute incubation. Absorbance was read at a wavelength of 450nm to quantify signal from each well. Quality of antibody pair performance was quantified by signal/background ratio, indicating sensitivity. This was calculated for every combination of capture and detection antibody concentration. Proceeding this screening exercise, standard curves were run for the best few antibody pairs to characterise performance across a range of analyte concentrations.

2.2.5.2 Cardiac troponin I

40µg/ml capture antibody was coated on a 96 well plate for one hour at room temperature, with lid fastened. After one hour, the antibody was tapped out of the plate into a bin, before tapping dry on a paper towel. Four washes of PBS-T 0.1% were conducted using a volume of 100µL wash per well. These were subsequently tapped out each time as described previously. 300µL of blocking solution was then added to each well, the lid was fastened again, and the plate agitated at 100rpm, room temperature for at least 30 minutes. Only when the plate was ready to be used for an experiment, should the blocking solution be tapped out.

When ready to conduct the experiment, 50µL of neat plasma sample was added to each well, followed immediately by 50µL troponin detection solution. This detection solution consisted of 2µg/ml antibody and 2µg/ml PolyHRP. The plate was incubated for 15 minutes at room temperature, at 450rpm on an orbital shaker, again with the lid fastened. After incubation, the plate was tapped dry, and 100µL wash solution (PBS-T 0.1%) was again added to the plate 4 times. After the final wash, if measuring optical density, 100µL of TMB is added to each well for 2 minutes, shaking at 450rpm, room temperature. Immediately after 2

minutes is up, 100µL sulfuric acid is added to each well to stop the reaction. The plate was then read at a wavelength of 450nm. In the case of a chemiluminescent reading, instead of TMB, 100µL of luminol is added to each well. After 2 minutes exactly, the plate was read optically.

2.2.5.3 sST2

In the sST2 assay, 5µg/ml capture antibody was coated, using the same procedure as the troponin assay for coating temperature, time, washing and blocking conditions. When plating up, 12.5µL neat plasma sample was added to each well, followed immediately by 62.5µL detection diluent. ST2 detection antibody was added at 1µg/ml, with single HRP added at 10µg/ml. Incubation occurs for 15 minutes at room temperature, 450rpm, with lid fastened. After this incubation was up, the rest of the protocol exactly follows the troponin protocol described in 2.2.5.2.

2.2.6 Duplex assay method

As a result of all the findings made in this chapter, the final duplex assay conditions were established to be as follows. 40µg/ml ST2 capture antibody, and 20µg/ml troponin capture antibody are diluted in PBS, then were co-coated in each well of a black 96 well plate. This was coated for one hour at room temperature. After one hour, four washes of 100µL of PBS-T 0.1% were performed, tapping the plate out after each wash. 300µL of blocking solution is added to each well and gently agitated at 100rpm at room temperature for at least 30 minutes. When reagents are ready for assay conduction, 50µL of diluted plasma sample (1:2 ratio in assay diluent) was added to each well, followed immediately by 50µL sST2 detection solution (1µg/ml detection antibody and 1 in 500 dilution of Qdot 800). If using spiked samples, both cTnI and sST2 should be spiked into the same sample. The assay is then incubated at 40 degrees for 20 minutes, at 450rpm. After the incubation, the plate is washed

4 times with 100µL PBS-T 0.1%. After washing, 100µL of troponin detection solution (1.5µg/ml detection antibody and 1.5µg/ml PolyHRP) was added to each well, and incubated in the same way for a further 10 minutes. After this step, another 4 washes are conducted. Finally, 50µL wash buffer is added to each well and the plate is immediately measured for fluorescence. Measurements for fluorescence were read at an excitation peak of 300nm and an emission peak of 792nm. Subsequently, the buffer should be tapped out, and luminol immediately added for exactly 2 minutes, after which the chemiluminescence can be read. The fluorescence reading will refer to the sST2 concentration, and the chemiluminescence reading will refer to the cTnI concentration.

2.3 Results

2.3.1 Selection of antibodies

As detailed in methods section 2.2.5.1, a screening exercise comparing signal to background ratios was performed to select optimal antibody pairs to proceed with development. Figure 2.1.7 denotes the best signal/background ratios for each pair combination at their most optimal concentrations.

		Capture		
		cTnI.3	cTnI.2	cTnI.1
Detection	cTnI.3		19.33	51.74
	cTnI.2	11.01		1.78
	cTnI.1	26.69	7.92	

		Capture		
		S103	S215	S501
Detection	S103		67.7	59.2
	S215	31		44.54
	S501	52.7	68.96	

Figure 2.1.7 – Tables to show, by colour conditional formatting, the size of signal to background ratios when antibodies are screened as both capture and detection antibodies. *Optical absorbance was measured in units of optical density, before dividing the signal from the positive spike by the background. Here shows only the best signal to background ratios of concentrations picked from a titration of each pair combination.*

For cTnI, this was 40µg/ml troponin capture antibody 1 with 2µg/ml detection antibody 3 and 2µg/ml polymer HRP. For ST2, this was 5µg/ml S215 with 1µg/ml S103 and 10µg/ml single HRP. Only one antibody pair for troponin gave performance significantly better than any other pair, clone 1 and 3, and so only this pair was run with standard curves. Unfortunately, the performance of the troponin pair significantly decreased to no sensitivity at all when moving from buffer to plasma (Figure 2.1.9), which is unsurprising given the relatively small size of troponin (24kDa) in comparison to a complex matrix of human proteins. It is expected that the kinetic efficiency of assay sandwich formation is hindered by the presence of a large amount of passive interferents. This phenomenon is described in the following section.

2.3.2 Matrix effects assessment

"Matrix effects" describes the negative influence of sample components on the performance of an assay by kinetic limitation. In ELISA for diagnostics, samples consist of different bodily fluids such as whole blood, plasma, urine and saliva. Biological factors within these samples, such as proteins, endogenous antibodies and lipids can interfere with the specific detection of target analyte. This may happen by sequestering binding sites on the antigen or the antibody, therefore preventing measurable interactions. Alternatively, in the absence of NSB (non-specific binding), matrix components may just physically interfere with the kinetics of the assay by being so abundant and large in comparison to antibody/analyte. Consequently, assays with neat, complex matrices often require longer incubation times in comparison to those with simpler matrices. However, with longer incubation time also comes the increase of all interactions, including NSB, and so it is important to find a balance between maximising the capture of analyte (which should occur more quickly than NSB), and not incubating for too long that would allow the lower affinity interactions to increase the

background signal measured. An example of matrix effects can be seen in Figure 2.1.8, where the standard curves were run in both calf plasma and PBS-T with 5% BSA. It was important in this early stage of screening and during pair selection, that performance was assessed in both a complex and simple matrix to determine the resilience of antibody pair performance to matrix factors. As shown in Figure 2.1.8, it was evident that the S215-S103 pair was preferable over S215-S501 due to the minimal difference in performance between matrices.

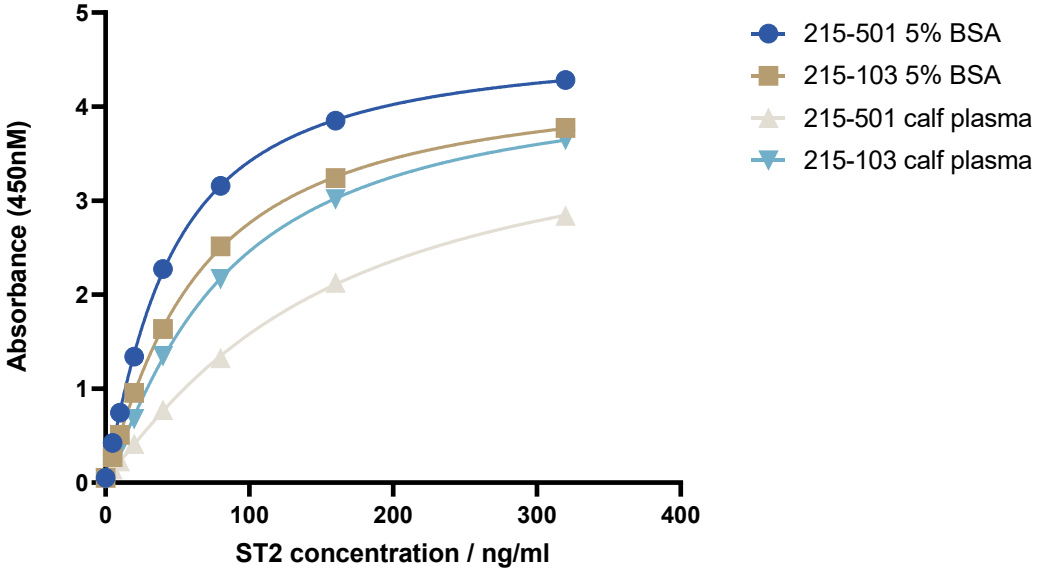

Figure 2.1.8 – Standard curves in PBS-T 0.1% or calf plasma as matrix to show sensitivity and linearity of the two best antibody pairs identified in Figure 2.5. *One pair is depicted by squares, and the other by circles. Each point is n=1.*

Unlike sST2, the initial screen of matrix effects with the best troponin pair demonstrated significant and disadvantageous matrix effects when moving from buffer to plasma (see Figure 2.1.9). The exact conditions were repeated a second time with fresh reagents and the result was exactly replicated. There was no sensitivity in detection of up to 1000ng/L troponin when spiked into calf plasma, however concentrations as low as 100ng/L were clearly distinguished in 5% BSA.

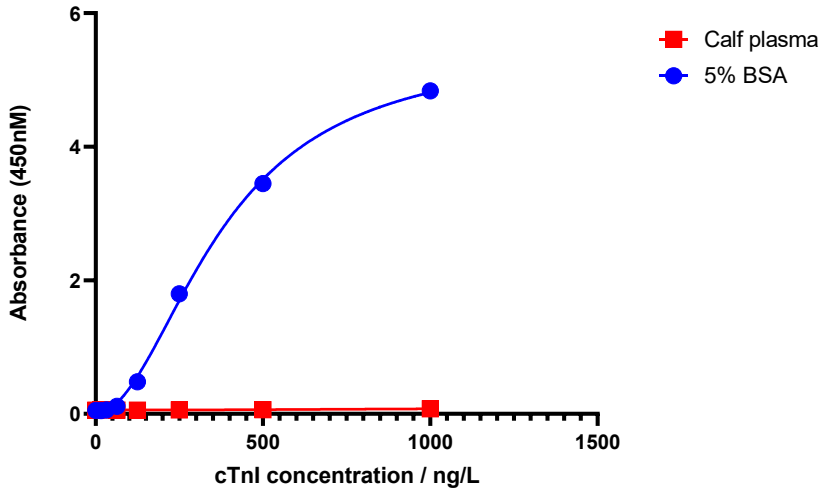

Figure 2.1.9 – Matrix effects present in calf plasma prevents sensitivity and cTnI detection up to 1000ng/L. *4PL regressions to show slope of the best troponin antibody pair from screening in both 5% BSA and calf plasma matrices. Each point is n=1.*

Based on the extent of vulnerability of the troponin antibody pairs to plasma proteins, significant alterations to the assay protocol were required. First to assess was the method of analyte detection by optical measurement type, as explored in the next section.

2.4 Assay detection method

2.4.1 Optical density vs chemiluminescence

During the screening phase of this assay development, analyte detection was measured using optical absorbance measurements, whereby light is passed through the oxidised substrate (in this case, TMB), to measure the ratio of light projected onto the sample, and the amount of light that passes through. This is known as optical density, The more optically dense the sample, the more light absorbed and therefore the less transmitted, indicating higher concentrations of analyte. The colour intensity of the sample depends on the turnover of TMB, which increases proportionally with sandwich assay formation.

In an attempt to improve the performance of the troponin assay, chemiluminescence-based detection was trialled, which has a reputation for superior sensitivity in comparison to optical density measurements. This technology requires the emission of light from a sample, rather than the absorbance of it, and uses a luminol based substrate to induce oxidation catalysed by HRP. Instruments measuring optical density are capped at an upper limit of 4, whereby 1, 2, 3 and 4 optical density allows for 10%, 1%, 0.1% and 0.01% of light to be transmitted through a sample, respectively. At the upper limits of optical density, single photons are being measured which can introduce a significant amount of imprecision.

By comparison, chemiluminescent technology has the capacity for a much larger dynamic range, and results are given as absolute numbers rather than a ratio. Below, Figure 2.2.1 shows a direct comparison of both measurement systems, using the same reagents except for the final oxidation-inducing substrate.

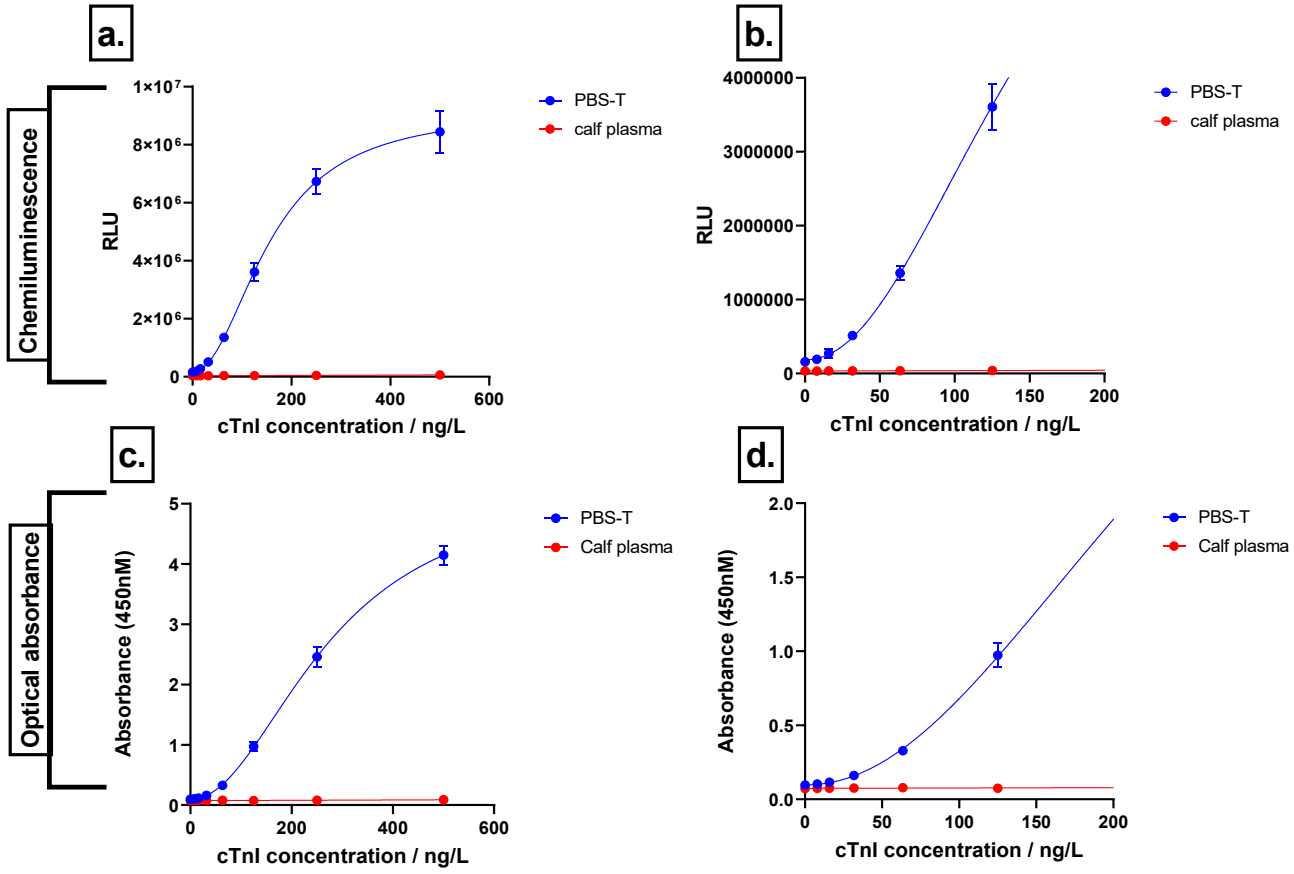

Figure 2.2.1 – 4PL plots to show sensitivity of the troponin assay in PBS-T and calf plasma in a chemiluminescent format (a and b) and optical absorbance (c and d). *b and d are plots with finer resolutions of the standard curves shown in a and c. Sensitivity in chemiluminescent format is superior to optical absorbance/density measurements. SD error bars for each concentration represent n=6.*

A simple division of background signal by specific signal at 125ng/L was made and showed increased magnitude using chemiluminescence detection as opposed to optical density. This was calculated to be 22.70 RLU and 10.05 RLU, respectively. However, as depicted, it did not solve the issue of using a plasma matrix in comparison to a cleaner buffer matrix, indicating that despite sensitivity advances in performance, there was much more work to be done with regards to matrix compatibility.

2.4.2 Biotin conjugation chemistries

It was at this point in development, after the initial screening exercise described in part 2.3.1 of this chapter, that a new antibody pair was made available for screening for the troponin assay. Given the poor performance so far, despite the change from optical density to chemiluminescence, this clone was optimistically screened immediately, and in human EDTA pooled plasma, the target matrix, to save time comparing matrices.

		Capture antibody concentration (ug/ml)											
		PBS						Bicarb					
		80	40	20	10	5	0	80	40	20	10	5	0
Detection antibody and HRP concentration (ug/ml)	4	148734	147320	125930	97536	68350	-11	123036	107934	91556	68910	51028.6	292.2
	2	151560	147740	125508	96694	67698	124.8	126242	107376	90522	68094	49049.8	49.8
	1	115060	112640	97380	79166	59510	52.52	117826	103912	82996	64151.4	48663.2	42.1
	0	15.02	-10.064	1.858	6.6632	0.1594	-7.5816	0.0606	-1.4904	1.526	0.0286	0.0858	0.016

Figure 2.2.2 – The optimal conditions for cTnI assay sensitivity were 40µg/ml capture antibody with 2µg/ml detection antibody and 2µg/ml polyHRP. *A table to depict slope (y2-y1)/(x2-x1), with slope increasing from red to green, where the most green indicates the highest slope (indicating higher sensitivity).*

When compared to previous slope data for the current troponin antibody pair, the new pair seemed extremely promising. Signal to background ratio was at 8.29 for this pair, in human EDTA plasma. Despite being incomparable to previous signal to background data as a result of different matrices used, detection of troponin was previously unachievable in calf plasma, let alone human plasma, and so it was logical to continue with assessment of this pair. The above sensitivity data, however, was calculated using a 500ng/L sample and a blank, so a subsequent ELISA was performed with a range of troponin levels to better characterise slope and linearity. This assay was also performed in human EDTA pooled plasma. These data are shown below in Figure 2.2.3:

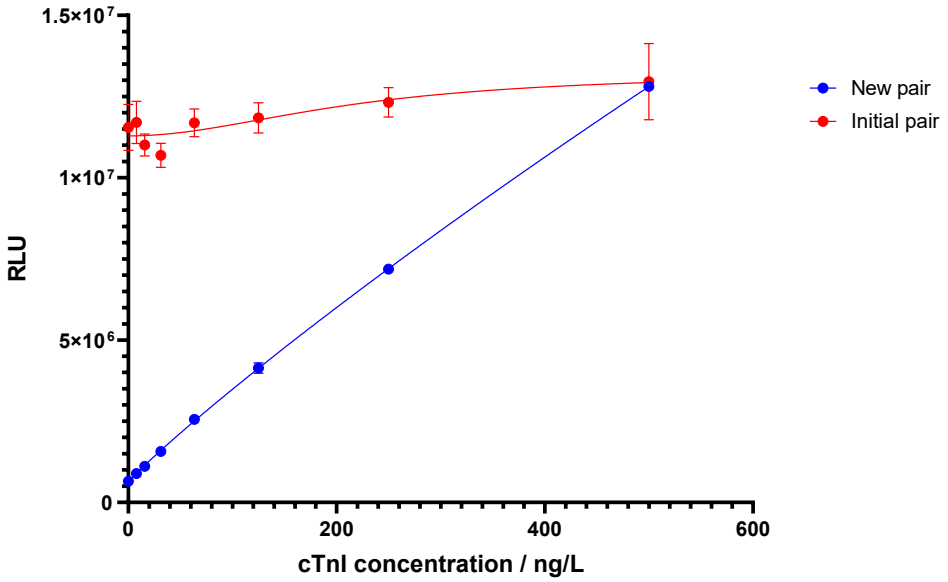

Figure 2.2.3 - 4PL regressions shows no sensitivity in the current pair, with improved sensitivity of the new pair for cTnI. *This shows complete inadequacy of the previous best pair in comparison to the newly assessed pair. This assay is performed in EDTA human pooled plasma.SD error bars for each concentration represent n=2.*

Clearly, the new antibody pair transformed the performance of the assay, highlighting the influence of epitope position and steric hindrance in the ability of monoclonal antibodies to bind analyte. The below table indicates the epitope targets for both the previous and new antibody pair for the consideration of spatial contribution to this new performance.

	Epitope region (amino acids)	
	Capture antibody	**Detection antibody**
Initial pair	86-90	23-29
New pair	83-93	24-40

Table 2.1 – A table to show comparison of epitope regions on capture and detection antibodies with the current underperforming pair and the new, significantly more sensitive pair.

Due to the magnitude of difference between the initial pair and new pair, the question arose about whether the quality of the biotinylation of the detection antibody in the initial

pair was inadequate and whether this was the cause of such poor performance. This naturally led assay development efforts into exploring alternative biotinylation chemistries and conjugations, rather than simply repeating the same conjugation for the initial pair. These biotinylation techniques are detailed in methods section 2.2.4.

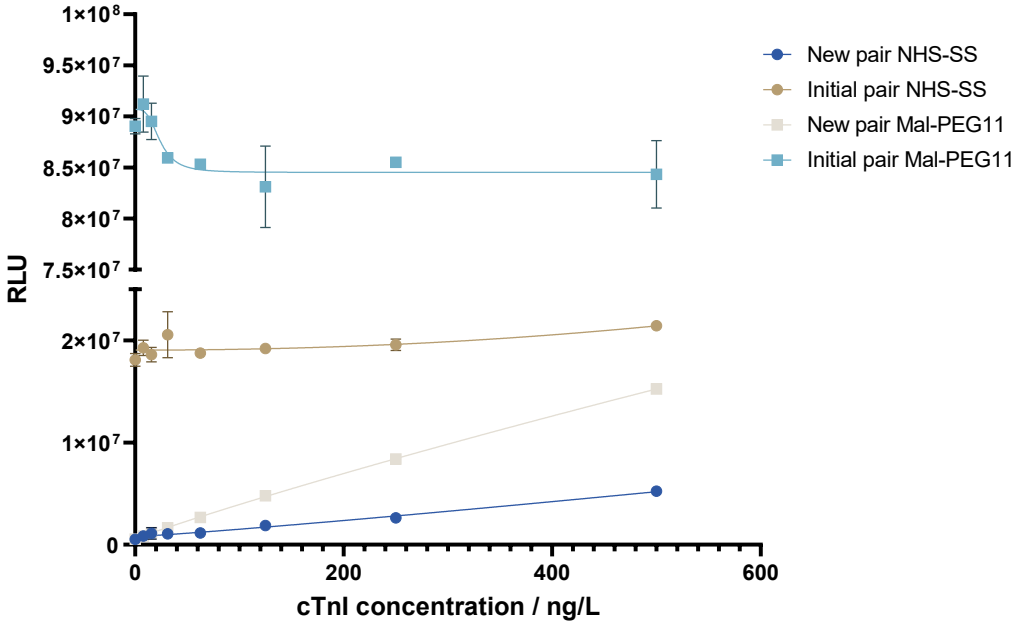

Figure 2.2.4 – Biotin conjugation chemistry has a vast impact on assay performance. *4PL regressions to demonstrate slope of troponin assay using two different antibody pairs (the originally assessed pair vs the newly available, higher performing pair) to show the effect of conjugation chemistry on performance. Error bars for each concentration represent n=2.*

The advantages of the new antibody pair and Mal-PEG11 biotinylation are two-fold. Firstly, the replication of the NHS-SS biotinylation allays the concern that one faulty biotinylation caused the poor performance observed in Figure 2.2.4, further evidence against the use of this specific antibody pair for slope. The complete lack of slope observed was repeatable with the same antibody, regardless of biotinylation technique. Secondly, the background signal produced when using the new antibody pair was substantially lower than using the current antibody pair, which will aid with donor-to-donor matrix disparity amongst other potential drivers of background as the assay develops.

Considering the success of the adoption of Mal-PEG11 biotinylation for the troponin detection antibody, the same conjugation was also trialled for the ST2 detection antibody (S103). The results are captured below in Figure 2.2.5.

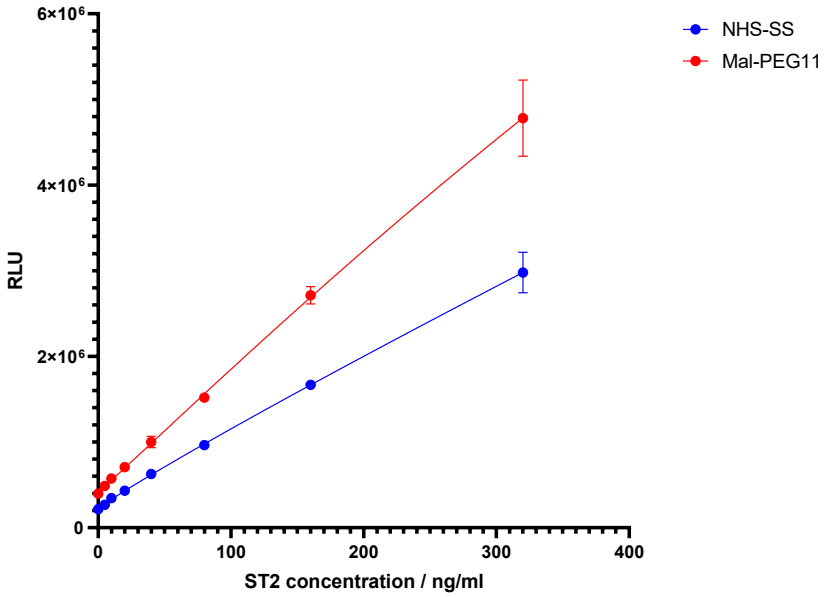

Figure 2.2.5 – Mal-PEG11 linker achieved an increased slope of 4840 RLU/ng/ml compared to the NHS-SS linker at 10ng/ml sST2. *Standard curves to show performance of two types of described biotinylation technique on assay sensitivity. SD error bars for each concentration represent n=2.*

Like the cTnI assay, the slope for sST2 detection in human plasma also increased, from 9335.6 RLU per ng/L to 14,015.6 RLU per ng/L at 80ng/ml. Unfortunately, assay background also increased, however, it was determined that the improvement in slope outweighed the slight increase in background. For the reasons explained in this section (2.4.2), assay development from this point forwarded proceeded with the new cTnI antibody pair, and with the Mal-PEG11 biotinylation of both the cTnI and sST2 detection antibodies.

2.5 Analyte commutability

The use of recombinant antigens for assay development is a common practice for several reasons. Firstly, it allows for the use of a consistent and controlled material for analytical validation. Secondly, it is relatively easy to produce on a mass scale and is not

contingent on a consenting patient with extremely high biomarker levels. All of these factors make obtaining a high concentration stock from native human sources difficult and costly due to its scarcity. Lastly, even if the aforementioned prerequisites were met, there is a risk in using a single donor to spike standard curves for matrix effects reasons, particularly from donors who have interfering co-morbidities associated with the reason for their high analyte concentration.

The entire purpose and commercial value of recombinant protein is to accurately replicate the characteristics of native protein without the shortcomings and restrictions of sourcing it. A significant finding of this thesis was that recombinant cTnI protein supplied by Hytest, does not in any way behave like native clinical protein. Below in Figure 2.2.6 is a demonstration of this analytical incongruence.

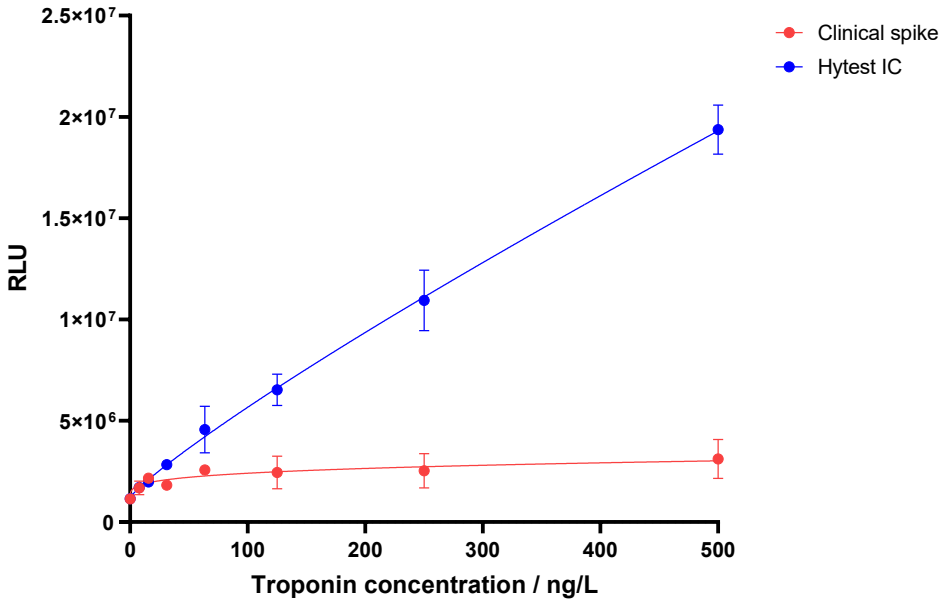

Figure 2.2.6 – The recombinant (Hytest IC) cTnI protein used for assay development does not corroborate the behaviour of clinical native cTnI. *These standard curves involve serial dilutions of Abbott Architect validated human plasma for high amounts of troponin analyte and Hytest commercially validated reconstitution of recombinant antigen. SD error bars for each concentration represent n=3.*

The experiment described in Figure 2.2.6 was repeated multiple times in case of an artefactual result but the relationship between clinical and recombinant spike was maintained upon each repeat. An additional pool of 3 high troponin donors were also screened with the same outcome which robustly demonstrated this disparity between native and recombinant activity. There is a negligible slope for the clinical spike condition, rendering the comparison of slope between the two proteins unquantifiable.

Despite some availability of high clinical donors to spike, it could not be a solution for the rest of the development of the duplex assay due to resource constraints. At this point in development, the experiments described in section 2.6 of this chapter proceeded whilst an alternative recombinant protein was ordered for troponin. Unfortunately, because the Abbott Architect does not have the capability to measure for sST2, it is much harder to determine whether the sST2 recombinant protein is also inaccurate in comparison to native protein. However, there was opportunity to validate the sST2 assay using clinical samples at the end of this chapter in a pilot clinical study (section 2.8).

Eventually, the new recombinant protein was received and tested and exhibited a much closer performance to clinical troponin as shown Figure 2.2.7. Note that due to the luminol formulation selected and the improvement in signal/background ratio from section 2.6.1, performance of the clinical troponin standard curve in Figure 2.2.6 differs from that of Figure 2.2.7.

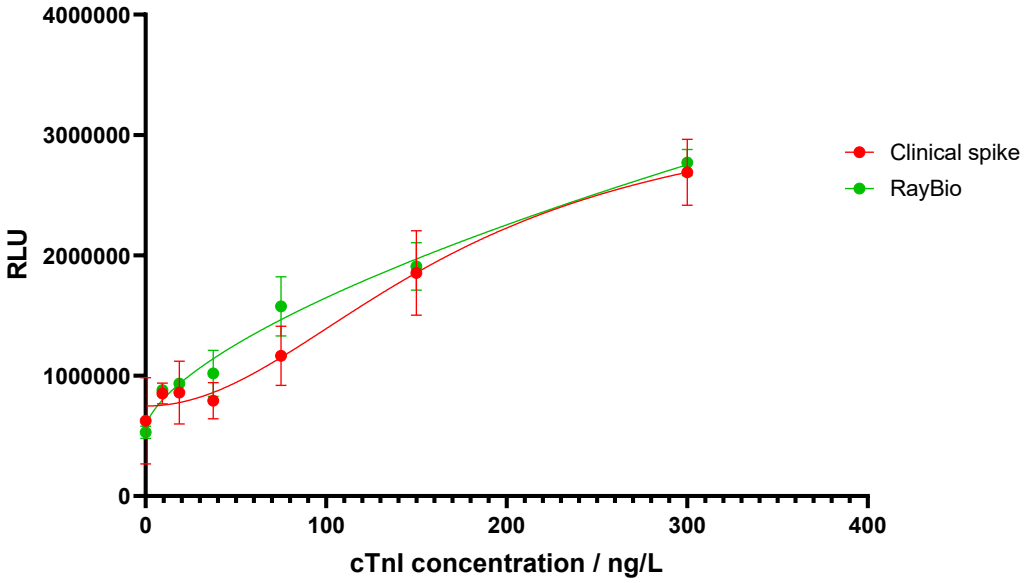

Figure 2.2.7 – RayBio recombinant cTnI resembles clinical troponin in assay response and therefore is a suitable calibrator. *Standard curves to show equivalency between recombinant troponin and a clinical high donor used as a spike for standard curves. RayBio recombinant protein shows much closer equivalency in comparison to Hytest. SD error bars for each concentration represent n=2.*

From this point forwards with assay development, the recombinant protein provided by RayBio® was utilised to ensure confidence that any further assay optimisations in the journey to duplex were in the best interest of clinical troponin performance.

2.6 Levers of sensitivity

2.6.1 Luminol formulation screen

As with most reagents involved in the assay protocol, substrate formulation also had an impact on analytical performance. The experiments involving chemiluminescent assays thus far has used a custom luminol manufactured by Neogen and supplied to this project by Osler Diagnostics. However, it was discovered that this particular formulation was discontinued when reorder was attempted, and so it was timely to investigate other formulations. The optimisation pipeline was relatively streamlined through the purchase of several commercially available luminols. No in-house formulations were investigated.

Performance was evaluated first, by calculating a signal to background ratio, in which signal achieved by each luminol at 200ng/L cTnI 300ng/ml sST2 were divided by their relative background signals. Results were considered by the comparison of luminol signal/background ratios within each analyte spiked. Ratios should not be interpreted across analytes. In Table 2.2 the performance of these substrates is described.

	Signal/background ratio		
	Hytest recombinant cTnIC	Troponin clinical sample spike	sST2
SuperSignal Femto	44.07	13.14	3.55
SuperSignal atto	29.56	8.91	3.02
SuperSignal pico	112.49	25.67	7.16
Neogen custom formulation*	31.86	8.24	2.91
Neogen K-Blue	113.74	23.28	5.47

Table 2.2 - A table to list comparative signal to background ratios of various luminol formulations (left) with three different types of analyte. *The condition highlighted in bold is the current formulation, that also appears to perform the worse (lowest signal to background ratio).*

Fortunately, the formulation of substrate turned out to be an influential lever in improving performance of clinical troponin sensitivity after the substantial differences uncovered in analyte commutability. The two best performing formulations by signal/background ratio, SuperSignal Pico® and Neogen K-Blue® were then assessed head-to-head with standard curves (Figure 2.2.8). Interestingly, the substrate formulation performance differed drastically between analyte type, with K-blue superior in all cases. The formulation shown in bold was the initial formulation, which also had the lowest sensitivity. The two best formulations for signal to background ratio were selected for the assessment of sensitivity at a greater range of analyte concentrations. Importantly, slope for clinical troponin improved from 2661.5RLU/ng/L for the old formulation, to 3894RLU/ng/L for the Neogen K-blue®

formulation when comparing 0ng/L and 500ng/L. This ~70% increase in slope is very promising for the assaying of clinical samples, however, is still 10-fold less sensitive than the Hytest recombinant protein, with a slope of 37980RLU/ng/L between 0-500ng/L. To reiterate, the target LoD (sensitivity) is set at 10ng/L, but it is more important to be robustly sensitive to donors that measure below and above the 99th percentile for troponin, around 20ng/L. At the time, the assay was not nearly reaching that target, and so although a change in luminol formulation improved performance, more optimisations of assay reagents and parameters were required.

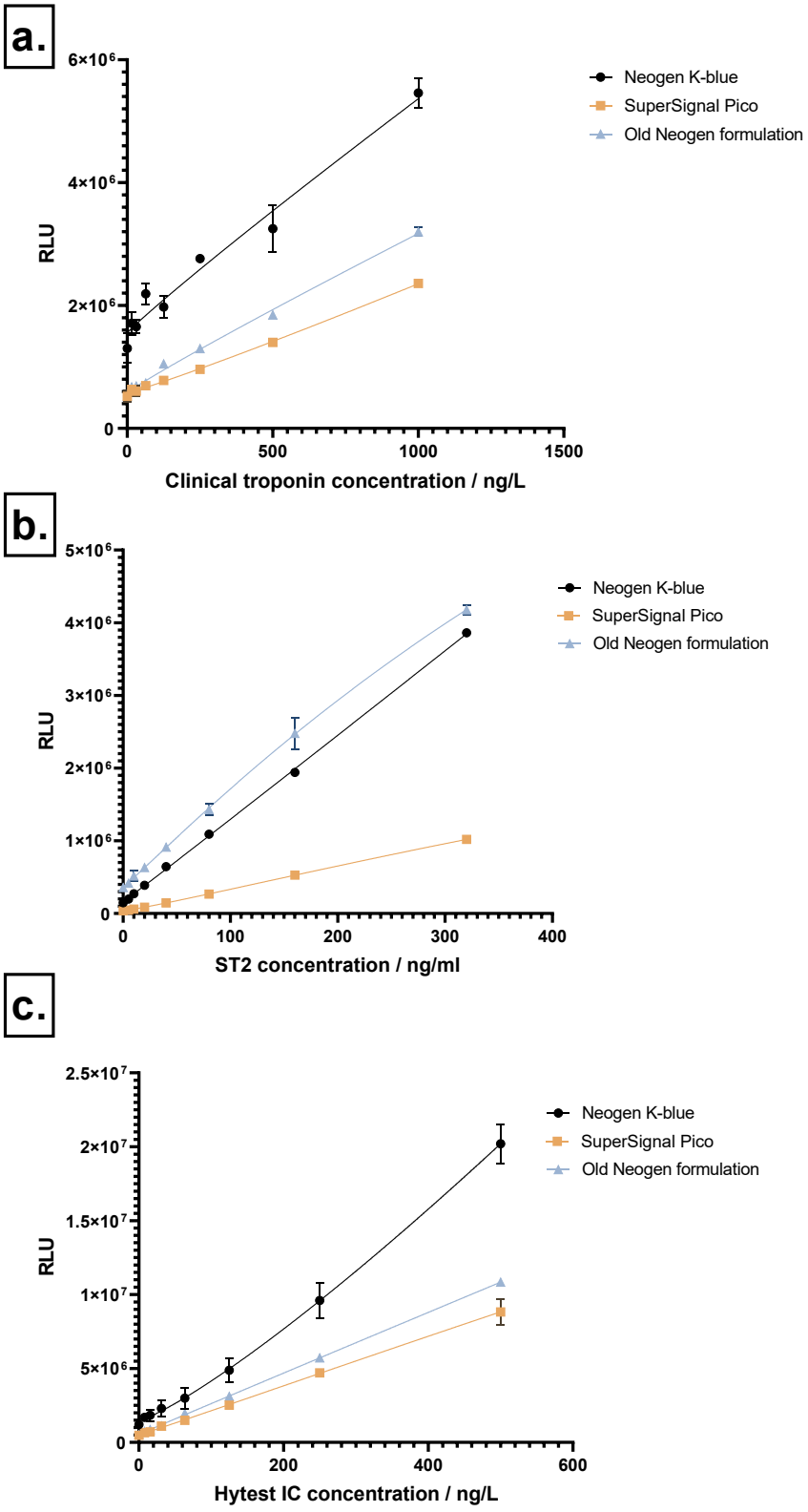

Figure 2.2.8 – Neogen K-blue luminol gives superior sensitivity to SuperSignal Pico and the old custom Neogen luminol formulation. *A demonstration of luminol formulation effect on assay slope, and the difference observed between proteins and sensitivity in relation to such formulation changes. SD error bars for each concentration represent n=2.*

2.6.2 Co-detection antibody screen

Another avenue explored for sensitivity improvement was the addition of a secondary detection antibody. The rationale behind this was to potentially boost specific signal by increasing the capacity of analyte bound by antibody, subsequently increasing turnover of substrate by increasing presence of specifically bound HRP.

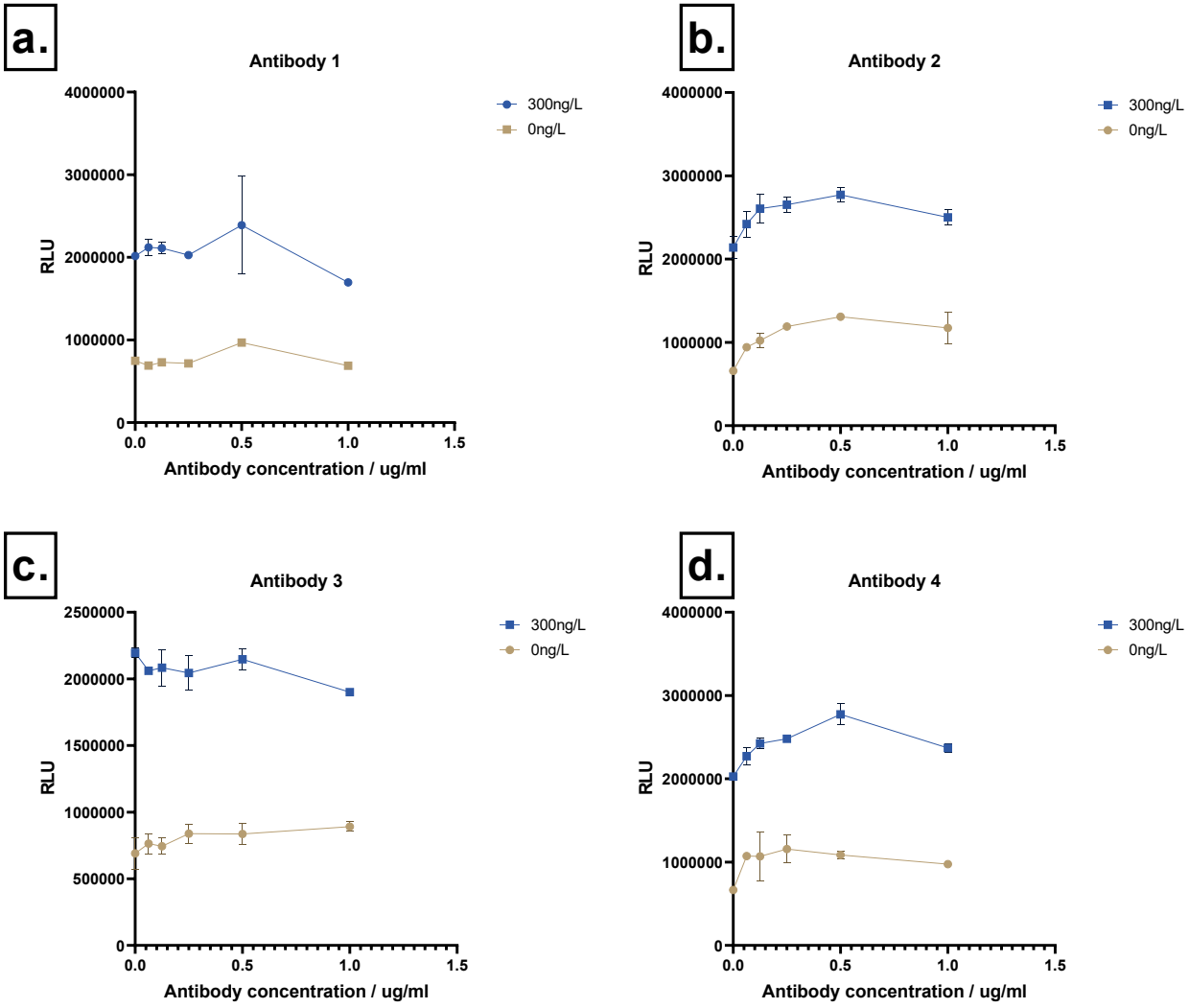

Figure 2.2.9 - The introduction of a second detection antibody does not improve the ability of the assay to detect native troponin. *Non-specific background increases in all cases, without a bigger increase in slope. SD error bars for each concentration of antibody represent n=2.*

As evident by Figure 2.2.9, this was not successful with the four antibodies trialled. In all cases, the difference between the 0ng/L and 300ng/L sample was greatest at 0µg/ml of extra antibody concentration, showing that adding an antibody targeting a different epitope did not boost sensitivity as hypothesised. Instead, it appears that adding more antibody is sterically compromising, and only entraps more HRP non-specifically, as indicated by the blank sample signal increasing and decreasing in parallel with the 300ng/L sample. Given the relevance of troponin epitope availability to this experiment, the high clinical troponin pooled human plasma was used to spike 300ng/L, instead of the Raybio® recombinant protein in this case. This was to negate the concern of optimising antibody efficacy with an analyte of unknown similarity to clinical troponin. Despite data to show equivalency in sensitivity between Raybio® spike and clinical troponin for sensitivity (Figure 2.2.7), it is unknown whether epitope character is also equivalent. Therefore, for experiments concerning epitope specificity, a high clinical donor spike is more appropriate. Clearly, the additional antibody does not aid capture of troponin, and so the hypothesis that clinical troponin capture is limited by capture antibody efficiency is not correct.

2.6.3 Assay diluent titrations

Titrating various salts, sugars, surfactants and proteins into assay diluent used for detection antibodies and HRP is an effective way to directly manipulate binding efficiency and kinetics in an immunoassay. This subsection of this chapter describes the hypotheses and impact of different chemical additives aimed at improving assay performance. Considering that troponin sensitivity is the main motivator of these sensitivity-driven experiments, the following titrations were only carried out with the troponin assay, not the sST2 assay. Thus far, sST2 assay sensitivity remained at target sensitivity. It was assumed that any changes made based on the results that follow should similarly improve with the sST2 assay, and if not, will

not hinder the sST2 assay beyond a tolerable degree. These optimisations were also done in a sequential, additive manner, such that, calcium chloride was optimised and added, followed by a magnesium chloride titration on top of the calcium chloride addition, and so on. This was to ensure that each consecutive additive did not negate or detrimentally affect the previous one.

2.6.3.1 Calcium chloride

An alternative hypothesis to the lack of sensitivity of the troponin assay is that rather than the detection system (antibodies, HRP) being suboptimal, the analyte itself is conformationally challenged. A relevant salt to titrate was calcium chloride due to troponin's ability to bind calcium during normal muscle function (Wakabayashi, 2015). As calcium is known to have this function in vivo, it is entirely possible that the same conformational change is achieved when troponin Is flooded with calcium Ions In an assay format.

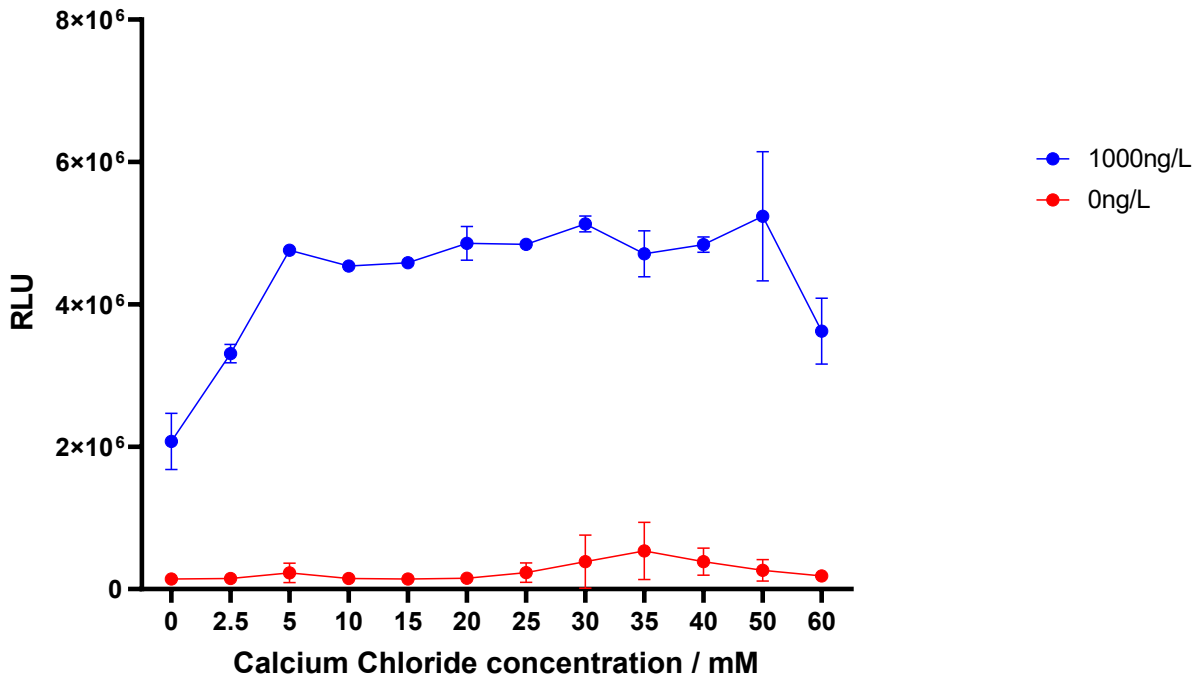

Figure 2.3.1 – A titration of calcium chloride in the assay diluent shows an increase in signal to background ratio before plateauing and decreasing after 10mM. *SD error bars for each concentration represent n=2.*

Figure 2.3.1 supports the hypothesis that calcium ions improve the availability of troponin for binding by antibody during assay incubation. The background of the assay does not significantly increase or decrease from 0mM up to 60mM calcium chloride, however specific signal increases by over double at 5mM, plateaus, then drops only at the highest concentration. The consistency of specific signal across the 5mM-50mM range infers an interaction between chloride ions and troponin that is at saturation point as, theoretically, there is a maximum amount of calcium able to bind to troponin. The slope of the assay using TBS-T 0.05% as a control, vs with 5mM was 1930.55RLU/ng/L, and 4531.5RLU/ng/L, respectively. It is tempting to assign the lowest effective concentration, 5mM, as a permanent change to assay diluent going forward, however, there is merit in considering a concentration from the middle of the effective range, such as 20mM. This would derisk the possibility that 5mM is only just effective enough in some donors, but not others, depending on unknown matrix influences. The slope for 20mM remains similar to 5mM, at 4704.3, and so it was decided to adopt this concentration of salt to the next titration.

2.6.3.2 Magnesium chloride

The interest in titrating magnesium chloride into the assay diluent comes from its inherent chaotropic activity. By definition, this salt is able to dismantle the stable hydrogen bonding dependent, structure of proteins held together by water molecules, inducing hydrophobicity. This in turn weakens protein-protein interactions, which, ultimately, could impair the efficiency of the assay. However, when used at a fine-tuned concentration, magnesium chloride could be influential enough to disrupt the non-specific, background provoking reactions; all whilst lacking the strength to disrupt the stronger, specific ones.

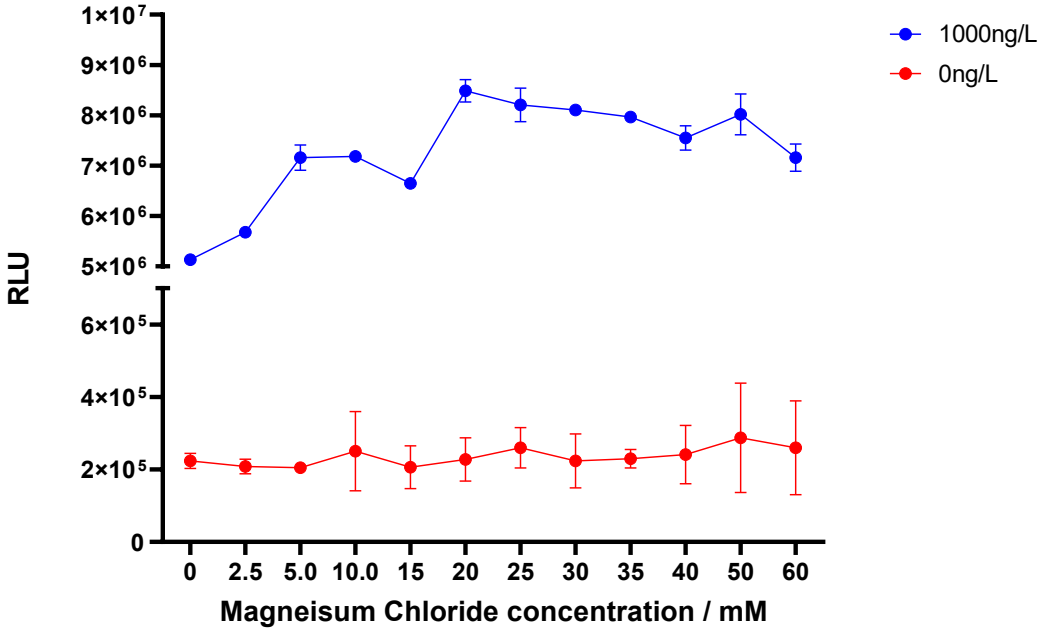

Figure 2.3.2 – The addition of 20mM magnesium chloride to assay diluent improved sensitivity (slope) to 8217RLU/ng/L. *Titrating up magnesium chloride increases signal to background ratio, increasing sensitivity of the assay. SD error bars for each concentration represent n=2.*

Somewhat surprisingly, the hypothesised effect of reducing background with maintained assay signal was not true (see Figure 2.3.2). The opposite occurs, whereby background signal remains the same but specific signal increases. However, on further thought, the same mechanism of removing NSB could still be occurring, but in a way that allows for additional detection of troponin in a sterically favourable way. In other words, the prevention of NSB by rendering the interaction energetically unfavourable could be removing the competition to capture analyte on the surface of the well. Based on another increase in slope to 8217.6 RLU/ng/L, 20mM magnesium chloride was the concentration selected to add to the diluent going forward.

2.6.3.3 Sodium chloride

Ionic stability is a key factor in the conformational stability of IgGs, in particular due to the concentration of Asp residues on the Fab (fragment, antigen binding) region that benefit

from ionic presence for conformational and aggregation reasons (Wang, et al., 2013). With this in mind, it is logical to titrate a salt such as sodium chloride when attempting to increase assay sensitivity. The more available antibody binding regions are to analyte through conformational optimisation, the more specific signal can be achieved. Below in Figure 2.3.3 is a characterisation of sodium chloride impact on signal to background ratio of the troponin assay. The titration started at 150mM as this is the concentration of sodium chloride in the TBS supplied to make the TBS-T 0.05% base of the buffer.

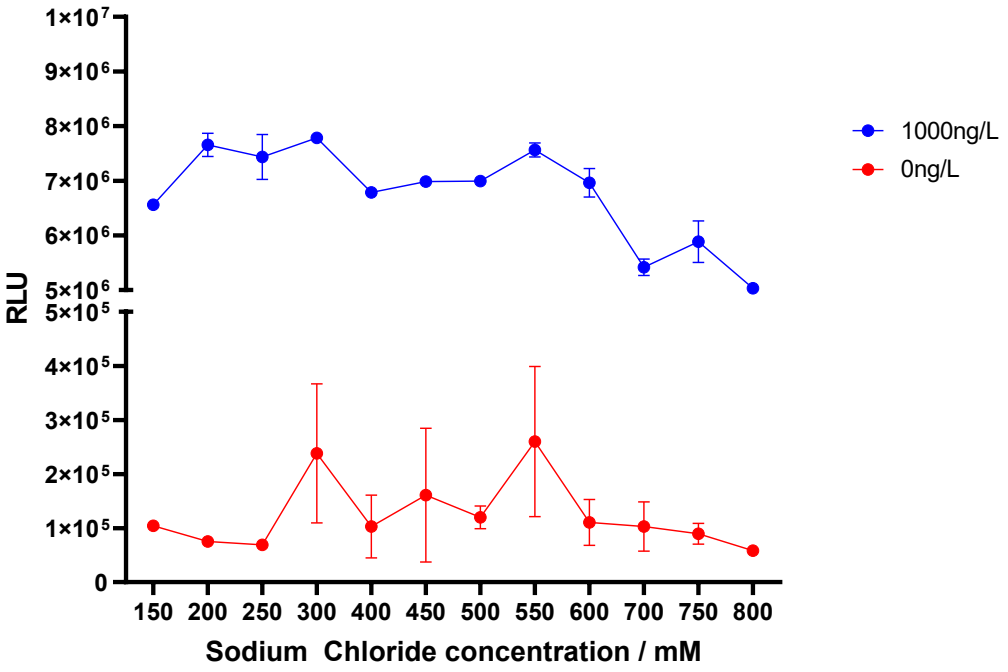

Figure 2.3.3 – Titrating sodium chloride into the assay diluent shows some, but minimal increase in sensitivity of the assay on top of the already added salts*. SD error bars for each concentration represent n=2.*

Fortunately, both an increase in signal and a decrease in background, albeit small, was observed in the addition of sodium chloride to TBS-T 0.05%. This benefit decreases after around 300mM, where specific signal starts to decrease. Slopes in RLU/ng/L for 150mM and 250mM were 6458.13 and 7366.155, respectively. It is acknowledged that the slope for the

addition of sodium chloride is slightly lower than when magnesium chloride was added in the previous section, however, these slope measurements are sensitive to even slight differences in background between plates, and so their use is for the observation of large delta in slope only.

2.6.3.4 Bovine serum albumin (BSA)

Another stabilising force in assay diluent is protein. It's action and benefits are twofold: firstly, if protein derived matrix effects are observed between different human plasma samples, dilution with a diluent containing a high concentration of protein is able to equalise any differences contributing to anomalous results. The second and most obvious role of BSA, as utilised in many difference applications across molecular biology, is as a blocking reagent. Passive interaction between BSA and potential assay inhibitors reduces competition and steric hinderance, having a similar effect as described with magnesium chloride, albeit by a different mechanism.

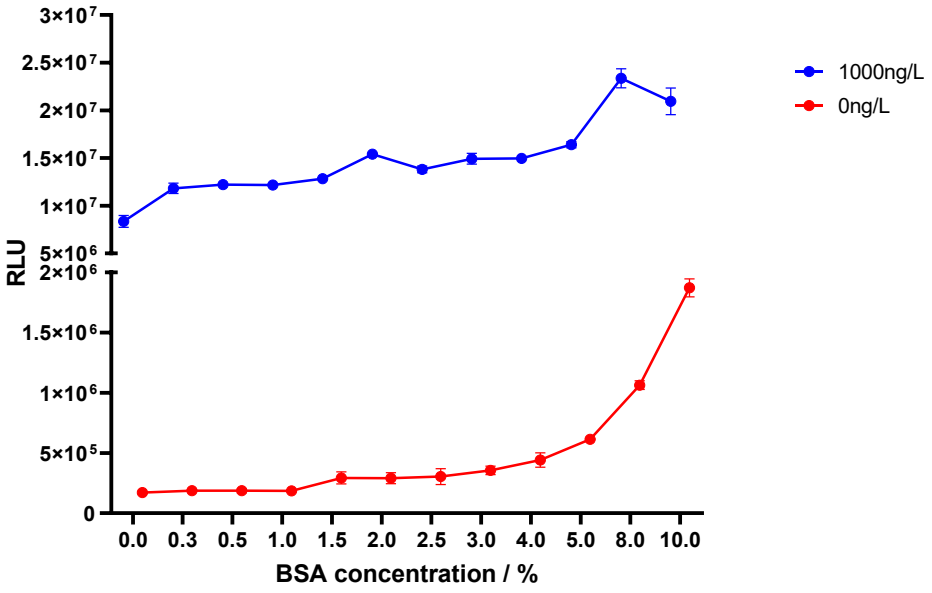

Figure 2.3.4 – 0.3-1% BSA addition to assay diluent improves slope to 11994.7RLU/ng/L. *SD error bars for each concentration represent n=2.*

As characterised by Figure 2.3.4, the addition of BSA, even at 0.3%, improved specific signal by increasing slope. As mentioned for calcium chloride, it could be safer to pick a concentration in the middle of the effective range. Based on this logic, and the observation that background starts to increase at 1.5%, 1% BSA was adopted for diluent formulation. The final slope calculation for all components combined: Calcium chloride, magnesium chloride, sodium chloride and BSA amounted to 11994.7 RLU, which is almost a 2-fold increase in sensitivity at 1000ng/L compared to initial estimations. This provides a vast improvement on the ability of the assay to detect clinical, native troponin which is imperative for the application of the assay in Chapter 4.

2.6.4 Final optimised single plex assay performance

After the promising improvements made as described in this chapter, it was decided that standard curves should be run with all the assay alterations combined to benchmark performance of both the troponin and the sST2 assay. To summarise, these improvements include the new MalPEG-11 biotinylation, luminol screening, diluent optimisation, a change of assay detection system (chemiluminescence) and the substitution of the troponin detection antibody. Importantly, this benchmark was run with human plasma spiked with a high clinical troponin sample. The performance of both assays with these changes is captured in Figures 2.3.5 and 2.3.6.

Troponin assay analysis:

A 4PL regression was fitted to the troponin assay standard curve from 125ng/L to 0ng/L, which was then used to self-interpolate raw signal to ng/L. The below formula, a 4PL

equation rearranged for χ, using the following values: 216260 (A), 1.558 (B), 72.88 (C), 833782 (D).

$$\chi = C\left(\frac{\mathrm{A} - D}{\gamma - D}\right) - 1^{\left(\frac{1}{\mathrm{B}}\right)}$$

The interpolated data are described in table 3. Once obtained, these were used to calculate LoB and LoD, to gauge sensitivity. Formulas described in Methods section of this chapter were applied and produced an LoD of 29.28ng/L, which was an enormous improvement from the data shown in Figure 2.2.6, where there was no analytical sensitivity up to 1000ng/L.

	Raw signal / RLU			**Interpolated value / ng/L**		
Sample	Replicate	Replicate	Replicate	Replicate	Replicate	Replicate
concentration / ng/L	1	2	3	1	2	3
15.6	276700	284200	372200	17.51	19.04	36.31
0	177800	187800	240800	0	0	9.43

***Table 2.3** - Values representing signal obtained at low concentrations of troponin and their interpolated values from the standard curve run on that plate.*

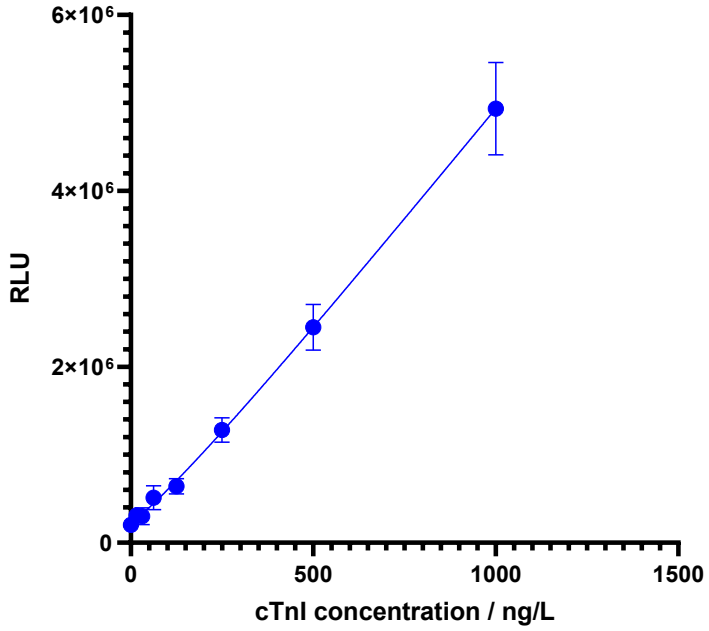

Figure 2.3.5 – After optimisation, the cTnI single plex assay had an LoD of 29.28ng/L. *Detection of native cTnI was made by chemiluminescent reagents, with a readout in RLU (relative light units). The standard curve 4PL regression seen in blue was used to produce the values in table 3. SD error bars for each concentration represent n=3.*

sST2 assay analysis:

For the sST2 standard curve, a simple linear regression was adequate for interpolation as the assay has a more linear lower end than the troponin assay. Again, raw and interpolated values are described below in table 4 and LoD was calculated to be 6.07ng/ml.

	Raw signal / RLU			**Interpolated value / ng/L**		
Sample concentration / ng/ml	Replicate 1	Replicate 2	Replicate 3	Replicate 1	Replicate 2	Replicate 3
10	149100	132600	129600	11.44	10.00	9.74
0	61490	51910	53950	3.90	2.96	3.14

Table 2. 4 - Values representing signal obtained at low concentrations of sST2 and their interpolated values from the standard curve run on that plate.

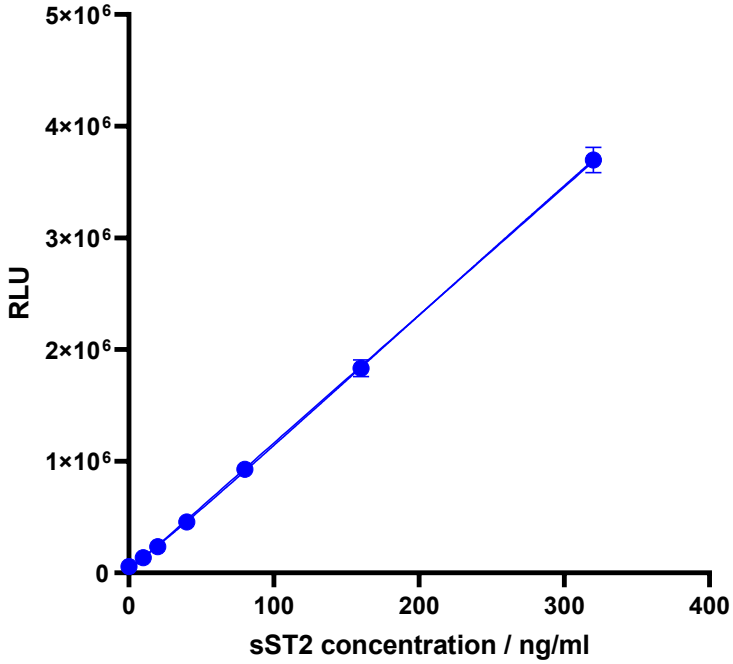

Figure 2.3.6 – After optimisation, the sST2 duplex assay had an LoD of 6.07ng/ml*. Detection of recombinant sST2 was made using chemiluminescent reagents, with a readout in RLU (relative light units). The standard curve with 4PL regression seen in blue was used to produce Figures in table 4. SD error bars for each concentration represent n=3.*

Given the clinical cutoff of approximately 20-35ng/ml for sST2, this assay achieves sensitivity well within the required limits for distinction between healthy and unhealthy individuals (Bagai, et al., 2018). This sensitivity would be satisfactory, were it maintained after duplexing with troponin.

For the troponin sensitivity, LoD is currently around the 99th percentile of the healthy population. This is the upper limit of assay efficacy, given that 99% of patient basal levels are below this and the resolution of increases in cTnI from baseline are involved in diagnosis. However, it is desired that sensitivity is robustly below the 99th percentile in the case that very early measurements after onset of MI symptoms can still be correctly flagged if actually raised in comparison to the patient's usual basal level. ROC analysis of duplex cTnI vs Abbott Architect cTnI will be assessed for false negativity in chapter 4. Based on the successful benchmarking of single plex performance, it was decided that the duplex exploration should commence.

2.7 Conversion of single plex to duplex assay

2.7.1 Interference studies

Before an attempt to detect both analytes in one coated well, it is important to methodically eliminate contributions of interfering non-specific assay signal from each system. For example, if the anti-troponin antibodies had some degree of specificity to sST2, troponin measurements would be incorrectly inflated, leading to false positive readings. Conversely, components of the opposite assay could have a negatively or positively interfering effect, preventing the binding of the target analyte and resulting in false negative or false positive readings.

2.7.1.1 Analyte interference

To assess the contribution of analyte interference on assay specificity, a simple experiment was conducted in which a clinically high concentration of the analyte was spiked into the sample of the opposite assay, in a standard curve of the target analyte. It is assumed that if the selected high concentration (300ng/ml for sST2 and 500ng/L for cTnI) does not interfere at each concentration of the standard curve, it is very unlikely to interfere at lower concentrations. The results of these experiments can be seen in Figure 2.3.7.

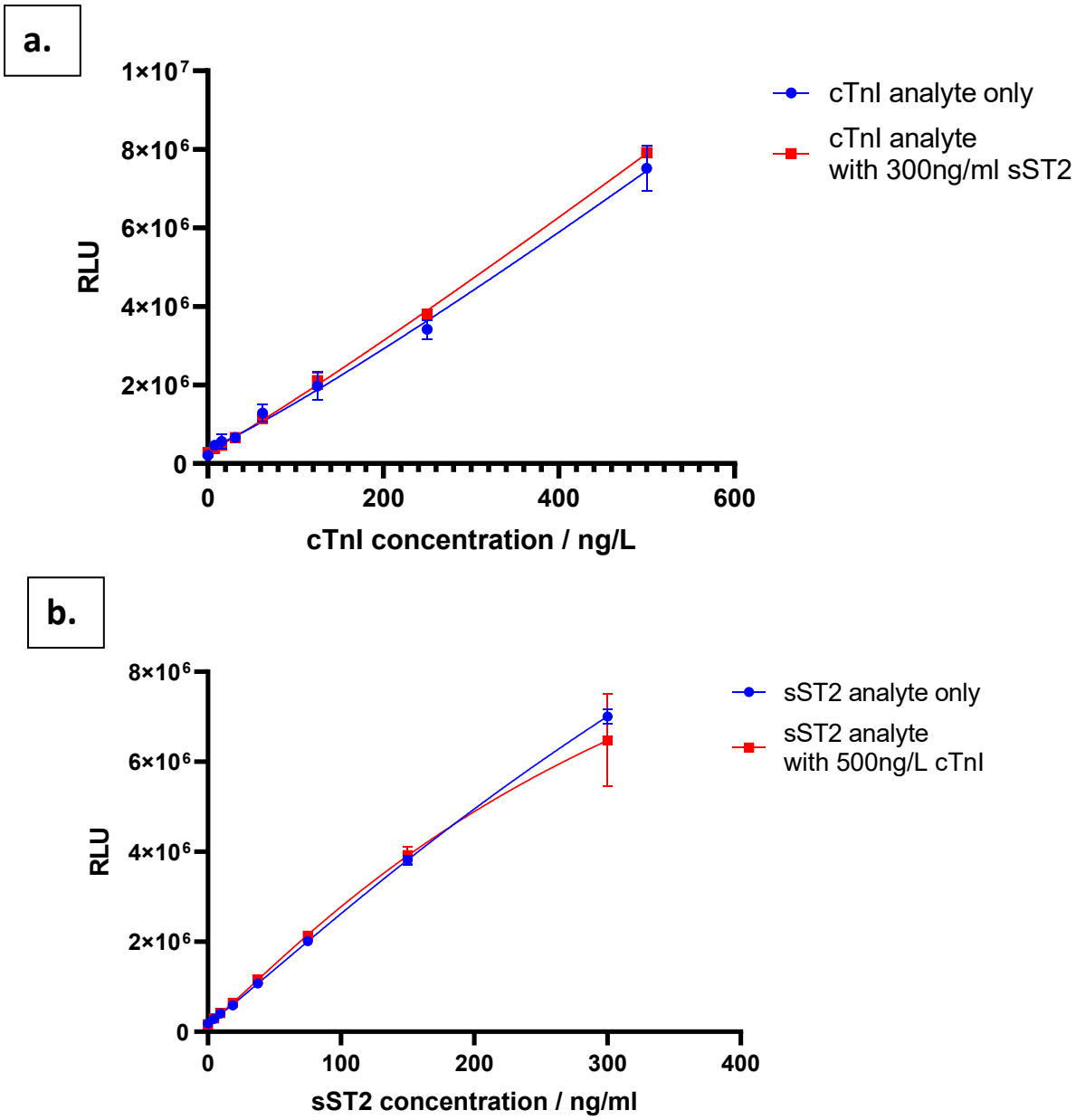

Figure 2.3.7 – There is no cross-interference of analytes when a.) a high amount of sST2 is spiked into the troponin assay and b.) a high amount of troponin is spiked into the sST2 assay. *SD error bars for each point represent n=3.*

There was no statistical difference between the response of both assays when spiked with the opposite analyte at high concentration. Evidently, the assay was robust to any interference from the opposite analyte, which derisked the continuation of duplex development.

2.7.1.2 Detection system interference

Further to the success of analyte compatibility evaluation, it was also important to assess antibody interference. At this point, both assays were measured using HRP-mediated enzymatic turnover of luminol, so ultimately the detection systems needed to be decoupled to use a different detection system for each to distinguish individual signals. However, given the effective performance of both the sST2 and cTnI detection antibodies, it was preferred that these are kept constant, and alternative streptavidin conjugates were explored. For that reason, similar to Figure 2.3.7, interference plots for antibodies on opposite assays are shown in Figure 2.3.8:

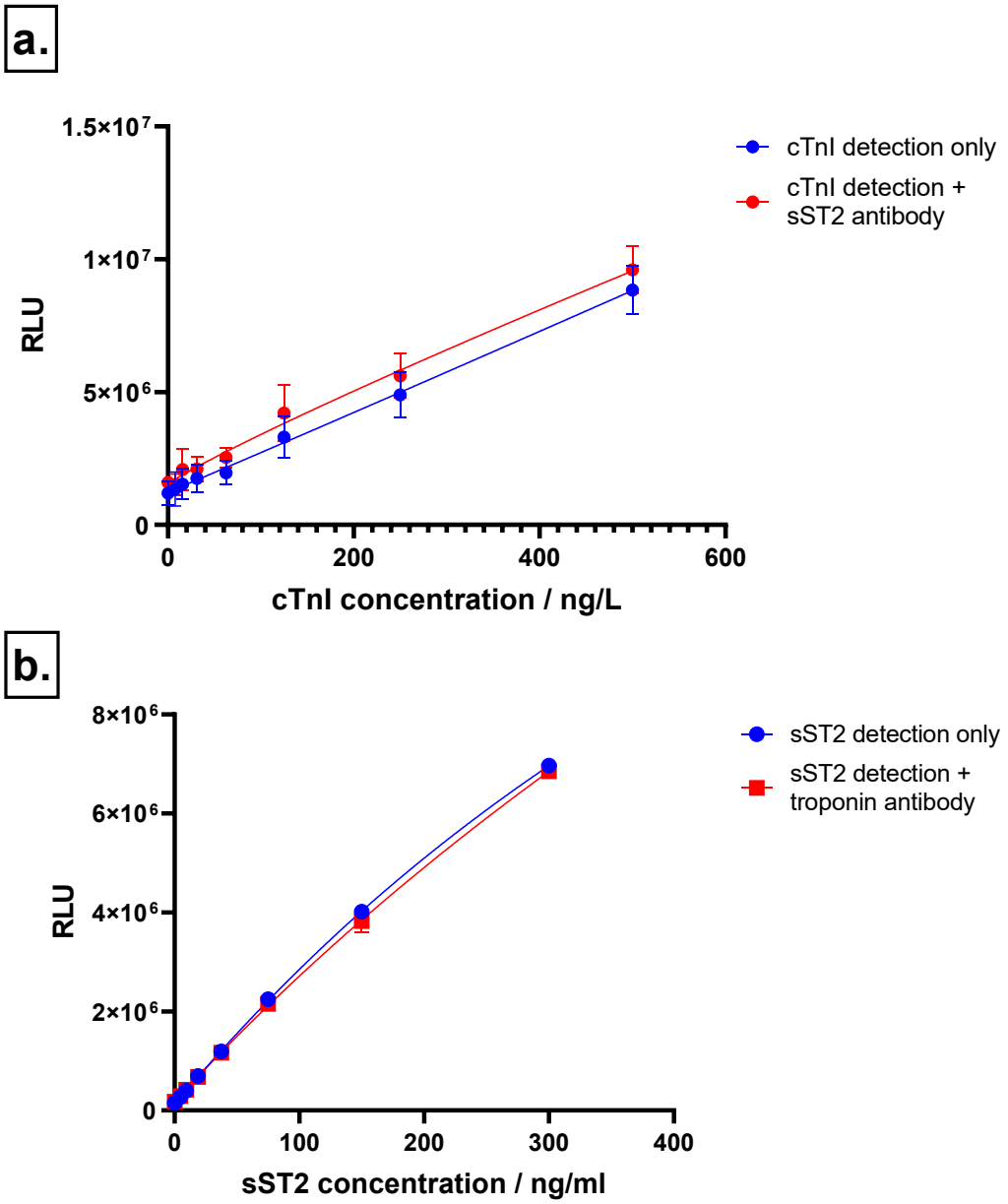

***Figure 2.3.8** - **Assay performance when a.) sST2 antibody at optimised concentration (1µg/ml) is spiked into the troponin detection solution, and b.) optimised concentration of troponin detection antibody (2µg/ml) is spiked into the sST2 assay.** SD error bars for a. represent n=3, and for b. n=2.*

Similarly, little interference was observed when the antibodies of each assay were added to the opposite detection solution, which is extremely beneficial. It was observed that the background of the cTnI assay increases but SD error bars still overlap. Importantly, the

slope of the assay remains unchanged, showing that despite an increase in non-specific signal, it does not introduce the effect of false positivity or negativity.

2.7.2 Quantum dot adoption for fluorescent signal distinction

As previously stated, it was hypothesised that a duplex assay could be achieved via the utilisation of two different light-associated detection systems. Theoretically, fluorescence could be employed to detect both analytes at different wavelengths of fluorophore excitation, however it was already known that chemiluminescence has the best chance of achieving the sensitivity required of the troponin assay. Conversely, the sST2 assay so far had demonstrated acceptable sensitivity for clinically relevant cutoffs, and so it was logical to trial alternative systems with this detection antibody. Known for their small size and benefit from a steric hindrance perspective, quantum dots posed a feasible solution for the detection of sST2 antibody-analyte sandwiches. An array of streptavidin conjugated quantum dots with various excitation wavelengths were screened in a similar "checkerboard" process as outlined in section 3.3.1. An arbitrary concentration of 200ng/ml sST2 was selected to calculate signal to background ratios in a titration of both the sST2 capture antibody and the detection antibody-quantum dot solution. In the interest of reducing complexity, the detection antibody and quantum dot were kept at equal concentrations, titrated together for this experiment. Results are defined in table 2.5.

		Q dot and detection antibody concentration					
		Qdot 800		Qdot 525		Qdot 655	
		1µg/ml	2µg/ml	1µg/ml	2µg/ml	1µg/ml	2µg/ml
Capture antibody coat / µg/ml	5	4.921	7.431	1.299	1.486	1.338	1.062
	10	6.957	6.384	1.279	1.379	0.932	1.002
	20	10.855	6.313	1.327	1.411	1.088	1.003
	40	7.050	4.550	1.353	1.335	1.142	0.999

Table 2.5 - Signal to background ratio using a checkerboard of different sST2 capture and detection antibody concentrations, whilst keeping quantum dot concentration equal to detection antibody.

Encouragingly, it was discovered that using Qdot800 at 1µg/ml produced almost an 11-fold difference in fluorescent signal when comparing a blank plasma sample to a sample spiked with 200ng/ml sST2. This reveals potential for the use of this specific quantum dot for detection of sST2 in a duplex assay format. The next step was to test interference of the Qdot with the troponin assay detection antibody and HRP. Given that both detection antibodies employ biotin-streptavidin affinity to generate signal, it was entirely possible that the Qdot could interfere by binding to the troponin antibody instead of PolyHRP. To mitigate this risk, it was concluded that the most practical assay method to adopt was a two-step protocol. This involved the separation of the detection of both analytes by a wash step, removing the large majority of free, unbound detection antibody before the introduction of the second detection antibody. To isolate any potential negative effect of the Qdot, the single plex assays were run with an added second step of the opposite assay detection system.

Characterised in Figure 2.3.9 is the effect of both detection systems separated by a wash step, which is statistically null. The two-step protocol was effective in preventing the cross-interaction of polyHRP or quantum dot with the unintended antibody, showing no interference in specific signal across a range of concentrations. In light of this success and the growing body of evidence to support the duplex proof of concept, it became reasonable to attempt the combination of the assays with this two-step technique, starting with the optimisation of co-coating the capture antibodies in the same well. Also undefined is the effect of luminol on the sST2 assay reading, the assessment of which is described in the next section of this chapter.

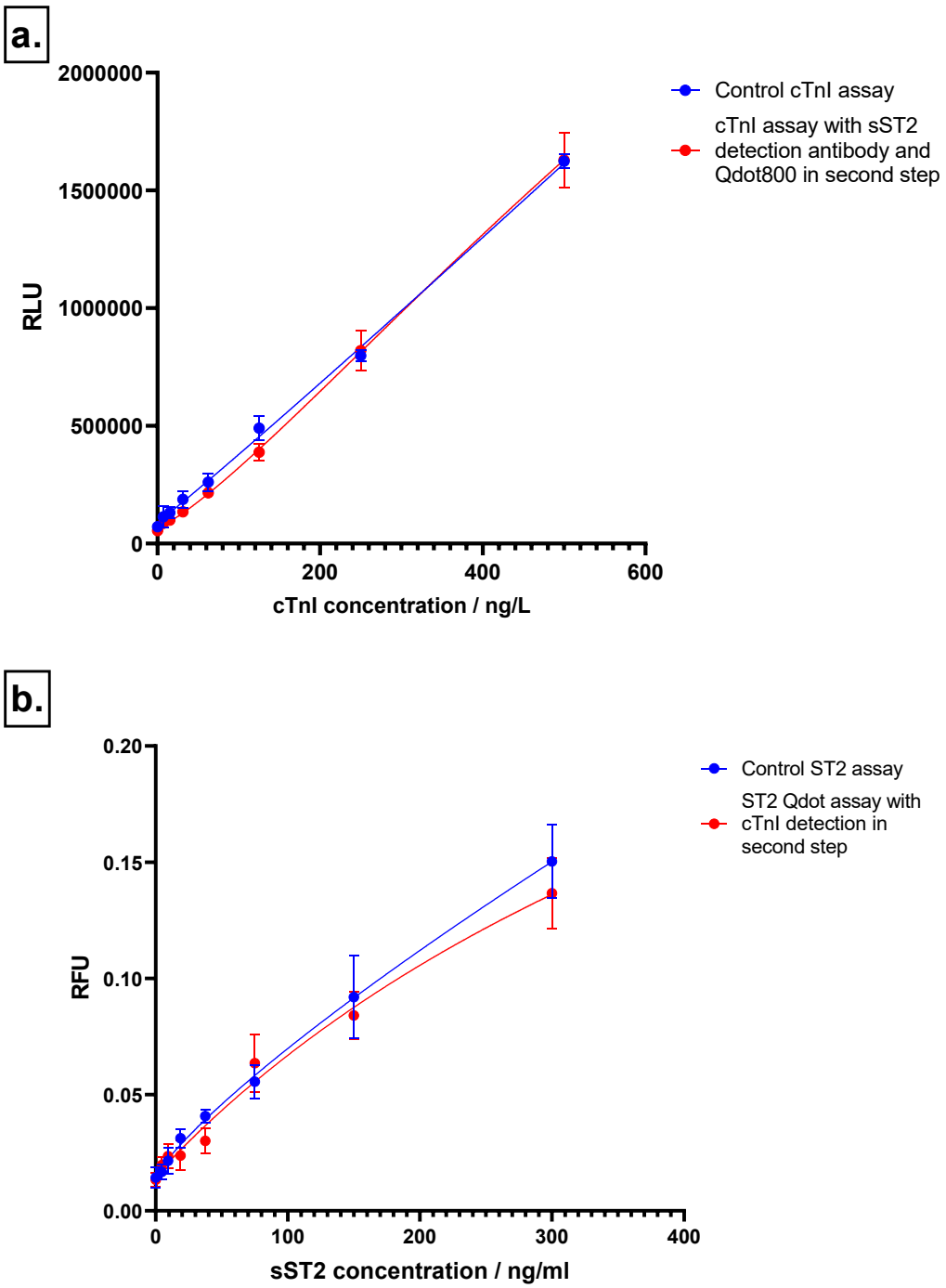

Figure 2.3.9 – sST2 detection reagents do not interfere with the cTnI assay (a.). Vice versa, cTnI detection antibody does not interfere with sST2 fluorescent-based detection (b.). *In blue shows the control single plex assay using only one set of reagents to detect one analyte. In red shows the combination of analyte detection reagents, where in a, cTnI capture antibody is coated and in b, sST2 capture antibody is coated. SD error bars for each concentration represent n=3.*

2.7.3 Final duplex assay optimisations

The most important part of the assay to address at this point was the co-coating optimisation. Solid phase ELISAs conducted on 96 well plates present kinetic limitations due to their limited surface area to volume ratio. Furthermore, the surface has a mathematical limit to the amount of IgG it can adsorb, even in the improbable case of perfect binding efficiency. When the surface must be shared between multiple capture antibodies, with potentially different binding efficiencies, it can become increasingly difficult to achieve target assay performance. It is expected that sensitivity and/or linear range will reduce with this reformat, and so to reduce this impact the capture antibodies were titrated and co-coated to select optimum concentrations.

Results are portrayed in Table 2.6 in the form of slope calculations between 0ng/L and 200ng/L for troponin and 0ng/ml and 300ng/ml for sST2. It appears that the most beneficial ratio of sST2 capture antibody to cTnI capture antibody is 40µg/ml and 20µg/ml respectively, which was adopted into the evolving protocol. Other areas of optimisation explored were shaking speed and temperature, which yielded steeper slope when incubated at 40°C, with the main effect being a reduction of background. This could be explained by the inhibition of NSB brought on by a temperature extreme enough to prevent weak interactions, but not strong enough to break the specific ones. It was also during these final optimisations that an issue became clear with the repeatability of the maleimide PEG-11 biotinylation of detection antibodies, namely with batch variation of 2MEA required to split the antibody in half to allow for access to disulfide regions. As a result, it was determined that a third alternative approach for biotinylation was required that did not involve antibody cleavage, but that maintained the sensitivity gained with the maleimide PEG-11 biotinylation. A good alternative was a Siteclick

biotinylation, that aims to reduce steric hindrance and uses click chemistry to attach biotin at an optimised 5-fold molar excess.

sST2 capture antibody coating concentration / µg/ml		Troponin capture antibody coating concentration / µg/ml							
		160		80		40		20	
		sST2 slope (RFU/ng/ml)	cTnI slope (RLU/ng/L)	sST2 slope (RFU/ng/ml)	cTnI slope (RLU/ng/L)	sST2 slope (RFU/ng/ml)	cTnI slope (RLU/ng/L)	sST2 slope (RFU/ng/ml)	cTnI slope (RLU/ng/L)
	80	0.031	12458748	0.051	13503278.67	0.095	15012922.67	0.114	16705193.33
	40	0.026	10249739.33	0.055	12403374.67	0.077	14055700.67	0.120	16852875.33
	20	0.017	8335616	0.035	11448835.33	0.053	13132965.33	0.096	16261300.67
	10	0.012	4800537.333	0.025	8913820	0.052	10866368.67	0.079	13756053.33

***Table 2.6** - **A colour schematic to show various combinations of sST2 capture antibody coating with troponin antibody coating for best slope between 0-200ng/L for troponin and 0-300ng/ml for sST2.** Values are shown in either RFU for sST2 or RLU for troponin.*

2.7.5 Final assay validation

2.7.5.1 Linearity

The linearity of an assay can be measured by the % deviation from the expected value after reading the observed value. To facilitate this, a standard curve containing a large range of points within the clinically relevant range was produced, then each point of the curve was interpolated using a 4PL fit. The reading of the curve in ng/L or ng/ml is ratioed to the intended spike amount of analyte for a % difference calculation.

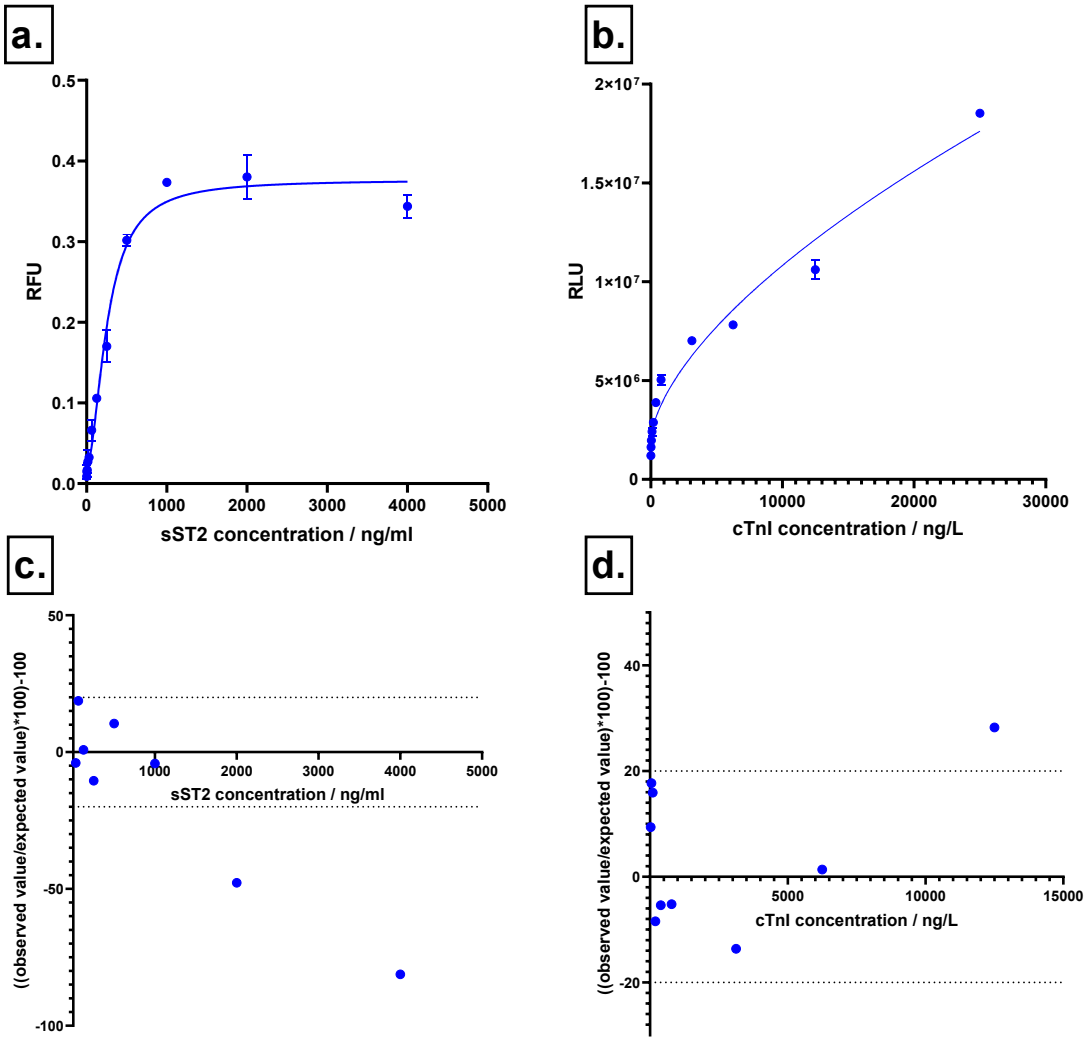

***Figure 2.4.1** - **Standard curves with broad ranges of sST2 and cTnI concentration run on the duplex assay format show loss of linearity starting between 1000-2000ng/ml and 6250ng/L-12500ng/L, respectively.** Standard curves are shown in a. (sST2) and b. (cTnI). C and D show deviation from linearity with dotted lines representing a 20% threshold. Points beyond the 20% threshold are considered a loss of linearity. For each concentration n=2.*

On the plots shown in Figure 2.4.1 loss of linearity occurred at some point between 1000-2000ng/ml for sST2 and around 12,500ng/L for troponin. Obviously, linearity is a continuous, scalable variable, and a loss of linearity does not mean that concentrations of analyte above that value cannot be measured. Having said that, the % recovery CV will increase as the curve gets flatter in proportional measure. This was certainly the case for sST2, as total assay saturation was met after 1000ng/ml, and since the actual human clinical range of sST2 is not completely elucidated, this will remain unknown until a sufficient number of representative clinical samples are measured. As for troponin, although some linearity was lost, the saturation or hook point of the assay is not reached, even up to concentrations of 25,000ng/L.

2.7.5.2 LoD

The limit of detection is a mathematical function of mean and standard deviation that has been used throughout this chapter as a tool to quantify assay sensitivity at various milestones of development. Finally, it was applied as a more rigorous validation step that aimed to follow the FDA-backed CLSI guidelines on LoD. Namely, a recommended 20 replicates of a blank and a low concentration are read from a standard curve before applying equations for LoB and LoD, noted in the introduction section 2.1.4. In Figure 2.4.2 the mean reading at a nominal spike of 30ng/ml was 33.3±11.8ng/ml, which was considered a lack of precision. For cTnI, the mean reading at a nominal spike of 30ng/L was 29.98±3.79ng/L, with the blank reading at 1.55±2.13ng/L. The precision was significantly better for cTnI readings, which infers a few hypotheses for the source of sST2 imprecision. Firstly, and believed most likely, was that the biotinylated antibody stock had been running low at the time of this assay, increasing the risk of pipetting aggregates from the stock. Aggregates could also have been forming in the quantum dot stock, with centrifugation recommended by the supplier in this case. Secondly,

the source of imprecision could derive from the contact between sST2 detection solution and plasma sample, as the troponin detection system does not have direct contact and does not suffer from non-specific interactions with plasma matrix components. A second biotinylation of the sST2 detection antibody will be performed to replenish stock, regardless, before the precision study, and so the opportunity to test this hypothesis will transpire.

For LoB, limits were determined as 5.4ng/ml and 5.07ng/L for sST2 and troponin respectively, which satisfies the sensitivity target for LoB, since these values are clinically irrelevant and would not change the course of treatment or diagnosis of a patient with any cardiovascular pathology. As for the LoD, this limit was calculated to be 11.3ng/L for troponin, which renders the assay suitable for use, considering this is around half of the 99th percentile for the healthy population.

This should ensure the assay is capable of reliably measuring pathological levels of troponin in the patients described in Chapter 4. For sST2, the story is different. The LoD is calculated to be 24.8ng/ml for sST2, which does not meet performance requirements for sensitivity. This is due to the LoD being almost exactly at the point of clinical cutoff for rule in/rule out significant levels of sST2, which would render the assay incapable of reliably measuring a range of samples between LoB and 25ng/ml. Based on the mean signals at 0ng/ml (0.00776 RFU) and 30ng/ml (0.02754 RFU), an LoD of much lower than 25ng/ml should be achievable, but the calculation is limited by the imprecision (standard deviation). Whilst analysing the data, it was also realised that the pool of EDTA plasma used to produce the standard curve, and the blank, is not validated for native sST2 level. It is possible, given that the pool was curated from multiple healthy donors, that the sST2 level could vary

anywhere from 0-25ng/ml. If at the higher end of that healthy range, the LoD could be completely confounded by these basal levels.

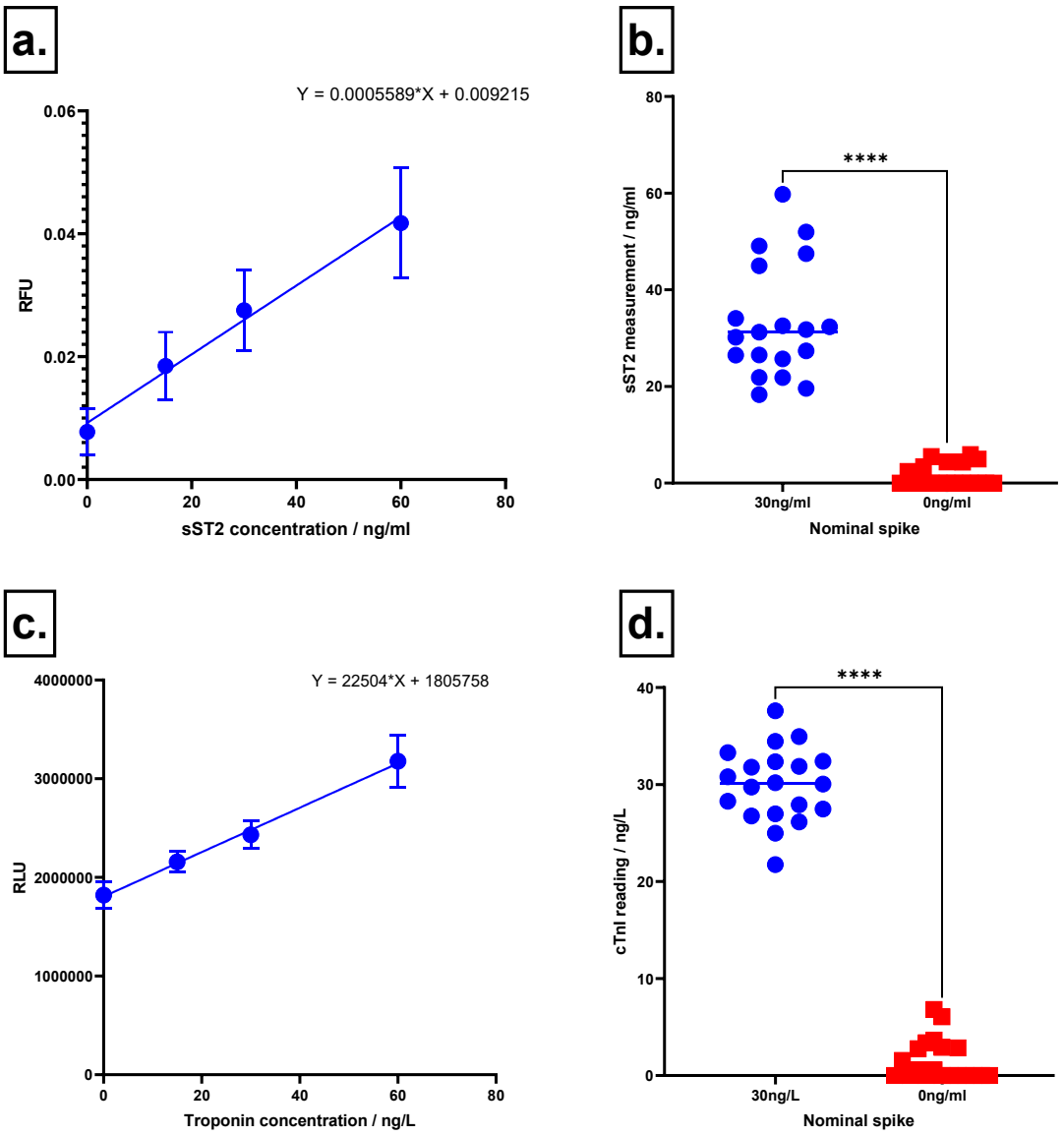

Figure 2.4.2 – Duplex LoD for sST2 (a. and b.) using pooled plasma was at 24.8nng/ml, confounded by basal analyte. LoD for cTnI was at 11.3ng/L (c. and d.). *T-test shows statistically significant differences (P=<0.0001) between the low positive spike and the blank in both cases (b. and d.). This assessment of LoD followed CLSI approved measurement of a blank and a low spike with 20 replicates, showing standard curve in a and c with LoD separation depicted in b and d. For each concentration, n=20. Error bars in a. and c. reflect SD.*

To investigate this concept, and in an attempt to measure the true value of this plasma, an approach was devised to “deplete” the plasma of sST2, by conjugating the sST2 capture antibody to 1µm diameter magnetic beads. The theory applied was that these beads, with anti-sST2 conjugated to their surface, when suspended in plasma could bind analyte before being separated using a magnet. The remaining plasma, now theoretically depleted, would be carefully pipetted away from the bead pile. This experiment was performed and yielded the results captured in Figure 2.4.3.

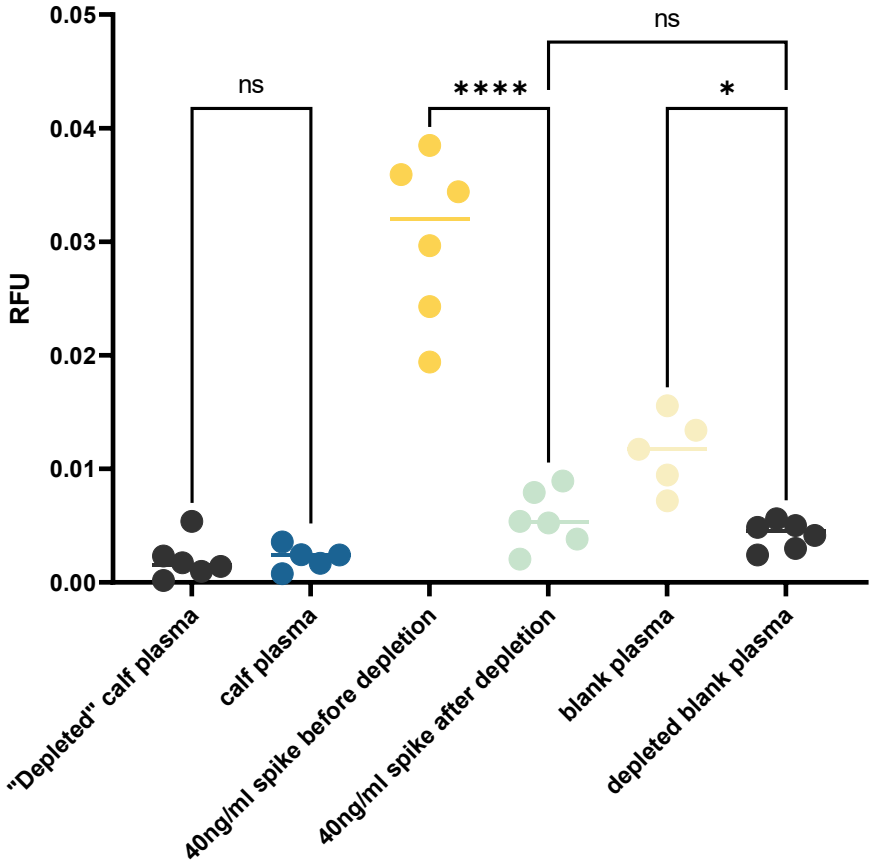

Figure 2.4.3 – A true “blank” human plasma pool sample is achievable via depletion of basal sST2 using antibody-conjugated magnetic particles. *There is a non-significant difference between the 40ng/ml depleted and the depleted blank plasma (P=0.1136), showing successful depletion. A significant different (p=0.0288) signal was found between the blank plasma and depleted blank plasma, indicating basal level. For each condition n=6, with error bars for SD.*

First to address is the result of the control sample, calf plasma. The anti-sST2 with human specificity is unable to bind bovine sST2 (and in fact, it is not confirmed whether cattle do produce sST2). This control was to match, as much as possible, human plasma from a protein abundance perspective, without risk of specificity. It was possible that the magnetic beads could just remove interfering matrix components non-specifically, allowing for a lower blank, rather than the complete absence of sST2 being attributable to lower blank signal. Based on this control, this concern is unlikely, based on the non-significance of signal in RFU between the "depleted" and non-"depleted" versions of calf plasma. Another control to corroborate this effect was the use of spiking the blank plasma to 40ng/ml, and measuring the signal produced by this sample before and after depletion with anti-sST2 conjugated beads. There was an extremely significant ($P=<0.0001$) difference between the spiked plasma before and after depleting, inferring a successful depletion protocol. In addition, there was a non-significant difference in the RFU signal of the spiked plasma after depleting, and the depleted "blank" plasma, which, in combination with the calf plasma control, confirms that the depletion was not only successful but also thorough. The spike of 40ng/ml was selected as a "stress test" for the depletion protocol, as it is impossible that any pool from healthy individuals will contain sST2 levels greater than, or even close to, 40ng/ml. This means that given 40ng/ml was successfully depleted, then the likely basal level of the pool (under 40ng/ml) will be successfully depleted too.

As for the main aim of this experiment, to determine whether basal levels of sST2 in the healthy pool were confounding the LoD calculations, it seems that this phenomenon was, in fact, skewing the sensitivity baseline of the sST2 assay. There was a somewhat significant difference ($P=0.0288$) between the "blank" plasma and the depleted "blank" plasma. In fact, if a linear regression is drawn between the latter and the 40ng/ml sample, the depleted

"blank" sample reads as containing 11.1±4.99ng/ml sST2. Again, this statistic lacks confidence due to size of CV, however, still confirms the presence of a basal sST2 concentration.

Upon repeating the LoD study, utilising the developed plasma depletion method, it was confirmed in Figure 2.4.4 that the actual LoD of the assay is around 10.3ng/L. This puts the assay well within the capability to distinguish between patients below and above the lower clinical cutoff of 25ng/ml. The LoB was also improved, at 2.24ng/ml. Since the previous LoD study, a new Siteclick™ biotinylation of the sST2 detection antibody was performed, and the quantum dot stock was spun down to remove any aggregates attributing to the imprecision. Concentration recovery CV using the standard curve is now at 16% for the 30ng/L spike which translates to 30.00+/4.88ng/L, which is within an acceptable range of imprecision, given the clinical decision made would not change drastically if a patient was to measure within this range. Patients on the borderline of clinical cutoffs are contextually assessed and the proximity of their biomarker levels to clinically relevant limits are taken into account.

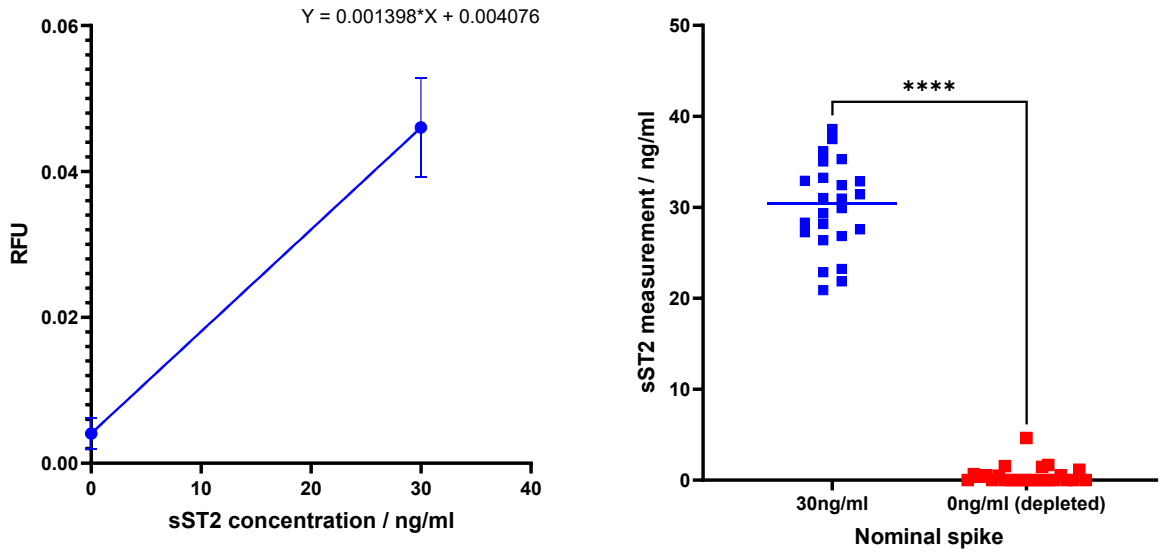

Figure 2.4.4 - A revised experiment using pooled plasma depleted of basal sST2 analyte shows a more accurate LoD of 10.3ng/ml. *A statically significant difference between the 30ng/ml sample and the blank (P=<0.0001) was identified by t-test. Error bars represent SD and n=24 technical replicates for each concentration.*

2.5.7.3 Matrix equivalency

Although not completely integral to the success of the assay, it is advantageous to achieve matrix equivalency in the most popular anticoagulants used for collection of whole blood in patients suspected of having MI. As already mentioned, these are lithium heparin (Lihep) and EDTA. Matrix equivalency is not only beneficial for optionality when drawing blood, but also reflects a robustness to Vacutainer© additive and matrix effects, producing more confidence in the accuracy of the assay. To thoroughly assess the effect, if any, of anticoagulant on the assay, fresh whole blood was obtained from 3 different healthy donors volunteering from Osler Diagnostics under anonymous donor numbers. This whole blood was subsequently centrifuged for 10 minutes at 3000 x g, before the plasma was separated from the buffy coat and erythrocytes to be used for the assay. 3 concentrations of both sST2 and cTnI were spiked into each donor's plasma and assayed following the duplex protocol. Figure 2.4.5 depicts the sensitivity and response of both the cTnI (plots a and b) and sST2 (plots c and d) assays at extreme ends of the linear range, to ensure equivalency across the whole curve.

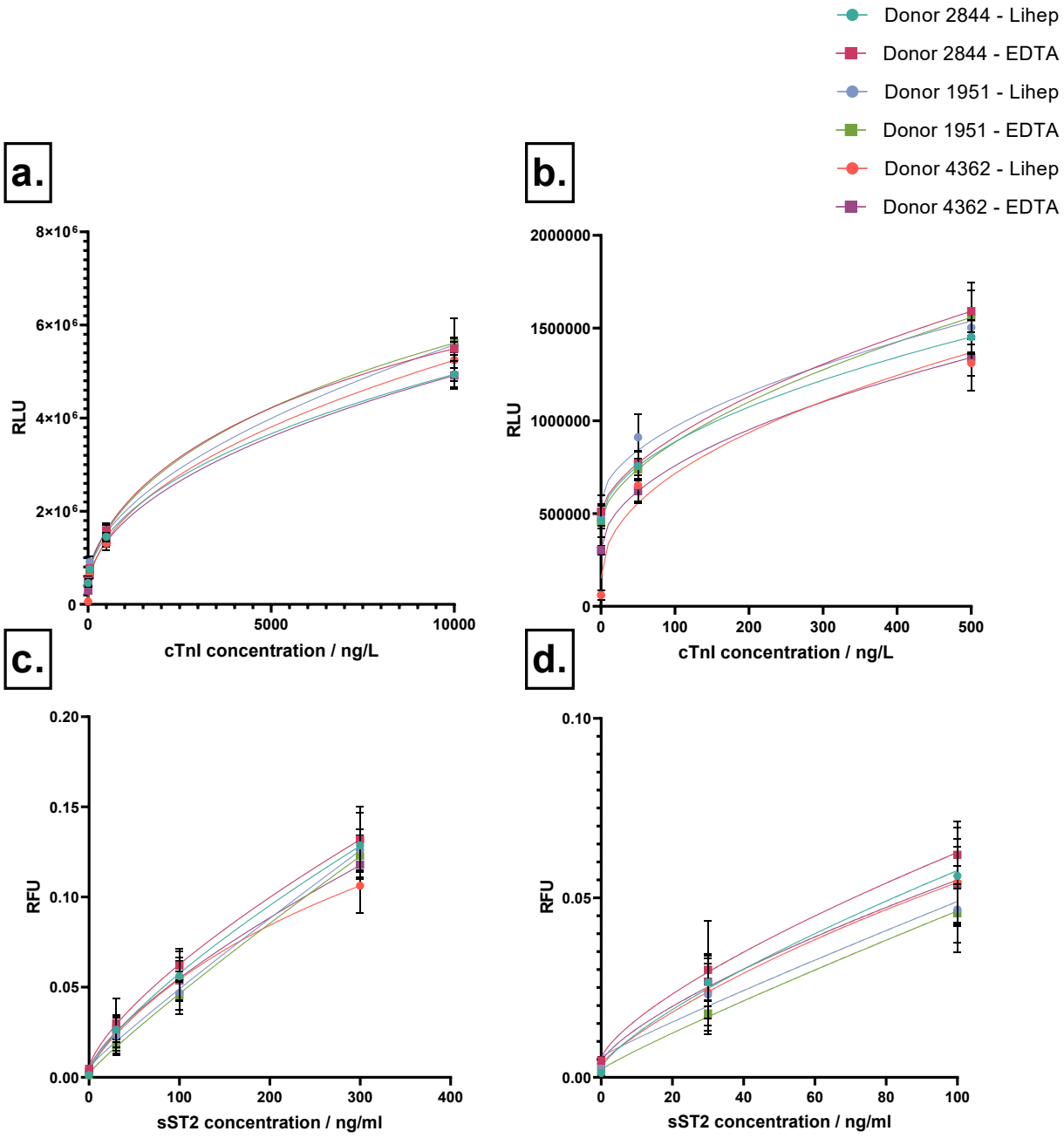

Figure 2.4.5 – Performance between EDTA and Lihep using the duplex assay is within error (error bars reflect SD), with the same equivalency observed between three different plasma donors. *Plots a. and b. show cTnI assay signal at different y axis resolutions. Plots c. and d. show sST2 assay response at different y axis resolutions. Standard curves were fit using a 4PL regression. n=4 for all concentrations except the blank, which was n=2.*

Based on the substantial overlap of response at all concentrations of both analytes, it was confirmed that the duplex assay was able to detect analyte at varying levels in both Lihep and EDTA anticoagulants. This is further supported by Figure 2.4.6, where a two-way ANOVA

shows no statistically significant difference between anticoagulant signal for all donors at two concentrations of both sST2 and cTnI on their respective curves. Although not an aim of this experiment, within the three donors tested it is also clear that the donor-to-donor variation is reasonably equivalent, again, demonstrating robustness to matrix effects outside of anticoagulant.

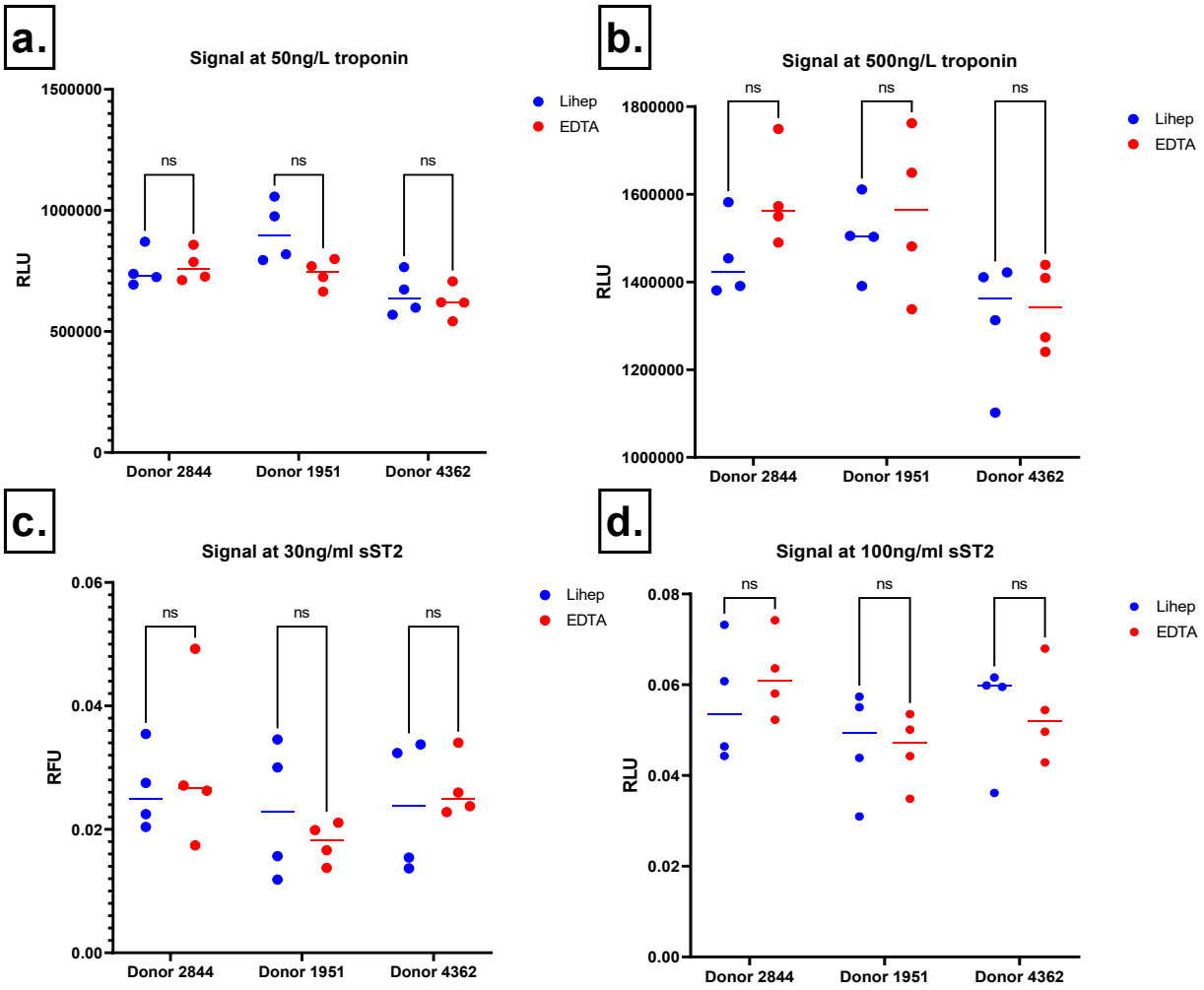

Figure 2.4.6 –2-way ANOVA showed no significant difference between types of anticoagulated plasma and cTnI readings at lower (a.) and higher (b.) spikes, with sST2 showing the same effect (c. and d.) *added to show complete equivalency between Lihep and EDTA anticoagulants at two different levels of cTnI and sST2, with n=4 for each condition.*

2.5.7.4 Precision

The CLSI guidelines on quantifying the precision of an assay recommends two main study designs: One involves measuring many replicates with the same operator in the same location over a short period of time, the other recommendation is reproducibility oriented, with different locations and operators. At this stage of the project, the first study design was considered most appropriate and feasible, given that it was not possible to test over a number of different sites. Therefore, precision assessment was carried out with 10 replicates on the same day with the same operator. In this exercise, human pooled plasma from healthy donors was spiked with cTnI and sST2 at different levels. Below, Table 2.7 capitulates the precision of a range of measurements in raw signal.

cTnI			**sST2**		
Concentration of analyte (ng/L)	Signal mean±SD (RLU)	**CV (%)**	Concentration of analyte (ng/ml)	Signal mean±SD (RFU)	**CV (%)**
25000	1.8E+07±644223	**3.51**	4000	0.34091±0.01279	**3.75**
12500	1.1E+07±871517	**7.95**	2000	0.36322±0.02114	**5.82**
6250	7570500±266815	**3.52**	1000	0.37168±0.00766	**2.06**
3125	7317700±265413	**9.91**	500	0.30158±0.00424	**1.41**
1562.5	6539400±265413	**4.05**	250	0.17336±0.01472	**8.49**
781.25	4988900±143339	**2.87**	125	0.1051±0.00213	**2.02**
390.63	3871200±106743	**2.75**	62.5	0.06624±0.00995	**15.02**
195.31	2895100±149669	**5.16**	31.25	0.03251±0.00215	**6.60**
97.66	2469500±142804	**5.78**	15.63	0.2745±0.00697	**25.39**
48.83	1926200±73775	**3.83**	7.81	0.01639±0.00420	**25.60**
24.41	1641800±79219	**4.82**	3.91	0.01177±0.00426	**36.16**
0	1214700±48805	**4.02**	0	0.00962±0.00229	**23.77**

Table 2.7 – The precision of the duplex assay at a wide concentration range of both cTnI and sST2, expressed as CV.

2.8 Pilot clinical study

To finalise the validation of the duplex assay, and to prepare for the clinical cohort, a pilot study evaluating sST2 and troponin levels in human clinical samples was conducted using 48 human plasma samples. The purpose of these experiments was twofold; firstly, to benchmark the relationship between the duplex assay troponin measurements against the

predicate Abbott Architect readings for assurance of accuracy. Secondly, to measure, for the first time, sST2 levels of patients diagnosed with MI. Also, amongst the samples measured are patients not diagnosed with MI, but with alternative diagnoses, with both cardiac and non-cardiac aetiology. It was deemed important to select samples of patients that presented to A&E with symptoms of MI, or that clinicians felt the need to rule out MI, for this is the demographic of patients for proposed application of the duplex assay. For the detailed process of sample acquisition at Salford Royal Hospital to preparing the sample for assay, please refer to the methods section of Chapter 4.

The measurement of human plasma samples was done in triplicate side by side, with the total number of samples spanning two 96 well plates. A standard curve, also in triplicate, was run on each plate, and samples were read off the 4PL regression on their respective plate, to control for any potential plate-to-plate differences. Firstly, sST2 levels were plotted against troponin levels, shown in three versions of the same data, in different resolutions, in Figure 2.4.7. As indicated by the dotted lines, cutoff was approximated at 35ng/ml for sST2, separating the positive from the negative samples. Additionally, patients diagnosed with either STEMI or NSTEMI are highlighted in red. Patients diagnosed with heart failure historically, or as a result of the hospital visit pertaining to these plasma samples, are marked in blue. In this Figure, plots A and B do not show a statistical correlation between troponin and sST2 concentrations. However, when a Pearson r test was run on plots c and f, a statistically significant correlation was found ($r=0.4093$ with a 95% confidence interval of 0.07073 to 0.6633, $p=0.02$). Importantly, this covers 32 of the 48 samples, which is most of this pilot cohort. Plots A and D of Figure 2.4.7 show that samples measuring the highest concentrations of troponin have sST2 concentrations of just around the clinical cutoff. This

hypothesis needs to be tested with more samples to establish its relevance, which will become apparent in Chapter 4.

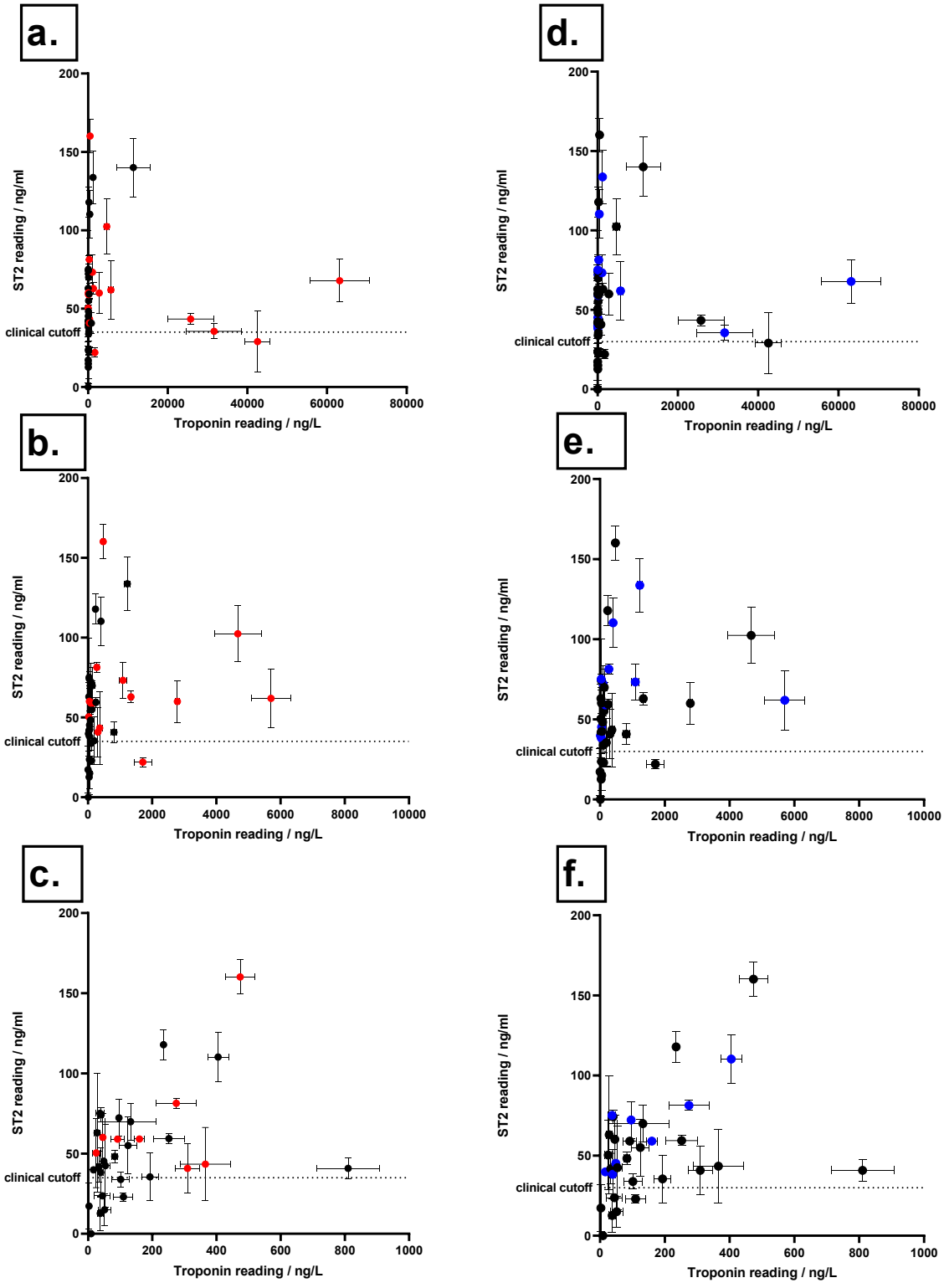

Figure 2.4.7 - Correlation plots between sST2 and cTnI readings produced by the duplex assay in sequential resolution from a-c and d-f show. *Plots a-c contain points in red, which depict patients diagnosed with MI. d-f show the same data except blue points highlight patients diagnosed with heart failure. Black data points represent patients that were suspected of MI, but had a differential diagnosis. Each point represents one donor with SD error bars reflecting n=3.*

An additional important observation is the correlation between the duplex assay reading of troponin and the hospital measurement of troponin, which was made on the Abbott Architect. As apparent from Figure 2.4.8, there are 3 outlying samples from the correlation, attributing to two false positive and one false negative reading, circled. Pearson r correlation coefficient for all samples was 0.39 (95% CI 0.1138 to 0.6119) and an R squared of 0.153. P value was 0.0072. This is somewhat skewed from the general population due to the circled outliers. All immunoassays, whether in the form of automated analysers or lab-based ELISA kits, are vulnerable to false positive and false negative results (Pretorius, et al., 2011). A comparative study in 2011 found the prevalence of outlying samples with clear clinical impact on the Abbott Architect to be between 0.02-0.2% (Pretorius, et al., 2011). By comparison, the duplex assay with 3 out of 48 samples giving false results is at 6.25%. However, this is with only 48 samples and may not be representative of a population, whereas the previously referenced study tested a total of 2391 samples. Considering the intention to read approximately 300 more samples in the clinical study of this thesis, false positivity and negativity will be re-evaluated with these data set and rates estimated again. Precautions via the addition of heterophile blocker to the diluent have been taken to negate human anti-species antibodies from interference by binding to the Fc regions of the mouse capture antibodies and the rabbit detection antibodies. When the data in Figure 2.4.8 are analysed with the removal of the three outlying samples, Pearson r increases to 0.9311 (CI 0.8756 to 0.9623) with an R^2 of 0.8669, P=<0.0001.

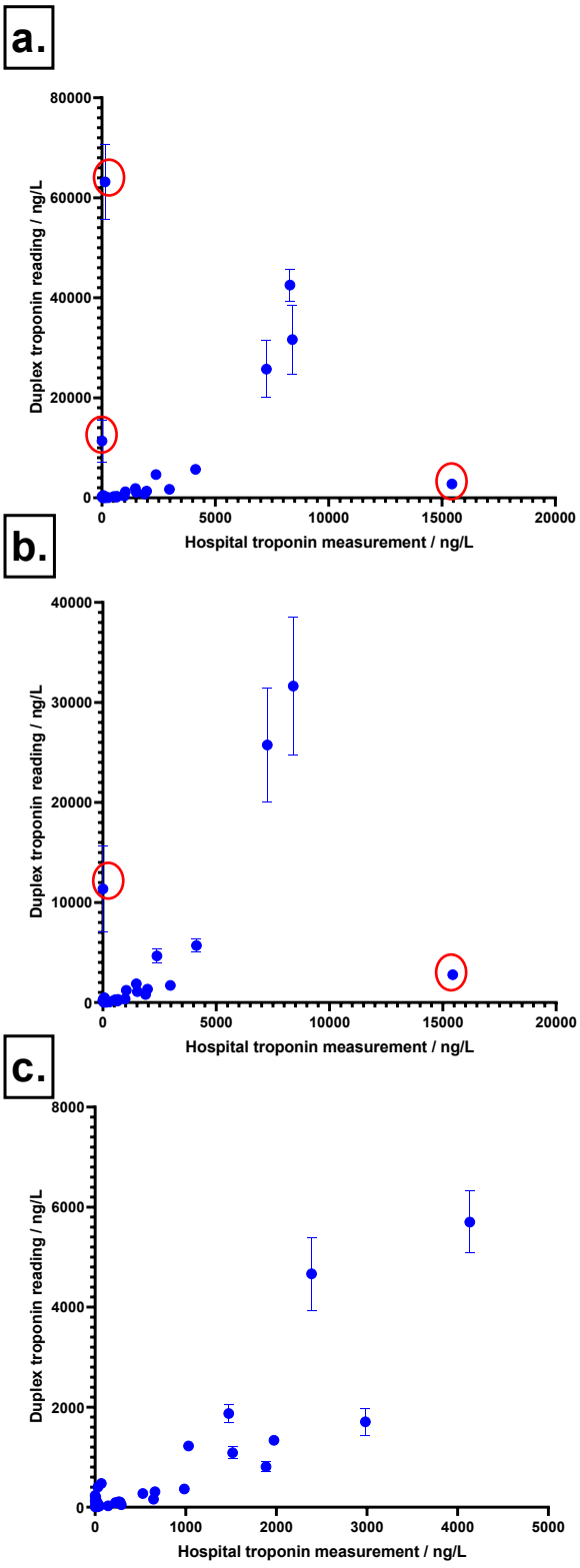

Figure 2.4.8 – Duplex cTnI readings correlate strongly with the hospital cTnI measurements (Pearson r = 0.9311, 95% CI 0.8756 to 0.9623). *Scatter plots in increasing XY resolution from A-C, showing the relationship between the hospital troponin measurement and the duplex troponin reading. Circled in red show particularly deviating samples from the correlation. Each point represents one donor and SD error bars reflect n=3. R^2 for agreement is 0.8669, (P=<0.0001).*

In addition to clinical sample measurements, an established cohort of normals is important for validation and for comparison against those with MI. A group of 37 healthy individuals, employees of Osler Diagnostics, donated their blood with consent for participation in assay development studies. These donors were assayed for sST2 to corroborate literature-derived limits for basal levels (under clinical cutoff). Upon a two-way ANOVA analysis, Figure 2.4.9 shows the relative measurements of sST2 of the normal samples in comparison to MI and HF diagnoses from the pilot clinical cohort samples. Each diagnosis group (MI, HF or MI and HF) had a very large statistically significant (P=<0.0001 in all cases) difference between the sST2 levels of normals, further confirming the presence of pathologically high levels of sST2 in MI.

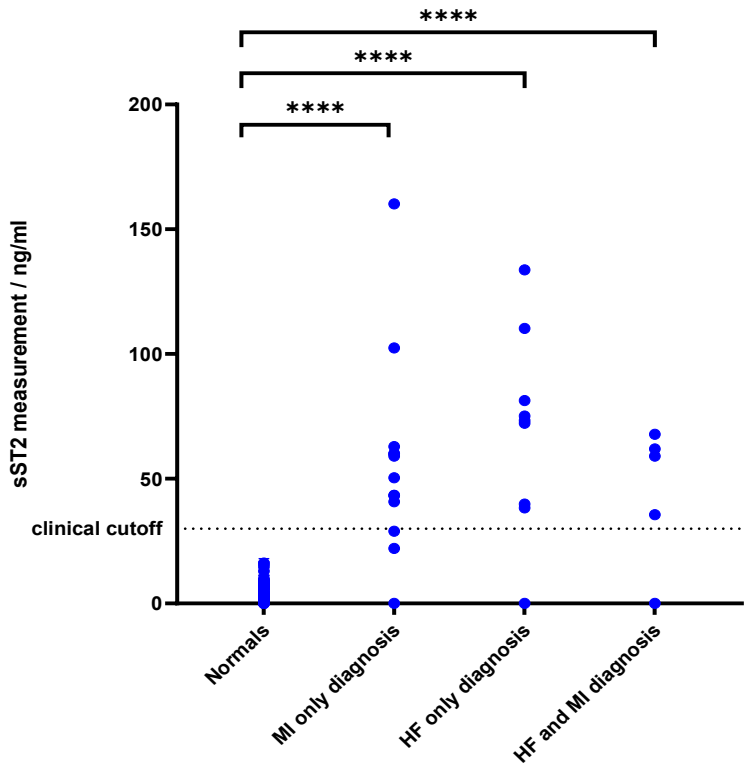

Figure 2.4.9 – The plasma sST2 levels of patients diagnosed with HF or MI (or both) are significantly higher than the average plasma level of sST2 in a cohort of normals (P<0.0001). *A grouped plot to show relative sST2 presence in the plasma of healthy (normals) (n=37), to MI (n=13), HF (n=9) and MI with HF diagnoses(n=5). All groups were equally statistically significantly (P=<0.0001) difference from the normals cohort.*

2.9 Discussion

This chapter presents a feasible solution for the measurement of cTnI and sST2 simultaneously in both EDTA and Lihep human plasma, with sensitivity capabilities that allow significant distinction between healthy and pathological levels of each analyte. This has been enabled by an extensive screen of the best commercially available reagents, as well as optimisation of in-house buffers, various antibody conjugations and incubation conditions. Using the described method, an sST2 and cTnI measurement can be obtained in 30 minutes, using only 25µL of plasma, which equates to just a few drops of blood. LoD targets are met for both assays as described in section 3.7.5.2, at approximately 10ng/L for cTnI and 10ng/ml for sST2. Linearity calculations also produced a successful outcome and span the entire clinically relevant ranges of both sST2 and cTnI.

After an extensive exploration into dual measurement methods, a streptavidin linked quantum dot was identified to be sensitive and compatible for assay alteration for the distinction of both biomarkers, keeping HRP-mediated chemiluminescent signal detection for cTnI readings. From an assay development perspective, the experiments designed to increase performance as transparently described hope to contribute to the growing body of knowledge surrounding assay development techniques, upon which the diagnostic industry completely relies. The addition of large (PEG-11) linkers for biotin attachment to IgG for reducing steric hindrance is not completely novel, but rarely compared directly for assay sensitivity, in addition to the cleavage of antibodies via disulfide bridge for smaller, more kinetically advantageous analyte detection. In addition, the industry of commercial assay diluents relies on secrecy of key players in the reduction of background and boosting of specific signal but is

broken down in this chapter to reveal influence of protein, salt and surfactant in formulation development, to enable academics to access this transparently.

Another finding of this chapter is a method of analyte depletion to enable blank sample production for LoD calculations. This is extremely important for the accurate read off of clinical samples from standard curves. If the blank sample in the standard curve actually contains basal levels of sST2, all clinical sample readings will be slightly underestimated. This may be the case for the pilot clinical study, since this finding of basal sST2 depletion was not found until after the clinical samples in the pilot study had been read, and so readings obtained for patients with MI and HF may, in reality, be slightly higher than stated. However, given the low level of basal sST2, this is not expected to change results in such a way that changes conclusions about the relationship between MI sST2 levels and healthy donor levels. If anything, the relationship in Figure 2.4.7 appears slightly less significant than in reality. In the same vein, it was also discovered that the blank measurement of sST2 had a CV of around 20%, which welcomes the question about whether the depletion method affected the blank, or if this is in fact representative of precision at such low signals.

Duplexing ensures that the time between drawing of the sample and measuring of the analyte is exactly the same for both biomarkers, negating concerns about unequal integrity of the target analyte as the stability of the sample decreases over time. Furthermore, obtaining both cTnI and sST2 results at the same time allows for consideration of sST2 level with potentially high cTnI, enabling clinicians to factor in sST2 determined cardiovascular risk at the at the 3-hour time point at which MI is confirmed. Theoretically, two patients with the exact same troponin increase profile between measurement at point of admission, and measurement 3 hours post admission, could have differing serum sST2 abundance. This is

supported by the data described in the pilot clinical study, where a weak but statistically significant correlation between cTnI and sST2 within the range of 0-1000ng/L and 0-300ng/ml respectively, shows that although it is likely that the higher the troponin, the higher the sST2, the degree of sST2 increase at a given cTnI concentration can differ. From a medical point of view, decisions about the strength of intervention could be supported by sST2 readings to assess risk of MACE and death in a physiologically novel way by comparison to NT-proBNP. It is acknowledge, however, that the performance of the sST2 part of the duplex assay could be strengthened by an additional comparison to the Presage® assay by Critical Diagnostics, the current FDA approved assay for sST2.

In addition to the relationship observed between cTnI and sST2, the relationship of sST2 between healthy and disease populations is of great interest. As stated in the introduction, there is some literature that observes increased sST2 levels beyond clinical cutoffs in MI, however some studies refute that claim. From this initial pilot study, it is clear that this assay does distinguish a stark contrast between the means of the normals group and the MI group, suggesting a clear association between oxidative stress-like injury and the release of sST2 into the circulation. As more confidently established in the literature, sST2 levels are also increased in the HF group, implying a role for this biomarker in both aetiologies. Despite these encouraging observations, the pilot study is limited in patient sample size, with only 20 patients in the cohort being diagnosed with MI. Having said that, this study served it's purpose as a preliminary snapshot of sST2 levels in MI and HF patients and the issue of sample size is rectified with the measurement of additional samples in Chapter 4.

In summary, the development of the duplex assay was successful, and meets all of the analytical pre-requisites outlined in the aims section. However, assay outliers (false positives

and negative) are the biggest limitation seen in performance so far, with precision also yet to be observed within and between plates using cardiac markers in the larger clinical cohort. A second re-appraisal of these concerns will be conducted upon the completion of the clinical study to ascertain the confidence in conclusions made as a result of those data.

3. Mechanistic investigations of sST2 pathway activation and expression in *in vivo* and *in vitro* injury models

3.1 Introduction

3.1.1 Aim and hypothesis

This chapter investigates hypotheses pertaining to the molecular influence of sST2 release downstream of the ST2L transmembrane receptor; specifically, that when cells are subjected to hypoxic conditions, sST2 will be increasingly released and the pathway downstream of ST2L becomes downregulated. Additionally, a HF model using AngII will be used for comparison of the contribution of both types of injury to sST2 upregulation on the protein level, where it was hypothesised that both will cause similar effects. Finally, the *in vivo* experiments tested the hypothesis that after LAD ligation to induce MI, sST2 is released quickly (within 24 hours) of injury, making sST2 an appropriate biomarker for measurement in the short time frame in which an MI diagnosis is made.

The aim of this chapter is to further explore the mechanistic basis and relevance of sST2 expression and release following myocardial injury, acknowledging that the upregulation of sST2 mRNA and protein can be systematically investigated, in an invasive and controlled manner in animal and cell culture models, that is impossible to achieve in human subjects. This broad objective can be categorised into four sub-objectives, namely 1) to characterise the release profile of sST2 in a controlled surgical model of MI, over a 28-day period; 2) to confirm both mRNA and protein release of sST2 in cardiomyocytes subjected to hypoxia and hypertrophic agonists; 3) to understand whether expression or activation of other IL-33/ST2L axis components correspondingly change with each type of injury; 4) to shed light on the

disagreement in the literature about whether sST2 release predominantly correlates with HF, MI, or both.

Human plasma samples, although useful for other objectives, have a number of confounding factors and variables contributing to inflammation physiology; however, animal studies allow the pairing and control of several characteristics contributing to injury such as infarct size and location of occlusion, etc. Additionally, animal models can provide information on serum concentration of sST2 in response to arterial occlusion by permanent coronary artery ligation in surgery, where exact timing of infarction, and ostensibly the size of it is controlled. In a human clinical setting, patients present at a variety of times post-onset of symptoms and researchers are required to rely on accurate self-reporting.

At the time of writing this thesis, a refined relationship between sST2 release and infarction of the myocardium over a concentrated period of 28 days was unknown, and its release profile assayed from mouse serum post-MI is under-explored. This is also true of sST2 pathway activity, in terms of upstream activators or downstream effectors, where nothing is currently published. After all, as mentioned in the literature review, only 10 papers have ever explored sST2 release in CM injury models, where focus has been on therapeutic agents to stimulate the protective pathway (Zheng, et al., 2022) or most recently, genetic knockouts of miRNA (miR-1268a) affecting sST2 expression associated with HF, but not MI (Xu, Xu, Zhang, Kao, & Li, 2024). Notably, both of the studies using H9c2 as a cell model did not state whether the cardiomyoblasts were differentiated before injury. If undifferentiated, one could argue that the injury model, and therefore responses, do not accurately recapitulate human CM behaviour.

Despite uncontrolled variables between patients, clinically concerning levels of sST2 have been detected by ELISA in patients within 5 hours of onset of MI symptoms (Pérez-Martínez, et al., 2018). What is equally important to decipher is not just the binary presence or absence of sST2 after MI (and because of MI), but the release profile and the stability of the protein in serum after the event. Whether the protein is continually secreted or broken down and excreted soon after the stimulus is removed, is highly relevant to its clinical utility. As a result of the studies described in the literature review of this work, it is hypothesised that sST2 expression and translation are increased in response to MI-specific injury (oxidative stress), and that the peptide is stable and present in the animal bloodstream within 24 hours of MI, and for at least 3 days post-MI.

As for the cell-based work, the aim is to establish an *in vitro* injury model using H9c2 cardiomyoblasts to investigate release (if any) of sST2 as a direct result of hypoxic injury, confirming mechanism of release as a result of injury stimulus to CMs. As previously mentioned, the literature contests the observation that humans with MI produce sST2, and there are only two published observations of sST2 upregulation in cardiomyocytes. As a consequence, a secondary aim of this chapter is to also clarify a HF-associated injury (hypertrophy) with sST2 expression on both the mRNA and protein level. In comparison to MI, there is more evidence to associate HF with sST2 release, but it is hypothesised that both injury stimuli will induce sST2 upregulation.

In addition to confirming sST2 presence, there is an additional objective to clarify and compare activation of various components of the pathway downstream of IL-33/ST2L interaction, namely, MAPK, AP-1, NF-κβ, IRAK-1 and MYD88. If significant downregulation of these factors is observed after injury, correlating with injury severity, more can be inferred

about how sST2 release affects the levels of transcription factors responsible for promoting anti-hypertrophic responses. If sST2 is indeed observed to increase with time subjected to H_2O_2 and the pathway is downregulated causing the promotion of adverse remodelling, sST2 arguably qualifies as a biomarker for MI.

3.1.2 Rationale

Despite the success of human duplex assay development, the mouse specific assays for cTnI and sST2 do not require impressive TTR or a defined range of sensitivity and linearity. Due to the fact that there is no time pressure to produce readings, given the purpose is animal and lab based rather than being pitched as a clinical solution, assay development was less requiring of rigorous validation and performance review.

Obviously, the rate at which sST2 is released post-MI specifically (if at all), is relevant to its value as a biomarker to be measured with troponin, and so this should be elucidated. The confidence in which this can be established informs the rationale of the whole thesis, and the practicality of a duplex assay. Regardless of the outcome, this chapter should fill the gap in current knowledge surrounding sST2 release as a result of MI, specifically. Understanding biomarker responses to specific injuries and pinpointing their roles following injury is essential to underpin their utilisation for diagnostic or prognostic tool in a clinical setting. As previously alluded to, the exact injury type(s) in which sST2 is upregulated have yet to be convincingly elucidated. To investigate this, assays for both sST2 and cTnI will be developed (for mouse antigen, rather than human antigen as per Chapter 2) for the assessment of biomarker release over time post-injury, with cTnI serving as a validator of infarction.

The end point user and application of the proposed sST2 measurements are for clinical use in the case of MI. However, the *in vivo* experiments involving LAD ligation in which a live

animal is subjected to MI – the closest and most controlled experiment that can be conducted to replicate human cardiac ischaemic injury and resulting necrosis, to inform on the injury response at the local and systemic levels, in a physiological context. In contrast, a CM model subject only to the physiology of its immediate surroundings without interaction with other organ and tissue systems, allows for the impact of specific and calculated injuries to be independently assessed. The work of this chapter is therefore integral to link cause and effect on a molecular scale between MI-like injury and sST2 expression *in vitro* and *in vivo.*

3.2 Methods

3.2.1 Mouse model study design

For the full assessment of sST2 association in serum with mechanical and physiological manifestations of MI, various methodologies took place within the study design. Mice were allocated to each time point across the range, which consisted of 1 day (n=3),3 days (n=2),7 days (n=1),14 days (n=2) and 28 days (n=2). Sham surgeries were conducted in additional animals at 1 day (n=1) and 28 days (n=1). Serum was collected following the procedures described in section 3.2.2.

3.2.2 Surgical method

As referred to at the beginning of this thesis, all surgeries and animal handling was conducted by Shih-Hsuan Mao. All animal procedures were approved by the institutional ethics committee and the United Kingdom Home Office and were performed on 12- to 14-wk-old female (C57BL/6J) (Charles River) mice. General anaesthesia was induced using 4% Isoflurane in oxygen. Next, the animal was intubated by a 22-gaµge IV catheter and connected to a ventilator (rate: 180-200/min; tidal volume: 6 to 8 µl/g) and injected with analgesia

Vetergesic (1.1 mg/kg). Once the animal was stabilized, the isoflurane was maintained at 2.5% in oxygen. Following sterilizing the left chest wall, a 1-cm incision was made to expose the underlying muscle. The pectoris muscles were carefully retracted without damaging them. Thoracotomy was then performed via 3rd or 4th intercostal space. The pericardium was removed, and the LAD ligated, 1.5 mm below the atrioventricular groove from the atrial appendage using a 8-0 nylon suture (S&T). This was an attempt to maintain consistent ligation site, as the anatomy of the LAD is known to vary. The occlusion was confirmed by myocardium blanching. The intercostal space was re-approximated by 6-0 Prolene sutures (Ethicon). The pectoris muscles were re-draped, and the skin was closed by 6-0 Prolene sutures (Ethicon). Following the return of spontaneous breathing, the animal was extubated and observed for one hour in the recovery chamber at 37°C. The animals were monitored closely in the first 7 days following surgery. Schedule 1 culling was performed if the animals reached a humane end point.

3.2.3 Assay development for mouse cTnI and sST2 targets

Antibodies for assay development were obtained by Hytest, and optimisation of their concentrations for sensitivity was assessed by titration with HRP for enzymatic turnover of luminol for chemiluminescent reading. Optimised conditions for the cTnI assay consisted of 80µg/ml capture antibody (clone 4C2cc) coated for 1 hour, followed by PBS-T 0.1% washing at 100µL for 4 repeats, then blocking using StabilBlock for 1 hour. After this, sample is pre-diluted 1:1 (25µL sample, 25µL diluent) using the assay diluent developed in chapter 2 for human assay development. This 50µL diluted sample is added to the 96-well plate immediately before 50µL of detection solution, which consisted of 1µg/ml detection antibody (clone 19C7cc) and 1µg/ml polyHRP supplied by Osler Diagnostics. This was incubated for 20 minutes in a 40-degree climate chamber, shaking at 450rpm. After the incubation period, the

plate was washed again four times using PBS-T 0.1%, then read spectrophotometrically using 100µL luminol supplied by Neogen. The sST2 assay followed the exact same procedure except with the substitutions of specific antibodies, where 40µg/ml S215 was coated for the capture step, and 2µg/ml S103 and 2µg/ml polyHRP was incubated in assay diluent for the detection step.

3.2.3 Cell culture and injury

The H9c2 cell line was selected for their ease of culture, cost effectiveness and well-cited ability to respond to stimuli simulating disease (Watkins, Borthwick, & Arthur, 2010) (Kuznetsov, Javadov, Sickinger, Frotschnig, & Grimm, 2014) (Osuru, Lavallee, & Thiele, 2022). Injury models to reflect HF and MI were selected from peer reviewed examples of injury in H9c2, where AngII (at concentrations between 50-400uM) was identified as a popular and robust agonist for simulation of HF-associated physiology and demonstrated equivalent hypertrophic responses to that of primary cardiomyocytes (Watkins, Borthwick, & Arthur, 2010) (Yang, et al., 2017) (Ren, et al., 2023) (Cheng, et al., 2024). For ischaemic injury to imitate MI, H_2O_2 was selected for it's ability to induce oxidative stress, which is also a widely acknowledged protocol for observation of myocardial ischaemia injury. (Witting, Liao, Harris, & Neuzil, 2006) (Oyama, Takahashi, & Sakurai, 2009) (Ihara, Urata, Goto, & Kondo, 2005) (Zhang Y. , Liu, Li, & Ye, 2021). The concentration of H_2O_2 used to induce oxidative stress from these papers has ranged from 10uM to 400uM with varying incubation times. Concentration of both AngII and H_2O_2 was optimised in a pilot study before the study described in the results section 3.3.2.

H9c2 cells were obtained from existing frozen stock and thawed for plating in a T75 flask using DMEM supplemented with 10% FBS and 1% penicillin-streptomycin. Cells were plated at passage 11 and cultured until passage 15, at which point there were sufficient cells

for differentiation. Once observed to have reached confluency, medium supplemented with 20% horse serum was given and replaced every 48-72 hours. Differentiation was visually affirmed by the formation of spindle fibres. At peak differentiation, medium was removed and replaced with DMEM spiked with two concentrations of H_2O_2 (50µM and 100µM) to initiate oxidative stress, for either 4 or 8 hours. This optimisation took place alongside a second injury study utilising AngII at either 100µM or 200µM for 24 or 48 hours as an agonist for hypertrophic cardiomyopathy, with the intention of inducing heart failure-like adaptations and injury for the observation of sST2 response. After injury, wells were washed with ice-cold PBS and frozen immediately at -80°C.

RNA extraction was performed using the RNeasy mini kit (product code 74104) according to the manufacturer's protocol. Post-extraction, cDNA synthesis was performed using New England Biolabs Protoscript® II reverse transcription (product code E6560), according to the manual provided with the kit. cDNA was quantified by nanodrop and frozen at -20°C before preparation for RT-qPCR.

3.2.4 rt-qPCR using SYBR green and TaqMan probes

Oligonucleotides and Taqman probes were purchased from ThermoFisher (sequences found in Appendix item C, Table 7.1, page 204). In a 20µL reaction, 10µL was mastermix, 1µL was TaqMan probe, 4µL of cDNA (50ng) and 5µL RNase free water. For SYBR green, two pairs of primers were screened for efficiency by melt curve analysis, with the best being selected for the injury study analysis. Targets were selected based on their involvement in hypertrophic and oxidative stress physiology.

3.3 Results

3.3.1 scRNA-seq for IL1rl1 in MI and uninjured mice

scRNA-seq is a useful tool for mapping expression of particular genes at the transcriptome level to visualise responses to injury stimuli. Using metadata collected from the literature, expression of different genes was evaluated by UMAP comparison to observe cellular diversity within a cardiac context vs an uninjured control. These metadata can be seen in Appendix item D, Table 7.2, page 205-206. The results of the UMAP analysis are shown in Figure 3.1.1. The plots provide insight into which cell types express particular genes and how their expression is influenced by injury such as MI. More specifically, *Il1rl1* is mainly expressed in CMs, myeloid cells, lymphocytes and fibroblasts (Figure 3.1.1, panel D), and appears to be modestly responsive to MI *in vivo* in CMs (Figure 3.1.1, panels B and C), giving reason for this cell type to be selected for culture for injury modelling since these data confirms expression both in the uninjured and injured conditions.

UMAP panels E-P in Figure 3.1.1 show the response of control gene markers for specific cell types (e.g. *Cd68* for macrophages and *Myh6* for CMs) for confirmation of ischaemic injury and comparative expression to *Il1rl1*. What can be observed from the figure as a whole is that *Il1rl1* expression, although increased after MI, is confined to a small proportion of CMs and immune cells, and is not a key player in the inflammatory response induced post-MI. However, the fact that it is upregulated at all still indicates a role as a biomarker, providing that sST2 expression is also observed accordingly at the protein level.

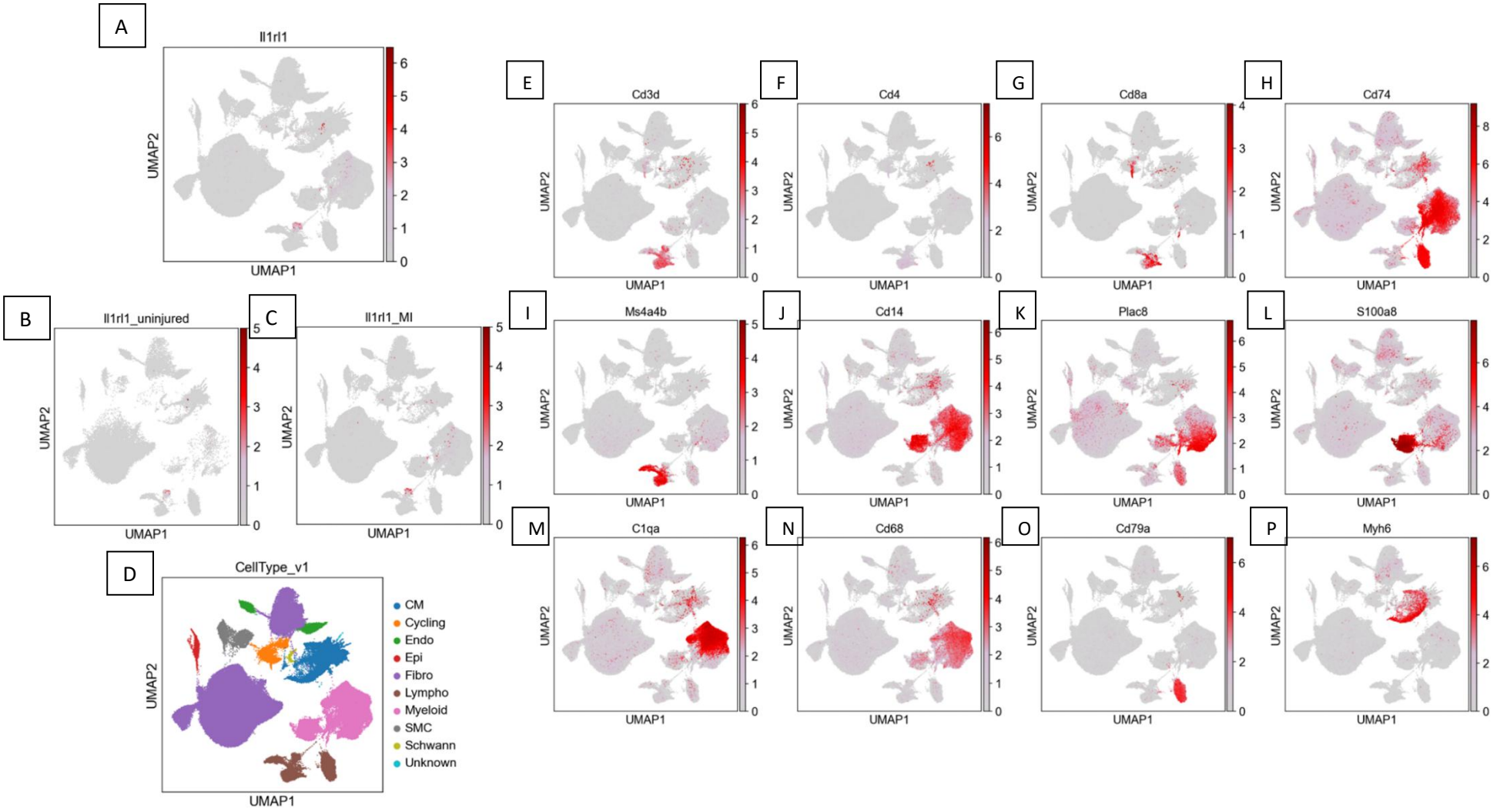

Figure 3.1.1 – A UMAP projections display the expression of various marker genes across different cell populations in the heart. *Feature plots for genes associated with immune cells (Cd3d, Cd4, Cd8a, Cd74, Ms4a4b, Cd14, Plac8, S100a8, C1qa, Cd68, Cd79a) and cardiac fibroblasts (**Il1rl1**, including comparisons between uninjured and myocardial infarction (MI) conditions). The colour scale represents normalized expression levels, with red indicating higher expression. (Bottom left panel) Cell type classification based on clustering, showing distinct populations including cardiomyocytes (CM), endothelial cells (Endo), fibroblasts (Fibro), myeloid cells, lymphocytes (Lympho), smooth muscle cells (SMC), and Schwann cells.*

3.3.2 Murine characterisation of sST2 release profile

3.3.2.1 ELISA optimisation

cTnI

Assays for the measurement of mouse sST2 and cTnI were developed from scratch for a couple of reasons. Firstly, the requirement from commercial ELISA kits of sample volume was too large (50µL for one replicate) for the volumes of the samples obtained from the MI study. Secondly, the development of an in-house assay allows for fine tuning of performance metrics such as sensitivity and range; by comparison, the widest analytical range available for mouse serum sST2 measurements is from 0.1-10ng/ml, which risks being insufficient.

Checkerboard titrations carried out under similar conditions as described in Chapter 2 were performed and evaluated by signal to noise ratio. The pair with the highest signal to noise ratio was then titrated in standard curves with varying detection antibody concentration. The best antibody pair was Hytest clones 4C2cc and 19C7cc, that have specificity for mouse troponin, with a signal to background ratio of 31.1 at 200ng/L cTnI and 0ng/L cTnI (see Figure 3.1.2).

Evidently, increasing the 19C7 and HRP concentration from 1µg/ml (Figure 3.1.2, plot a) to 2µg/ml (Figure 3.1.2, plot b) increases slope for all concentrations of capture antibody. Slope was calculated as 41265 RLU/ng/L for the condition using 80µg/mg 4C2 capture antibody and 1µg/ml 19C7 detection antibody with an equal amount of polyHRP. This was very close to the slope achieved with 2µg/ml detection solution and so it was decided to proceed with 1µg/ml for cost/benefit reasons. The data described in Figure 3.1.2 were acquired using the optimised assay diluent from Chapter 2 to first evaluate performance in a simple matrix.

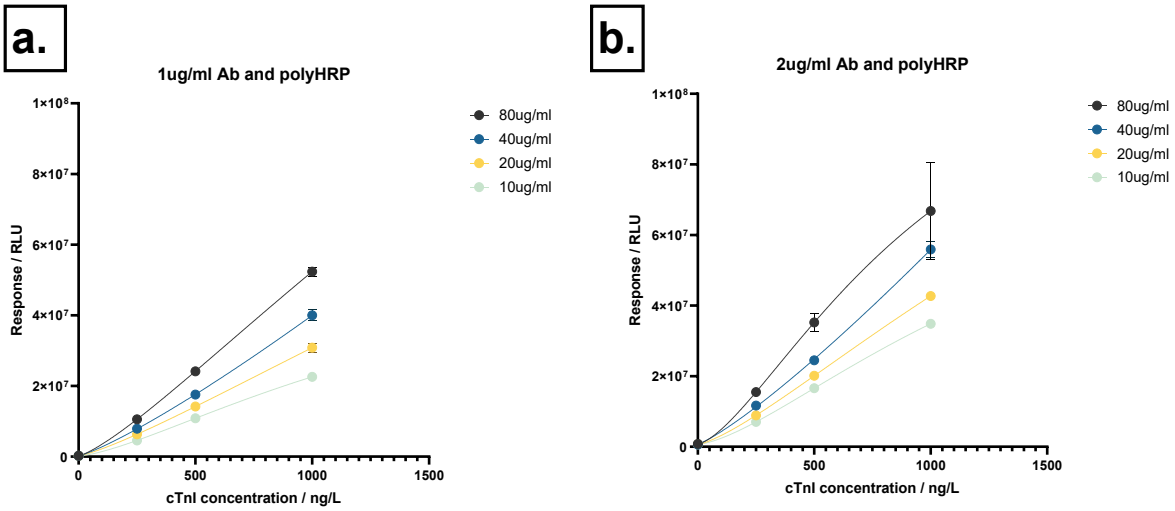

Figure 3.1.2 – Titrations of primary antibody with either 1µg/ml Ab (antibody) and polyHRP (a.) or 2µg/ml Ab and polyHRP (b.) *Highest sensitivity was recorded by the highest amount of capture antibody (80µg/mg) as quantified by slope (41265 RLU/ng/L). There was very little benefit for slope when increasing detection antibody and polyHRP due to an increase in non-specific background. SD error bars represent SD for n=3.*

Considering the benefit of a two-step assay as discovered in Chapter 2, where detection solution with the propensity to cause high non-specific background was prevented from having contact with biological samples, the same procedure was trialled and compared for the mouse troponin assay. Figure 3.1.3 demonstrates how influential the removal of sample containing excess matrix components can be on the response of the assay. Here, the response of the one step protocol provides significantly increased sensitivity at the lower end of the standard curve, with a slope of 16937235RLU/ng/L, in comparison to the two step which has an inferior slope of 4860377RLU/ng/L, when calculated relatively at 312.5ng/L and 0ng/L. However, the most obvious trait of the one step assay is the point at which it reaches analyte saturation, which is at 5000ng/L cTnI. Two-step assay saturation is not observed up to 20,000ng/L by comparison, which is an attractive aspect of performance. This experiment is a classic example of the trade-offs commonly confronted in assay development, where sensitivity is sometimes sacrificed for linear range. Given the intended use of this assay, and the fact that it was completely unknown how much troponin is to be expected in the serum

of a mouse post-MI, it was tempting to proceed with the two-step protocol. However, it also must be acknowledged that this experiment used assay diluent as a sample matrix, and so it is likely that when moving from buffer to plasma matrices, sensitivity is likely to suffer and the curve is likely to flatten, as observed in Figures 2.1.8 and 2.1.9 in Chapter 2. For this reason, development continued using 1µg/ml antibody and polyHRP in a one-step format in anticipation of matrix effects.

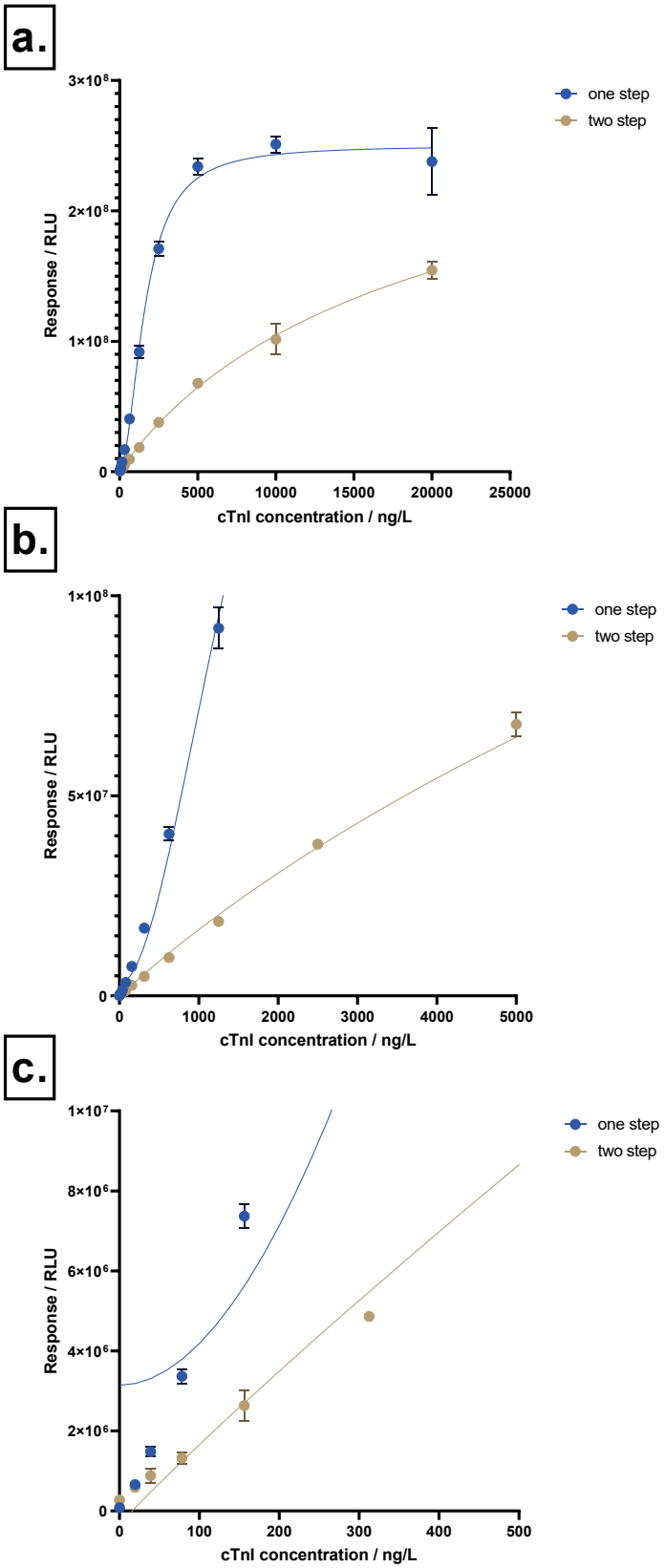

Figure 3.1.3 – 4PL regressions show sensitivity and linear range of one-step and two-step versions of the troponin assay, with increasing XY resolution from a-c. *The one step assay provides superior sensitivity (steeper curve in plot c) in comparison to the 2-step assay; however, the 2-step assay provides superior linearity, most obvious in plot a. SD error bars represent n=3.*

Predictably, the next step in assay development was the equivalence testing of using diluent as a matrix vs mouse serum (target matrix) in the format previously described. The results are shown in Figure 3.1.4 where, exactly as predicted, there is a drop in signal to background ratio (from 1.434 to 1.282, as described by a 4PL fit) when moving into mouse serum, demonstrating matrix effects. Consequently, the LoD of the assay increases from 7.24ng/L in diluent, to 25.5ng/L in mouse serum. It is also observed that linearity improves with the R^2 of a linear fit increasing from 0.96 to 0.99, caused by matrix effects slowing the rate of analyte capture. Although assay sensitivity is always important to some degree, a LoD of 25.5ng/L is deemed sufficiently sensitive for the purpose of this assay, which is not to accurately quantify analyte in ng/L, but to be able to detect significant relative changes in cTnI over time.

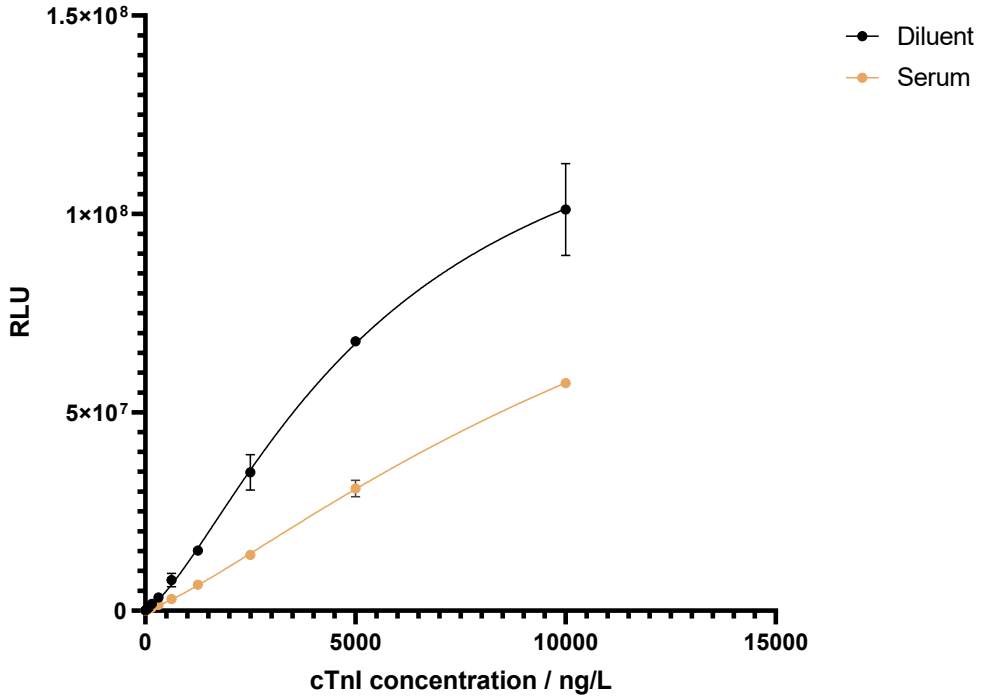

Figure 3.1.4 – A demonstration of matrix effects in serum that are absent in assay diluent. *There is a decrease in slope when moving to serum (orange), however, still maintains adequate sensitivity for the purpose of its intended use, with an LoD of 25.5ng/L.SD error bars represent n=2.*

sST2

sST2 assay development followed the same path as described for cTnI. However, only one antibody pair was available with sensitivity to mouse antigen – the same pair used for the human duplex assay. The capture antibody, S215, was titrated from 40µg/ml to 5µg/ml with traversing titrations of detection antibody and HRP, which was maintained at a ratio of 1:2. The positive spike of sST2 for comparison of signal and blank was fixed at 300ng/ml and the screen was conducted in mouse serum to prevent the need for rescreening if initially optimised in diluent. Results in the form of signal to background ratio and signal minus background are displayed in Table 3.1.

	Signal to background ratio			**Signal minus background / RLU**		
capture coating concentration / µg/ml	0.25µg/ml S103, 0.5µg/ml polyHRP	0.5µg/ml S103, 1µg/ml polyHRP	1µg/ml S103, 2µg/ml polyHRP	0.25µg/ml S103, 0.5µg/ml polyHRP	0.5µg/ml S103, 1µg/ml polyHRP	1µg/ml S103, 2µg/ml polyHRP
40	1.764	3.953	3.542	1267000	11299500	28702000
20	1.471	2.448	2.775	981500	9094000	30185000
10	1.159	2.089	2.744	295000	4338500	20045000
5	1.073	1.414	2.003	115500	1302000	8301500

***Table 3.1** - **Capture antibody (S215) is titrated in a checkerboard fashion with detection solution, which contains a fixed ratio (1:2) of secondary antibody (S103) with polyHRP.** Ratios of signal vs non-specific background and also signal minus background are depicted in increasing order from red to green.*

As depicted by colour gradient, the best coating concentration with the highest signal to background ratio was 40µg/ml. As for detection antibody concentrations, it appears a near tie between 0.5µg/ml S103 and 1µg/ml HRP, and 1µg/ml S103 and 2µg/ml HRP. In order to decide between these, the signal minus background metric reveals that there is a far greater difference between the blank and 300ng/ml for the highest concentration of antibody and HRP. Despite confirmation that these antibodies can in fact detect sST2, the signal to noise

ratio of around 3.5-3.9 is still lower than desired. If the difference between signal obtained at 300ng/ml is only 3.5 times higher than that of 0ng/ml, then roughly, the assay would not be able to detect sST2 concentrations lower than 85ng/ml as signal in RLU would be indistinguishable. Similar to the cTnI assay, there is no quantifiable LoD target for the sST2 assay and the only way to loosely extrapolate these targets is from human reference ranges which when considered, proves an 85ng/ml LoD as insufficient.

As a consequence of unmet sensitivity needs, it was decided that the ratio of S103 detection antibody and polyHRP should be titrated with a fixed capture antibody coating concentration of 40µg/ml. It cannot be assumed that a 1:2 ratio is optimal, and this titration was likely to provide an opportunity to improve sensitivity. Results from this titration are shown below in Table 3.2:

	Signal to background ratio			**Signal minus background / RLU**		
PolyHRP concentration / µg/ml	0.5µg/ml S103	1µg/ml S103	2µg/ml S103	0.5µg/ml S103	1µg/ml S103	2µg/ml S103
0.5	2.418	1.855	1.722	830200	1745500	2410000
1	2.768	3.931	4.678	1565000	12224500	32299000
2	1.449	5.212	4.366	956000	19711000	67775000
3	2.062	2.097	1.559	393450	1117000	1006000

Table 3.2 - After selection of 40µg/ml as capture antibody concentration, ratio and concentration of secondary antibody (S103) and polyHRP were titrated in a similar checkerboard fashion. *Ratios of signal vs non-specific background and also signal minus background are depicted in increasing order from red to green.*

Clearly, there is a significant improvement in blank subtracted signal when moving from 1µg/ml S103 and 2µg/ml polyHRP to 2µg/ml S103 and 2µg/ml polyHRP. This difference was previously around 29,000,000 RLU, but with added S103 has been boosted to 67,775,000

RLU. This result reveals that antigen was not fully saturated with antibody and so not all of the analyte was able to be detected by HRP turnover. Moreover, the ratio of signal to background increased from around 3.5 to 4.4. As a result of these improvements, development then continued focusing on sample dilution.

A key consideration in developing the assay for mouse serum was the need to obtain as many technical replicates as possible whilst conserving sample. Only around 50-100µL of mouse serum was obtained for measurement and given the requirement of 50µL of sample per replicate, dilution is required to achieve multiple repeats of the same sample.

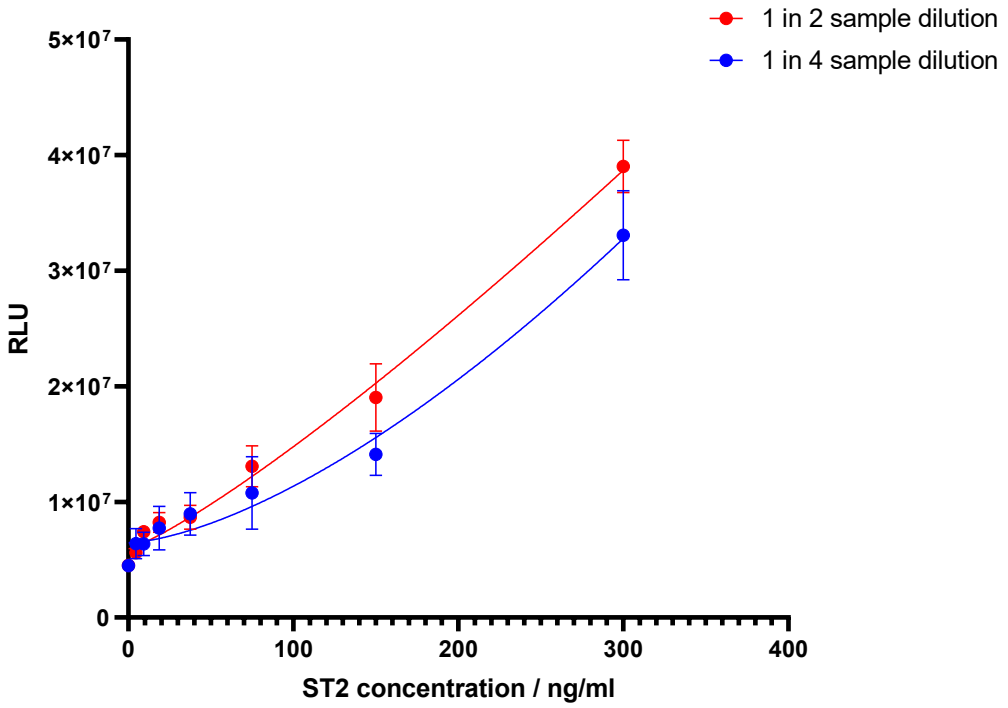

Figure 3.1.5 – The sST2 assay demonstrates similar sensitivity at both a 1 in 2 and a 1 in 4 sample dilution. *Standard curves show response at each concentration is within error (SD), with minimal decrease in average response. N=3 technical replicates.*

Figure 3.1.5 describes the profile of sST2 response using pooled mouse serum as a matrix, with a 1 in 2 (50µL requirement) sample dilution and a 1 in 4 (25µL requirement)

sample dilution. Due to limited resources, sample dilution was only investigated for sST2, the most important biomarker to measure in the mouse MI time course given its novelty and lack of characterisation so far in the field. Unfortunately, slope decreased from 1.531 to 1.192 when moving from a 1 in 2 to 1 in 4 dilution of sample. A decrease in sensitivity is expected, given that analyte concentration is halved when doubling the dilution, but the question is whether that decrease is tolerable within the targets of sensitivity. In this case, considering that the lower end of the curve (0-50ng/ml) is equivalent, and only above 75ng/ml do the curves start to diverge, the conclusion that the assay is still capable of measuring sST2 at high clinical levels at a 1 in 4 dilution is still true and so the assay is fit for purpose.

3.3.2.2 Assaying mouse serum post-LAD ligation for sST2 and cTnI

As a result of the development previously described, both assays were responding to recombinant mouse protein spiked into the target matrix of mouse serum, using only 25µL of sample. Following LAD ligation serum was collected at days 1, 3, 7, 14 and 28 and assayed. The profile of cTnI release post infarct is depicted in Figure 3.1.6.

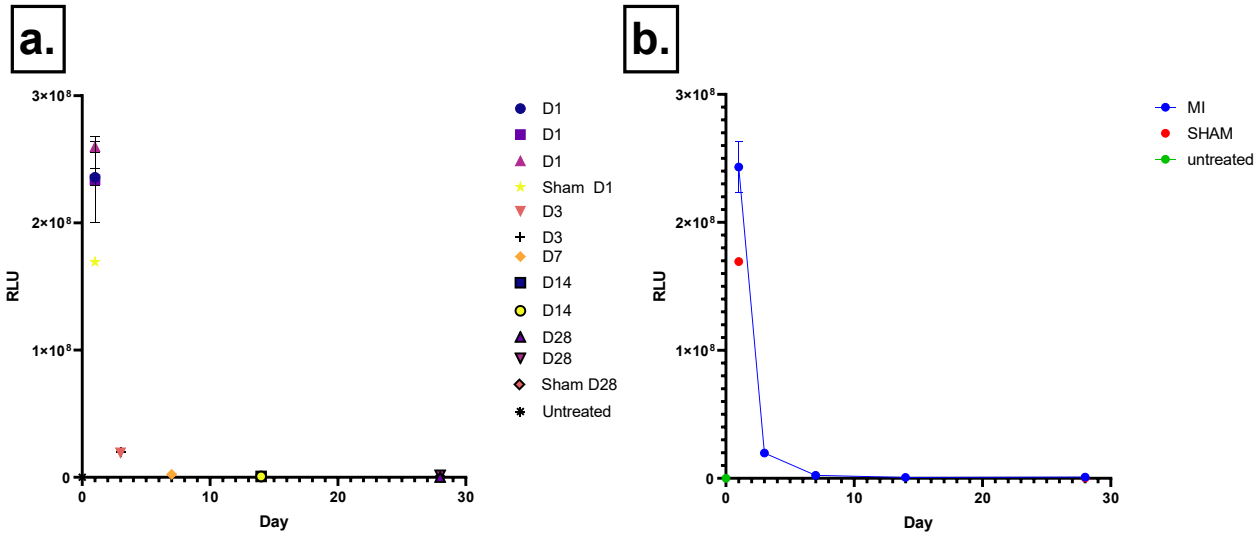

Figure 3.1.6 – When mice were subjected to LAD ligation, cTnI increased by 3000-fold within 24 hours, and then declines rapidly. *Plot a. shows the responses of individual animals, and the replicates associated with each day post-ligation. Plot b. shows the collated response to plot a curve indicating average cTnI decline over 28 days.SD error bars represent n=2 or n=3.*

Within 24 hours of LAD ligation, signal obtained for cTnI response increased by 3000-fold, which is characteristic of serous presence of troponin post-infarction. Then, the response curve drops steeply to near basal levels (untreated control) by day 14. This profile confirms success of the induction of MI and matches historical and well characterised literature on troponin release in mice post-MI (Frobert, et al., 2015).

Additionally, the sST2 levels in mice were measured simultaneously from the same samples, in different wells on the 96 well plate. The results are shown in Figure 3.1.7 in RLU:

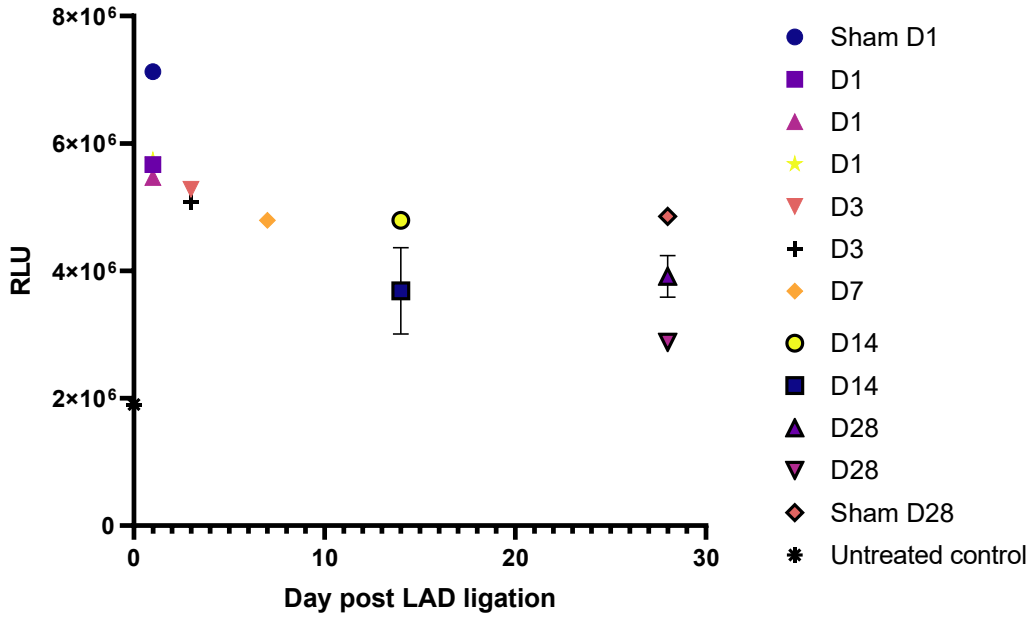

Figure 3.1.7 – sST2 is very responsive to LAD ligation in mice, with a 2.95-fold increase in the biomarker within 24 hours of infarction. *Levels decline slowly in comparison to cTnI (Figure 49), and are maintained at around double that of baseline, even after 28 days post-surgery. SD error bars represent n=2.*

When mice were subjected to MI by LAD ligation, sST2 spiked and rose by 2.95X within 24 hours of surgery. After day 1, the assay response slowly decayed over one week and started to plateau between day 14 and day 28, although never reaching baseline levels (or even close to) within a 28-day period post-injury. Additionally, when the data were collated such that each reading in RLU from serum measured from the same time point were considered biological replicates (excluding sham), and assessed for correlation between day 1 and day 28, there is a statistically significant correlation (P=0.011, 95% CI -0.9972 to -0.4717) between signal obtained by the sST2 assay and day post LAD ligation, with an R^2 of 0.68 (see Figure 3.1.8).

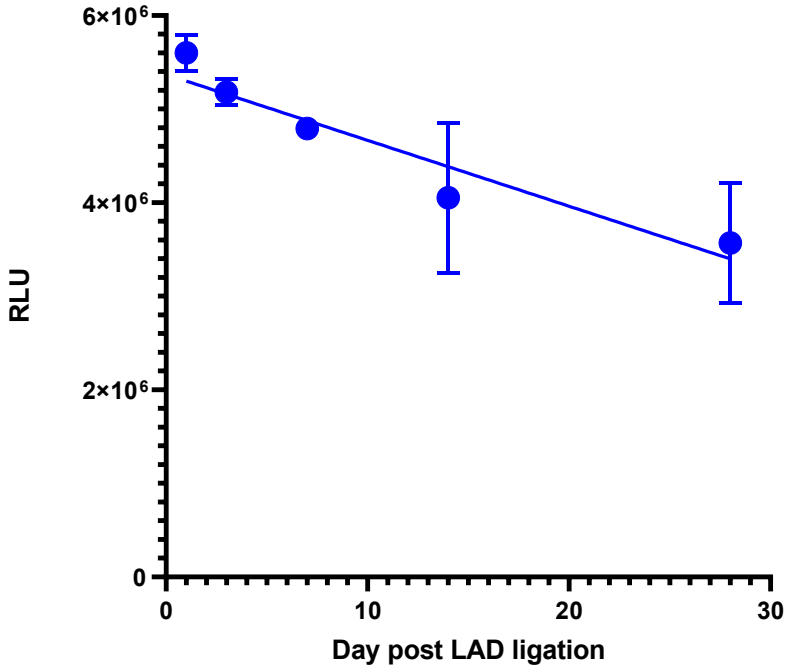

***Figure 3.1.8 – Collectively, there is a negative correlation between signal obtained by the murine sST2 assay and day post-LAD ligation**. This relationship was statistically significant (P=0.0011). SD error bars represent either n=2 or n=3.*

This was extremely encouraging evidence that sST2 was, in fact, released as a result of isolated and controlled ischaemic injury to the myocardium, therefore could be used as a biomarker for MI. Unfortunately, the sham mice could not offer a robust surgical control due to the high sera readings of both sST2 and cTnI. Given that cTnI was raised, it is likely that there was unintended myocardial damage during the surgery. This is relatively unsurprising given the perforation (via a stitch) of the pericardium, epicardium and myocardium during the sham procedure, resulting in damage to the small branches of coronary vessels, or induced some degree of ischaemic injury due to excessive manipulation of the LAD.

3.3.3 H9c2 injury modelling for MI and HF

In order to assess the differences, if any, between expression of various proteins including sST2 and the components of the IL-33/ST2L signalling pathway, models of MI and HF were optimised in H9c2 cells. For an "MI-like" injury, it was decided that H_2O_2 was the most appropriate activator of ischaemic injury, based on its popularity in the literature and ease of use (Yang, Jiang, & Shi, 2017) (Liu, et al., 2020). Secondly, a "HF-like" injury was inflicted using AngII, for similar reasoning including the accessibility of a protocol from the literature and it's well-elucidated mediation of hypertrophy in CMs (Ren, et al., 2023) (Yang, et al., 2012).

3.3.3.1 Confirmation of sST2 expression pre and post differentiation

Given that the only literature exploring sST2 expression in H9c2 examined cells were in their cardiomyoblastic form, in order to compare findings retrospectively, it was required to check sST2 expression pre and post differentiation. This was conducted in the form of a qRT-PCR time course, using *Tnni3* as a control, and *gapdh* as a housekeeper. *Gapdh* is known to stay relatively consistent across H9c2 differentiation, and any small decrease in mRNA is likely to be due to some cell death (Masilamani, Loiselle, & Sutherland, 2013). Differentiation success was confirmed visually by the formation of spindle fibres. This is evidence is shown in the images in Figure 3.1.9 (b and c).

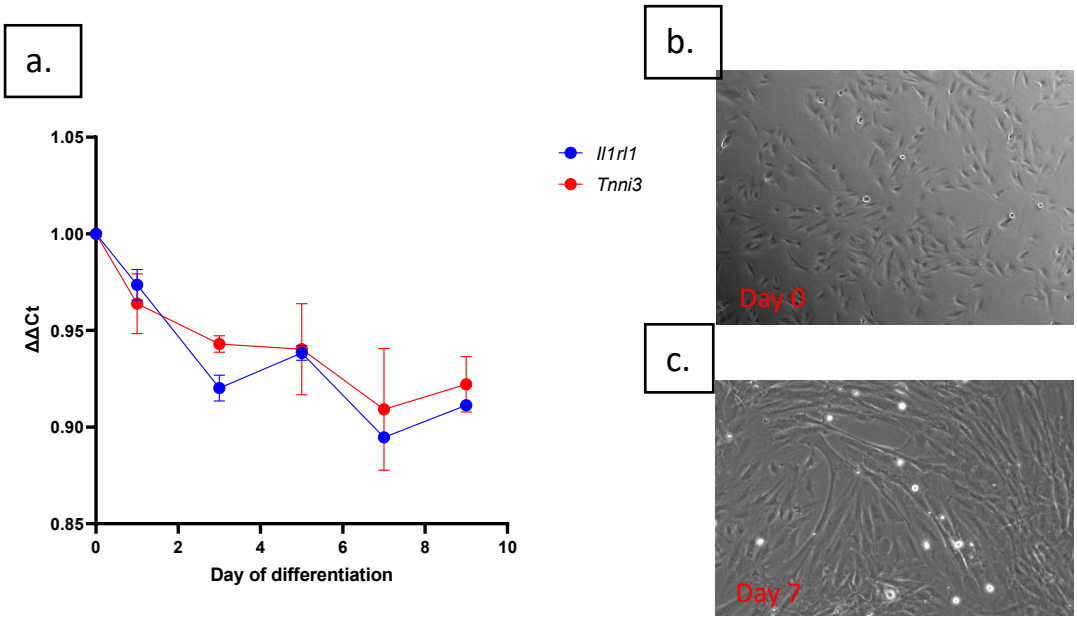

Figure 3.1.9 – ΔΔCT data (a.) shows a very minimal (~10%) decrease in expression of sST2 mRNA over a differentiation time course. *Images provide confirmation of differentiation to CM phenotype from day 0 (b.) to day 7 (c.). sST2 still maintains modest mRNA expression at the CM level as well in cardiomyoblast form. SD error bars represent n=2.*

As shown in Figure 3.1.9, there was a modest decrease in expression of both the control *(Tnni3)* and *il1rl1* over the 9 days of differentiation with horse serum. However, at a 10% reduction, there appeared to be no meaningful difference in the expression (and presumably therefore, the role) of sST2 in cardiomyoblasts vs cardiomyocytes, especially considering that this same change is reflected in cTnI, which is an essential CM sarcomeric component. Additionally, the difference in *Tnni3* mRNA levels between day 0 and day 7 was statistically insignificant (P= 0.203). The literature corroborates this finding, where *Tnni3* mRNA was only observed to increase from 12 days onwards (Machado, Sachinidis, & Futschik, 2021).

3.3.3.2 MI modelling with hypoxia

RT-qPCR

H9c2 cells were subjected to hypoxic conditions varying in severity by increasing hydrogen peroxide concentration (from 50µM to 100µM) and time of incubation (from 4-8 hours). This protocol was first optimised in a small pilot study, after consulting the literature

for the most successful protocols that implement H_2O_2 as a popular metabolite in ischaemic injury in the H9c2 cell line (Yang, Jiang, & Shi, 2017) (Liu, et al., 2020). *Il1rl1* was probed using qRT-PCR with *Il6*, *Tnf* and *Nfkb* as control genes to confirm injury.

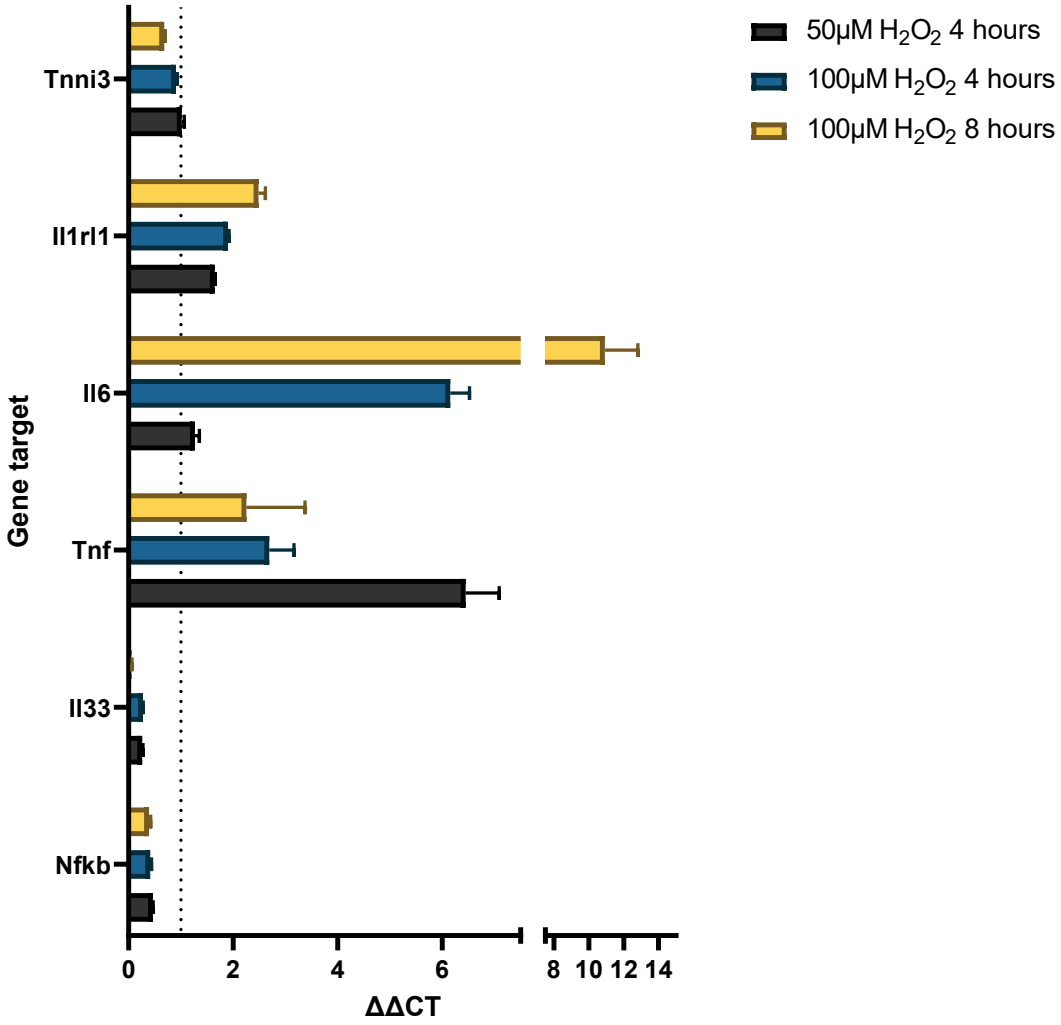

Figure 3.2.1 – Increased mRNA levels of Il6, Tnf and Il1rl1 were observed after ischaemic injury with H2O2 at either 50μM or 100μM. *Tnni3 did not change, with Il33 and Nfkb transcript levels reducing. SD error bars reflect n=2 technical replicates.*

Figure 3.2.1 demonstrates that *Il1rl1* mRNA upregulation takes place in CMs as a response to ischaemic injury. At the most severe injury, 100μM of H_2O_2 for 8 hours, *Il1rl1* upregulation is 2.5-fold that of the uninjured control, and decreases to around 1.9-fold when the time of incubation of the agonist is halved to 4 hours. With the shortest time of incubation and lowest concentration of H_2O_2 (4 hours, 50μM), *Il1rl1* mRNA is still produced in comparison

to the uninjured control at a ratio of approximately 1.65. Figure 3.2.2 (a.) shows the relationship between *Il1rl1* and *Il33* expression. As *Il1rl1* increases with injury severity, *Il33* decreases, particularly when H9c2s are incubated for 8 hours in 100µM H_2O_2. Additionally, the response of *Tnfα* and *Il6* (Figure 3.2.2 (b.)) suggests success in inducing the injury, given these characteristic observations of mRNA upregulation are observed, especially in the case of *Il6* where expression also increases with severity of injury.

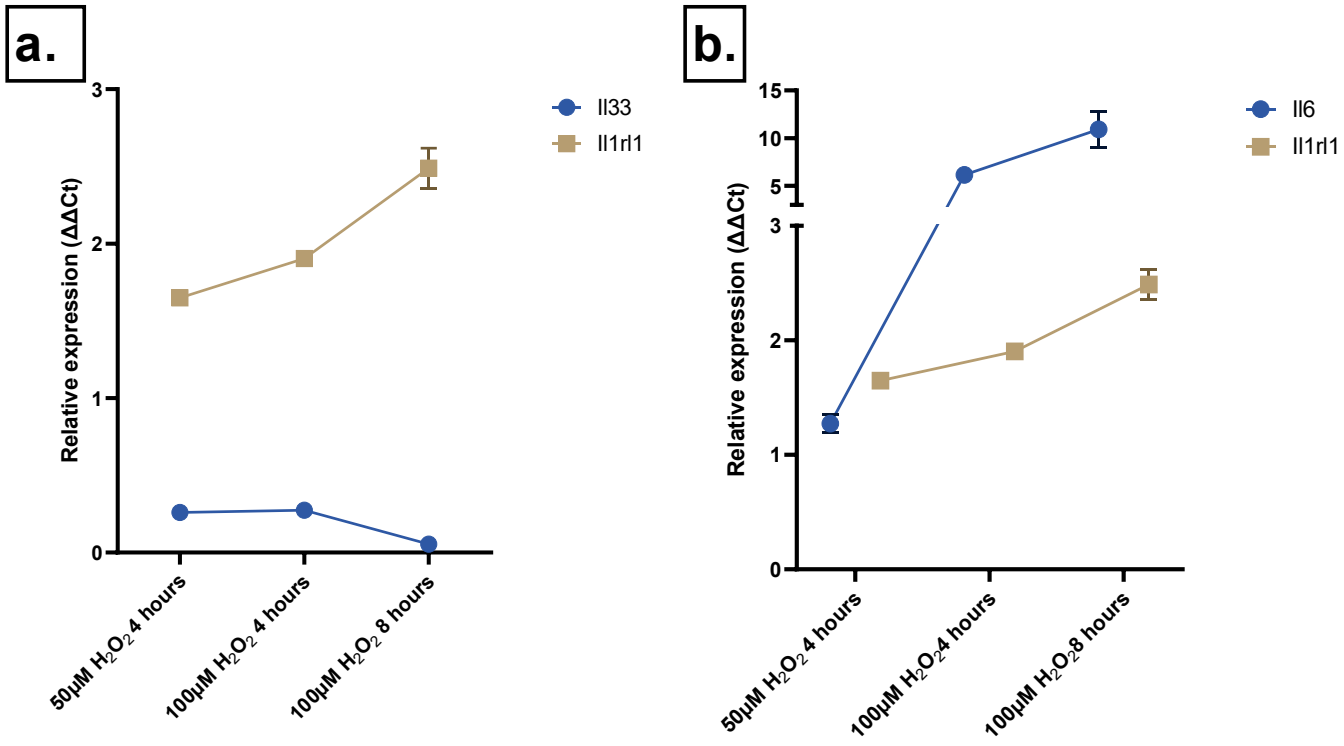

Figure 3.2.2 – Plots to show the relationship between mRNA levels of Il1rl1 with other closely related interleukins. *Il1rl1 is a decoy for Il33, and mRNA shows opposite responses whereby upregulation of Il1rl1 is compared to downregulation of Il33. Additionally, Il6 (plot B) shows positive correlation with Il1rl1 levels, denoting increasing injury. SD error bars represent n=2.*

These findings proved for the first time with this specific injury protocol, that oxygen starvation is substantial environmental motivation for *Il1rl1* upregulation and its inhibition of the IL-33/ST2L pathway. Consequently, this may lead to the decrease in anti-hypertrophic signalling which could contribute to the adverse remodelling known to cause HF. This

conclusion assumes a matching presence of sST2 protein as a result of the mRNA upregulation, which was investigated in the next section.

SDS-PAGE and Western blots

sST2 was quantified at the protein level, alongside caspase-9 and α-smooth muscle actin (controls). Caspase-9 was selected to control for successful AngII injury for several reasons, firstly, that caspase-9 is widely cited as a control for AngII injury in a variety of cells (including H9c2s), and secondly, is known to be involved in the initiation stage of apoptosis and signals mitochondrial stress (Lee, Mungunsukh, Tutino, Marquez, & Day, 2010) (Prathapan, Raj, Rani, & Raghu, 2018). When caspase-9 is upregulated, it can be assumed that the apoptotic pathway is activated which would later recruit effector caspases (Guerrero, Schmitz, Chen, & Wang, 2013). Given the short time frames of injury used in this study, early apoptotic activity has a better chance of detection (and confirmation of injury) than total apoptosis. For α-SMA, if H_2O_2 injury was successful in inducing ischaemia that results in the sequestration of anti-hypertrophic signalling (based on the downregulation of the IL-33/ST2L pathway), then there is likely to be reorganisation of actin filaments via α-SMA upregulation (Claridge, et al., 2023) (Ahmed, et al., 2011). This, if correlated with sST2 upregulation, could indicate that remodelling is occurring partly due to the lack of chemokines and cytokines recruited in the anti-inflammatory response usually signalled via the IL-33/ST2L pathway.

Protein was extracted from cells undergoing the same injury time course. The downstream signalling pathway triggered by IL-33/ST2L interaction was also evaluated. Observations about the pathological response to oxygen starvation were made first, as shown in Figure 3.2.3 below, as a second validation (alongside RT-qPCR results) of injury.

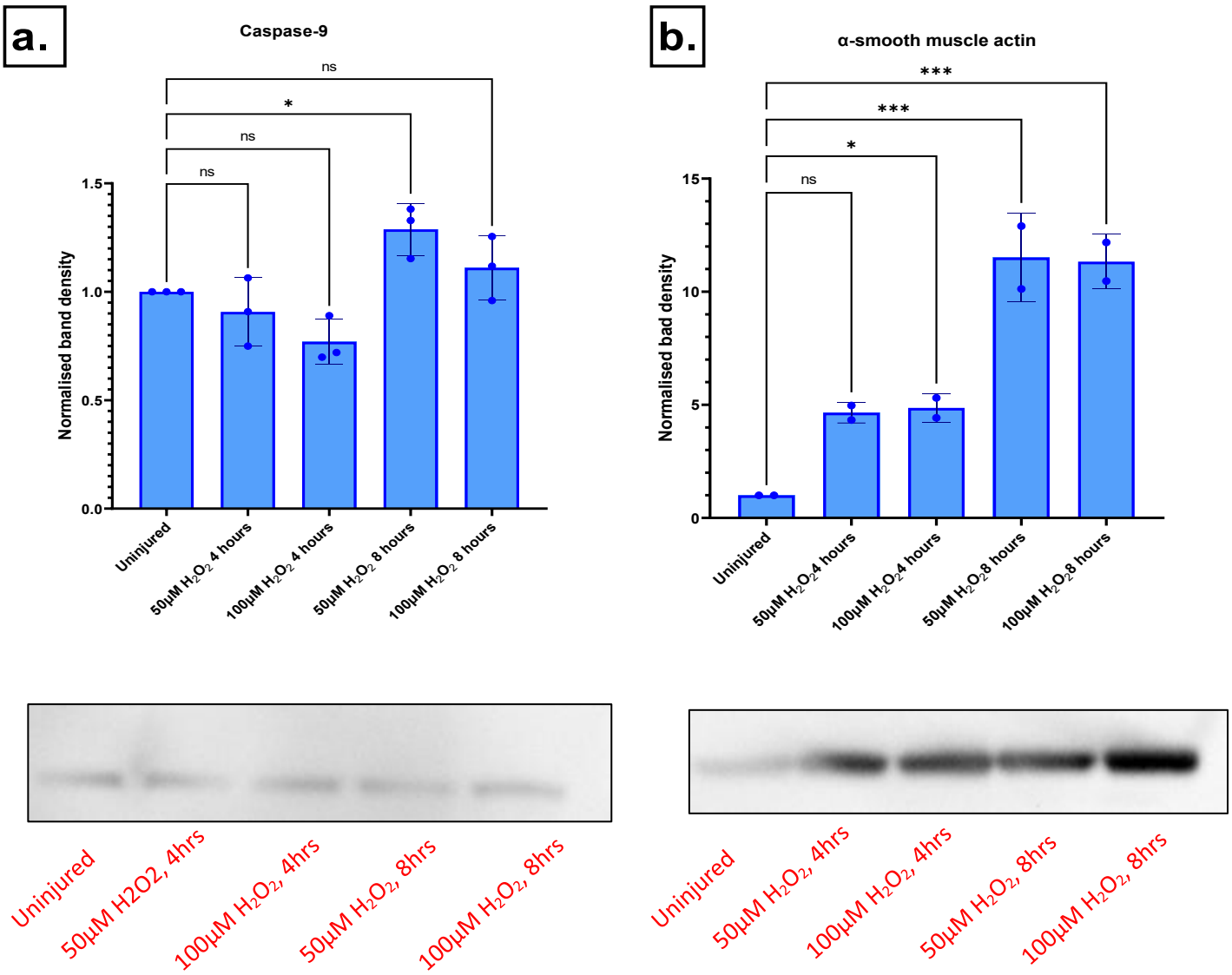

Figure 3.2.3 – Longer periods of H_2O_2 incubation (plot a) show moderate increases of caspase-9, whilst most injury conditions mediated significant increases in α-smooth muscle actin (plot b). *For caspase-9, only one injury condition (50μM H_2O_2 for 8 hours) caused a significantly higher expression of caspase-9 (P=0.0463). As for α-smooth muscle actin and its response to H2O2, significant increases were detected after 100μM for 4 hours, 50μM for 8 hours and 100μM for 8 hours, with P values of 0.0461, 0.0006 and 0.0007, respectively. This confirms and controls for induction of injury, which gives confidence that further conclusions made about sST2 presence is directly associated with oxidative stress.*

Western blot analysis reveals a statistically significantly increased presence of α-smooth muscle actin upon hypoxic injury in both of the 100μM conditions and when 50μM is spiked into medium for 8 hours (Figure 3.2.3b). An additional observation is the somewhat unstable amount of caspase-9 in shown in Figure 3.2.3, however, shows a modest increase for the longer, 8-hour injury indicating the start of apoptotic activity (Brentnall, Rodriguez-

Menocal, Guevara, Cepero, & Boise, 2013). sST2 protein response to both injury models will be compared in section 3.3.5.

3.3.4 *IL1RL1* response in HF modelling with AngII

AngII is a popular mediator of HF-like physiology in cell models, specifically through RAAS activation, simulating hypertrophy and apoptosis (Liu, et al., 2010) (Qin, Patel, Yan, & Liu, 2006). AngII was implemented at concentrations of 100µM and 200µM for 24 or 48 hours after consultation of the literature as to commonly used protocols for injury in H9c2 cells (Abdulrahman, et al., 2022) (Siti, Jalil, Asmadi, & Kamisah, 2021). H9c2 cells differentiated to CMs were somewhat responsive to AngII over a period of 24 hours, showing mean mRNA upregulation of 55% for *IL6* (P=0.0113), 75% for *Pikc3b* (P=0.0174) and 200% for *mmp9* (P=0.222). MMPs are strongly associated with hypertrophic pathways via cytokine and growth factor immunomodulation pertaining to thickening of the left ventricle, with their main influence (given the name) involving degradation of the extracellular matrix (Jager & Hoefer, 2017). There are several groups of MMP according to their enzymatic domains (Loffek, Schilling, & Franzke, 2010). MMP-2 and MMP-9 were selected for confirmation of injury due to their involvement in progressive ventricular hypertrophy observed in mice; despite the roles for other MMPs in heart failure (e.g. MMP-1 and MMP-3), MMP-2 and MMP-9 have long been recognised as the primary contributors to hypertrophy and adverse remodelling in the left ventricle in HF models (Spallarossa, et al., 2006) (Thomas, et al., 1998) (Li & Feldman, 2012). However, in the results shown in Figure 3.2.4, *Mmp9*, not *Mmp2*, was upregulated in response to injury. Despite the average ΔΔCT increasing by 2-fold, however, this increase is statistically insignificant. It may be that the introduction of ROS via AngII-mediated NADPH oxidase activation causes a down regulatory effect on MMP-2, but not MMP-9, furthermore, MMP-9 is regulated by p38 kinase as opposed to ROS, and so the data may point to the

differential influence of these two mediators of MMP upregulation (Spallarossa, et al., 2006). Also of interest is the significant downregulation of *Tnf* post-injury, which was not expected given that the literature widely documents the opposite effect (Prathapan, Raj, Rani, & Raghu, 2018) (Yu, Yang, Guo, & Sun, 2020).

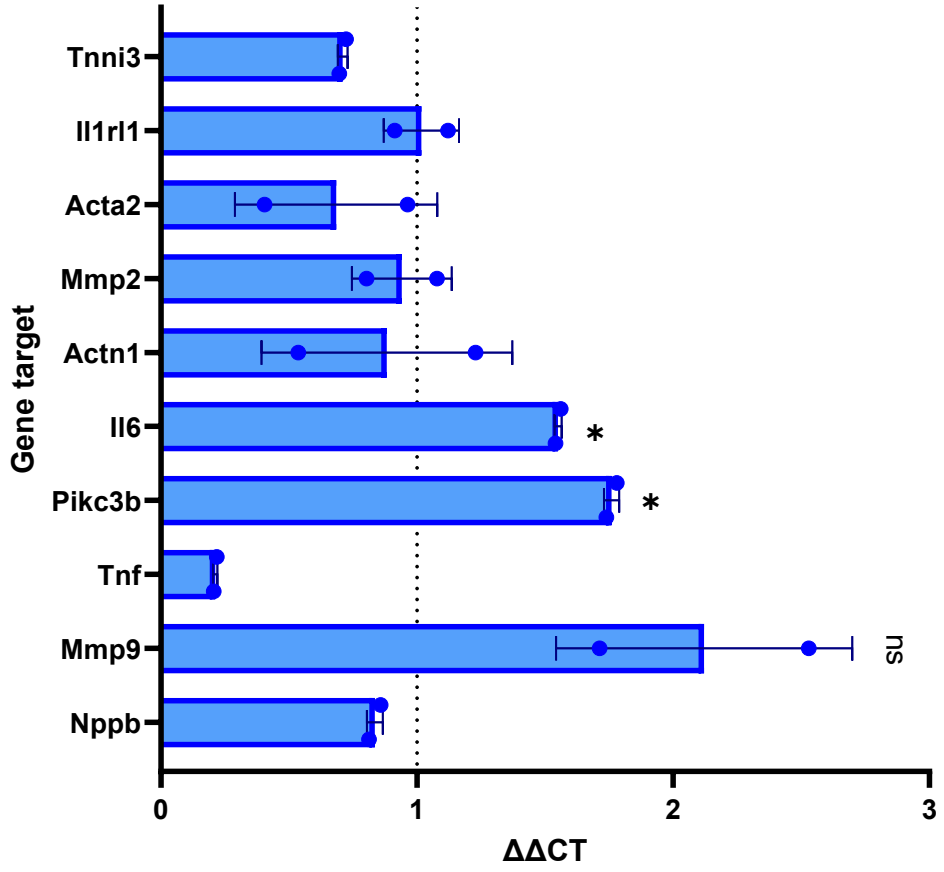

Figure 3.2.4 - Relative expression of 100μM AngII for 24 hours shows increase of mmp9, pikc3b and IL-6 mRNA, however sST2 expression remains constant. *Paired t-test found significant upregulations' in Il6 and Pikc3b transcripts (P=0.0113 and P=0.0174, respectively), but a non-significant increase in Mmp9 (P=0.2225).*

A significant increase in *Il6* mRNA could induce hypertrophy; the role of *Il6* is described as essential for hypertrophy in the literature, as demonstrated with *Il6* knockout mice (Zhao, et al., 2017) (Muñoz-Cánoves, Scheele, Pedersen, & Serrano, 2013). Additional reassurance of successful achievement of HF/hypertrophy-like state is the increased mRNA production of

Pikc3b; a known component of the PI3K-AKT signalling pathway for the promotion of CM proliferation (Lin, et al., 2014). Despite the upregulation of multiple genes associated with pro-hypertrophic signalling, *Il1rl1* is not upregulated in response to AngII, which raises questions about sST2 isoform involvement in remodelling and chamber stress as opposed to necrosis and cell death.

SDS-page and Western blots

Western blot was performed on protein extract from cells that had undergone the same AngII injuries. The results are plotted in Figure 3.2.5. There was a significant increase in caspase-9 when H9c2 cells were incubated with 100µM of AngII for 24 hours, indicating the initiation of apoptotic activity that can lead to subsequent hypertrophic cardiomyopathy in the survivors, thus acting as a control for successful injury induction (Putinski, et al., 2013). The other AngII conditions (200µM for 24 hours and 100µM for 48 hours) showed an average increase in caspase-9, although this was statistically non-significant. Mean α-smooth muscle actin levels were increased in one of the injury conditions (200µM for 24 hours), although this was statistically non-significant. There was no change in α-smooth muscle actin in the other two injury conditions. This could call into question the validity of this model, as AngII has previously demonstrated a positive α-smooth muscle actin response using similar concentrations for a similar incubation period (Oh, et al., 2012).

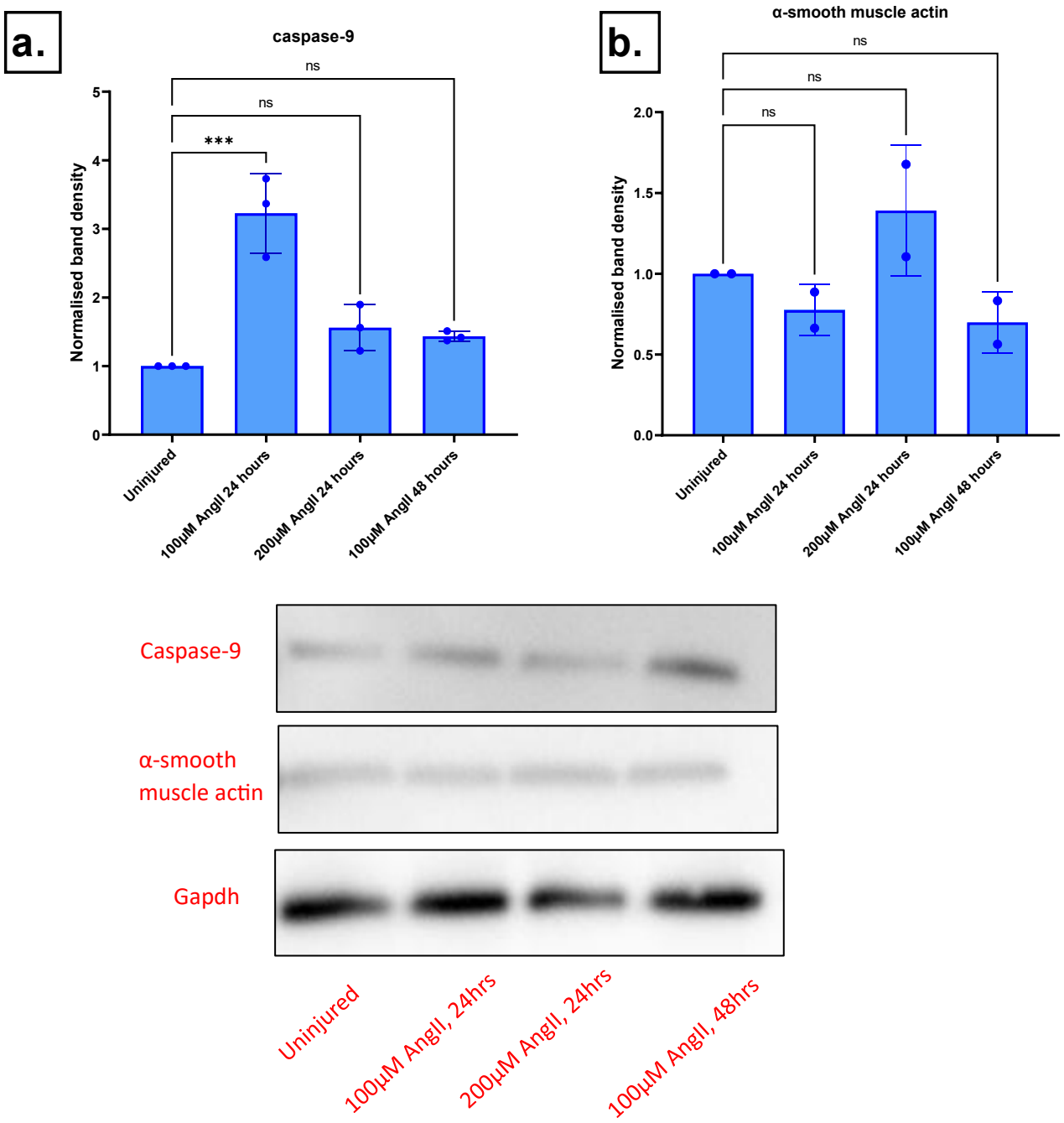

Figure 3.2.5 – Caspase-9 (plot a.) mean protein level increased with all concentrations of AngII (however only significantly so to 100µM for 24 hours, P=0.0005)), indicating increased apoptotic activity associated with hypertrophy and remodelling*. α-smooth muscle actin (plot b) was only responsive (non-significantly, P= in the highest concentration of AngII.*

3.3.5 sST2/IL-33 pathway comparison between models

The signalling pathway downstream of the IL-33/ST2L interaction was next explored by western blotting, and compared for both injury models, as shown in Figure 3.2.6. Statistical significance was assessed by one-way ANOVA comparison of each injury condition to the uninjured control. The first, most obvious observation when comparing each plot is the difference in the magnitude of response between the two injury models, indicating separate effects of AngII and H_2O_2 on the Intracellular signalling pathway. Firstly, if ST2L transmembrane protein was able to bind IL-33, the adaptor protein MYD88 is implicated in the transmission of signal of successful interleukin activation. In Figure 3.2.6, there were significantly increased responses detected when 50µM H_2O_2 was incubated for both 4 hours (P=0.0052) and 8 hours (P=0.0002). Interestingly, when the concentration of H_2O_2 was increased to 100µM, there was a decrease in expression, which was non-significant at 4 hours (P=0.2513) but significant at 8 hours (0.0365). As for AngII-mediated injury, Myd88 expression changes were more modest, in fact, expression increase only reached statistical significance at the longest time point (100µM AngII for 48 hours, P=0.0173), whereas the other 24-hour conditions (100µM and 200µM) showed increases in means that were non-significant (P=0.6031 and P=0.0579, respectively).

The next pathway component in the downstream signalling towards the nucleus is IRAK-4, which is recruited and bound by Myd88. IRAK-4 is a critical member in TLR-mediated signalling and is responsible for the upregulation of transcription factors (such as Nf-κB) for cytokinetic response to inflammatory stimuli (Kim, et al., 2007). In the case of AngII injury, the increase in IRAK-4 expression was much larger than that of Myd88, where all injury conditions showed statistical significance. Within 24 hours, injuring differentiated H9c2s with AngII caused a 2-fold increase in IRAK-4 when using 100µM, and a 2.2-fold increase when using

200µM (P=0.0003 and <0.0001, respectively). The mean IRAK-4 expression decreases slightly at 100µM for 48 hours, although still shows a significant 1.8-fold increase in expression to the uninjured control (P=0.0057). When H9c2s were exposed to 50µM or 100µM H_2O_2, increase in expression of IRAK-4 was only significant for the longer injury period of 8 hours (P=0.0027 for 50µM, and P=0.0017 for 100µM), although mean increases were still observed without statistical significance for the 4-hour periods.

After IRAK-4 recruitment, MAPKs such as p38 are activated to further transduce signalling to the nucleus and have established roles in apoptosis, survival and inflammation (Zhang & Liu, 2002). Their influence in downstream signalling usually involves phosphorylation and so for completeness, an antibody targeting both phosphorylated and dephosphorylated protein was used for western blot. Interestingly, there is no observed upregulation of MAPK in AngII injury over all time points and concentrations, however there is significant upregulation in C-Jun for all time points and concentrations (P=0.0066, P=0.0441, P=0.0009 for 100µM for 24 hours, 200µM for 24 hours and 100µM for 48 hours, respectively). C-Jun is a transcription factor that is activated by phosphorylation by JNKs, which are a subset of MAPKs (Guma & Firestein, 2012). In hindsight, if more specific members of the MAPK family had been probed (e.g. JNK), there may have been more insight into which MAPK specifically caused the upregulation of C-jun. Nonetheless, the 2-4-fold increase in C-Jun in all AngII injury conditions demonstrates a significant effort to continue signalling to the nucleus and the activation of other transcription factors. By comparison, MAPK is significantly upregulated (~3-fold) when either 50µM or 100µM H_2O_2 is spiked into medium for 8 hours (P=0.0002 and P=0.0009, respectively). This is followed by significant increases in intracellular C-Jun recruitment observed for the 50µM H_2O_2 conditions at 4 and 8 hours (P=0.0014 and P=0.0053, respectively), but not for the 100µM conditions at 4 and 8 hours (P=0.9990 and P=0.9306), respectively. Given that the

relationship between C-Jun and MAPK expression is again, not in correlation, suggests more specific subsets of MAPK (i.e. as previously suggested, JNK) are responsible for the activation of c-Jun that were not resolved on western blot.

Finally, Nf-κβ, a component at the end of the IL-33/ST2L pathway showed no significant increases in expression in any of the injuries by AngII or H2O2, despite some conditions (100µM AngII for 24 hours and 100µM H2O2 for 8 hours) showing non-significant increases in mean protein abundance. It could be that during the time periods of this study (4-48 hours) the window for Nf-κβ upregulation was missed, as it is widely cited that Nf-κβ activation can occur within minutes of exposure to cytokines or DAMPS (Gallego-Selles, et al., 2022) (Giridharan & Srinivasan, 2018).

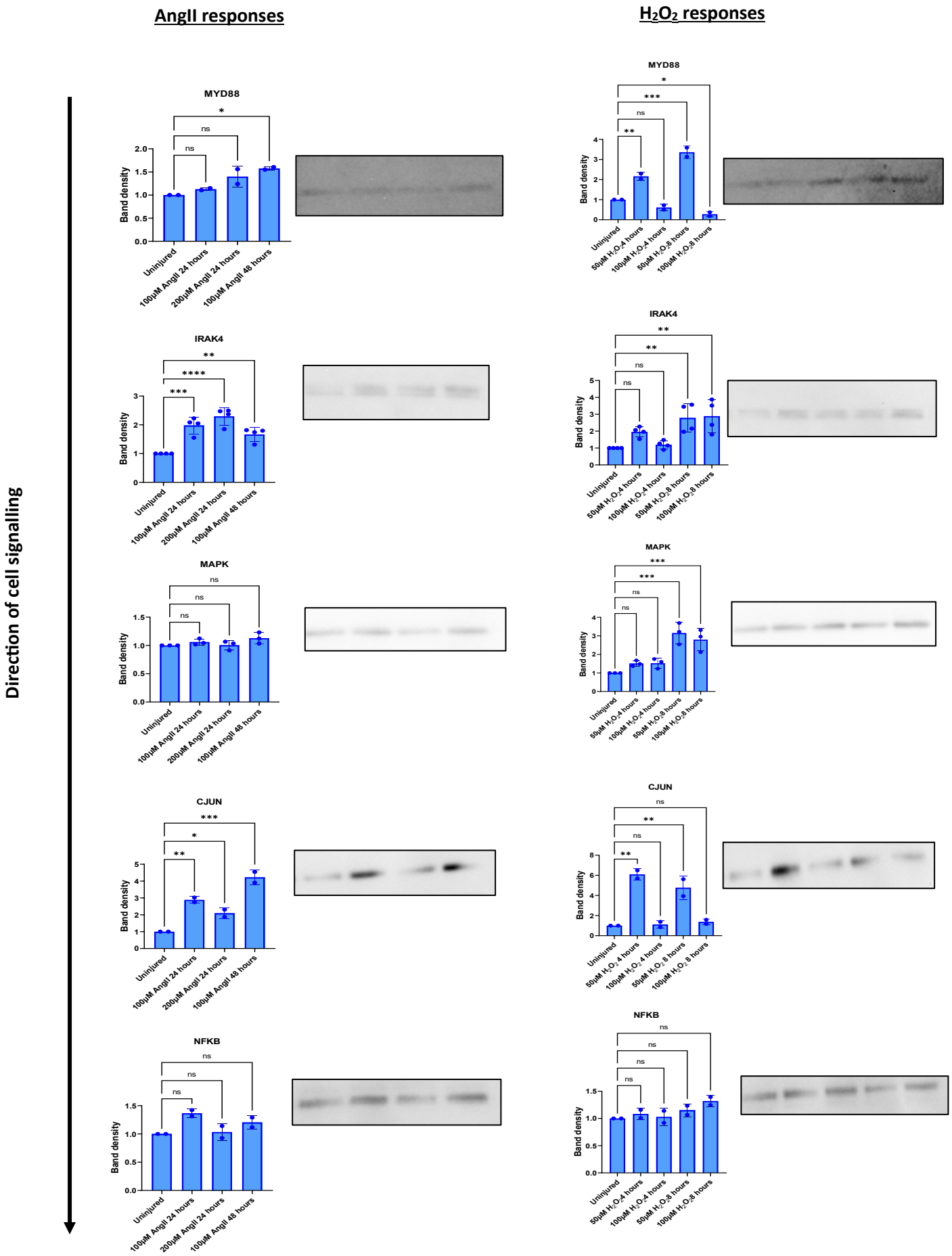

Figure 3.2.6 – AngII and H_2O_2 agonists have very different influences on the expression of the constituents of the IL-33/ST2L signalling pathway. *H_2O_2 causes the biggest response, with up/downregμLation showing dependency on concentration.*

Finally, Figure 3.2.7 demonstrates the protein level expression response of sST2 in both injury protocols. It is irrefutable that sST2 production is injury-responsive for both AngII and H_2O_2 antagonists, however, this did not always reach statistical significance. The conditions that did reach statistical significance were 100µM AngII for 24 hours (P=0.0172) and 50µM H_2O_2 for 4 hours (P=0.0337).

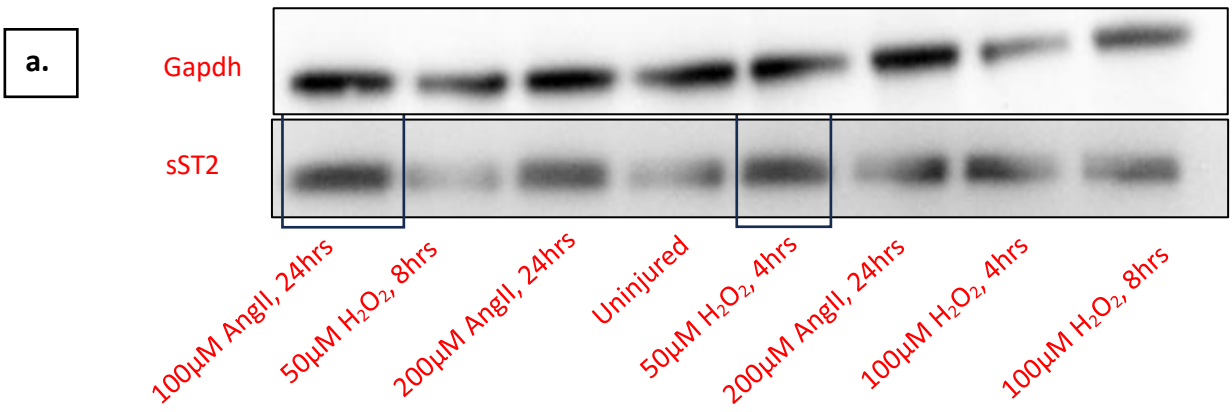

b.

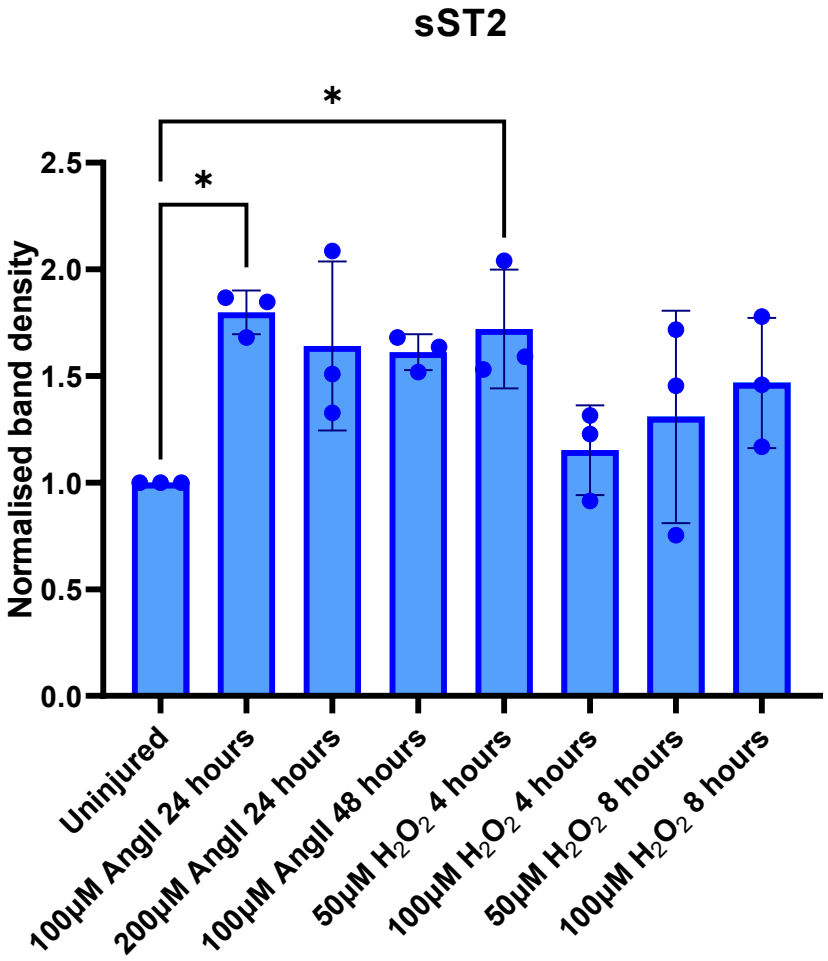

Figure 3.2.7 – sST2 protein expression increased in all injury conditions involving AngII and H_2O_2. *This was significant by on-way ANOVA for the 100uM AngII for 24 hours (P=0.0172) and 50uM H_2O_2 for 4 hours (P=0.0337). Western blot quantification made from the bands in Figure a were compared after normalisation to GAPDH in plot b.*

3.4 Discussion

This chapter presents supportive data for the association of sST2 with MI, demonstrated at the whole animal and cellular levels. Notably, these data contribute novel and first-time investigation of sST2 release over time in LAD ligated mice, as well as sST2 observation with AngII and H_2O_2 in differentiated H9c2s.

Firstly, scRNA-seq data provide cardiac cellular mapping data for the expression of Il1rl1. These data were collected in the absence of RNAscope images that were attempted

many times on tissue sections from mice post LAD ligation, although without success. Despite not being able to collect primary data on intra-cellular expression of sST2, secondary data from 7 studies (Farbehi, et al., 2019) (Forte, et al., 2020) (Tombor, et al., 2021) (Kretzschmar, et al., 2018) (Ruiz-Villalba, et al., 2021) (Molenaar, et al., 2021) (Wang, et al., 2020) provide information about the expression of *Il1rl1* throughout immune and cardiac cells, including CMs, which validates the use of differentiated H9c2s as an appropriate cell type for sST2 investigation. However, despite there being some injury-responsive expression in the collective scRNA-seq data, it is modest. Before the acquisition of these data, there was an effort to obtain primary data on Il1rl1 expression in the heart using RNAscope which was unsuccessful despite much optimisation and many repeats. The low abundance of Il1rl1 expression evident by the scRNA-seq data may explain the trouble in visualising sST2 protein in MI heart sections using RNAScope. In an ideal world, the RNAscope experiments could reflect a more controlled comparison of IL1RL1 expression with injury response, where strain and age etc are constant.

In the release profile experiments, there is a regrettable lack of fMRI, fibrosis and ultrasound data to compliment the serum samples, due to a change in circumstances during the course of the collaboration. These data would have strengthened the conclusions, by determining size of infarct and correlating those measurements with sST2. However, the experiment is still controlled by cTnI that was measured in addition to sST2, which as mentioned, is an incredibly specific biomarker for myocardial necrosis. The literature also confidently and consistently reports the release profile of troponin, said to have reached depletion between 10-14 days post-infarction, which exactly matches the profile displayed by the assay in Figure 3.1.6 (Katrukha & Katrukha, 2021) (Bertinchant, et al., 1996) (Laugaudin,

et al., 2015). This gives additional confidence in the success of the surgical protocol, and therefore the sST2 response by extension.

With this in mind, sST2 response follows the hypothetical prediction, that the protein is released very quickly into serum, and depletes slowly (in comparison to troponin). The implications of this observation could be huge on a clinical scale. Stable levels of biomarker post injury, that are raised quickly, allow clinicians to make decisions more accurately without risk of missing transient peak of biomarker expression (if depleted quickly, or take a long time to express). The most encouraging and applicable result is the fact that sST2 was significantly raised within 24 hours. If this study could be repeated, it would be interesting to home in on the time points before 24 hours. For example, the NICE guidelines direct treatment suggestions within a 12 hour period from onset of symptoms to presentation at A&E (NICE: NG185, 2020) (NICE: NG185, 2020). It is also likely that patients will present to A&E and have their blood taken for biomarker measurements well within the 12-hour period, and so characterising the sST2 release profile within this time could be informative, albeit, difficult to investigate in practice given that LAD ligation surgery on mice takes a couple of hours.

However, the cell injury study in section 3.3.3 in which AngII and H_2O_2 were used to replicate HF-like and MI-like injury, respectively, showed that sST2 protein is upregulated within 4 hours. Although there was no trend in duration of injury and sST2 level (given there were only 2 timepoints of 4 and 8 hours for H_2O_2 incubation), mRNA upregulation of *Il1rl1* was able to translate sST2 protein to double the control quantity within 4 hours. This is important for application of sST2 measurements in acute disease diagnosis and could be considered unsurprising given the IL-33/sST2 axis is a firm member of acute inflammatory response, designed to act quickly to prevent physiological damage from injury. Also worthy of note is

the difference that injury activator (AngII and H_2O_2) and by extrapolation, injury (HF or MI) have on the expression of ST2L/IL-33 pathway components. As commented on during the introduction of this thesis, the literature contests the involvement of sST2 in MI pathophysiology, with more data available for HF pathophysiology. This chapter presents the first cellular study comparing models for the two disease processes and sST2, and their impact on intracellular messaging conducted by transcription factors that elicit protective mechanisms. Undeniably, both H_2O_2 and AngII had very different effects on translation responses concerning proteins in the pathway, although both caused considerable increases in sST2.

Intracellular signalling and cellular physiology in general is incredibly complex and pathways rarely activate linearly, with each component in the pathway having potential for crossover with other pathways that could be responsible for upregulation. An example of this in the IL33-ST2L axis is the involvement of NF-κβ, an integral transcription factor in many inflammatory stimuli and responses (Qing Guo, et al., 2024). *Tnfα* mRNA was expressed 3-6 times more in the hypoxic model (Figure 3.2.6), which is a known mediator of a canonical pathway resulting in the activation of NF-κβ, and so it is possible that this pathway contributed to increased levels of the transcription factor (Qing Guo, et al., 2024).

Most puzzling about the western blot data is the polarity between MyD88 expression after varying severities of H_2O_2 exposure. It was hypothesised that an increase in sST2 would result in less MyD88 translation, given that the ST2L would be under-utilised as a result of IL-33 interception by sST2. This seems to certainly be the case with the highest concentration of H_2O_2, where MyD88 expression drops by half at 4 hours, and then half again at 8 hours. However, this does not explain the response elicited by the lower concentrations of H_2O_2,

where MyD88 doubles at 4 hours, and increases further again at 8 hours of 50µM H_2O_2. It is important to remember that an increased signal of a protein on western blot does not necessarily correlate with increased accessibility or activation of a pathway, and so the increase of MyD88 in the 50µM H_2O_2 conditions could reflect an *attempt* to boost immune response by escalating MyD88 presence intracellularly, as it is plausible that the signalling isn't entirely inhibited but just reduced. In other words, an increased expression of Myd88 may not be able to boost downstream signalling if it cannot be activated by IL-33/ST2L interaction. However, despite increases in MyD88, if ST2L isn't activated by IL-33, downstream signalling for this specific pathway cannot occur. MyD88 in the H_2O_2 model loosely correlates with the expression of protein in the rest of the pathway, where IRAK4, C-Jun and NF-κβ loosely correlate with injury intensities, inferring that MyD88 fluctuations impact protein levels downstream.

The final point to address is that despite exciting developments in the understanding of sST2 release post-infarction and its steady decline, it cannot provide information about patient-to-patient differences in decline. If the collaboration had not ended abruptly, the acquisition of more serum from more animals would have added more data points to Figure 3.1.7. Having said that, with lower n it is less likely to observe a trend that might be there, which means adding more animals would only strengthen the trend observed in Figure 3.1.8 and therefore not change the conclusion of the experiment. Additionally, it would be interesting to study sST2 changes in patients' post-MI in the days after the event, up to a few weeks and months post injury. The only study to come close to observing this was conducted by Tyminska et al., although time points were limited to 72 hours and 1-year post-MI (Tymińska, et al., 2019). Because cTnI is released based on a necrotic event at a discrete time, rather than continual strain, release profile of this biomarker may be more consistent amongst

patients. In contrast, if sST2 is affected by both strain AND necrosis, as evident by the injury modelling study, levels may not decline as consistently across patients. This additional study in humans would be the next step in understanding sST2 physiology after the definition of its behaviour in a surgical animal model. As the literature suggests, if sST2 is continually released and remains high in one patient and not another, risk of MACE may differ.

4. A clinical cohort evaluation of sST2 presence in myocardial infarction

4.1 Introduction

4.1.1 Aims and hypothesis

Translatable findings from basic science experiments are fundamental to the success of extrapolating academic research into applied medicine. Given the relationship confirmed by western blots in cellular injury mechanisms explored in chapter 3, it is expected that myocardial necrosis as a result of ischaemia in humans induces similar sST2-mediated pathophysiological changes, and as a result of it's serological release, are measurable. Consequently, the aim of this chapter is, firstly, to corroborate findings that sST2 is raised in patients with MI. Generally speaking, this observation could also contribute to the limited available literature looking specifically at sST2 expression in MI, accounting for both STEMI and NSTEMI aetiology. Secondly, data about patients' development of HF post-MI, and whether they suffered a second MI after the one they were admitted for, will be compared to their serum sST2 to determine correlation, if any. It is hypothesised that sST2 will be significantly higher in those with these adverse outcomes.

Finally, NT-pro BNP measurements will also be obtained from the hospital to evaluate whether sST2 or NT-proBNP, perform best for AUC for outcome predicting. As discussed in the introduction, there is conflicting literature about the relative utility of NT-proBNP and sST2 for predicting outcome after MI, however, given the rapid release of sST2 into serum confirmed by Chapters 2 and 3, it is hypothesised that sST2 is a better predictor of outcome based on level of biomarker at presentation.

4.1.2 Rationale

Consented donations of human plasma samples of those who have suffered MI are essential to establishing a relationship, if any, between biomarker expression and MACE/prognosis, and also between biomarkers themselves (i.e. NT-proBNP, cTnI, sST2). Acquiring sufficient clinical samples in order to validate the developed duplex assay is also necessary to comment on its efficacy in a clinical setting, hence forms the rationale of this chapter. If it is confirmed that patients with MI do, in fact, develop MACE at a higher rate with a pathological level of sST2, the development of an applicable solution (i.e this duplex assay) to such findings is crucial to further prove its utility beyond a theoretical and basic science concept.

4.2 Methods

4.2.1 Patient inclusion and exclusion criteria

All clinical samples were donated by patients attending Salford Royal hospital A&E department over a period of 3 years with symptoms of ACS. The primary aim of this chapter was to observe sST2 levels in MI, and patient samples within this criterion will be defined and measured as such. However, the arrangement between the NCARC (Northern Care Alliance Research Collection) and Osler Diagnostics allows for the acquisition of plasma from consenting patients with symptoms of ACS, and where the responsible clinician feels that cTnI measurements are necessary to rule in/out MI. Given the opportunity to assess these samples for the intended purpose of the duplex assay, where diagnosis is unknown and biomarkers are used as a tool to diagnose, all samples were measured initially for “all-cause” contribution of biomarker levels and subsequently excluded from further analysis when appropriate. For scrutiny of sST2 presence solely attributed to confirmed MI by t-test analysis, inclusion and exclusion criteria further in analysis were as follows:

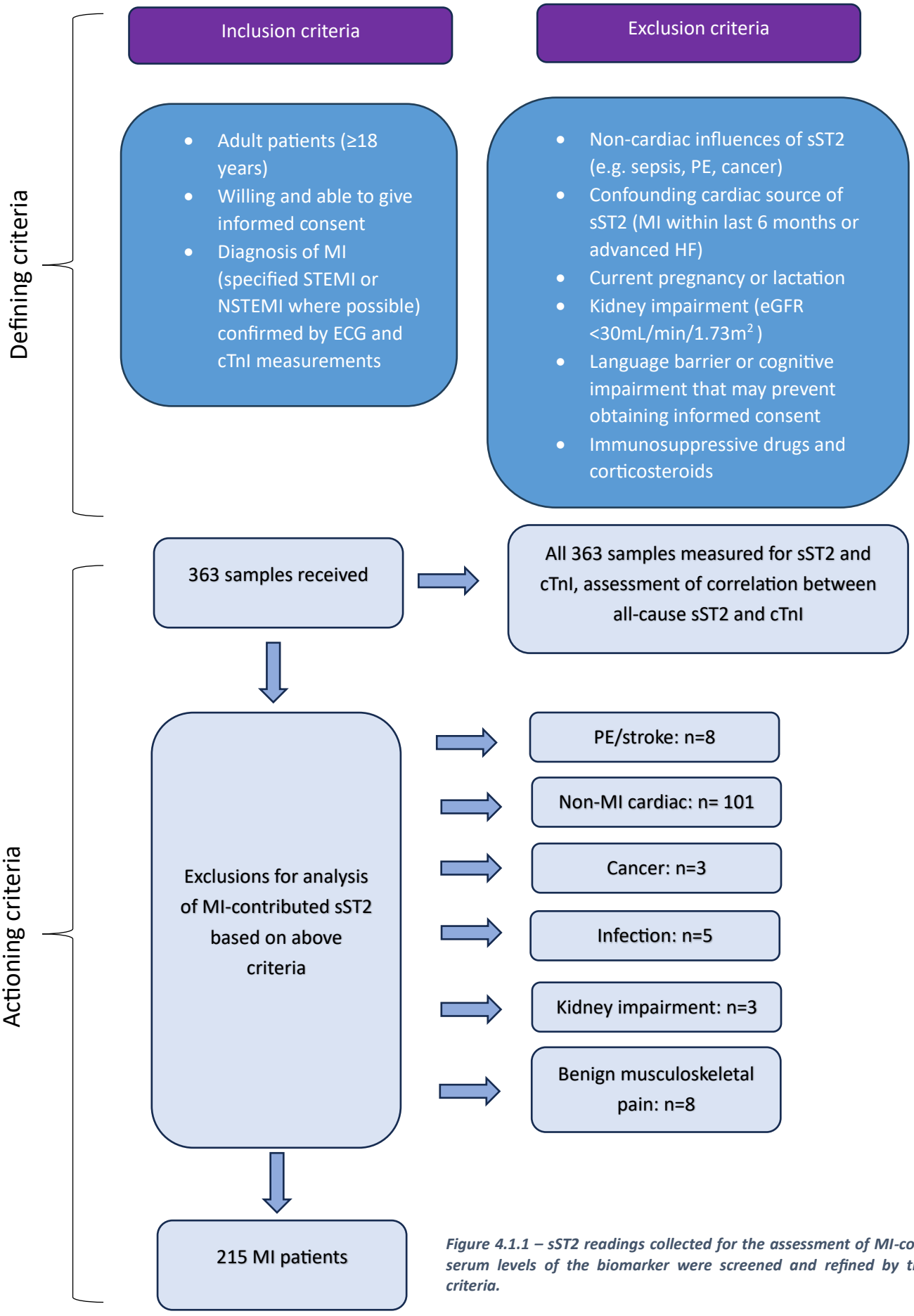

Figure 4.1.1 – sST2 readings collected for the assessment of MI-contributed serum levels of the biomarker were screened and refined by the above criteria.

Additional parameters requiring control were the timescale in which the patient arrived in A&E with symptoms of MI, and the point at which the blood sample was obtained from the patient. This information was not available until 24th March 2025 due to retrospective additional data collection, and as a result, all samples were measured before knowledge of their age post-symptomatic onset. Collecting samples at different times is not ideal, however, due to the severity of MI and the way it can cause incapacitation, it is difficult to obtain informed consent at the earliest opportunity, when the patient first presents with symptoms. In some cases, consent was only obtained after a few days after admission post-MI, when the patient was well enough. However, this information is known for each donor and will be plotted for transparency in the results section of this chapter. This also provides opportunity to observe time effect, if any.

A donut chart detailing the prevalence of each diagnosis attributed to each patient is shown below in Figure 4.1.2, with age and gender breakdown in figure 4.1.3

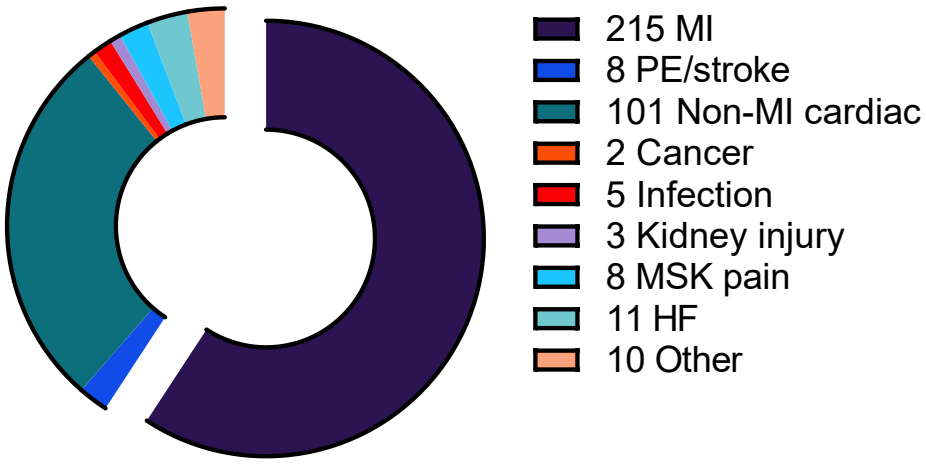

Figure 4.1.2 – A donut graph to show distribution of diagnoses among patients involved in the clinical cohort. *Most patients presenting to A&E with chest pain where the clinician responsible suspected an MI, were in fact later diagnosed with MI. These 215 patients were further analysed to fulfil the chapter's hypotheses. Other causes of high sST2 could be infection, kidney injury, and other cardiac conditions, and so these patients were removed from the final dataset.*

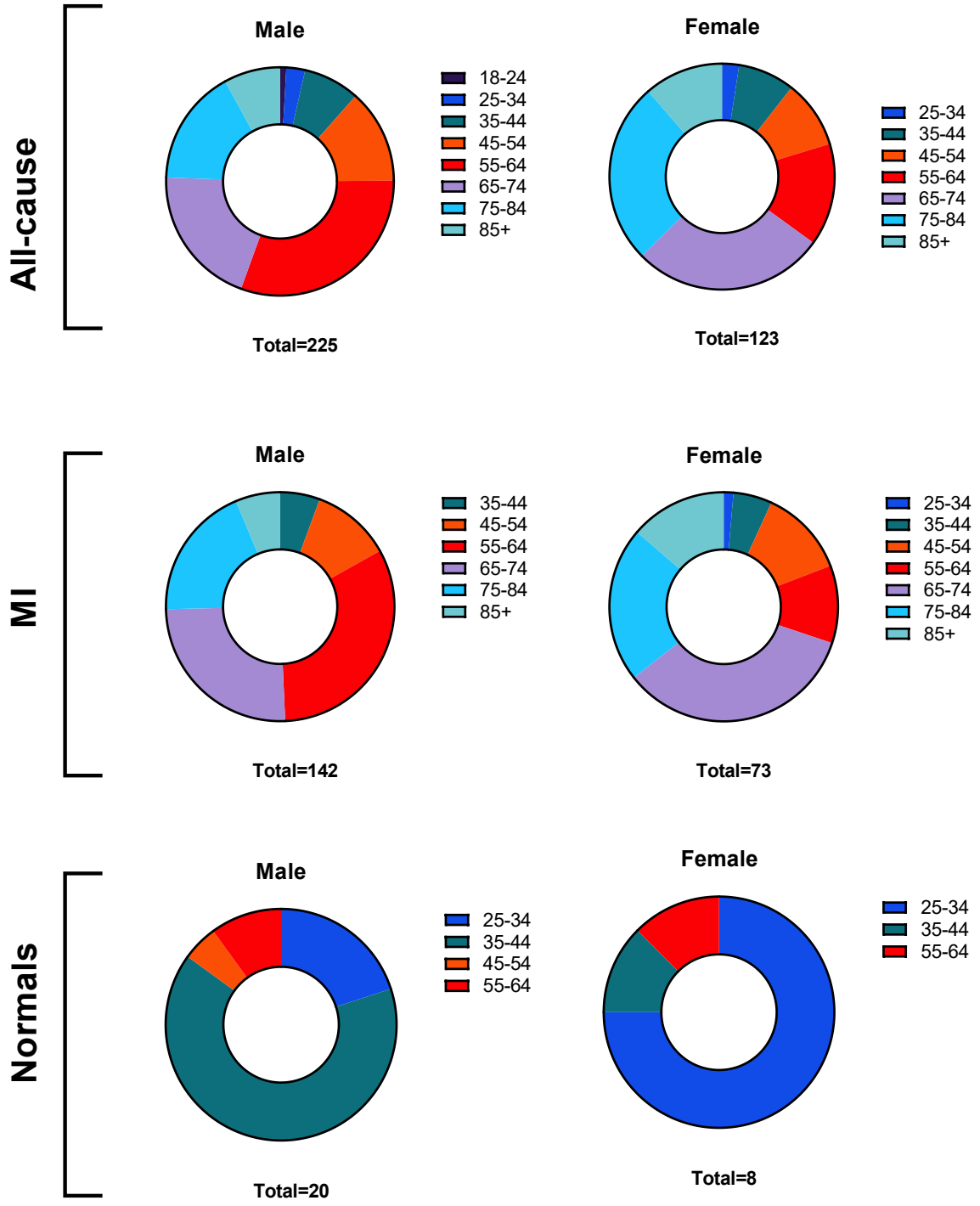

Figure 4.1.3 – Donut charts show the distribution of age and gender by all-cause with a total n=348. *Patient total in Figure 4.1.1 describes 363 patients, however there was not age and gender data for 15 of these cohort. All 415 MI patients consented to age and gender data collection. For normals, 28 donors consented to releasing their age and gender.*

4.2.2 Sample handling, preparation, transport and storage

The arrangement between Osler Diagnostics and the NCARC is as follows: Whole blood was acquired from a consenting patient that has attended A&E with symptoms of ACS, or that a doctor has suspected ACS and a troponin measurement is ordered. Blood was taken from patients who have entered A&E within the last 12 hours. Both EDTA and LiHep anticoagulated vacutainers were used for collection, with 18ml and 9ml drawn, respectively. The whole blood sample was refrigerated immediately (4-8°C) and shipped to Osler Diagnostics by temperature control within 8 hours. Upon receipt in Oxford, the sample was immediately centrifuged at 3000 x g for 15 minutes, plasma was separated by pipette and aliquoted into 400µL microtubes. 200µL of plasma was reserved for measurement of troponin and NT-proBNP on the Abbott Architect. Once aliquoted, each of the tubes were frozen immediately at -80°C. For the clinical study, only Lihep samples were tested. To prepare the plate maps for the clinical study, the samples were removed from the freezer and thawed in a 37°C water bath for 5 minutes to achieve complete thaw. Once thawed, samples were pipetted into a 96 well plate format outlined in section 6.2.3, before being sealed with tape and frozen again at -80°C. For confidence in the sample handling procedure, stability of freeze thawed standard curves were assessed before the study on both the duplex assay and the Abbott Architect to ensure analyte integrity (see Appendix item B, Figure 7.1.2, page 203).

4.2.3 96 well plate layout and study plan

Each 96 well plate of donor samples was mapped to contain enough plasma for triplicate measurements of both troponin and sST2. On the day of the clinical study, the 96 well plates were thawed at 37°C, then centrifuged at 3000 x g for 1 hour. Thawing from -80°C to 37°C enables minimal cryoprecipitate formation, which in turn reduces the possibility of precipitate interference in the immunoassay. Furthermore, the centrifugation step ensures

that any cryoprecipitate that has formed from thawing is pelleted at the bottom of the well, allowing for removal of clean supernatant post centrifugation.

To derisk the potential of analyte degradation throughout the day, each plate was thawed and centrifuged four at a time, such that when it came to assaying the samples, each plate had an equal vulnerability to degradation at room temperature. Two 96 well plates were assayed at one time, to keep the duration in which it took to load the plate with detection reagents and therefore the catalysis of analyte detection equal to prevent accidentally prolonging incubation times for some samples and not others. The plate layout for each plate is seen below:

	1	2	3	4	5	6	7	8	9	10	11	12
A	clinical sample 1			clinical sample 9			clinical sample 17			STD CURVE		
B	clinical sample 2			clinical sample 10			clinical sample 18					
C	clinical sample 3			clinical sample 11			clinical sample 19					
D	clinical sample 4			clinical sample 12			clinical sample 20					
E	clinical sample 5			clinical sample 13			clinical sample 21					
F	clinical sample 6			clinical sample 14			clinical sample 22					
G	clinical sample 7			clinical sample 15			CONTROL 1					
H	clinical sample 8			clinical sample 16			CONTROL 2					

Figure 4.1.4 - A 96 well plate design to show the layout of each clinical sample study plate, where this plate was repeated 17 times with different groups of 22 samples each run.

The timetable in which samples were assayed and collected can be found in Appendix item E, Table 7.3, page 207.

To control for, and to quantify, the inevitable degree of variation between 96 well plates, a cardiac control material sourced from BioRad (IntelliQ Plus) was included in triplicate for each well plate measurement. These samples are usually human serum based and contain a variety of different cardiac analytes at various levels. However, due to the novelty of sST2 as an indicator of disease and the lack of analysers with solutions for detecting the protein, the

cardiac controls used to control the clinical study in this chapter were for the reading of cTnI only. The benefit of having control samples from a reputable supplier is that the material is highly stable and validated on multiple different FDA approved commercial analysers. However, the agreement of value assignment between commercial analysers is not tightly consistent and so instead of cardiac marker values having been assigned to the controls, they are denoted as “levels”, increasing in analyte from 1-4. Mid-range controls (2A and 3) were selected with the aim of the level to be within the linear range of detection, and far enough away from the LoD to derisk undetectable levels. Due to the manufacturer advising against freeze-thaw, the control samples were used having no previous freeze-thaw cycles and were diluted at the beginning of the day in assay diluent, kept on ice and used on every plate for the duration of the study.

4.2.4 Statistical analysis

All statistical analysis throughout this chapter was conducted using GraphPad Prism. Data were collected in Excel as raw values from spectrophotometer outputs, then interpolated from standard curves using a 4-parameter logistic regression. After raw data were converted to measurements of biomarker in their respective concentration units, multiple comparisons were made between biomarker readings within donors, plotted simply in XY format. Normality testing is integral for selecting the appropriate correlation algorithm and was done by running D’Agostino Pearson normality for larger data sets (n=>50). Shapiro-Wilk and K-S normality tests were also outputted, however are not as suitable for larger sample sets, where D’Agostino Pearson is recognised to have the most power (D'Agostino & & Pearson, 1973) (Shapiro & Wilk, 1965) (Massey, 1951) (Razali & Wah, 2011). ROC and AUC calculations were

also done on discrete data grouping and are essential for evaluation of diagnostic efficacy, as well as determining clinical cutoff for the duplex assay specifically

4.3 Results

4.3.1 Control material

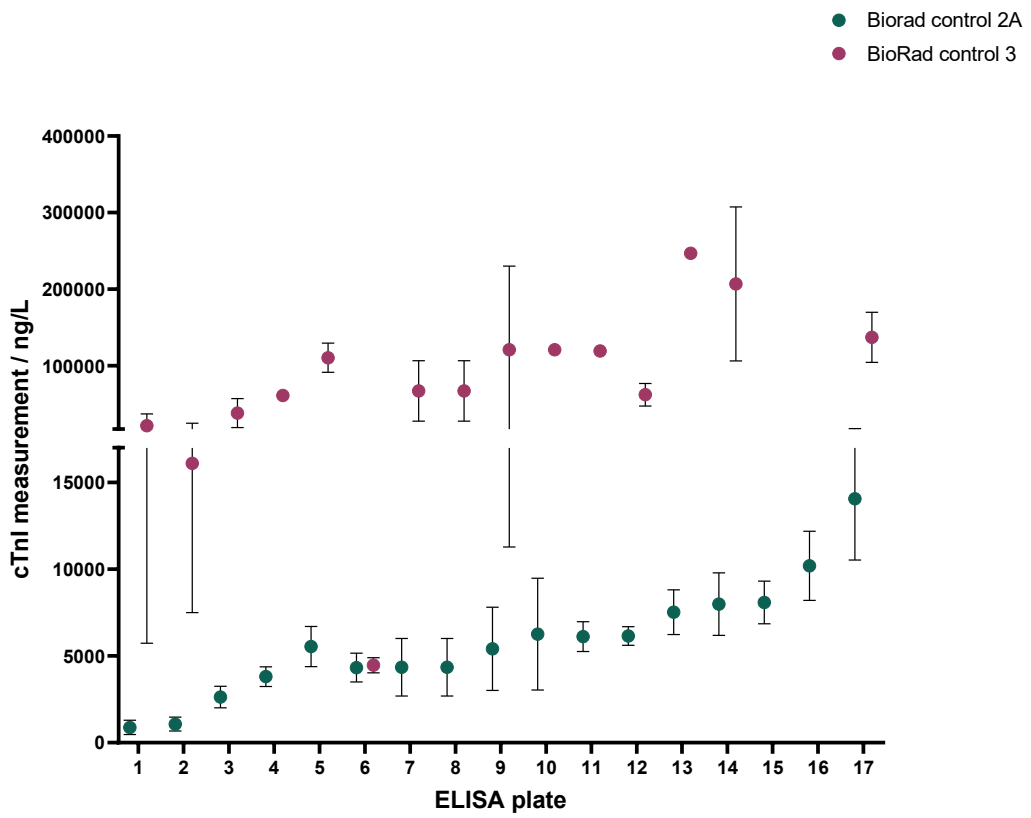

Figure 4.1.5 – A Levy-Jennings plot to show distribution of control sample (BioRad IntelliQ Cardiac Plus) on each plate for clinical sample measurement over time. *The spread of control sample measurements across all 17 ELISA plates used for the clinical study follows an upward trend in interpolated cTnI value, where the number of ELISA plate reflects the order in which they were run. It is clear that there is disparity between measurements, and thus each clinical sample should be normalised to the standard curve on each plate. Also to be noted is that not all points represent n=3; some readings were outside the range of the standard curve and therefore could not be plotted, e.g. plate 16 control 3 was outside of assay limits.*

Figure 4.1.5 shows the interpolated values of the controls with each point representing the control reading from each of the 17 plates. Despite being on ice for 8 hours, there is a trend in the increasing signal of control sample over time, showing positive interference. This raises questions about the stability of the control material and does not give confidence in the variability between ELISA well plates. The BioRad controls are said to contain a range of

different cardiac-related analytes, and so sST2 was also measured. However, all readings came back as negligible.

However, the standard curves run on each plate (see Figure 4.1.6) also showed some disagreement for cTnI, with better comparison between plates observed for sST2. This could be due to a variety of reasons, such as stability of coated capture antibody, blocking efficiency, degradation etc. Despite a lesser than expected agreement between cardiac controls, standard curves using recombinant protein also serve as a useful additional control. Given that the signal obtained from each donor sample was read from its respective standard curve, it is expected that any inevitable variation between plates is normalised this way. Inevitably, if the incongruence observed in Figure 4.1.6 causes significant detriment to cTnI accuracy, this will become apparent when comparing readings to commercial analysers.

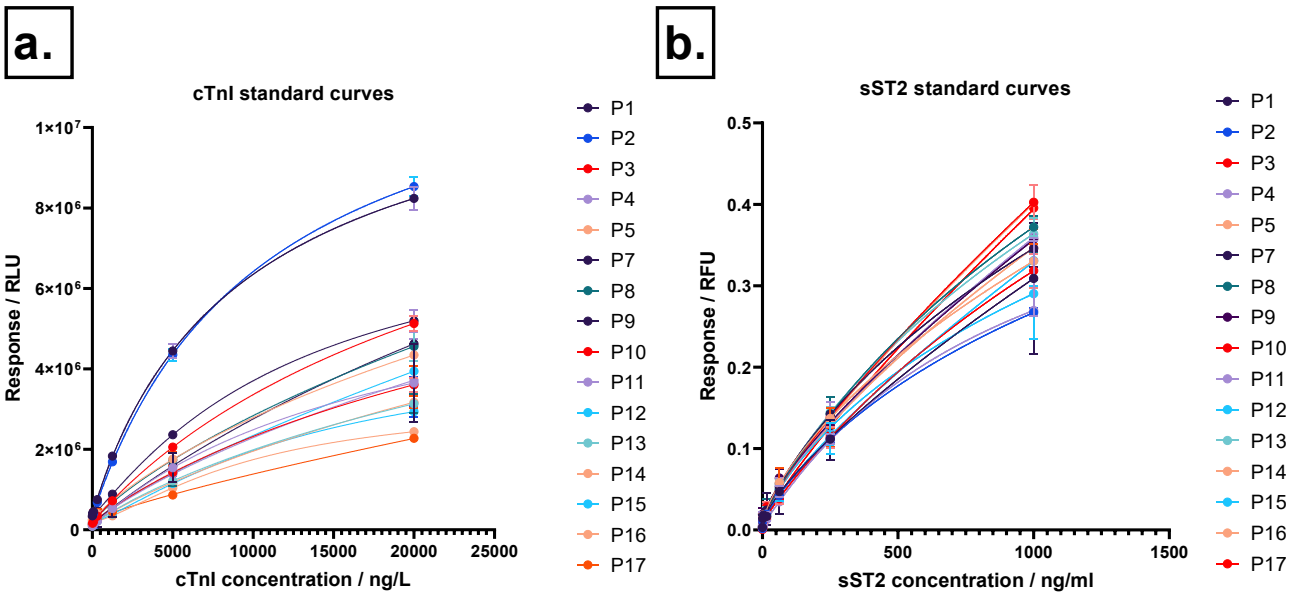

Figure 4.1.6 – The spread of standard curve response across all 17 ELISA plates used for the clinical study. *There was more agreeance in sST2 standard curves between plates compared to the troponin samples, perhaps indicating stability of each antigen.*

4.4 Comparison of duplex sST2 with commercial analysers

For each clinical sample obtained, troponin was measured three times on three different assays. Firstly, at the hospital on the Siemens Centaur hs-cTnI assay, secondly upon receipt and centrifugation in Oxford on the Abbott Architect, and thirdly in the duplex assay. It is important to consider that the Siemens Centaur result was using fresh plasma, the Abbott Architect had an 8-hour delay (although refrigerated) and the duplex assay result used plasma that had been freeze-thawed once and centrifuged. Correlations between all 3 measurement systems are plotted in Figure 4.1.7, and statistical analysis of their correlation and normality are made in Table 4.1.

Given that none of the troponin data sets were considered normally distributed, Spearman's correlation matrix was favoured over Pearson's. Correlation analysis was conducted to quantify the agreement between each measurement system across the whole range of troponin values. In all cases, a very statistically significant correlation ($P<0.0001$) was found when all measurement systems were compared to each other. This gives high confidence in the validation of specificity of the duplex troponin assay, considering its comparators are two commercially robust and globally used analysers. However, Spearman R does decline when one of the variables introduced is the duplex assay, perhaps reflecting variation seen from Figure 4.1.7.

Variable 1	Variable 2	Number of XY pairs (patients)	D'agostino-Pearson normality P value	Spearman R (95% CI)	P value
Abbott Architect (Oxford) cTnI	**Siemens Centaur (Salford) cTnI**	336	<0.0001 (not normal)	0.9054 (0.8840 to 0.9230)	<0.0001
Siemens Centaur (Salford) cTnI	**Duplex cTnI**	316	<0.0001 (not normal)	0.6198 (0.5443 to 0.6853)	<0.0001
Abbott Architect (Oxford) cTnI	**Duplex cTnI**	340	<0.0001 (not normal)	0.6598 (0.5932 to 0.7174)	<0.0001

Table 4.1 – Normality and correlation significance data for cTnI measurements across all systems. *All correlations were very statistically significant (P=<0.0001), with the highest correlation (spearman r= 0.9054) observed for both commercial analysers.*

As obvious from Table 4.1, the number of XY pairs involved in analysis differed between instruments. This is due to the fact that firstly, some of the samples measured out of range for the duplex assay standard curve, and as a result, were not able to be interpolated (n-=23, making the total number of samples measured on duplex n=340). Secondly, not all cTnI results from the hospital were made available. However, this is mitigated by the ability to measure all samples on the Abbott Architect, and so comparison between the duplex and a commercial analyser was still possible for all 340 samples.

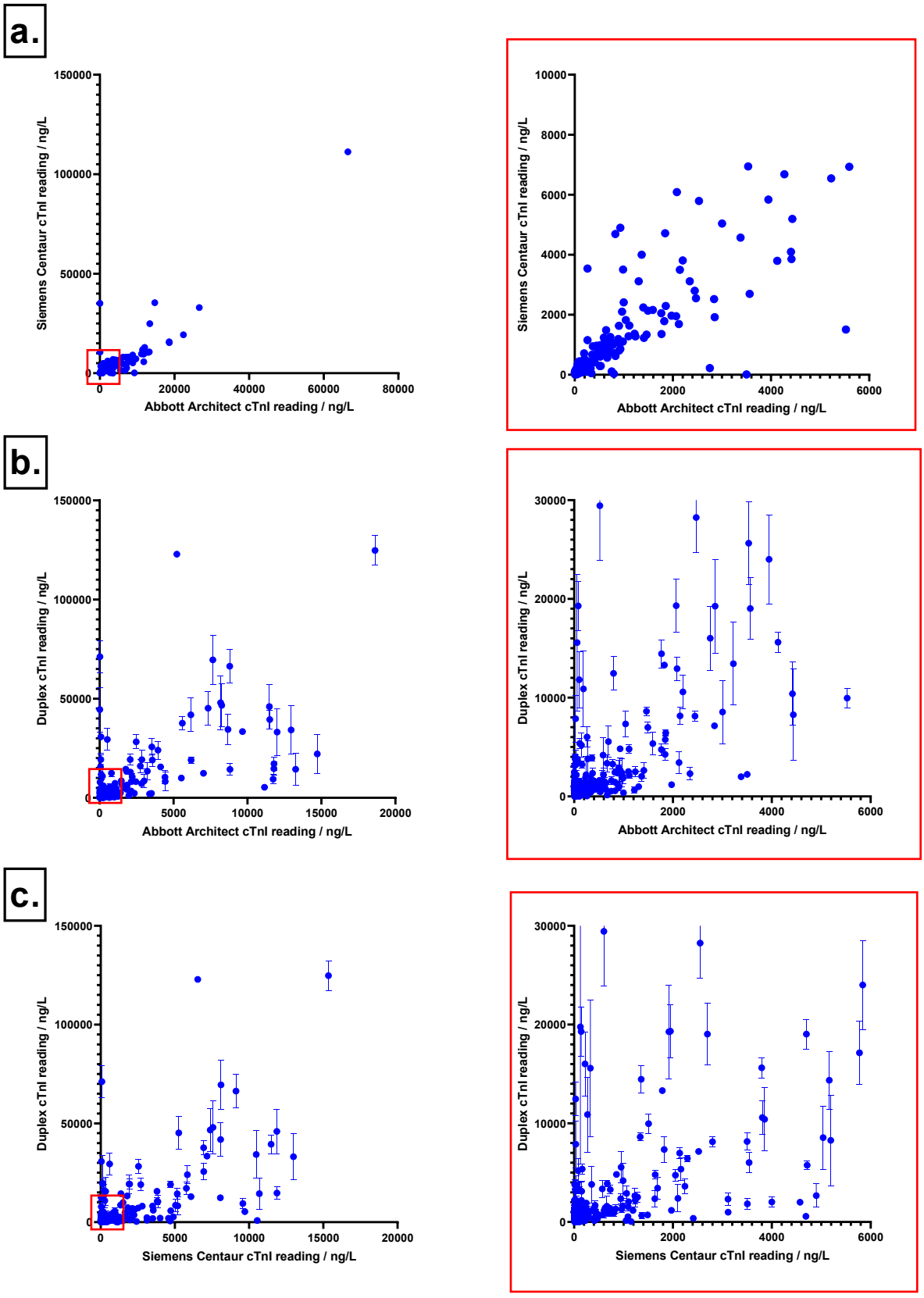

Figure 4.1.7 – Scatter plots to show agreement between cTnI measurement systems, where a) shows Siemens Centaur vs Abbott Architect, b) Duplex vs Abbott Architect and c) Duplex vs Siemens Centaur. *Statistically significant (P<0.0001) correlations were observed in all comparisons. Panels on the left side are shown in higher resolution on the right-hand side as indicated by red squares. SD error bars represent n=3.*

4.5 sST2 correlation with cTnI readings

The most anticipated results from this research were the comparisons between cTnI (diagnostic of MI) and sST2. From cTnI measurements, myocardial necrosis was inferred without risk due to the biomarker's sensitivity and, thus, sST2 can be correlated to this injury using cTnI. As before, all measurement systems for cTnI were compared to the duplex assay for assessment of agreement. The results broken down by all-cause vs MI upregulation of sST2 are tabulated below (Table 4.2):

Aetiology	cTnI test platform	sST2 test platform	Number of samples	D'agostino-Pearson normality P value	Spearman R (95% CI)	P value
All-cause	Abbott Architect (Oxford) cTnI	Duplex sST2	364	<0.0001 (not normal)	0.1200 (0.01449 to 0.2228)	0.0219
STEMI or NSTEMI	Abbott Architect (Oxford) cTnI	Duplex sST2	213	<0.0001 (not normal)	0.2137 (0.07766 to 0.3420)	0.0017
All-cause	Siemens Centaur (Salford) cTnI	Duplex sST2	337	<0.0001 (not normal)	0.0820 (-0.02822 to 0.1903	0.1330
STEMI or NSTEMI	Siemens Centaur (Salford) cTnI	Duplex sST2	199	<0.0001 (not normal)	0.2257 (0.08533 to 0.3573)	0.0013
All-cause	Duplex cTnI	Duplex sST2	291	<0.0001 (not normal)	-0.01094 (0.1291 to 0.1076)	0.8526
STEMI or NSTEMI	Duplex cTnI	Duplex sST2	189	<0.0001 (not normal)	0.3390 (0.2021 to 0.4628)	<0.0001

Table 4.2 – Statistical analysis shows significance in all cases for the correlation between cTnI and sST2 in MI patients. *In patients with all-cause presence of biomarkers, significance is only shown for the Abbott Architect, and is much weaker than for MI patients only (P=0.0219 and 0.0017, respectively).*

There are several relationships to observe here. The first is that in all measurement systems, the correlation between cTnI and sST2 was significant when cause of sST2 release was attributed to MI, with the most significant correlation being found between the duplex measurements (P=<0.0001). The Spearman R value for cTnI-sST2 relationship with duplex measurements only was 0.3390, which would still be seen as a moderate correlation rather than a strong one, however was noticeably higher than the Spearman R values observed for the Architect or the Centaur (R= 0.2137 and 0.2257 respectively). This supports the notion that there is significant value in measuring the same sample at the same time when measuring biomarkers. Although these data cannot inform whether simultaneous measurement is the reason for better agreement between biomarkers here, this factor is one of the few differences between the duplex in comparison and other analysers.

Another interesting observation is the relationship between correlation significance when going from a cohort of all-cause biomarker release and MI-mediated biomarker release. The Architect was the only platform to demonstrate significant correlation between cTnI and sST2 when including all-cause patients. Neither the Centaur nor the duplex assays yielded significant P values when comparing biomarkers in the same group (P= 0.1330 and 0.8526 respectively). cTnI-sST2 relationship in all-cause patients was particularly insignificant in the duplex assay, demonstrating that the duplex assay showed the strongest attribution of sST2 to MI pathology compared to commercial analyser measurements. However, it is essential to acknowledge the differing sample sizes for each comparison. The Architect may have been able to detect significance in all-cause biomarker release due to having a higher sample size, meaning, there is potential for type II error (failing to reject the null hypothesis) due to smaller sample size for the Centaur and the duplex. Despite this factor making it difficult to compare

across measurement systems, this does not confound the judgements made about the differences in aetiological relationships within the analysis of one measurement system.

This relationship between sample size and statistical power, where one increases with the other, is well observed in scientific research (Faber & Fonseca, 2014). With this in mind, it is perhaps even more striking that the duplex assay was able to achieve the highest level of statistical significance when observing cTnI and sST2 in MI patients. These data shown in table 4.2 and depicted in Figure 4.1.8 contribute very clear support for the hypothesis that sST2 is upregulated specifically in MI now at the human level.

Duplex cTnI vs duplex sST2

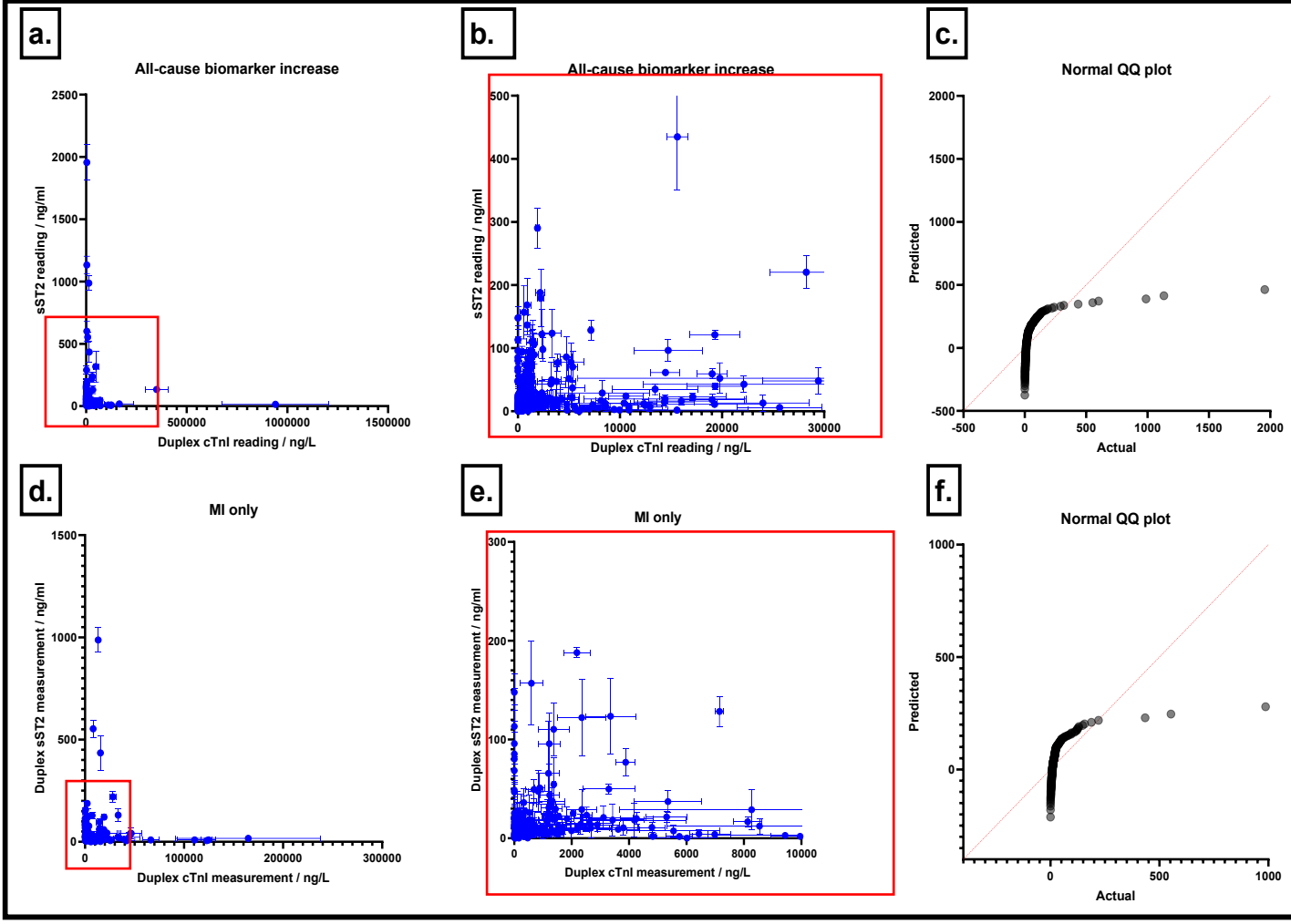

Abbott Architect cTnI vs duplex sST2

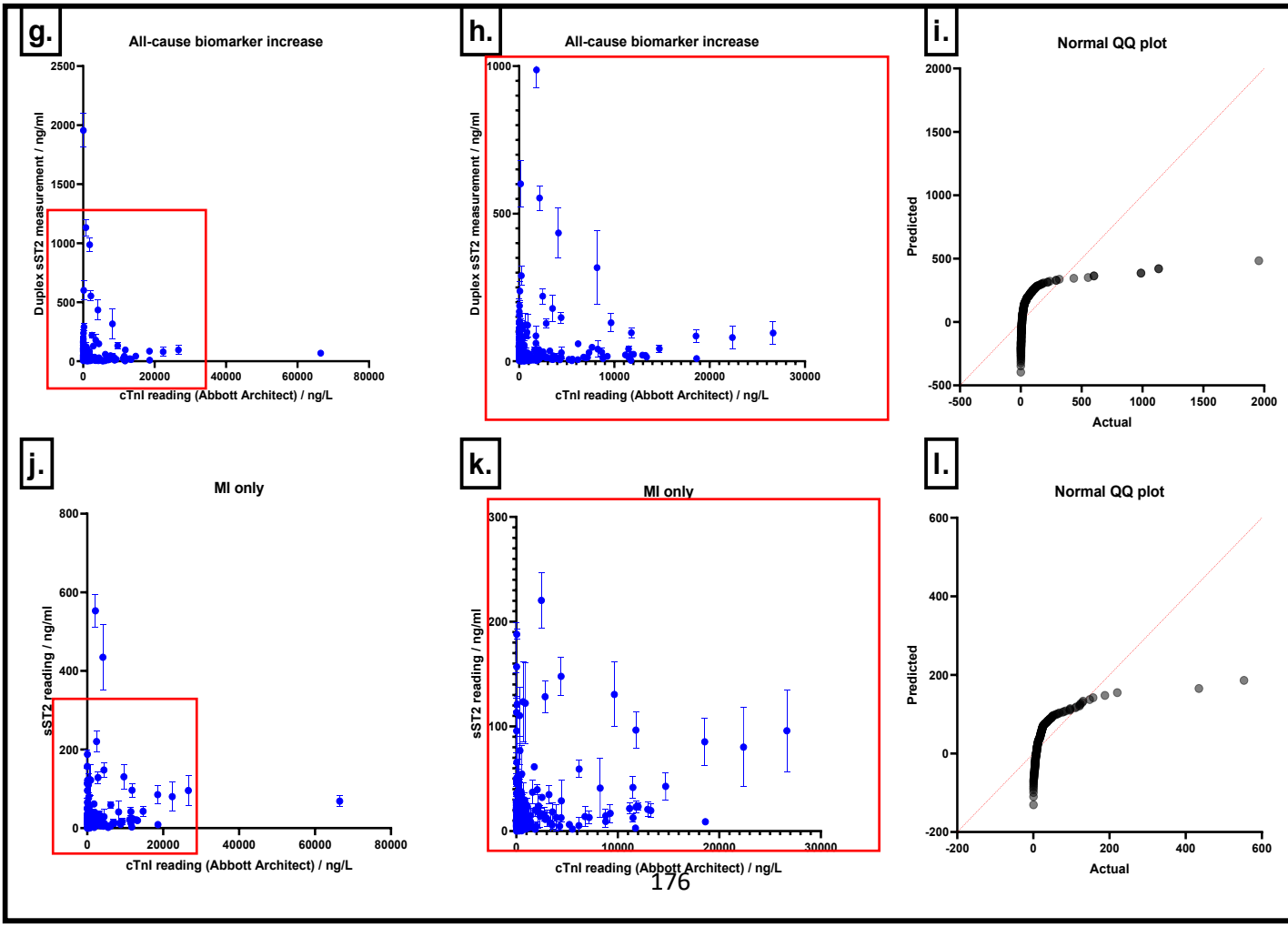

Figure 4.1.8 – sST2 does not correlates with cTnI in all-cause measurements of biomarker, however, correlates strongly in MI patients (P=<0.0001) when comparing duplex readings only. *QQ plots for normality to justify spearman's correction to correlation matrix analysis is also shown in the far right panels (panels a-f). For the Abbott Architect comparison of cTnI measurement vs the duplex sST2 measurements, significance is achieved in both all-cause and MI patients, however significance is much higher for that of MI (P=0.0219 and 0.0017, respectively).*

4.6 sST2 response with diagnosis

In addition to the cTnI-sST2 observations, it is also important to examine whether sST2 levels could discriminate between a cohort of healthy plasma donors (normals) and the MI patients from the clinical study. Figure 4.1.8 clearly presents a significantly higher sST2 reading in patients diagnosed with MI compared to a cohort of normals. An unpaired t-test (two-tailed) with Welch's correction for unassuming SD yielded a very significant difference in means between the populations (P=<0.0001 difference between means = 21.17±3.153, CI: 14.96 to 27.39), along with an equally significant difference in variance according to an additional F-test. The difference in variance amongst cohorts potentially reflects the difference in magnitude of injury (MI), as suggested by the data in section 4.5. Although the sample size is much smaller for the cohort of normals, it suggests that sST2 is fairly stable and non-responsive in this population.

The ability of sST2 to predict MI was also evaluated by plotting a ROC curve (also Figure 4.1.8), where the AUC was 0.8067 (P=<0.0001, 95% CI 0.7607 to 0.8527). By a Youdens index (*J*) calculation (*J* = sensitivity + specificity -1), the optimal clinical cutoff for this assay was 12.27ng/ml sST2, with a *J* value of 146.15.

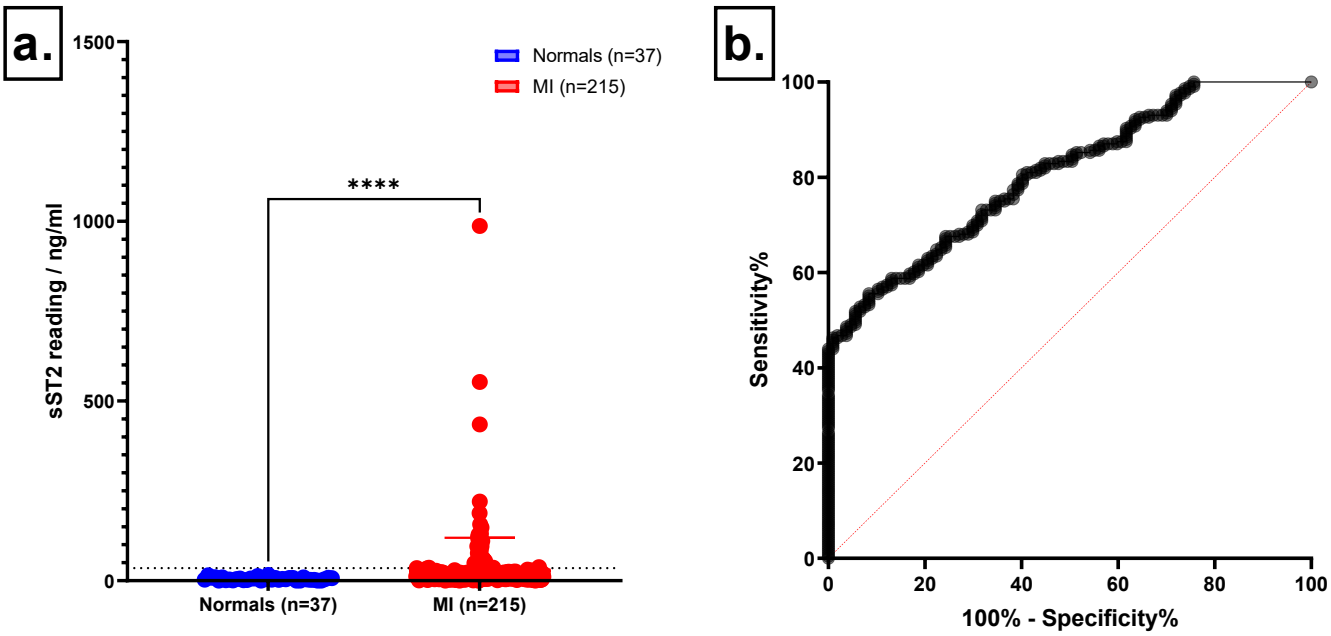

Figure 4.1.9 – sST2 levels are significantly (P=<0.0001) higher in MI patients than a cohort of healthy individuals. *Panel A shows the results of an unpaired t-test (with Welch's correction for abnormal distribution) for significance of difference between means. Panel B shows ROC analysis of the same data, with an AUC of 0.8067.*

Additional analysis was conducted by compartmentalising type of MI with healthy donor responses, again using an unpaired t-test with Welch's correction for unequal standard deviations. The results are plotted in Figure 4.2.1. Comparisons between STEMI, NSTEMI and the healthy cohort were examined to reveal a significant difference in the means of sST2 readings between NSTEMI and normals (P <0.0001), at 18.74 +- 3.444ng/ml, 95% CI 11.94 to 25.54. By comparison, the difference in means between STEMI and normals (P 0.0038) was 27.23 +- 8.224, 95% CI 9.9774 to 44.49. This *could* demonstrate a much more significant difference in the sST2 of those with NSTEMI compared to STEMI, however, this conclusion would not be robust given that the number of STEMI patients (n=19) was much smaller than NSTEMI (n=163). When both MI types are compared, the t test for NSTEMI vs STEMI reveals a non-significant difference in means at P of 0.3597, where the difference in means was -8.492 +- 8.862, 95% CI-26.76 to 9.77. Further analysis using ROC showed AUC values of 0.88 (95%

CI: 0.7758 to 0.9994), 0.80 (95% CI: 0.7291 to 0.8673) and 0.65 (95% CI: 05245 to 0.7833) for normals vs STEMI, normals vs NSTEMI and STEMI vs NSTEMI, respectively.

Another interesting observation regarding readings around the clinical cutoff value of 35ng/L. For STEMI, the average reading for sST2 was 32.18ng/ml (+- 37.7ng/ml), with a median of 19, which is situated around the clinical cutoff. This means that only 5 out of 19 (26.32%) STEMI patients exceeded the clinical cutoff for pathological levels of sST2 as stated by Critical Care Diagnostics. AUC for STEMI was 0.8876 (95% CI: 0.7758-0.9994, P=<0.0001). For NSTEMI, the average reading was 23.5ng/ml (+- 43.6ng/ml), with a median of 11.18ng/ml, which is again just below the clinical cutoff. AUC for NSTEMI was 0.7982 (95% CI: 0.7291 to 0.8673, P=<0.0001). By stark comparison, the average reading for sST2 for the normals cohort was 4.94ng/ml (+- 4.49ng/ml) with a median reading of 3.5ng/ml. Clearly, the range of readings for those with MI, regardless of ECG presentation, is much higher than healthy donors. This was quantified using an F-test, in which there was a very significant (P>0.001) difference in the variances between both normals and STEMI, and normals and NSTEMI, with a non-significant difference (P 0.3597) in variance between STEMI and NSTEMI. Given the ROC analysis made from the previous Figure (Figure 4.1.9), the clinical cutoff would be considered much different. This brings light to the nuanced and intricate factors producing clinical cutoff values, where assay performance can change these thresholds significantly (Woo & Kim, 2020). In sections 4.8.1 and 4.8.2, where incidence of MACE, specifically subsequent HF diagnosis and secondary MI are recorded, clinical cutoff will be revaluated by ROC analysis to assess whether the arbitrary 35ng/ml extrapolated from the assay developed by Critical Care Diagnostics is accurate for the duplex.

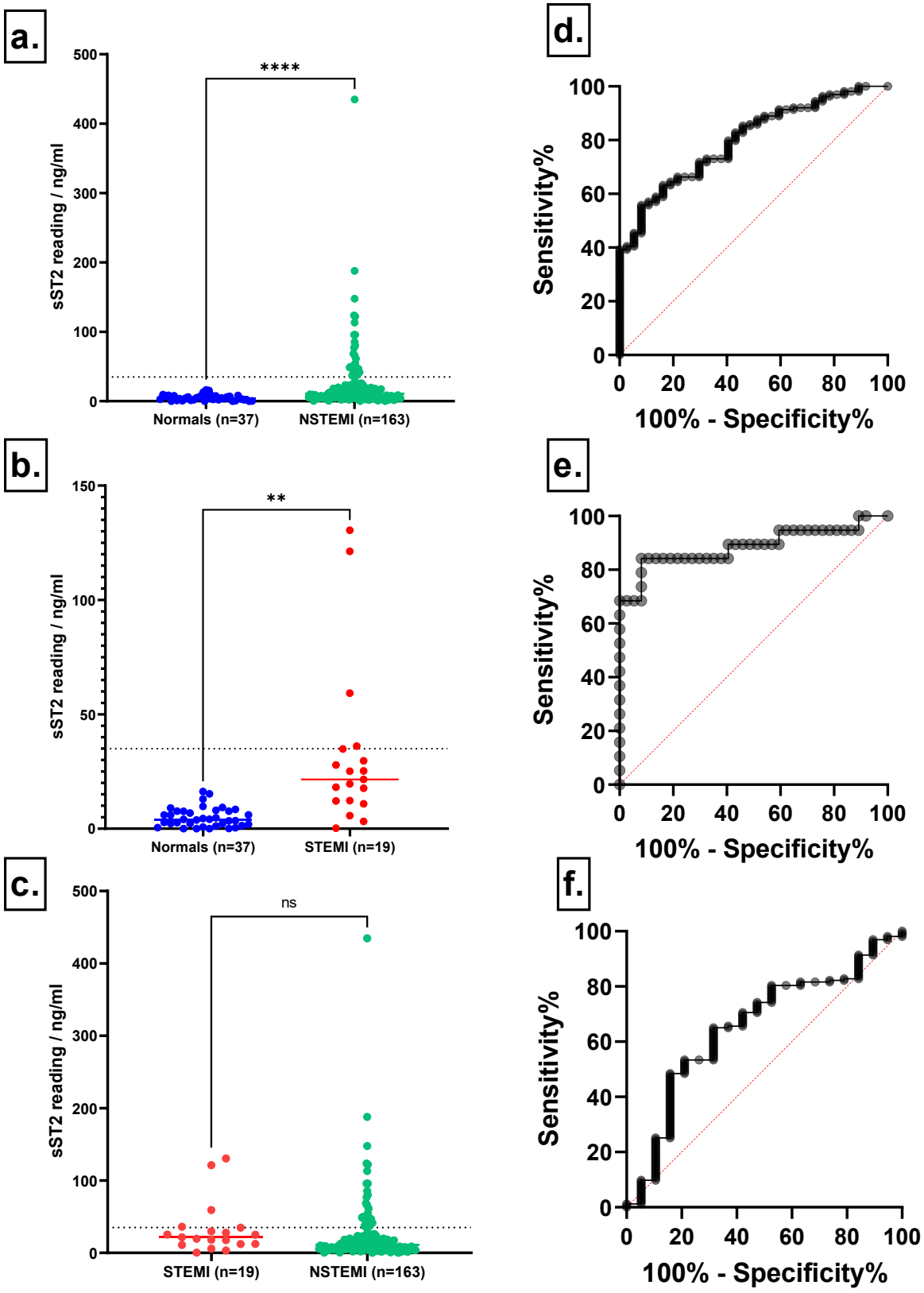

Figure 4.2.1 - sST2 is able to distinguish both (a.) NSTEMI (P=<0.0001) and (b.) STEMI (P=0.0381) from a healthy cohort. There is no difference in sST2 levels between STEMI and NSTEMI patients (plot c. P=0.3473). *sST2 had positive predictive value (PPV) for both NSTEMI (d., AUC:0.7982) and STEMI (e. AUC:0.8876), but a much smaller PPV for distinguishing STEMI from NSTEMI (f. AUC:0.6539).*

4.7 sST2 reading broken down by time post MI symptom onset

The date and time in DD/MM/YYYY and HH:MM format was collected for each patient, for when the patient was registered as arriving at A&E at Salford Royal Hospital and the time in which their bloods were taken for troponin. These analyses only contain data from patients diagnosed with MI.

Figure 4.2.2 shows the distribution of time between post presentation to A&E, and the point in which the patient donated a blood sample to be sent to us in Oxford. Given that the time was recorded down to the minute, the data was plotted in minutes rather than hours for higher accuracy (a) but for higher resolution at the earlier quartiles and distinction of days, a focused plot is also provided in the same Figure 4.2.2 (b). These two plots show that the median time of sample collection was 2 days post-presentation, and coincidentally, the first quartile contains all of the sample measured within 24 hours, and the second quartile contains the large majority of patients donating to this study between 24-48 hours post-presentation. Plots c and d in Figure 4.2.2 show the distribution of sST2 readings from patients within each quartile. Based on the study in Chapter 3 (Figure 3.1.7) where sST2 peaks at 24 hours post-infarction and declines slowly, it would be reasonable to expect a similar relationship in these patients over time.

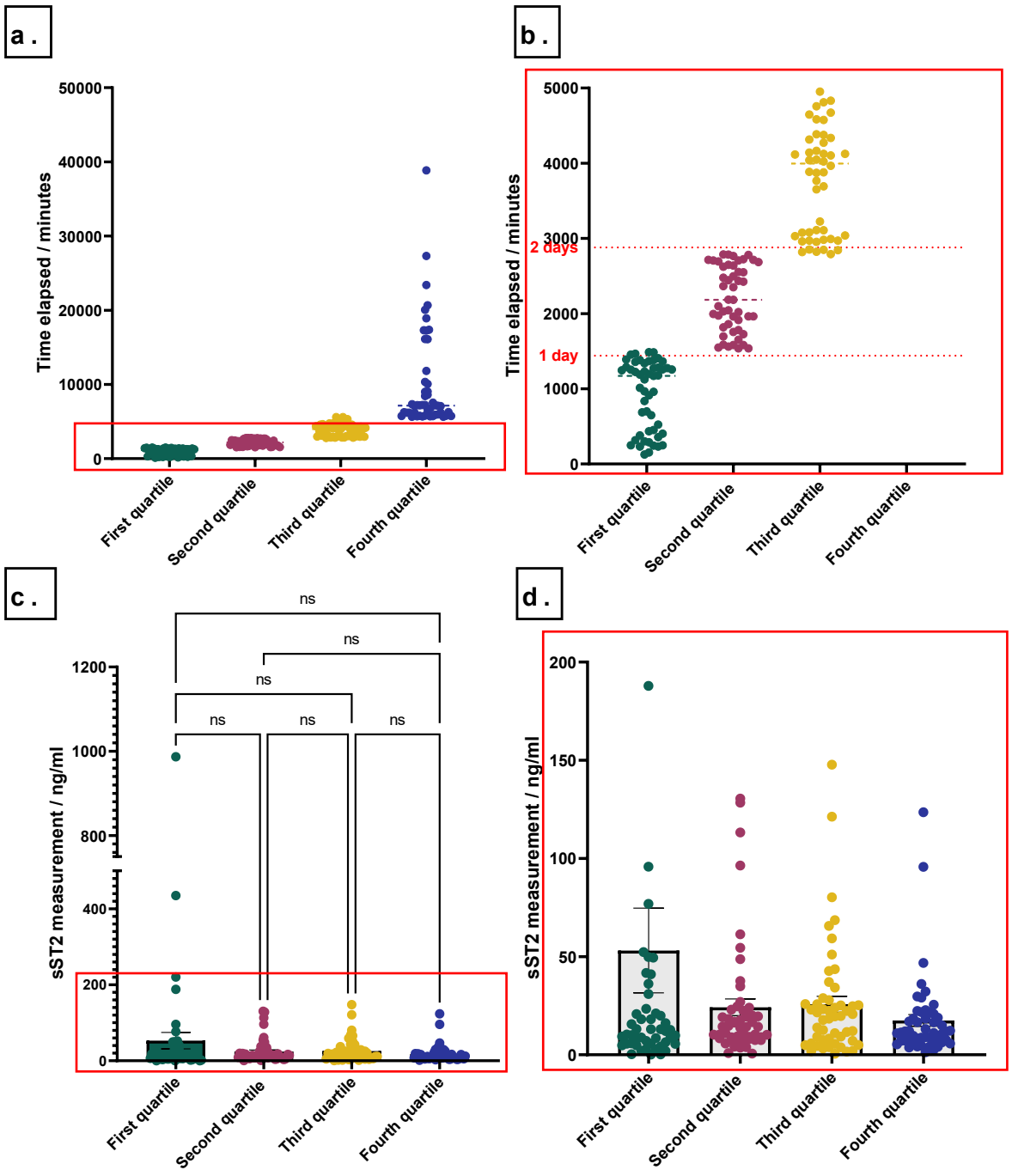

Figure 4.2.2 – The median time between patient presentation to A&E and the sample which was donated to this study was drawn was 2876 minutes (2 days). *The distribution of sST2 levels within each time quartile is shown in a., and in greater resolution (indicated by red squares) in b. There was no significant difference, according to one-way ANOVA, between sST2 levels in each of the quartiles, however, an F-test showed a significantly different variance (P=<0.0001) of sST2 levels within the first quartile in comparison to the other quartiles.*

An F test declared a statistically different variance (P<0.0001) in the first quartile group of sST2 measurements in comparison to the other quartiles, which perhaps reflects peak sST2 post-infarction since the first quartile patients were measured within 24 hours. To refine this observation, all sST2 readings from the first quartile were plotted in isolation for correlation analysis (Figure 4.2.3 plot a), however no correlation was observed (P=0.994). Given that size of infarct was not controlled in this plot, a second analysis was carried out on the same data but normalising for peak cTnI levels. All patients consented to share retrospective cTnI values from when they were registered at A&E, as well as their 2–3-hour post-presentation cTnI measurement to observe delta for MI diagnosis requirement. Peak cTnI was identified from these sequential measurements and used to normalise sST2 level after conversion of concentrations to equivalent units. The results are shown in plot b of Figure 4.2.3. After normalisation, correlation was still non-significant (P=0.493), although slope increased to 1.74 from 0.

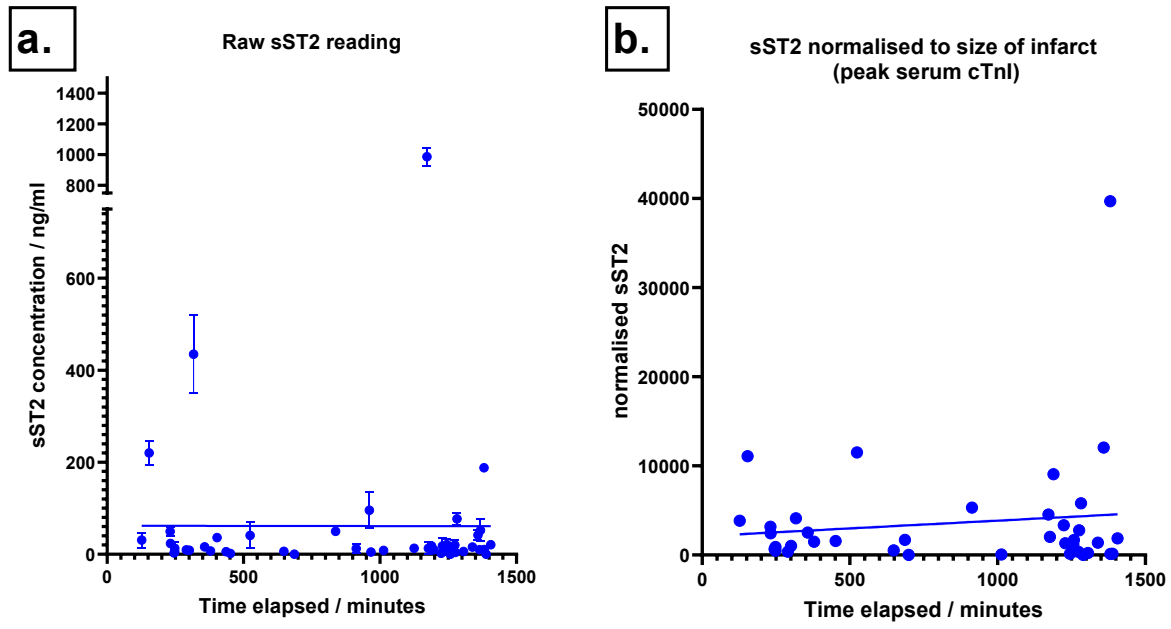

Figure 4.2.3 – When patients were able to donate their plasma within 24 hours of MI, there was no correlation between time elapsed and sST2 concentration (plot a.) (P=0.9942). This was still true when normalising for size of infarct (cTnI) of the same sample (plot b.) (P=0.4602). *A linear regression was plotted where slope was non-significantly non-zero in both cases.*

4.8 MACE incidence (either HF or secondary MI)

So far in this chapter, the relationship between sST2 and MI in a diagnostics sense has been thoroughly explored, yielding results that are robustly suggestive of a connection between MI pathophysiology and the upregulation of serous sST2, implicating a role in diagnosis. Given the seriousness of this disease and the lasting damage inflicted onto the myocardium, risk stratification is also an integral piece of the MI patient handling pathway, for indication of treatment aggression and monitoring. Two of the most severe outcomes (MACE) post-MI (not including death) are a consequential diagnosis of HF and subsequent MI. The incidence of these events was recorded in the entire patient cohort and analysed in the next sections 4.8.1 and 4.8.2.

4.8.1 Subsequent diagnosis of HF post-presentation to A&E

The incidence of HF between the period of presenting to A&E at the time in which the sample measured was drawn for each patient, and 24th March 2025 was recorded as a binary Y/N incidence. The data for all-cause (entire cohort, n=361) incidence of HF during this period is shown in Figure 4.2.4. To reiterate, this includes all patients that present to A&E with MI symptoms, but do not necessarily leave with that diagnosis. The left column of plots shows the comparison of incidence of HF (n=55) and non-HF (n=295). Significance of mean difference between groups is denoted by bars and represents a T-test with Welch's correction for an assumption of unequal variance. The only biomarker capable of detecting a difference between the group at risk of subsequent HF and those who had not acquired HF was NT-proBNP, where the difference in means was 2715±1183, 95% CI 377 to 5053 (P=0.0232). The confidence intervals for the difference between groups is very wide considering the extreme difference in variance between the groups, which was confirmed significant by an additional F test (P<0.0001). On the other hand, the difference between means was not significant for

sST2 (56.73±35.12, 95% CI -13.59 to 127, P=0.1118) nor cTnI (6831±24022, 95% CI -40824 to 54485, P=0.7767). Analysis by ROC in the right-hand panel of plots tells a similar story, where AUC for sST2, NT-proBNP and cTnI were 0.71, 0.75 and 0.61, respectively. These data indicate a positive predictive value to NT-proBNP and sST2, which are not too dissimilar, however NT-proBNP has a slight advantage.

When the patient cohort is sectioned by a diagnosis of MI without confounding aetiologies such as kidney injury (as stated in methods Figure 4.1.1) (n=205) and the data is analysed in the same way as the whole cohort (Figure 4.2.5), no biomarkers were able to differentiate HF from non-HF when pooled as a group and analysed for mean difference. Unpaired T-tests with Welch's correction for unequal variance yielded P values of 0.28, 0.10 and 0.88, with F test P values of <0.0001, 0.0008 and 0.033 for NT-proBNP, sST2 and cTnI, respectively. This confirms that Welch's correction was the appropriate statistic to apply given that all biomarkers showed significantly different variance between HF and non-HF groups. ROC plots for biomarker prediction of subsequent HF also yielded similar results to the all-cause cohort ROCs, where AUCs were 0.72 (95% CI: 0.6149 to 0.8348), 0.70 (95% CI 0.5917 to 0.8069) and 0.53 (95% CI: 0.4095 to 0.6664) for NTpro-BNP, sST2 and cTnI, respectively. Important to consider is the very close overlap of sST2 and NT-proBNP predictive value, showing almost the same ability to predict HF in MI patients. This is an important finding, considering that NT-proBNP is the current gold standard biomarker for HF prediction.

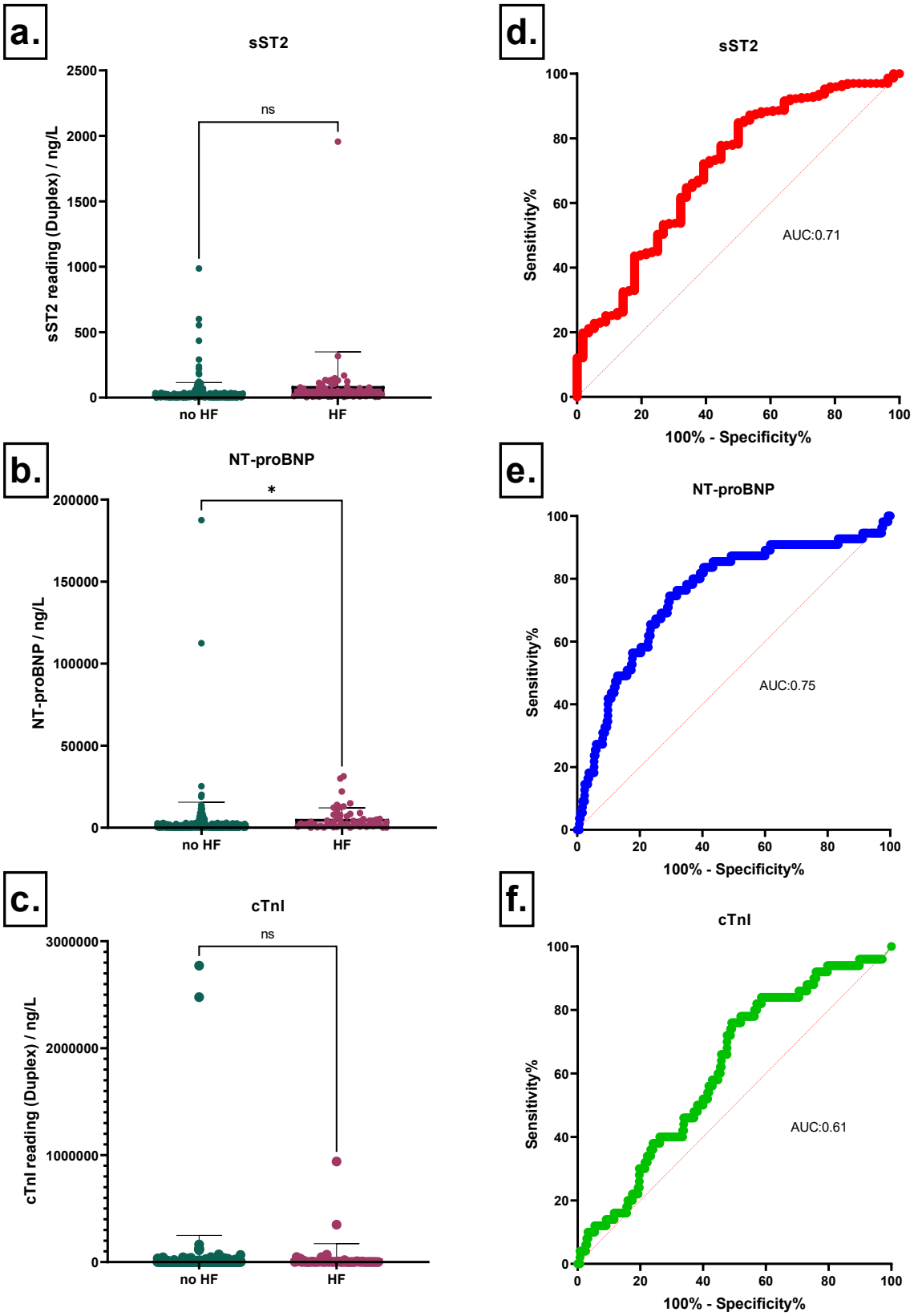

Figure 4.2.4 – Comparison of biomarker levels in entire patient cohort (all-cause) between HF (n=295) and non-HF (n=55) with corresponding ROC. *Plots a., b., and c., show the difference in means for sST2 (P=0.1118), NT-proBNP (P=0.0232) and cTnI (P=0.7767), respectively. AUC annotated on plots d., e., and f., showed highest PPV for NT-proBNP, closely followed by sST2.*

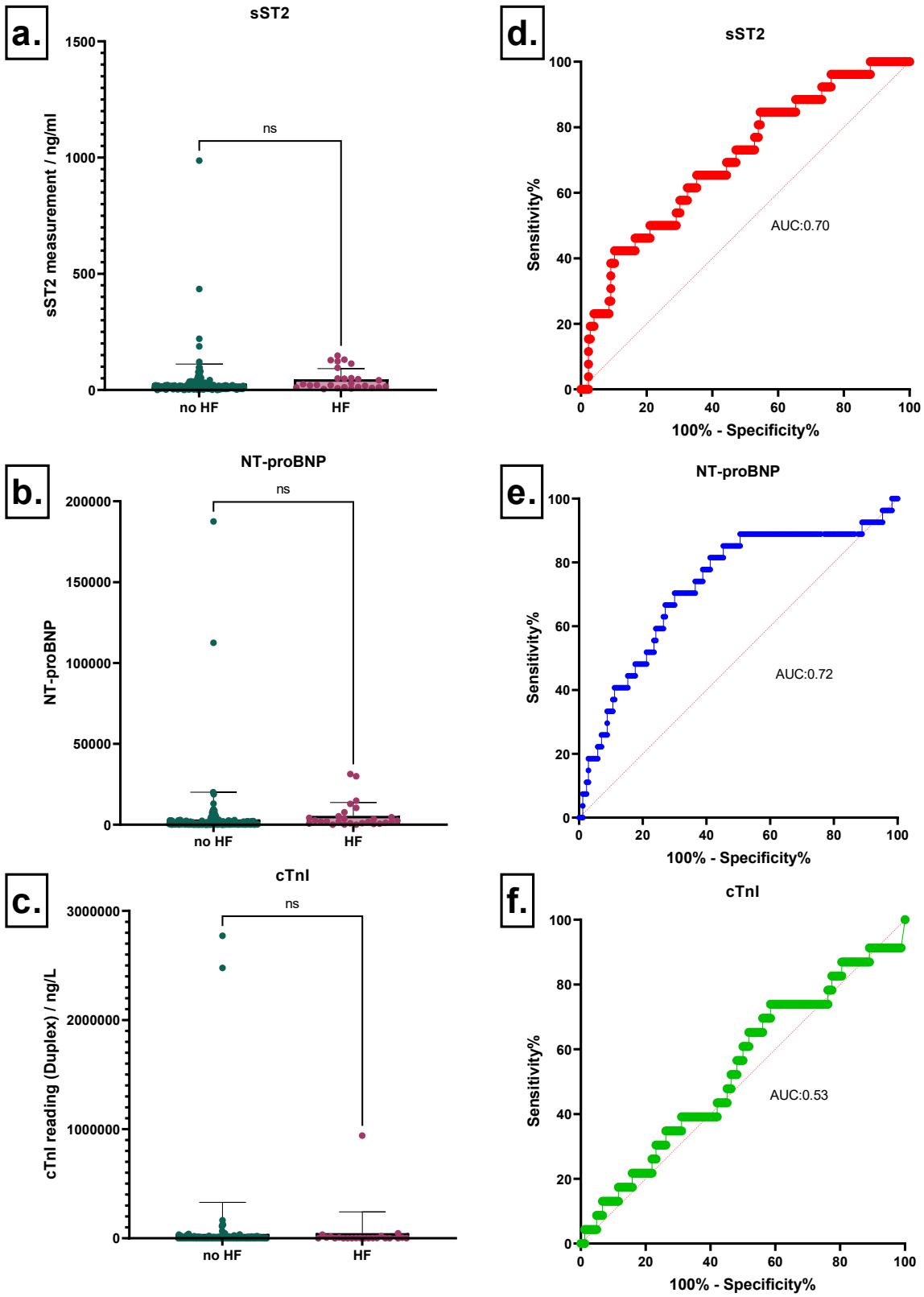

Figure 4.2.5 – Comparison of biomarker levels in MI subsection of clinical cohort (n=202: n=176 no HF and n=27 HF) with corresponding ROC. *Plots a., b., and c., show the difference in means for sST2 (P=0.1032), NT-proBNP (P=0.02840) and cTnI (P=0.8794), respectively. AUC annotated on plots d., e., and f., showed similar AUC for sST2 and NT-proBNP (0.70 and 0.72, respectively).*

4.8.2 Second MI incidence and prediction

Another metric that poses a significant threat to MI patients is the possibility of another MI. The incidence of these in the MI cohort was analysed similarly to the subsequent HF incidence by t-test and ROC. In total, 113 patients out of 205 had a second MI, which is a prevalence of 55%. This is significantly higher than the AMA statistic of 20% incidence within 5 years, with another study quoting 10% incidence within 1 year (Nair, et al., 2021). In comparison to the HF records, there was no relationship between any biomarker and incidence of second MI (Figure 4.2.6). This is evident both by the t-test (again with Welch's correction) and the ROCs. All ROCs showed 0.5 AUC, denoting equal chance between subsequent MI or not. T-test P values were 0.2618, 0.7906 and 0.2690 for sST2, NT-proBNP and cTnI, respectively.

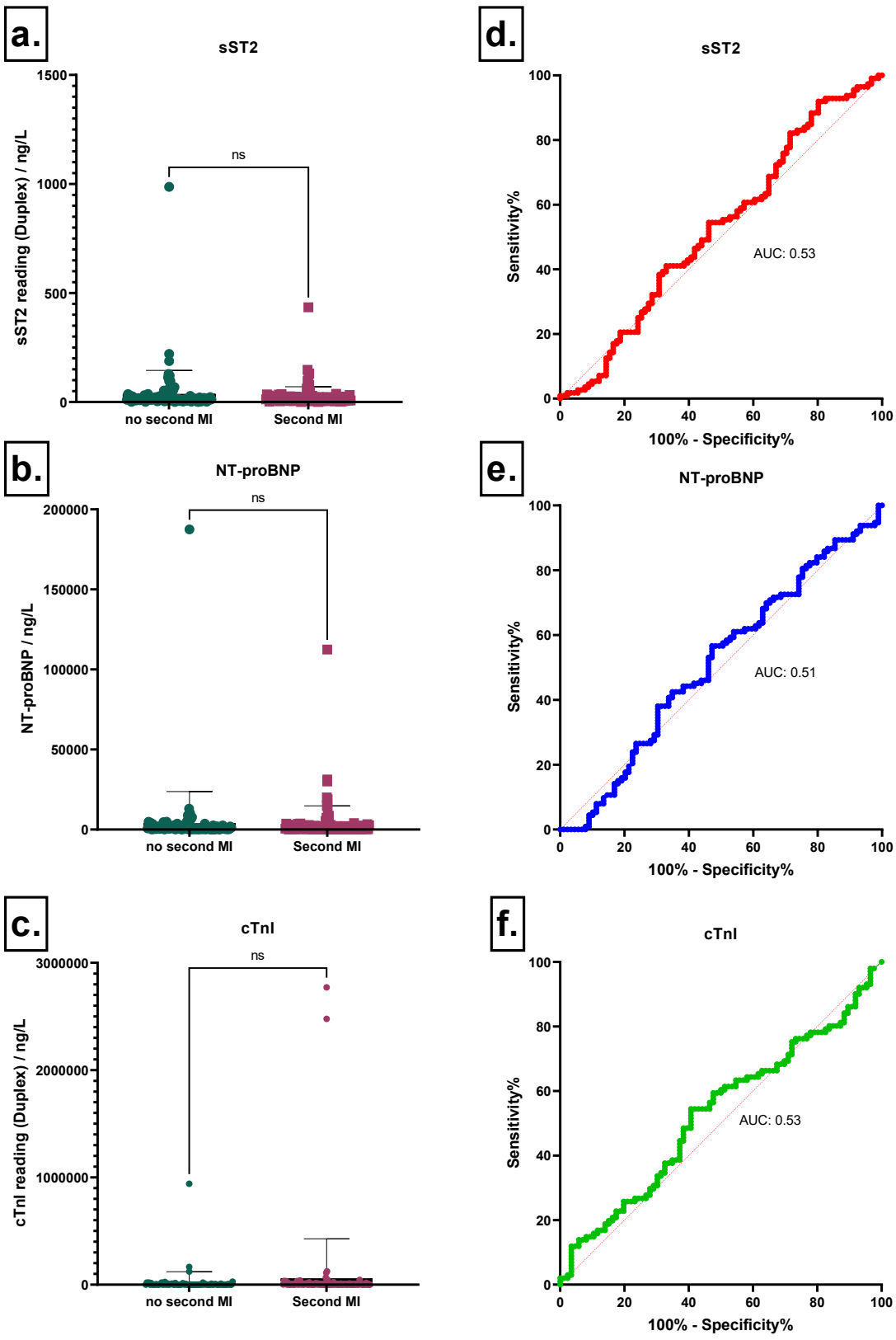

Figure 4.2.6 - Comparison of biomarker levels in the MI cohort between second MI (n=113) and no second MI (n=92) with corresponding ROC. *All plots show no relationship between biomarker levels and incidence of second MI.*

4.9 Discussion

In an area of literature so sparse with elucidative data on sST2 in MI, this chapter contributes valuable information on the topic, not only observing sST2 in MI patients but de-risking the variables associated with measuring plasma at different intervals, negated by a duplex, one well assay. The results first explored were the degrees of disparity between hospital (Salford Royal, Siemens Centaur), Oxford site (Osler Diagnostics, Abbott Architect) and duplex troponin measurements. It was perhaps unsurprising that the two commercial analysers, the Architect and the Centaur, had the best R out of all the analysers tested, given they have undergone rigorous FDA validation and are popular all over the world for diagnosis of MI. However, even these analysers showed degrees of false positivity and false negativity, highlighted by several points. For example, patient number 121 measured 1507ng/L at the hospital, but 5525ng/L onsite here in Oxford. Additionally, patient number 195 measured at 222ng/L at the hospital, but 2753.9ng/L at Oxford. Of course, false positivity and negativity are not discrete rulings but based on continuous data and can vary in degree. The most important outcome to consider is whether treatment based on a false reading would differ with each contextual comparison of troponin levels between analysers. One could argue that given troponin measurements are taken serially and compared to each other, as long as the discrepancy between analysers were kept at a constant ratio between different time points, the influence of inaccuracy is low. The most unfortunate scenario would be a completely false completely negative cTnI (below 99th percentile of around 25ng/L), with an inability to detect changes, due to some interferent rendering the assay unable to capture troponin. In this case, ECG readings and other methods of diagnosis via multifactorial assessment are key to prevent a single metric from potentially inaccurately determining the fate of an unwell patient. This applies to the entire diagnostic field, even outside of MI and cardiology, which further

reinforces the increasingly recognised value of multiplexed biomarkers in assessment of disease severity and risk.

On the subject of combining biomarkers, the next finding of this chapter was the relationship between cTnI and sST2. The pilot study conducted in Chapter 2 revealed a loose but significant (P=0.02) correlation between sST2 concentration and cTnI readings below 1000ng/L. This relationship was strengthened with a larger sample size, except this time across the entire range of cTnI levels. The imperfection in correlation between cTnI and sST2 does not render it a poor biomarker for MI. In fact, if correlation between these two readings was perfect, it would imply no additional value in mapping patient physiology. The comparison between all-cause cTnI and sST2 readings and MI patients' readings of these biomarkers was the focus of this experiment. Given that the P value is either insignificant, or close to insignificance, for all-cause increases denotes an attributable influence of MI on sST2 physiology, even before separating patient values by time post-presentation.

In the next section of the results, there is an important comparison of sST2 readings between the cohort of normals and those with MI, separated between ECG observations (STEMI and NSTEMI). The mean sST2 reading is very significantly different between healthy and MI cohorts, with an additionally large amount of variation in sST2 measurements in the MI cohort in comparison to the normals. Although the number of donors for MI and healthy donors vary (n=263 and n=37 respectively), the P >0.0001 resulting from the F test implies a variable within MI pathology that promotes a presence of sST2. This variance can be attributed to differing MI severities, extrapolated from the results in the previous section. In the absence of data that would further physiologically characterise each patient with MI, it could be predicted that the variable is not singular, and is probably affected by dilation-related

cardiomyopathy of the left ventricle, degrees of existing and resulting hypertrophy, presence of arrythmias, degrees of aortic stenosis etc. In turn, if it were elucidated that one or more of these variables contribute to sST2 measurement, it would add logic to the hypothesis that sST2 is able to predict risk of MACE and death.

In addition, the non-significant difference in sST2 levels between STEMI and NSTEMI renders sST2 useful in MI before this distinction has been made by ECG, giving even further reason to its measurement in addition to cTnI. Another hypothesis of this chapter was that sST2 would be a significant predictor of adverse outcome (HF or second MI) post-MI. This turned out to be true for the case of HF, but not for second MI. Firstly, a limitation of this study is that the time that the patient is observed for both of these outcomes post-MI varies. The cutoff for analysis was 24th March 2025, with the earliest patient sample being collected on 8th August 2021, and the last patient being 16th December 2024. According to a 2020 study, 13% of MI patients develop HF within 30 days, and 20-30% develop HF at 1-year post-MI (Jenča, et al., 2020). The data from the study in this chapter showed a HF prevalence of 13.26% in the MI cohort, which considering the differing length of time between sample collection and end time point, lines up with the previous statistic. However, ideally, all patients would be observed for a stated amount of time post-MI (e.g., 5 years), with the starting point being from when MI was diagnosed. Nevertheless, sST2 produced an AUC that is statistically equivalent (based on overlapping confidence intervals) to NT-proBNP, the current gold standard biomarker for HF prediction post-MI. Given that sST2 is not affected by age and renal impairment like NT-proBNP, there is an argument to be made for the addition of sST2 to risk factor analysis. On the other hand, it may be that sST2 is also implicated by other inflammatory stimuli.

As for subsequent MI, the prevalence was 55% in the MI cohort, with none of the biomarkers (cTnI, NT-proBNP or sST2) being able to predict incidence. To reiterate an earlier point, this could have been because of the timings associated with each patient, in that depending on when the patient was diagnosed with MI, depended on how long they were observed for MACE (including second MI).

5. Discussion

5.1 Contribution of this work to the field

The popularity of high sensitivity diagnostics in point of care settings is increasing, and with it, the expertise of assay development with human samples. Chapter 2 demonstrates the intricacy required in fine tuning assays with human plasma both as single plex, not to mention the added delicacy of multiple detection using the same sample (multiplexing). For the first time, cTnI and sST2 measurements are accessible using a small amount of sample (25uL) and within 30 minutes, with the devised protocol. The chapter reveals vital levers of sensitivity and linearity in assay development to achieve commercial standard of performance, that are not usually accessible to academia. Bridging the gap between academic findings and commercial implementation allows for the application of novel medicine as quickly as possible. It is a delicate symbiosis where one depends on the other, and so the harmony of both sectors is in the best interest of not just the scientists involved, but the worldwide community.

Aside from the obvious goal of producing a successful duplex assay, which was certainly achieved, there are other more subtle learnings from this chapter worth noting. The first, and most tedious, was the incongruence between recombinant cTnI and that of a native source. This phenomenon cannot be understood without transparency from the manufacturer (Hytest) beyond what is currently shared and poses questions about the use of all recombinant proteins in general. Due to the lack of sST2 validation, it is still uncertain whether recombinant sST2 does effectively replicate native sST2, however it is expected that any disagreement would have been observed in the pilot clinical study, whereby measurements would be too high or too low if the calibration curve was assigned inaccurately.

Researchers developing assays should, where possible, quantify the relationship between their recombinant protein and a high reading clinical sample(s) early on to allow for screening of the best antigen for continued development.

Another technical learning from this chapter is the value of a validated blank sample for inclusion in standard curves. In assays such as sST2, where novelty presents difficulties in validation, magnetic particles may be used for the depletion of a sample for basal levels. For most of the development of the duplex, a pool of human plasma was used for spiking a standard curve for some time without consideration of baseline sST2 skewing sensitivity. Once this was realised, the blank plasma could be depleted, the pool quantified and therefore sensitivity statements were more accurate. Depletion of any sample matrix in this way, using magnets is theoretically possible, and is useful where validated assays are not available.

Chapter 3 saw the novel contribution of pathway elucidation based on injury pathology, whereby it was observed that both contributions of serum sST2 (HF and MI) saw different levels of pathway stimulation on the protein level. Although the exact reason for this cannot be explained with the data provided, this is the first time that this difference has been observed. This observation is unsurprising given that the literature available contests which (or if both) disease processes cause sST2 upregulation, showing an intricacy to the IL-33/ST2L/sST2 relationship that is perhaps underappreciated. Nonetheless, the focus of this chapter, and of this thesis, is sST2 involvement in MI specifically, which is where the animal study had a significant contribution to the field's understanding of sST2 release. The knowledge that sST2 almost triples within 24 hours, with data showing decline up to 30 days post-MI, gives undeniable support to sST2 as a biomarker in MI. The next step followed through into Chapter 4, was the observation of sST2 in humans.

The literature review at the start of this thesis identified 18 papers of relevance to the relation of sST2 in MI disease process in humans. The latest paper in this list was published in 2021, when this DPhil work commenced. Since then, nothing has been published linking sST2 levels with MI pathophysiology in a diagnostic or prognostic sense. Perhaps an exception is the latest (considered unrelated) research, conducted by the OXAMI (Oxford Acute Myocardial Infarction) group in the Cardiovascular Medicine Department at the University of Oxford, which however only included patients with cardiovascular injury specifically as a result of COVID-19 (Shiwani, et al., 2024). If the intended use of sST2 measurements as proposed in this work is for corroboration of an MI event and subsequent risk, it is important that sST2 is appropriate and indicative of risk in all causes of MI. It is evident that sST2 fulfils this requirement based on the data in section 4.5 that shows a statistically significant sST2 correlation with cTnI in 189 MI patients, corroborating the only study in the literature review to explicitly compare sST2 and cTnI levels in patients with MI as a result of any aetiology (Mzoughi, et al., 2019). This study saw a much more significant correlation ($p < 0.001$), however had a sample size of only 74 patients, and drew all samples 72 hours after admission (Mzoughi, et al., 2019). Producing a dataset with all-cause MI patients, with some restrictions on AKI (acute kidney injury), is important for understanding the applicability of sST2 measurements in patients immediately presenting to A&E, with an additional indication that sST2 correlates with severity of infarction.

One of the main benefits of duplexing is the mitigation of risk surrounding time differences between biomarker measurements. For example, it has been observed within this project that degradation of samples can be unique to the donor, depending on their plasma matrix components that may accelerate this process. In single plex assays, particularly in busy hospitals, there is often delay between measuring one biomarker compared to another. If a

patient sample is particularly unstable, or haemolyses over time, the relationship between biomarker measurements can be confounded. This is why the relationship between troponin and sST2 is particularly robust, given that this variable is an impossibility when measured in duplex. This makes this the first time ever (publicly and to my knowledge), that sST2 and cTnI have been measured in MI patients at exactly the same time. An additional benefit of multiplexing is the acquisition of data more quickly, without having to wait for two separate readings to make a collective decision on diagnosis and/or treatment. A criticism of adding another biomarker to the stratification of risk, and therefore intensity of treatment in MI, is the time taken to reach this conclusion. Theoretically, if the assay from this thesis was implemented in hospitals tomorrow, there would be no additional time required to wait for rule in/rule out MI and decision on treatment, not to mention that no additional sample would need to be drawn, with a choice of either of the most popular anticoagulants.

Finally, the applicability of the sST2/cTnI duplex is proven by the initial data collected from Osler Diagnostics' proprietary development platform

5.2 Limitations

As with any scientific study, there are limitations. These are extremely important to acknowledge and demonstrate reflection and areas of work that require clarification. The work in this thesis is no exception.

Firstly, the assay produced in Chapter 2 is expensive to run. The reagents are very high quality, which is beneficial for sensitivity and specificity, but perhaps tip the balance of cost effectiveness. It is a personal conviction and belief that everyone deserves quality healthcare, and as such, expensive diagnostics are not always accessible to developing countries. If the

assay was to be commercialised, from both a community and a business perspective, the cost should be minimised as much as possible.

Limitations surrounding the robustness of the mouse serum data have already been specifically addressed in the discussion of Chapter 3, however will be touched upon here also. It was the intention of myself and the collaborator Shih-Hsuan Mao to complete the project with additional samples and the collection of additional functional and histological data, however due to reasons beyond their control, this could not be fulfilled by them in time for the thesis completion. It is thoroughly acknowledged that additional verification and quantification of infarct size, in addition to a larger sample size per time point, would have contributed to the robustness of the conclusions, however the data were still considered important and impactful enough to include in the thesis, especially given its novelty.

Finally, Chapter 4 includes a reasonable number of samples, although they were not each taken at the same time post-MI. The variability of time of presentation to time of draw varied from 0-7 days, which is likely to affect levels of biomarker given the release profile data. Having said that, it is believed that this disadvantage is somewhat mitigated by the fact that it was recorded on which day each sample was drawn post-MI, and the data are plotted to reflect that in section 4.7. The relationship between biomarker levels and time post-draw is also discussed in section 4.7. It would be ideal to collect each sample at the point of presentation, and perhaps one and two days after, when decisions about that patient's care are made, however this is near impossible due to the fact that the patient cannot consent to providing their blood sample to a third party for research when unconscious or not lucid. This is a limitation in all studies associated with donation of samples in very unwell patients. In the same vein, biomarker levels may be confounded by the time between onset of symptoms and

presentation to A&E. This also relies on perfect reporting by patients on when their symptoms started, which may not always be accurate. Again, this is a limitation of all studies collecting blood from MI patients and is not a limitation of this study design in isolation.

In the interest of further development of the duplex assay to Osler Diagnostics' technology, the sST2 assay was trialled on the proprietary platform that utilises sensors and electrochemistry for analyte detection. The proprietary platform harbours the same sensors built within Osler's single use cartridges for point of care application but does not require lyophilised reagents. With the initial data presented in Appendix item A, Figure 7.1.1, page 203, the reagents optimised in this thesis show capability to translate to electrochemical readings and perform similarly to the optical ELISA duplex, indicating feasibility for further development. This insight into real-world application demonstrates the maturity of the assay and it's potential for enabling people to live healthier, happier and longer lives.

5.3 Future work

The work involved in the 3.5 years of the curation of this thesis was genuinely exciting and enjoyable from start to finish. Having proposed the concept of the project myself, and watched it evolve whilst collecting data is something I am still passionate about and proud of as this work comes to a close. Despite feeling like this work has significantly contributed to the understanding of sST2 in MI patients and it's potential to improve care, there are a few experiments that could follow on to either explore new unanswered questions raised by the results, or to improve robustness to the existing results. These are outlined below:

i) The addition of more data involving both serum (ideally n=10 total) with matching MRI data to corroborate sST2 relation to infarct size in the murine LAD ligation study.

ii) The further commercialisation of the assay as a follow-up from the preliminary data using Osler Diagnostics' proprietary immunosensing platform.

iii) Further exploration into the IL-33/ST2L signalling pathway of seemingly vital components such as MyD88, IRAK4 and C-Jun. This could involve the phenotypic characterisation of knockout mice, lacking key pathway components, for evaluation of altered pathway activity and cardiac repair following induced MI.

iv) Expansion of the clinical study (you can never have too many samples) with a focus on recruiting patients with STEMI, given the small number of STEMI patients in this study.

v) Serial measurements of sST2 levels in patients upon arrival at A&E, and every day post-MI up to 7 days, for the characterisation of early response of sST2 within the same patients (not comparing across patients, which introduces uncontrolled variables). This experiment would also be difficult to conduct given that all of the patients would need to be well enough to consent on admission, and survive 7 days post-MI. By comparison, only four patients were able to consent on admission in the cohort described in Chapter 4, however consent was obtained within 24 hours for 25% of patients, which would still be considered an early time point.

vi) IL-33 may be useful to investigate in a therapeutic sense in the same cell injury models with AngII and H_2O_2. Additional experiments could include spiking injured cells with IL-33 in an attempt to overwhelm sST2 production and prevent inhibition of IL-33/ST2L.

6. Conclusions and final remarks

In conclusion, my work demonstrates that the duplexing of sST2 with cTnI to satisfactory (clinically relevant) limits is possible, enabling the theoretical application of this assay to clinical use in health care settings with laboratories. There is additional promise, given the data produced on Osler's proprietary development platform, that the assay can be transformed from lab-based to point of care, further increasing the value of these measurements. Clarification about the release profile of sST2 was also obtained, where it was observed that sST2 is raised within 24 hours in vivo and slowly depletes over the course of a month. This is a significant contribution to the limited existing knowledge on the release kinetics of the biomarker and provides strong rationale for it's measurement as early as possible in MI patients, but also serially over time as the patient recovers. This thesis also finds that both MI and HF contribute to the production of sST2 intracellularly and the transcription factors responsible for it's mRNA upregulation. Most importantly, the clinical study evaluates the plasma levels of sST2 and cTnI in a cohort designed to replicate the scenario in which the assay should be used, where it was indeed found that sST2 and cTnI do correlate in patients with MI. This study also allowed for the evaluation of MACE post-MI, where sST2 could predict HF about as well as NT-proBNP – the current gold standard for HF assessment. Collectively, these findings contribute data that further elucidates sST2 behaviour and its relationship with heart disease, where sST2 should be seriously considered for application in clinical practice.

7. Appendix

Appendix A: Point of care feasibility

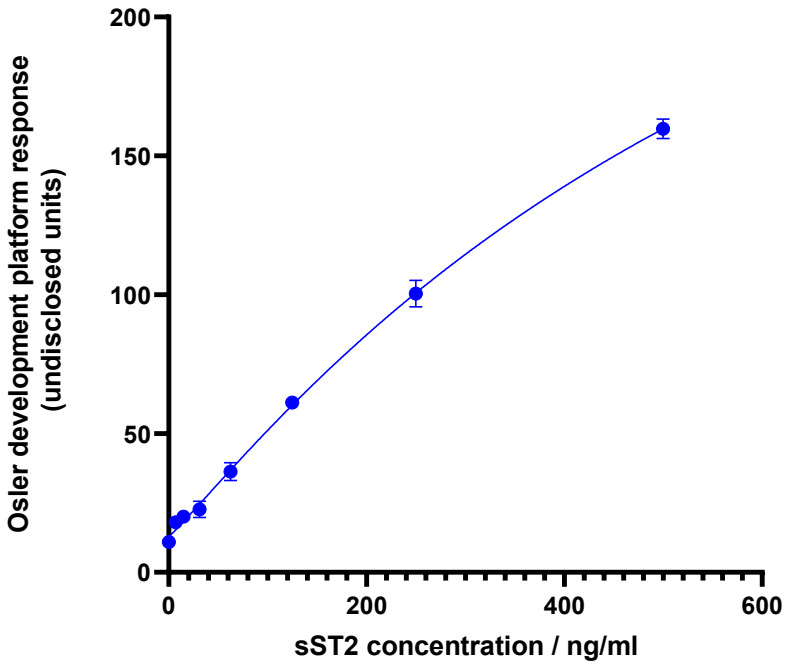

Figure 7.1.1 – The response when the sST2 assay is optimised for Osler Diagnostics proprietary development platform, showing feasibility for assay commercialisation.

Appendix B: Standard curve stability

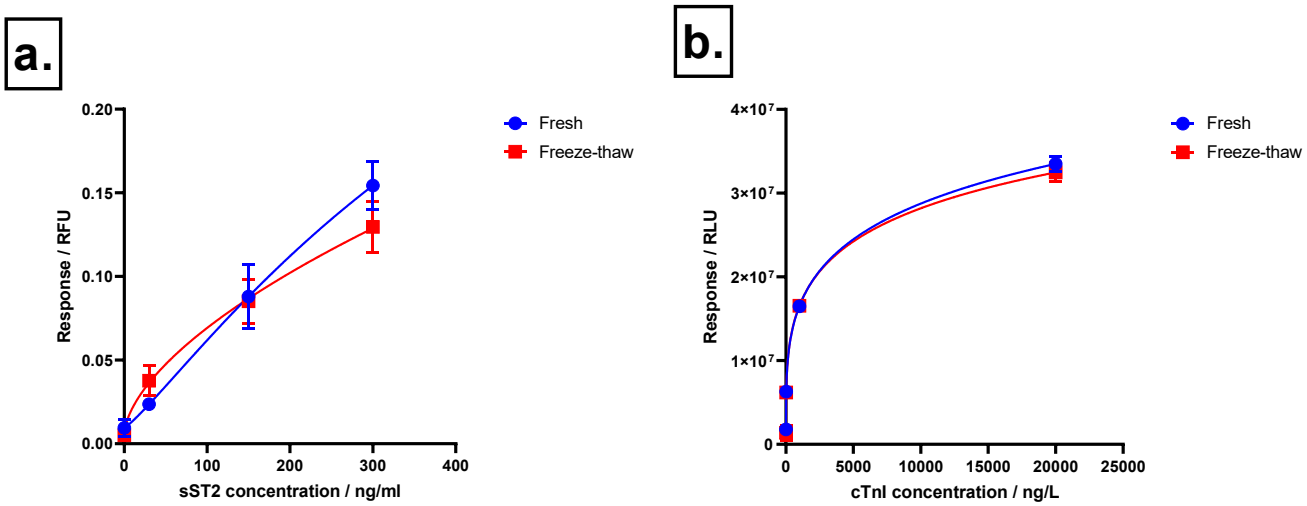

Figure 7.1.2 – Analytes are unaffected by freeze-thaw cycles required for clinical study preparation.

Appendix C: Primer information

Target	Forward/Reverse?	Sequence
MMP9	F	CCTTTCTTATTGCCCGCACG
	R	ACATTTTGCGCCCAGAGAAG
IL-33	F	GCCCTGAGCACATACAACGA
	R	TCCACACCGTCTCCTGATTGT
NPPB	F	ACAATCCACGATGCAGAAGCTG
	R	TGTAGGGCCTTGGTCCTTTG
MMP9	F	TGGGGACAAGTTCTGGAGATACA
	R	AGGTGAAGGAGAAGGCTGATT
TNF-A	F	ATGGGCTCCCTCTCATCAGT
	R	GCTTGGTGGTTTGCTACGAC
PIKC3B	F	TAGAGGCATACTGTCGGGGA
	R	CCATAGGGGAGCATTCGCAG
IL-6	F	AGCCCACCAGGAACGAAAG
	R	GGCTGGAAGTCTCTTGCGG
ACTN1	F	CCAACTATACAATGGAGCACATC
	R	TCTTTTCCATTTAAGACTGGTGGA
MMP2	F	TGTGTTCTTCGCAGGGAATG
	R	CCCGGTGTGCAGTGAAGATT
ACTA2	F	TCGTGACTACTGCTGAGCG
	R	AAGGCGCTGATCCACAAAAC

Table 7.1 – Primer sequences for RT-qPCR.

Appendix D: scRNA-seq metadata

Author	StudyID	Genotype	CellType	Age	Strain	Condition	Day	Tissue	Development_stage	Organism	Gender
Farbehi	EMTAB7365	Pdgfra+/Sca1+/Cd31	Fibroblasts	8	C57BL/6J	Uninjured	0	ventricle	adult	Mus musculus	male
Farbehi	EMTAB7376	Pdgfratm11(EGFP)+CD31-	TIP	8	C57BL/6J	MI	3	ventricle	adult	Mus musculus	male
Farbehi	EMTAB7376	Pdgfratm11(EGFP)+CD31-	TIP	8	C57BL/6J	Sham	3	ventricle	adult	Mus musculus	male
Farbehi	EMTAB7376	Pdgfratm11(EGFP)+CD31-	TIP	8	C57BL/6J	MI	7	ventricle	adult	Mus musculus	male
Farbehi	EMTAB7376	Pdgfratm11(EGFP)+CD31-	TIP	8	C57BL/6J	Sham	7	ventricle	adult	Mus musculus	male
Farbehi	EMTAB7376	WT	TIP	8	C57BL/6J	MI	3	ventricle	adult	Mus musculus	male
Farbehi	EMTAB7376	WT	TIP	8	C57BL/6J	MI	7	ventricle	adult	Mus musculus	male
Farbehi	EMTAB7376	WT	TIP	8	C57BL/6J	Sham	7	ventricle	adult	Mus musculus	male
Forte	EMTAB7895	WT	Interstitial cells	10	C57BL/6J	Sham	7	ventricle	adult	Mus musculus	male
Forte	EMTAB7895	WT	Interstitial cells	10	C57BL/6J	Sham	7	ventricle	adult	Mus musculus	male
Forte	EMTAB7895	Wt1Cre;RosaZsgreenf/+	Interstitial cells	10	C57BL/6J	Uninjured	0	ventricle	adult	Mus musculus	male
Forte	EMTAB7895	Wt1Cre;RosaZsgreenf/+	Interstitial cells	10	C57BL/6J	MI	1	ventricle	adult	Mus musculus	male
Forte	EMTAB7895	Wt1Cre;RosaZsgreenf/+	Interstitial cells	10	C57BL/6J	MI	3	ventricle	adult	Mus musculus	male
Forte	EMTAB7895	Wt1Cre;RosaZsgreenf/+	Interstitial cells	10	C57BL/6J	MI	5	ventricle	adult	Mus musculus	male
Forte	EMTAB7895	Wt1Cre;RosaZsgreenf/+	Interstitial cells	10	C57BL/6J	MI	7	ventricle	adult	Mus musculus	male
Forte	EMTAB7895	Wt1Cre;RosaZsgreenf/+	Interstitial cells	10	C57BL/6J	MI	14	ventricle	adult	Mus musculus	male
Forte	EMTAB7895	Wt1Cre;RosaZsgreenf/+	Interstitial cells	10	C57BL/6J	MI	28	ventricle	adult	Mus musculus	male
Forte	EMTAB7895	WT	Interstitial cells	10	129S1/SvImJ	Sham	7	ventricle	adult	Mus musculus	male
Forte	EMTAB7895	WT	Interstitial cells	10	129S1/SvImJ	MI	3	ventricle	adult	Mus musculus	male
Tombor	EMTAB9816	Cdh5-CreERT2/+; mT/mG	Non-CM	12	Cdh5-CreERT2;mT/mG	Uninjured	0	heart	adult	Mus musculus	male
Tombor	EMTAB9816	Cdh5-CreERT2/+; mT/mG	Non-CM	12	Cdh5-CreERT2;mT/mG	MI	1	heart	adult	Mus musculus	male
Tombor	EMTAB9816	Cdh5-CreERT2/+; mT/mG	Non-CM	12	Cdh5-CreERT2;mT/mG	MI	3	heart	adult	Mus musculus	male
Tombor	EMTAB9816	Cdh5-CreERT2/+; mT/mG	Non-CM	12	Cdh5-CreERT2;mT/mG	MI	7	heart	adult	Mus musculus	male
Tombor	EMTAB9816	Cdh5-CreERT2/+; mT/mG	Non-CM	12	Cdh5-CreERT2;mT/mG	MI	28	heart	adult	Mus musculus	male
Tombor	EMTAB9816	mT/mG	Non-CM	12	Cdh5-CreERT2;mT/mG	Uninjured	0	heart	adult	Mus musculus	male
Tombor	EMTAB9816	Cdh5-CreERT2/+; mT/mG	Non-CM	12	Cdh5-CreERT2;mT/mG	MI	14	heart	adult	Mus musculus	male
Tombor	EMTAB9817	Col1a2-CreERT2/+; mT/mG	Non-CM	88to91	Col1a2-CreERT2;mT/mG	MI	28	heart	adult	Mus musculus	male
Tombor	EMTAB9817	Col1a2-CreERT2/+; mT/mG	Non-CM	88to91	Col1a2-CreERT2;mT/mG	MI	28	heart	adult	Mus musculus	male
Tombor	EMTAB9817	Col1a2-CreERT2/+; mT/mG	Non-CM	12	Col1a2-CreERT2;mT/mG	MI	28	heart	adult	Mus musculus	male
Tombor	EMTAB9817	Col1a2-CreERT2/+; mT/mG	Non-CM	12	Col1a2-CreERT2;mT/mG	MI	28	heart	adult	Mus musculus	male
Tombor	EMTAB9817	Col1a2-CreERT2/+; mT/mG	Non-CM	88to91	Col1a2-CreERT2;mT/mG	Uninjured	28	heart	adult	Mus musculus	male
Tombor	EMTAB9817	Col1a2-CreERT2/+; mT/mG	Non-CM	88to91	Col1a2-CreERT2;mT/mG	Uninjured	28	heart	adult	Mus musculus	male
Tombor	EMTAB9817	Col1a2-CreERT2/+; mT/mG	Non-CM	12	Col1a2-CreERT2;mT/mG	Uninjured	28	heart	adult	Mus musculus	male
Tombor	EMTAB9817	Col1a2-CreERT2/+; mT/mG	Non-CM	12	Col1a2-CreERT2;mT/mG	Uninjured	28	heart	adult	Mus musculus	male

Kretzschmar	GSE102048	Ki67TagRFP	remote area	8	C57BL/6	MI	14	heart	adult	Mus musculus	male
Kretzschmar	GSE102048	Ki67TagRFP	infarcted area	8	C57BL/6	MI	14	heart	adult	Mus musculus	male
Kretzschmar	GSE102048	Ki67TagRFP	remote area	8	C57BL/6	Sham	14	heart	adult	Mus musculus	male
Kretzschmar	GSE102048	Ki67TagRFP	apex area	8	C57BL/6	Sham	14	heart	adult	Mus musculus	male
Kretzschmar	GSE102048	Ki67TagRFP	infarcted area	8	C57BL/6	IR	14	heart	adult	Mus musculus	male
Kretzschmar	GSE102048	Ki67TagRFP	ventricles	8	C57BL/6	Uninjured	0	heart	adult	Mus musculus	male
Kretzschmar	GSE102048	WT	ventricles	8	C57BL/6	Uninjured	0	heart	adult	Mus musculus	male
Kretzschmar	GSE102048	WT	infarcted area	8	C57BL/6	MI	14	heart	adult	Mus musculus	male
Kretzschmar	GSE102048	Ki67TagRFP	heart	8	C57BL/6	Uninjured	0	heart	adult	Mus musculus	male
Ruiz	GSE132146	Col1a1-GFP+/CD31-/CD45-	heart	10	C57BL/6	Uninjured	0	heart	adult	Mus musculus	male
Ruiz	GSE132146	Col1a1-GFP+/CD31-/CD45-	heart	10	C57BL/6	MI	7	heart	adult	Mus musculus	male
Ruiz	GSE132146	Col1a1-GFP+/CD31-/CD45-	heart	10	C57BL/6	MI	14	heart	adult	Mus musculus	male
Ruiz	GSE132146	Col1a1-GFP+/CD31-/CD45-	heart	10	C57BL/6	MI	30	heart	adult	Mus musculus	male
Ruiz	GSE132146	Cthrc1-KO mEFSK4+/CD31-/CD45-	heart	10	C57BL/6	MI	7	heart	adult	Mus musculus	male
Molenaar	GSE146285	WT	infarcted area	8	C57BL/6	Sham	1	left ventricle	adult	Mus musculus	male
Molenaar	GSE146285	WT	infarcted area	8	C57BL/6	Sham	14	left ventricle	adult	Mus musculus	male
Molenaar	GSE146285	WT	infarcted area	8	C57BL/6	IR	1	left ventricle	adult	Mus musculus	male
Molenaar	GSE146285	WT	infarcted area	8	C57BL/6	IR	3	left ventricle	adult	Mus musculus	male
Molenaar	GSE146285	WT	infarcted area	8	C57BL/6	IR	14	left ventricle	adult	Mus musculus	male
Molenaar	GSE146285	WT	infarcted area	8	C57BL/6	MI	3	left ventricle	adult	Mus musculus	male
Wang	GSE153480	WT	Cardiac cells	8	ICR/CD1	MI	1	ventricle	adult	Mus musculus	male
Wang	GSE153480	WT	Cardiac cells	8	ICR/CD1	Sham	1	ventricle	adult	Mus musculus	male
Wang	GSE153480	WT	Cardiac cells	8	ICR/CD1	MI	3	ventricle	adult	Mus musculus	male
Wang	GSE153480	WT	Cardiac cells	8	ICR/CD1	Sham	3	ventricle	adult	Mus musculus	male

Table 7.2 – Metadata from scRNAseq analysis

Appendix E: Clinical study schedule

<table>
<tr><th>Time</th><th>Prep</th><th>Thawing and centrifugation</th><th>Assaying</th></tr>
<tr><td>08:00</td><td rowspan="3">Coat capture antibodies on all 17 plates, then wash and leave blocking</td><td rowspan="4">Clinical samples for plates 1-4</td><td rowspan="4"></td></tr>
<tr><td>08:30</td></tr>
<tr><td>09:00</td></tr>
<tr><td>09:30</td><td rowspan="19"></td></tr>
<tr><td>10:00</td><td></td><td rowspan="2">Plates 1 & 2</td></tr>
<tr><td>10:30</td><td rowspan="4">Clinical samples for plates 5-8</td></tr>
<tr><td>11:00</td><td rowspan="2">Plates 3 & 4</td></tr>
<tr><td>11:30</td></tr>
<tr><td>12:00</td><td></td></tr>
<tr><td>12:30</td><td></td><td rowspan="2">Plates 5 & 6</td></tr>
<tr><td>13:00</td><td rowspan="4">Clinical samples for plates 9-12</td></tr>
<tr><td>13:30</td><td rowspan="2">Plates 7 & 8</td></tr>
<tr><td>14:00</td></tr>
<tr><td>14:30</td><td></td></tr>
<tr><td>15:00</td><td></td><td rowspan="2">Plates 9 & 10</td></tr>
<tr><td>15:30</td><td rowspan="4">Clinical samples for plates 13-17</td></tr>
<tr><td>16:00</td><td rowspan="2">Plates 11 & 12</td></tr>
<tr><td>16:30</td></tr>
<tr><td>17:00</td><td></td></tr>
<tr><td>17:30</td><td rowspan="5"></td><td rowspan="2">Plates 13 & 14</td></tr>
<tr><td>18:00</td></tr>
<tr><td>18:30</td><td rowspan="2">Plates 15 & 16</td></tr>
<tr><td>19:00</td></tr>
<tr><td>19:30</td><td>Plate 17</td></tr>
</table>

Table 7.3 – A timetable for the execution of the clinical sample study, designed to ensure protection of analyte stability.

Appendix F: Literature reviewed including clinical studies on human subjects

Study type	Author, year published, PMID	Sample size	Main finding(s)	Supportive of use of sST2 peri/post-MI?
Prospective enrolment of patients admitted with MI	Weir et al, 2010,20117403	100	sST2 positively correlated with infarct volume at baseline (P=0.005) and at 24 weeks post-MI (P=0.037).	Yes
A randomised control trial including patients with NSTE-ACS	Eggers et al, 2010, 20435187	403	sST2 predicted 1 year mortality after NSTE-ACS independently of clinical risk factors (P=0.03), but lost its predictive ability after additional adjustment for NT-proBNP measurement.	Mixed
Unselected emergency admission of patients with NSTEMI	Dhillon et al, 2011, 21641364	577	sST2 predicted MACE, including reinfarction (P=0.03), however did not predict MACE better than NT-proBNP or GRACE scoring.	No
Prospective enrolment of unselected patients with STEMI	Dhillon et al, 2012, 22835988	677	Adding sST2 measurement to GRACE score significantly improved c statistic for 30 day mortality from 0.82 to 0.90 sST2 was significantly associated with increased mortality and showed incremental value with NT-proBNP.	Yes
Recruitment of patients from the FINRISK97 cohort (a prospective cohort for CV risk factors and disease development)	Hughes et al, 2014, 25080471	8444	sST2 showed suggestive but non-significant correlation with HF. sST2 significantly correlated with death, but no improvement in c index by adding sST2 to risk stratification. This study was done in a healthy population, not post-MI	Mixed
Randomised controlled clinical trial in patients with NSTE-ACS	O'Malley et al, 2014, 24530676	4432	sST2 was not focus of the study, however, was measured and correlated with CV death or HF 1-year post-MI (P<0.001).	Mixed

Prospective patients with MI monitored over 3 years	Minamisawa et al, 2016, 26742699	430	sST2 did not distinguish STEMI and unstable angina and could not predict adverse outcome after MI. sST2 only measured 1 month after MI, missing acute phase of release	No
Prospective recruitment of patients with STEMI	Minana et al, 2018, 29954670	109	sST2 independently predicted changes in CMR-derived left ventricular volume and LVEF 1 week post-MI (P<0.01).	Yes
Observational cohort over 2 centres	Tuegel et al, 2018, 29866459	883	sST2 did not correlate with risk of CVD. Only 41 patients developed HF, so small sample size	Mixed
1027 patients retrospectively enrolled and 333 patients for prospective validation cohort	Wang et al, 2018, 29146682	1360 total, 234 MI and 67 healthy control	sST2 was significantly elevated in patients with MI (P<0.001) in comparison to healthy controls.	Yes
Prospective clinical trial of patients with STEMI undergoing PCI	Liu et al, 2018, 30464124	295	Baseline levels of sST2 (immediately after STEMI) significantly associated with MACE (P=0.048).	Yes
Longitudinal prospective study on patients with MI between Apr-Oct 2016	Mzhougi et al, 2019, 31539092	74	78% patients with MI had sST2 above 35ng/ml. Correlation between sST2 and cTnI (r=0.398, p=<0.0001).	Yes
Prospective study on patients with first time STEMI	Tyminska et al, 2019, 31642446	117	Primary end point after MI AUC for sST2 was 0.64, although this was only 8 patients.	Mixed
Single centre prospective recruitment of patients with STEMI between May 2017-Apr 2018	Somuncu et al, 2019, 30996145	379	sST2 levels above 14.2ng/ml predicted no-reflow phenomenon after MI.	Yes

Prospective enrolment of patients with ACS, monitored for 1 year post-admission	Van den Berg et al, 2020, 32383686	161	sST2 was measured in 15 patients at 24,48 and 72 hours, and the rest measured on admission and after 1 year. sST2 stabilised after day 5 generally. Within patient variation of ST2 did not differ as much as NT-proBNP, which might make sST2 better at personalised risk stratification.	Yes
Randomised clinical trial from CHILL-MI cohort, where CHILL-MI used hypothermia in parallel with PCI to improve outcome	Mohammad et al, 2020, 33122738	119	sST2 had strong association with infarct size and LVEF post-STEMI.	Yes
Multicentre study: 9 hospitals in 8 European countries, prospective enrolment of patients with cardiogenic shock	Hongisto, 2021, 33522124	219	Those with cardiogenic shock with primary aetiology of MI was 84%. sST2 measurements improved mortality risk stratification (AUC went from 0.75 to 0.84). Elderly patient cohort.	Yes
Retrospective analysis from a registry of patients admitted with STEMI or NTSEMI	Hjort et al, 2021, 34496288	538 STEMI, 544 NTSEMI	sST2 showed higher concentration in STEMI and could generally predict adverse outcome, but did not distinguish between different adverse outcomes between STEMI and NSTEMI. STEMI and NSTEMI pts should not be treated different based on sST2.	Mixed

Table 7.4 – The results and comparison of a literature review on human clinical studies evaluating sST2 plasma levels in MI patients.

Appendix G: Literature reviewed including sST2 release in non-human subjects (cellular or animal)

Study subject	Author, year published, PMID	Main finding(s)	Supportive of sST2 mechanistically relating to MI?
AC16	Zhang et al, 2012, 22682001	Influx of IL-33 to the media of AngII injured CMs could not reduce oxidative stress exacerbated by increased levels of sST2	Yes
HL-1 and mice	Yang et al, 2019, 31674275	The IL-33/ST2L pathway is involved in cell apoptosis and heart function after MI *in vivo* and *in vitro* and can be controlled with long non-coding RNA.	Yes
H9c2 and rats	Yang et al, 2019, 30265647	Hypoxic CMs saw increased sST2 expression	Yes
Rabbits and HL-1	Li et al, 2020, 32325147	Valsartan reduces structural remodelling in rabbits with atrial fibrillation, confirmed by reducing levels of sST2	Only addresses atrial fibrillation, not MI
H9c2	Zheng et al, 2022, 35347547	Nicorandil reduced expression of IL-33 and sST2 after hypoxia-reoxygenation injury which in turn reduced incidence of apoptosis	Yes
HL-1	Zhan et al, 2023, 37403470	Vericiguat prevented atrial fibrillation-associated remodelling, where remodelling process was confirmed by increased sST2.	Yes
HL-1	Cheng et al, 2024, 38244770	IL-33 treatment promoted cardiac remodelling via sST2.	Yes
AC16 and H9c2	Wu et al, 2024, 38724005	Anti-sST2 antibody mitigated remodelling effects caused by IL-33.	Yes
AC16	Xu et al, 2024, 38619643	Treating cells with AngII increased sST2 expression	For HF, yes. Does not address MI
HL-1 and mice	Zhang et al, 2025, 40088120	The ST2L/IL-33 pathway is involved in improving myocardial function after injury	Yes

Table 7.5 - The results and comparison of a literature search where sST2 expression in cardiomyocytes (HL-1, AC16 or H9c2 cell line) has been explored.

8. References

Abdulrahman, N., Ibrahim, M., Joseph, J. M., Elkoubatry, H. M., Al-Shamasi, A.-A., Rayan, M., . . . Mraiche, F. (2022). Empagliflozin inhibits angiotensin II-induced hypertrophy in H9c2 cardiomyoblasts through inhibition of NHE1 expression. *Molecular and Cellular Biochemistry, 477*, 1865-1872.

ACCF/AHA Task Force on Practice Guidelines. (2017). 2013 ACCF/AHA guideline for the management of ST-elevation myocardial infarction: a report of the American College of Cardiology Foundation/American Heart Association Task Force on Practice Guidelines. *Circulation, 127*(4), 362-425.

Ahmed, M. I., Gladden, J. D., Litovsky, S. H., Lloyd, S. G., Gupta, H., Inusah, S., . . . Dell'Italia, L. J. (2011). Increased Oxidative Stress and Cardiomyocyte Myofibrillar Degeneration in Patients with Chronic Isolated Mitral Regurgitation and Ejection Fraction > 60%. *Journal of the American College of Cardiology, 55*(7), 671-679.

Aurora, L., Peterson, E., Gui, H., Zeld, N., McCord, J., Pinto, Y., . . . Lanfear, D. E. (2020). Suppression tumorigenicity 2 (ST2) turbidimetric immunoassay compared to enzyme-linked immunosorbent assay in predicting survival in heart failure patients with reduced ejection fraction. *Clinica Chemica Acta*, 767-771.

Aydin, S., Ugur, K., Aydin, S., Sahin, İ., & Yardim, M. (2019). Biomarkers in acute myocardial infarction: current perspectives. *Vascular Health and Risk Management, 15*, 1-10.

Backus, B. E., Six, A. J., Kelder, J. C., Bosschaert, M. A., Mast, E. G., Mosterd, A., . . . Doevendans, P. A. (2013). A prospective validation of the HEART score for chest pain patients at the emergency department. *International Journal of Cardiology, 168*(3), 2153-2158.

Bagai, A., Alexander, K. P., Berge, J. S., Senior, R., Sajeev, C., Pracon, R., . . . Chaitman, B. (2018). Use of Troponin Assay 99th Percentile as the Decision Level for Myocardial Infarction Diagnosis. *American Heart Journal, 190*, 135-139.

Bay, M., Kirk, V., Parner, J., Hassager, C., Nielsen, H., Krogsgaard, K., . . . Aldershvile, J. (2003). NT-proBNP: a new diagnostic screening tool to differentiate between patients with normal and reduced left ventricular systolic function. *Heart, 89*(2), 150-154.

Bers, D. (2002). Cardiac excitation–contraction coupling. *Nature, 415*, 198-205.

Bertinchant, J. P., Larue, C., Pernel, I., Ledermann, B., Fabbro-Peray, P., Beck, L., . . . Pau, B. (1996). Release kinetics of serum cardiac troponin I in ischemic myocardial injury. *Clinical Biochemistry, 29*(6), 587-594.

BHF. (2024). *England Factsheet.*

Brentnall, M., Rodriguez-Menocal, L., Guevara, R. L., Cepero, E., & Boise, L. H. (2013). Caspase-9, caspase-3 and caspase-7 have distinct roles during intrinsic apoptosis. *BMC Cell Biology, 14*(32), 14-32.

Brogan, R. A., Malkin, C. J., Batin, P. D., Simms, A. D., McLenachan, J. M., & Gale, C. P. (2014). Risk stratification for ST segment elevation myocardial infarction in the era of primary percutaneous coronary intervention. *World Journal of Cardiology, 6*(8), 865-873.

Brunetti, G., Barile, B., Nicchia, G. P., Onorati, F., Luciani, G. B., & Galeone, A. (2023, June). The ST2/IL-33 Pathway in Adult and Paediatric Heart Disease and Transplantation. *Biomedicines, 11*(6), 1676.

Cao, Z., Jia, Y., & Zhu, B. (2019). BNP and NT-proBNP as Diagnostic Biomarkers for Cardiac Dysfunction in Both Clinical and Forensic Medicine. *International Journal of Molecular Sciences, 20*(8).

Chan, M. Y., Shah, B. R., Gao, F., Sim, L. L., Chua, T., Tan, H. C., . . . Tai, S. (2011). Recalibration of the Global Registry of Acute Coronary Events risk score in a multiethnic Asian population. *Americal Heart Journal, 162*(2), 291-299.

Cheng, Y., Lin, G., Xie, Y., Xuan, B., He, S., Shang, Z., . . . Shen, A. (2024). Baicalin ameliorates angiotensin II-induced cardiac hypertrophy and mitogen-activated protein kinase signaling pathway activation: A target-based network pharmacology approach. *European Journal of Pharmacology, 981*.

Claridge, B., Rai, A., Lees, J. G., Fang, H., Lim, S. Y., & Greening, D. W. (2023). Cardiomyocyte intercellular signalling increases oxidative stress and reprograms the global- and phospho-proteome of cardiac fibroblasts. *Journal of Extracellular biology, 2*(12).

D'Agostino, R. B., & & Pearson, E. S. (1973). Tests for Departure from Normality. Empirical Results for the Distributions of b2 and √b1. *Biometrika, 60*(3), 613-622.

Dhillon, O. S., Narayan, H. K., Khan, S. Q., Kelly, D., Quinn, P. A., Squire, I. B., . . . Ng, L. L. (2013). Pre-discharge risk stratification in unselected STEMI: is there a role for ST2 or its natural ligand IL-33 when compared with contemporary risk markers? *International Journal of Cardiology, 167*(5), 2182-2188.

Dhillon, O. S., Narayan, H. K., Quinn, P. A., Squire, I. B., Davies, J. E., & Ng, L. L. (2011). Interleukin 33 and ST2 in non-ST-elevation myocardial infarction: comparison with Global Registry of Acute Coronary Events Risk Scoring and NT-proBNP. *American Heart Journal, 161*(6), 1163-1170.

Dieplinger, B., Egger, M., Gegenhuber, A., Haltmayer, M., & Mueller, T. (2015). Analytical and clinical evaluation of a rapid quantitative lateral flow immunoassay for measurement of soluble ST2 in human plasma. *Clinica Chemica Acta, 451*(Pt B), 310-315.

Dieplinger, B., Jr, J. L., Steinmair, M., Gabriel, C., Poelz, W., Haltmayer, M., & Mueller, T. (2009). Analytical and clinical evaluation of a novel high-sensitivity assay for measurement of soluble ST2 in human plasma--the Presage ST2 assay. *Clinica Chimica Acta, 1-2*, 33-40.

Duchesne, M., Okoye, I., & Lacy, P. (2022). Epithelial cell alarmin cytokines: Frontline mediators of the asthma inflammatory response. *Frontiers in Immunology, 13*.

Eggers, K. M., Armstrong, P. W., Califf, R. M., Simoons, M. L., Venge, P., Wallentin, L., & James, S. K. (2010). ST2 and mortality in non-ST-segment elevation acute coronary syndrome. *American Heart Journal, 159*(5), 788-794.

Espinosa, A. S., Hussain, S., Al-Awar, A., Jha, S., Elmahdy, A., Kalani, M., . . . Redfors, B. (2023). Differences between cardiac troponin I vs. T according to the duration of myocardial ischaemia. *European Heart Journal: Acute Cardiovascular Care, 12*(6), 355-363.

Faber, J., & Fonseca, L. M. (2014). How sample size influences research outcomes. *Dental Press Journal of Orthodontics, 19*(4), 27-29.

Farbehi, N., Patrick, R., Dorison, A., Xaymardan, M., Janbandhu, V., Wystub-Lis, K., . . . Harvey, R. P. (2019). Single-cell expression profiling reveals dynamic flux of cardiac stromal, vascular and immune cells in health and injury. *eLife, 8*.

Forte, E., Perkins, B., Sintou, A., Kalkat, H. S., Papanikolaou, A., Jenkins, C., . . . Sattler, S. (2020). Cross-Priming Dendritic Cells Exacerbate Immunopathology After Ischemic Tissue Damage in the Heart. *Circulation, 143*(8), 821-836.

Frobert, A., Valentin, J., Magnin, J.-L., Riedo, E., Cook, S., & Giraud, M.-N. (2015). Prognostic Value of Troponin I for Infarct Size to Improve Preclinical Myocardial Infarction Small Animal Models. *Frontiers in Physiology, 6*(353).

Gallego-Selles, A., Galvan-Alvarez, V., Martinez-Canton, M., Garcia-Gonzalez, E., Morales-Alamo, D., Santana, A., . . . Martin-Rincon, M. (2022). Fast regulation of the NF-κB signalling pathway in human skeletal muscle revealed by high-intensity exercise and ischaemia at exhaustion: Role of oxygenation and metabolite accumulation. *Redox Biology, 55*.

Gandhi, S., Garratt, K. N., Li, S., Wang, T. Y., Bhatt, D. L., Davis, L. L., . . . Kontos, M. C. (2022). Ten-Year Trends in Patient Characteristics, Treatments, and Outcomes in Myocardial Infarction From National Cardiovascular Data Registry Chest Pain–MI Registry. *Circulation: Cardiovascular Quality and Outcomes, 15*(1).

Ghali, R., Altara, R., Louch, W. E., Cataliotti, A., Mallat, Z., Kaplan, A., . . . Booz, G. W. (2018). IL-33 (Interleukin 33)/sST2 Axis in Hypertension and Heart Failure. *Hypertension, 72*(4), 818-828.

Giridharan, S., & Srinivasan, M. (2018). Mechanisms of NF-κB p65 and strategies for therapeutic manipulation. *Journal of Inflammation Research, 11*, 407-419.

Griesenauer, B., & Paczesny, S. (2017, April). The ST2/IL-33 Axis in Immune Cells during Inflammatory Diseases. *Frontiers in Immunology, 8*.

Guerrero, A. D., Schmitz, I., Chen, M., & Wang, J. (2013). Promotion of Caspase Activation by Caspase-9-mediated Feedback Amplification of Mitochondrial Damage. *Journal of Clinical and Cellular Immunology, 3*(3).

Guma, M., & Firestein, G. S. (2012). c-Jun N-Terminal Kinase in Inflammation and Rheumatic Diseases. *The Open Rheumatology Journal, 6*, 220-231.

Harrison, L. J. (2013). *Pulmonary and Critical Care Medicine. 2nd ed.* McGraw-Hill Education.

Hartopo, A. B., Sukmasari, I., & Puspitawati, I. (2018). The Utility of Point of Care Test for Soluble ST2 in Predicting Adverse Cardiac Events during Acute Care of ST-Segment Elevation Myocardial Infarction. *Cardiology Research and Practice*.

Hautamäki, M., Järvensivu-Koivunen, M., Lyytikäinen, L.-P., Eskola, M., Lehtimäki, T., Nikus, K., . . . Hernesniemi, J. (2024). The association between GRACE score at admission for myocardial infarction and the incidence of sudden cardiac arrests in long-term follow-up - the MADDEC study. *Scandinavian Cardiovascular Journal, 58*(1).

Homsak, E., & Gruson, D. (2020, August). Soluble ST2: A complex and diverse role in several diseases. *Clinica Chimica Acta, 507*, 75-87.

Hongisto, M., Lassus, J., Tarvasmäki, T., Sionis, A., Sans-Rosello, J., Tolppanen, H., . . . Harjola, V.-P. (2021). Mortality risk prediction in elderly patients with cardiogenic shock: results from the CardShock study. *ESC Heart Failure, 8*(2), 1398-1407.

Hughes, M. F., Appelbaum, S., Havulinna, A. S., Jagodzinski, A., Zeller, T., Kee, F., . . . investigators, F. a. (2014). ST2 may not be a useful predictor for incident cardiovascular events, heart failure and mortality. *Heart, 100*(21), 1715-1721.

Huot, J., Houle, F., Marceau, F., & Landry, J. (1997). Oxidative stress-induced actin reorganization mediated by the p38 mitogen-activated protein kinase/heat shock protein 27 pathway in vascular endothelial cells. *Circulation Research, 80*(3), 383-392.

Ihara, Y., Urata, Y., Goto, S., & Kondo, T. (2005). Role of calreticulin in the sensitivity of myocardiac H9c2 cells to oxidative stress caused by hydrogen peroxide. *American Journal of Cell Physiology, 290*(1), 208-221.

Jager, S. C., & Hoefer, I. E. (2017). Beyond the matrix: MMP2 as critical regulator of inflammation-mediated vascular dysfunction. *Cardiovascular Research, 113*(14), 1705-1707.

Jenča, D., Melenovský, V., Stehlik, J., Staněk, V., Kettner, J., Kautzner, J., . . . Wohlfahrt, P. (2020). Heart failure after myocardial infarction: incidence and predictors. *ESC Heart Failure, 8*(1), 222-237.

Kakkar, R., & Lee, R. T. (2008, October). The IL-33/ST2 pathway: therapeutic target and novel biomarker. *Nature Reviews Drug Discovery, 7*(10), 827-840.

Katrukha, I. A., & Katrukha, A. G. (2021). Myocardial Injury and the Release of Troponins I and T in the Blood of Patients . *Clinical Chemistry, 67*(1), 124-130.

Keller, T., Zeller, T., Peetz, D., Tzikas, S., Roth, A., Czyz, E., . . . Blankenberg, S. (2009). Sensitive Troponin I Assay in Early Diagnosis of Acute Myocardial Infarction. *The New England Journal of Medicine, 361*(9), 868-877.

Kim, H., Lee, T.-H., Hur, M., Kim, H.-J., Yang, H. S., Lee, K. R., & Somma, S. D. (2023). Performance Evaluation of AFIAS ST2 and Ichroma ST2 Assays in Comparison with Presage ST2 Assay. *Reviews in Cardiovascular Medicine, 24*(4).

Kim, T. W., Staschke, K., Bulek, K., Yao, J., Peters, K., Oh, K.-H., . . . Li, X. (2007). A critical role for IRAK4 kinase activity in Toll-like receptor-mediated innate immunity. *The Journal of Experimental Medicine, 204*(5), 1025-1036.

Kretzschmar, K., Post, Y., Bannier-Hélaouët, M., Mattiotti, A., Drost, J., Basak, O., . . . Clevers, H. (2018). Profiling proliferative cells and their progeny in damaged murine hearts. *Biological Sciences, 115*(52), 2245-2254.

Kristensen, J. H., Hasselbalch, R. B., Strandkjær, N., Jørgensen, N., Østergaard, M., Møller-Sørensen, P. H., . . . Vaku, M. (2024). Half-Life and Clearance of Cardiac Troponin I and Troponin T in Humans. *Circulation, 150*(15), 1187-1198.

Kuznetsov, A. V., Javadov, S., Sickinger, S., Frotschnig, S., & Grimm, M. (2014). H9c2 and HL-1 cells demonstrate distinct features of energy metabolism, mitochondrial function and sensitivity to hypoxia-reoxygenation. *1853*(2), 276-284.

Laugaudin, G., Kuster, N., Petiton, A., Leclercq, F., Gervasoni, R., Macia, J.-C., . . . Roubille, F. (2015). Kinetics of high-sensitivity cardiac troponin T and I differ in patients with ST-segment

elevation myocardial infarction treated by primary coronary intervention. *European Heart Journal: Acute Cardiovascular Care, 5*(4).

Lee, Y. H., Mungunsukh, O., Tutino, R. L., Marquez, A. P., & Day, R. M. (2010). Angiotensin-II-induced apoptosis requires regulation of nucleolin and Bcl-xL by SHP-2 in primary lung endothelial cells. *Journal of Cell Science, 123*(10), 1634-1643.

Li, Y. Y., & Feldman, A. M. (2012). Matrix Metalloproteinases in the Progression of Heart Failure. *Drugs, 61*, 1239-1252.

Lin, Z., Zhou, P., Gise, A. v., Gu, F., Ma, Q., Chen, J., . . . Pu, W. T. (2014). Pi3kcb Links Hippo-YAP and PI3K-AKT Signaling Pathways to Promote Cardiomyocyte Proliferation and Survival. *116*(1), 35-45.

Liu, J., Wu, P., Xu, Z., Zhang, J., Liu, J., & Yang, Z. (2020). Ginkgolide B inhibits hydrogen peroxide-induced apoptosis and attenuates cytotoxicity via activating the PI3K/Akt/mTOR signaling pathway in H9c2 cells. *Molecular Medicine Reports, 22*(1), 310-316.

Liu, J.-J., Li, D.-L., Zhou, J., Sun, L., Zhao, M., Kong, S.-S., . . . Zang, W.-J. (2010). Acetylcholine prevents angiotensin II-induced oxidative stress and apoptosis in H9c2 cells. *Apoptosis, 16*, 94-103.

Liu, X., Hu, Y., Huang, W., Zhang, G., Cao, S., Yan, X., . . . Zheng, X. (2019). Soluble ST2 for Prediction of Clinical Outcomes in Patients. *International Heart Journal, 60*(1), 19-26.

Loffek, S., Schilling, O., & Franzke, C.-W. (2010). matrix metalloproteinases in lung health and disease": Biological role of matrix metalloproteinases: a critical balance. *European Respiratory Journal, 38*(1), 191-208.

Lu, L., Liu, M., Sun, R., Zheng, Y., & Zhang, P. (2015). Myocardial Infarction: Symptoms and Treatments. *Cell biochemistry and biophysics, 72*(3), 865-867.

Machado, R., Sachinidis, A., & Futschik, M. E. (2021). Detection of Novel Potential Regulators of Stem Cell Differentiation and Cardiogenesis through Combined Genome-Wide Profiling of Protein-Coding Transcripts and microRNAs. *Cells, 10*(9).

Martínez, M. J., Rueda, F., Labata, C., Oliveras, T., Montero, S., Ferrer, M., . . . García-García, C. (2022). Non-STEMI vs. STEMI Cardiogenic Shock: Clinical Profile and Long-Term Outcomes. *Journal of Clinical Medicine, 11*(12).

Masilamani, T. J., Loiselle, J. J., & Sutherland, L. C. (2013). Assessment of Reference Genes for Real-Time Quantitative PCR Gene Expression Normalization During C2C12 and H9c2 Skeletal Muscle Differentiation. *Molecular Biotechnology, 56*, 329-339.

Massey, F. J. (1951). The Kolmogorov-Smirnov Test for Goodness of Fit. *Journal of the American Statistical Association, 46*(253), 68-78.

Meyers, H. P., Bracey, A., Lee, D., Lichtenheld, A., Li, W. J., Singer, D. D., . . . Smith, S. W. (2021). Comparison of the ST-Elevation Myocardial Infarction (STEMI) vs. NSTEMI and Occlusion MI (OMI) vs. NOMI Paradigms of Acute MI. *Journal of Emergency Medicine, 60*(3), 273-284.

Michael Attwaters, S. M. (2021). Cellular and molecular pathways controlling muscle size in response to exercise. *The FEBS Journal, 289*(6), 1428-1456.

Mildner, M., Storka, A., Lichtenauer, M., Mlitz, V., Ghannadan, M., Hoetzenecker, K., . . . Ankersmit, H. J. (2010, April 02). Primary sources and immunological prerequisites for sST2 secretion in humans. *Cardiovascular Research, 87*(4), 769-777.

Mills, E. H., Møller, A. L., Engstrøm, T., Pedersen, F., Køber, L., Gnesin, F., . . . Torp-Pedersen, C. (2024). Time From Distress Call to Percutaneous Coronary Intervention and Outcomes in Myocardial Infarction. *JACC: Advances, 3*(7).

Miñana, G., Núñez, J., Bayés-Genís, A., Revuelta-López, E., Ríos-Navarro, C., Núñez, E., . . . Bodí, V. (2018). ST2 and left ventricular remodeling after ST-segment elevation myocardial infarction: A cardiac magnetic resonance study. *International Journal of Cardiology, 1*(270), 336-342.

Mitsis, A., & Gragnano, F. (2021). Myocardial Infarction with and without ST-segment Elevation: a Contemporary Reappraisal of Similarities and Differences. *Current Cardiology Reviews, 17*(4).

Moledina, S. M., Kontopantelis, E., Wijeysundera, H. C., Banerjee, S., Spall, H. G., Gale, C. P., . . . Mamas, M. A. (2022). Ethnicity-dependent performance of the Global Registry of Acute Coronary Events risk score for prediction of non-ST-segment elevation myocardial infarction in-hospital mortality: nationwide cohort study. *European Heart Journal, 43*(24), 2289-2299.

Molenaar, B., Timmer, L. T., Droog, M., Perini, I., Versteeg, D., Kooijman, L., . . . Rooij, E. v. (2021). Single-cell transcriptomics following ischemic injury identifies a role for B2M in cardiac repair. *Communications Biology, 4*(146).

Montalescot, G., Dallongeville, J., Belle, E. V., Rouanet, S., Baula, C., Degrandsart, A., & Vicaut, E. (2007). STEMI and NSTEMI: are they so different? 1 year outcomes in acute myocardial infarction as defined by the ESC/ACC definition (the OPERA registry). *European Heart Journal, 28*(12), 1409-1417.

Monti, C. B., Ambrogi, F., & Sardanelli, F. (2024). Sample size calculation for data reliability and diagnostic performance: a go-to review. *European Radiology Experimental, 8*(1).

Moraes-Silva, I. C., Rodrigues, B., Coelho-Junior, H. J., Feriani, D. J., & Irigoyen, M.-C. (2017). Myocardial Infarction and Exercise Training: Evidence from Basic Science. *Advances in experimental medicine and biology*, 139-153.

Mueller, T., Zimmermann, M., Dieplinger, B., Ankersmit, H. J., & Haltmayer, M. (2012). Comparison of plasma concentrations of soluble ST2 measured by three different commercially available assays: the MBL ST2 assay, the Presage ST2 assay, and the R&D ST2 assay. *Clinica Chimica Acta, 413*(19-20), 1493-1494.

Mullins, K. E., & Christenson, R. H. (2020). Optimal Detection of Acute Myocardial Injury and Infarction with Cardiac Troponin: Beyond the 99th Percentile, into the High-Sensitivity Era. *Current Cardioloy Reports, 22*(101).

Muñoz-Cánoves, P., Scheele, C., Pedersen, B. K., & Serrano, A. L. (2013). Interleukin-6 myokine signaling in skeletal muscle: a double-edged sword? *The FEBS Journal, 280*(17), 4131-4148.

Mzoughi, K., Chouaieb, S., Zairi, I., Fredj, S., Kilani, M. B., Berriri, S., . . . Kraiem, S. (2019). Prognostic value of ST2 in myocardial infarction. *La Tunisie Medicale, 97*(2), 335-343.

Nadlacki, B., Dennis Horton 2, S. H., Ali, A., Aliprandi-Costa, B., Ellis, C. J., Adams, R. J., . . . Ranasinghe, I. (2021). Long term survival after acute myocardial infarction in Australia and

New Zealand, 2009-2015: a population cohort study. *The Medical Journal of Australia, 214*(11), 519-525.

Nair, R., Johnson, M., Kravitz, K., Huded, C., Rajeswaran, J., Anabila, M., . . . Menon, V. (2021). Characteristics and Outcomes of Early Recurrent Myocardial Infarction After Acute Myocardial Infarction. *Journal of the American Heart Association, 10*(16).

NICE: NG185. (2020). *NSTEMI/unstable angina: early management.* Retrieved from https://www.nice.org.uk/guidance/ng185/resources/visual-summary-unstable-angina-nstemi-pdf-8900622109

NICE: NG185. (2020). *STEMI: early management.* Retrieved from https://www.nice.org.uk/guidance/ng185/resources/visual-summary-stemi-pdf-8900623405

Ogbu, I., Ayutyanont, N., Wilson, S., & Akhondi, H. (2023). The Impact of Gender and Race When Using the GRACE ACS Score to Predict Mortality. *HCA Healthcare Journal of Medicine, 4*(3), 235-242.

Oh, K.-S., Oh, B. K., Park, C. H., Mun, J., Won, S. H., & Lee, B. H. (2012). Baicalein potently inhibits Rho kinase activity and suppresses actin stress fiber formation in angiotensin II-stimulated H9c2 cells. *Biological and Pharmaceutical Bulletin, 35*(8), 1281-1286.

O'Malley, R. G., Bonaca, M. P., Scirica, B. M., Murphy, S. A., Jarolim, P., Sabatine, M. S., . . . Morrow, D. A. (2014). Prognostic performance of multiple biomarkers in patients with non-ST-segment elevation acute coronary syndrome: analysis from the MERLIN-TIMI 36 trial (Metabolic Efficiency With Ranolazine for Less Ischemia in Non-ST-Elevation Acute Coronary Syndromes-Th. *Journal of the American College of Cardiology, 63*(16), 1644-1653.

Osuru, H. P., Lavallee, M., & Thiele, R. H. (2022). Molecular and Cellular Response of the Myocardium (H9C2 Cells) Towards Hypoxia and HIF-1α Inhibition. *Frontiers in Cardiovascular Medcine, 9*.

Oyama, K., Takahashi, K., & Sakurai, K. (2009). Cardiomyocyte H9c2 Cells Exhibit Differential Sensitivity to Intracellular Reactive Oxygen Species Generation with Regard to Their Hypertrophic vs Death Responses to Exogenously Added Hydrogen Peroxide. *Journal of Clinical Biochemistry and Nutrition, 45*(3), 361-369.

Pérez-Martínez, M. T., Lacunza-Ruiz, J., Lara, J. G., Noguera-Velasco, J. A., Lax, A., Hernández-Vicente, Á., . . . Pascual-Figal, D. A. (2018). Noncardiac Production of Soluble ST2 in ST-Segment Elevation Myocardial Infarction. *Journal of the American College of Cardiology, 72*(12), 1429-1430.

Piepoli, M. F., Corrà, U., Dendale, P., Frederix, I., Prescott, E., Schmid, J. P., . . . Pelliccia, A. (2016). Challenges in secondary prevention after acute myocardial infarction: A call for action. *European Journal of Preventative Cardiology, 23*(18), 1994-2006.

Poldervaart, J. M., Langedijk, M., Backus, B. E., Dekker, I. M., Six, A. J., Doevendans, P. A., . . . Reitsma, J. B. (2017). Comparison of the GRACE, HEART and TIMI score to predict major adverse cardiac events in chest pain patients at the emergency department. *International Journal of Cardiology, 227*, 656-661.

Prathapan, A., Raj, P. S., Rani, M. P., & Raghu, K. (2018). Apoptosis in angiotensin II-stimulated hypertrophic cardiac cells -modulation by phenolics rich extract of Boerhavia diffusa L. *Biomedicine and Pharmacotherapy, 108*, 1097-1104.

Pretorius, C. J., Dimeski, G., O'Rourke, P. K., Marquart, L., Tyack, S. A., Wilgen, U., & Ungerer, J. P. (2011). Outliers as a cause of false cardiac troponin results: investigating the robustness of 4 contemporary assays. *Clinical chemsitry, 57*(5).

Putinski, C., Abdul-Ghani, M., Stiles, R., Brunette, S., Dick, S. A., Fernando, P., & Megeney, L. A. (2013). Intrinsic-mediated caspase activation is essential for cardiomyocyte hypertrophy. *Biological Sciences, 110*(43), 4079-4087.

Puymirat, E., Simon, T., Cayla, G., Cottin, Y., Elbaz, M., Coste, P., . . . Danchin, N. (2017). Acute Myocardial Infarction: Changes in Patient Characteristics, Management, and 6-Month Outcomes Over a Period of 20 Years in the FAST-MI Program (French Registry of Acute ST-Elevation or Non-ST-Elevation Myocardial Infarction) 1995 to 2015. *136*(20).

Qin, F., Patel, R., Yan, C., & Liu, W. (2006). NADPH oxidase is involved in angiotensin II-induced apoptosis in H9C2 cardiac muscle cells: Effects of apocynin. *Free Radical Biology and Medicine, 40*(2), 236-246.

Qing Guo, Y. J., Chen, X., Ye, X., Shen, X., Lin, M., Zeng, C., . . . Zhang, J. (2024). NF-κB in biology and targeted therapy: new insights and translational implications. *Nature, 9*(53).

Razali, M. N., & Wah, B. Y. (2011). Power Comparisons of Shapiro-Wilk, Kolmogorov-Smirnov, Lilliefors, and Anderson-Darling Tests. *Journal of Statistical Modeling and Analytics, 2*(1), 21-33.

Ren, S., Wang, Y., Zhang, Y., Yan, P., Xiao, D., Zhao, Y., . . . Lin , Y. (2023). Paeoniflorin alleviates AngII-induced cardiac hypertrophy in H9c2 cells by regulating oxidative stress and Nrf2 signaling pathway. *Biomedicine and Pharmacotherapy, 165*.

Ruiz-Villalba, A., Romero, J. P., Hernandez, S. C., Vilas-Zornoza, A., Fortelny, N., Castro-Labrador, L., . . . Prósper, F. (2021). Single-cell RNA-seq analysis reveals a crucial role for Collagen Triple Helix Repeat Containing 1 (CTHRC1) cardiac fibroblasts after myocardial infarction. *142*(19), 1831-1847.

Salari, N., Morddarvanjoghi, F., Abdolmaleki, A., Rasoulpoor, S., Khaleghi, A. A., Hezarkhani, L. A., . . . Mohammadi, M. (2023). The global prevalence of myocardial infarction: a systematic review and meta-analysis. *BMC Cardiovascular Disorders, 23*(206).

Schellings, D. A., Adiyaman, A., Dambrink, J.-H. E., Gosselink, A. M., Kedhi, E., Roolvink, V., . . . Hof, A. W. (2016). Predictive value of NT-proBNP for 30-day mortality in patients with non-ST-elevation acute coronary syndromes: a comparison with the GRACE and TIMI risk scores. *Vascular Health and Risk Management, 12*, 471-476.

Shapiro, S. S., & Wilk, M. B. (1965). An Analysis of Variance Test for Normality (Complete Samples). *Biometrika, 52*(3-4), 591-611.

Sherwood, M. W., & Newby, L. K. (2014). High-Sensitivity Troponin Assays: Evidence, Indications, and Reasonable Use. *JAMA, 3*(1).

Shiwani, H., Artico, J., Moon, J. C., Gorecka, M., McCann, G. P., Roditi, G., . . . Greenwood, J. (2024). Clinical Significance of Myocardial Injury in Patients Hospitalized for COVID-19: A Prospective, Multicenter, Cohort Study. *JACC Cardiovascular Imaging, 17*(11), 1320-1331.

Siti, H. N., Jalil, J., Asmadi, A. Y., & Kamisah, Y. (2021). Rutin Modulates MAPK Pathway Differently from Quercetin in Angiotensin II-Induced H9c2 Cardiomyocyte Hypertrophy. *International Journal of Molecular Sciences, 22*(10).

Spallarossa, P., Altieri, P., Garibaldi, S., Ghigliotti, G., Barisione, C., Manca, V., . . . Barsotti, A. (2006). Matrix metalloproteinase-2 and -9 are induced differently by doxorubicin in H9c2 cells: The role of MAP kinases and NAD(P)H oxidase. *Cardiovascular Research, 69*(3), 736-745.

Takeji, Y., Shiomi, H., Morimoto, T., Yamamoto, K., Matsumura-Nakano, Y., Nagao, K., . . . Kimura, T. (2021). Differences in mortality and causes of death between STEMI and NSTEMI in the early and late phases after acute myocardial infarction. *16*(11).

Taylor, C. J., Ordóñez-Mena, J. M., Roalfe, A. K., Lay-Flurrie, S., Jones, N. R., Marshall, T., & Hobbs, F. D. (2019). Trends in survival after a diagnosis of heart failure in the United Kingdom 2000-2017: population based cohort study. *BMJ, 364*(223).

Terkelsen, C. J., Sørensen, J. T., Maeng, M., Jensen, L. O., Tilsted, H.-H., Trautner, S., . . . Lassen, J. F. (2010). System Delay and Mortality Among Patients With STEMI Treated With Primary Percutaneous Coronary Intervention. *JAMA, 304*(7), 763-771.

Thomas, C. V., Coker, M. L., Zellner, J. L., Handy, J. R., Crumbley, A. J., & Spinale, F. G. (1998). Increased Matrix Metalloproteinase Activity and Selective Upregulation in LV Myocardium From Patients With End-Stage Dilated Cardiomyopathy. *Circulation, 97*(17), 1708-1715.

Tombor, L. S., John, D., Glaser, S. F., Luxán, G., Forte, E., Furtado, M., . . . Dimmeler, S. (2021). Single cell sequencing reveals endothelial plasticity with transient mesenchymal activation after myocardial infarction. *Nature Communications, 12*(681).

Tymińska, A., Kapłon-Cieślicka, A., Ozierański, K., Budnik, M., Wancerz, A., Sypień, P., . . . Filipiak, K. J. (2019). Association of Galectin-3 and Soluble ST2, and Their Changes, with Echocardiographic Parameters and Development of Heart Failure after ST-Segment Elevation Myocardial Infarction. *Disease Markers*.

Wakabayashi, T. (2015). Mechanism of the calcium-regulation of muscle contraction--in pursuit of its structural basis. *Proceedings of the Japan Academy, Series B physical and biological sciences, 91*(7), 321-350.

Wang, T., Kumru, O. S., Yi, L., Wang, Y. J., Zhang, J., Kim, J. H., . . . Volkin, D. B. (2013). Effect of ionic strength and pH on the physical and chemical stability of a monoclonal antibody antigen-binding fragment. *Journal of pharmaceutical sciences, 102*(8), 2520-2537.

Wang, Z., Cui, M., Shah, A. M., Tan, W., Bassel-Duby, R., & Olson, E. N. (2020). Cell-Type-Specific Gene Regulatory Networks Underlying Murine Neonatal Heart Regeneration at Single-Cell Resolution. *Cell Reports, 33*(10).

Watkins, S., Borthwick, G., & Arthur, H. (2010). The H9C2 cell line and primary neonatal cardiomyocyte cells show similar hypertrophic responses in vitro. *In Vitro Cellular and Developmental Biology - Animal, 47*(2), 125-231.

Weir, R. A., Miller, A. M., Murphy, G. E., Clements, S., Steedman, T., Connell, J. M., . . . McMurray, J. J. (2010). Serum soluble ST2: a potential novel mediator in left ventricular and infarct remodeling after acute myocardial infarction. *Journal of the American College of Cardiology, 55*(3), 243-250.

Witting, P., Liao, W.-Q., Harris, M., & Neuzil, J. (2006). Expression of human myoglobin in H9c2 cells enhances toxicity to added hydrogen peroxide. *Biochemical and Biophysical Research Communications, 348*(2), 485-493.

Woo, S. Y., & Kim, S. (2020). Determination of cutoff values for biomarkers in clinical studies. *Precision and Future Medicine, 4*(1), 2-8.

Wu, L., Zhu, X., Luo, C., Zhao, Y., Pan, S., Shi, K., . . . Jie, W. (2024). Mechanistic role of RND3-regulated IL33/ST2 signaling on cardiomyocyte senescence. *Life Sciences, 348*.

Xu, G., Xu, Y., Zhang, Y., Kao, G., & Li, J. (2024). miR-1268a Regulates Fatty Acid Metabolism by Targeting CD36 in Angiotensin II-induced Heart Failure. *Cell Biochemistry and Biophysics, 82*(2), 1193-1201.

Xu, Q., Huff, L. P., Fujii, M., & Griendling, K. K. (2017). Redox regulation of the actin cytoskeleton and its role in the vascular system. *Free Radical Biology and Medicine, 109*, 84-1078.

Yang, C., Wang, Y., Haiyan Liu, N. L., Sun, Y., Liu, Z., & Yang, P. (2012). Ghrelin protects H9c2 cardiomyocytes from angiotensin II-induced apoptosis through the endoplasmic reticulum stress pathway. *Journal of Cardiovascular Pharmacology, 59*(5), 465-471.

Yang, J., Hu, F., Fu, X., Jiang, Z., Zhang, W., & Chen, K. (2018). MiR-128/SOX7 alleviates myocardial ischemia injury by regulating IL-33/sST2 in acute myocardial infarction. *Biological Chemistry, 400*(4), 533-544.

Yang, J., Hu, F., Fu, X., Jiang, Z., Zhang, W., & Chen, K. (2019). MiR-128/SOX7 alleviates myocardial ischemia injury by regulating IL-33/sST2 in acute myocardial infarction. *Biological Chemistry, 400*(4), 533-544.

Yang, W., Liu, Z., Xu, Q., Peng, H., Chen, L., Huang, X., . . . Shi, R. (2017). Involvement of vascular peroxidase 1 in angiotensin II–induced hypertrophy of H9c2 cells. *Journal of the American Society of Hypertension, 11*(8), 519-529.

Yang, X., Jiang, H., & Shi, Y. (2017). Upregulation of heme oxygenase-1 expression by curcumin conferring protection from hydrogen peroxide-induced apoptosis in H9c2 cardiomyoblasts. *Cell and Bioscience, 7*(20).

Yanqiao, L., Shen, L., Yutong, M., Linghong, S., & Ben, H. (2022). Comparison of GRACE and TIMI risk scores in the prediction of in-hospital and long-term outcomes among East Asian non-ST-elevation myocardial infarction patients. *BMC Cardiovascular Disorders, 22*(1).

Ye, Z., Chen, C., Chen, S., Xu, M., & Xu, J. (2023). Analytical performances of a new rapid assay of soluble ST2 for cardiac and inflammatory diseases and establishment of the reference intervals for children and adolescence in China. *Practical Laboratory Medicine*.

Yu, S., Yang, H., Guo, X., & Sun, Y. (2020). Klotho attenuates angiotensin II-induced cardiotoxicity through suppression of necroptosis and oxidative stress. *Molecular Medicine Reports, 23*(1).

Zhang, H., & Dhalla, N. S. (2024). The Role of Pro-Inflammatory Cytokines in the Pathogenesis of Cardiovascular Disease. *International Journal of Molecular Sciences, 25*(2).

Zhang, W., & Liu, H. T. (2002). MAPK signal pathways in the regulation of cell proliferation in mammalian cells. *Cell Research, 12*, 9-18.

Zhang, Y., Liu, S., Li, X., & Ye, J. (2021). Protective Effect of Fasudil on Hydrogen Peroxide-Induced Oxidative Stress Injury of H9C2 Cardiomyocytes. *Disease Markers, 2021*(1).

Zhao, L., Cheng, G., Jin, R., Afzal, M. R., Samanta, A., Xuan, Y.-T., . . . Dawn, B. (2017). Deletion of Interleukin-6 Attenuates Pressure Overload-Induced Left Ventricular Hypertrophy and Dysfunction. *Circulation Research, 118*(2), 1918-1929.

Zheng, Y., Li, X., Zhang, F., Zhao, B., Du, W., Sun, D., & Li, G. (2022). Protective effect of nicorandil against myocardial ischemia/reperfusion injury mediated via IL33/ST2 signaling pathway. *Molecular and Cellular Biochemistry, 477*(7), 1921-1929.